Dimet

Ph.D. Program
Translational and Molecular Medicine

Mitochondrial diseases: from gene function to therapy

EMANUELA BOTTANI
Matr. 034194

Coordinator: Prof. Andrea Biondi
Tutor: Prof. Massimo Zeviani
Co-Tutor: Dr. Carlo Viscomi

Index

Chapter 1 General Introduction 1

1. Mitochondria 2
2. Mitochondrial DNA 4
3. Mitochondrial biology 8
   - 3.1. Complex I 9
   - 3.2. Complex II 11
   - 3.3. Complex III 12
   - 3.4. Complex IV 13
   - 3.5. Complex V 14
   - 3.6. Mitochondria Respiratory Chain Supercomplexes 15
4. Mitochondrial disorders 18
   - 4.1. Mutations in mtDNA 18
     - 4.1.1. Large-scale rearrangements of mtDNA 19
     - 4.1.2. Point mutations of mtDNA 20
   - 4.2. Mutations in nuclear genes 23
     - 4.2.1. Genes encoding structural subunits of complexes I-V 24
       - I Structural subunits of Complex I 24
       - II Structural subunits of Complex II 25
       - III Structural subunits of Complex III 26
       - IV Structural subunits of Complex IV 26
       - V Structural subunits of Complex V 26
     - 4.2.2. Genes encoding assembly factors of complexes I-V 27
       - I Assembly factors of Complex I 27
       - II Assembly factors of Complex II 28
       - III Assembly factors of Complex III 28
       - IV Assembly factors of Complex IV 33
       - V Assembly factors of Complex V 34

4.2.3. Genes encoding factors affecting mtDNA maintenance, replication and protein synthesis 35
4.2.4. Genes encoding mitochondrial proteins indirectly involved in oxidative phosphorylation 37
5. The MDDS due to mutations in MPV17 gene and the animal models used to study the disease 39
5.1. The Mpv17$^{-/-}$ mouse model 44
5.2. Sym1, the yeast orthologue of Mpv17 48
5.3. The mutant transparent zebrafish 51
5.4. What is the lesson learned by studying different species? 52
6. Treatment of mitochondrial diseases 53
6.1. Adeno-associated virus 54
7. Scope of the thesis 59
References 62
Chapter 2 Ttc19 is an assembly factor of respiratory complex III leading to slowly progressive neurodegeneration 84
Abstract 85
1. Introduction 86
2. Results 88
I Neurological and metabolic characterization of Ttc19$^{-/-}$ mice. 88
II Neuropathological characterization of Ttc19$^{-/-}$ mice 90
III Biochemical analysis of Ttc19$^{-/-}$ tissues 91
IV Analysis of cIII$_2$ assembly status in Ttc19$^{-/-}$ tissues 93
V TTC19 co-purifies with cIII$_2$ in HEK cells 96
3. Discussion 98
4. Methods 100
5. Supplemental information 111
References 119
Acknowledgments 122

Chapter 3 AAV-mediated liver-specific MPV17 expression restores mtDNA levels and prevents diet-induced liver failure 123

Abstract 124

1. Introduction 125
2. Results 128

I Mpv17 is part of a high molecular weight complex.... 128

II AAV2/8-mediated hMPV17 expression rescues the Mpv17$^{-/-}$ mouse liver phenotype 129

III Ketogenic diet induces severe cirrhosis in Mpv17$^{-/-}$ mice 132

IV AAV-mediated Mpv17 expression corrects liver damage of ketogenic diet 134

3. Discussion 141
4. Materials and Methods 143
5. Supplemental Information 147

References 155

Acknowledgments 159

Chapter 4 Emerging concepts in the therapy of mitochondrial disease 160

Abstract 161

1. Introduction 162

1.1. Basic concepts of mitochondrial biology and medicine 162

1.2. Experimental therapeutic strategies 166

2. Pharmacological and metabolic interventions 168

2.1. Increasing mitochondrial biogenesis 168

2.2. Endurance training 176

2.3. Scavenging toxic compounds 177

2.4. Supplementation of nucleotides 181

2.5. Targeting autophagy 183

2.6. Dietary manipulations 186

2.7. Targeting the PTP 188
3. Molecular approaches to treat mitochondrial diseases 189
3.1. Targeted re-expression of the mutated gene 189
3.2. Manipulating mtDNA heteroplasmy 195
3.3. Stabilizing mutant mt-tRNA 198
3.4. Targeting fission and fusion 200
3.5. Bypassing the block of the respiratory chain 201
3.6. Somatic nuclear transfer 202
4. Conclusions 203
References 204
Acknowledgements 223
Chapter 5 Summary, conclusions and future perspectives 224
1. Summary 225
2. Conclusions 228
3. Future perspectives 231
References 233
Publications 236

Chapter 1

General Introduction

1. Mitochondria

Mitochondria are double-membrane-enclosed, dynamic, plastic organelles that participate in a variety of physiological processes through the production of ATP, regulation of cellular signalling and programmed cell death [1]. These cytoplasmic organelles are thought to have arisen about 1.5 billion years ago; the discovery of mitochondrial DNA (mtDNA) and the following evidence about the close genetic relations between mitochondria and the photosynthetic α-proteobacteria led to the development of the endosymbiotic hypothesis [2], which has now been widely accepted among the scientific community. Most cells contain hundreds to thousands and more mitochondria. From a structural perspective, mitochondria are characterized by a double-membrane system delimitating four "mitochondrial compartments" where different metabolic pathways occur: the outer membrane, the inner membrane, the intermembrane space and the matrix (Figure 1). The outer mitochondrial membrane (OMM) is permeable to ions and small proteins (MW <10 kDa) because of the abundance of a large conductance channel, known as mitochondrial porin or voltage-dependent anion channel (VDAC). The intermembrane space (IMS) contains pro-apoptotic proteins as well as enzymes that are involved in the energy metabolism (adenylate kinase and creatine kinase): the most abundant member of the IMS is cytochrome c, a component of the oxidative phosphorylation (OXPHOS) system. The IMS also harbours proteins involved in reactive oxygen species removal and in the structural

organisation of the inner mitochondrial membrane (IMM). The IMM is indeed organized in numerous invaginations protruding into the matrix, called cristae. The cristae forms a network of tubular structures joined to IMM through the so-called cristae junctions (CJs) [3]. Thus, the inner mitochondrial compartment is delimited by the IMM and contains a soluble space, the mitochondrial matrix (MM). In turn, the IMM is composed of three membrane systems: outer and inner boundaries and cristae membrane [4]. The inner boundary contains proteins involved in mitochondrial fusion and protein import, whereas the complexes of the respiratory chain and the proteins involved in the biogenesis of iron/sulfur clusters accumulate in the cristae membrane [5].

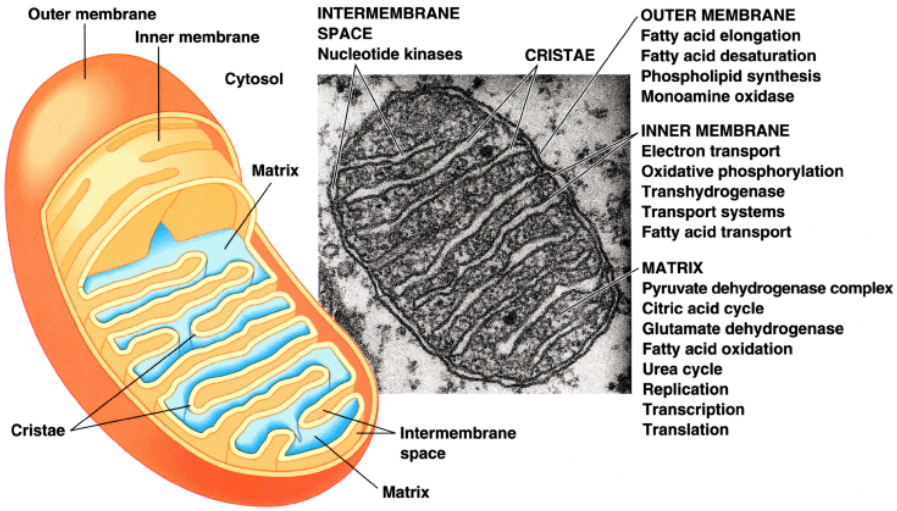

Figure 1. Mitochondria structure. Schematic representation of mitochondrial compartments (left) and ultrastructural image of a mitochondrion (right).

This organization is not static and the redistribution of these proteins between the two compartments is indeed an index of

the physiological state of mitochondria [5, 6]. The mitochondrial matrix contains several proteins involved in β-oxidation of fatty acids and Krebs cycle. Also, the matrix houses all the components of the mitochondrial protein synthesis machinery and several copies of mitochondrial DNA molecules as well as antioxidant enzymes.

2. Mitochondrial DNA

Mitochondria have their own genome (Figure 2), a circular DNA molecule of 16.5 Kb, consisting of two complementary strands that can be separated on denaturing cesium chloride gradients and are therefore referred to as the heavy strand (H-strand) and the light strand (L-strand). Mitochondrial DNA (mtDNA) is packaged into DNA–protein complexes called nucleoids, the major protein component of which is mitochondrial transcription factor A (TFAM) [7]. In addition to replication and transcription proteins, nucleoids also contain known components of the inner membrane, suggesting that mtDNA may be membrane associated [8]. MtDNA contains two non-coding regions: a 1 kb sequence known as the non-coding control region (NCR), and a distant 30 nt sequence containing the origin of replication for the L-strand (OriL). The NCR contains one transcription promoter for each strand (light strand promoter—LSP; heavy strand promoter—HSP). It also contains the origin of replication for the H-strand (OriH), classically annotated at nucleotide position 191, though less dominant origins have been reported nearby [9].

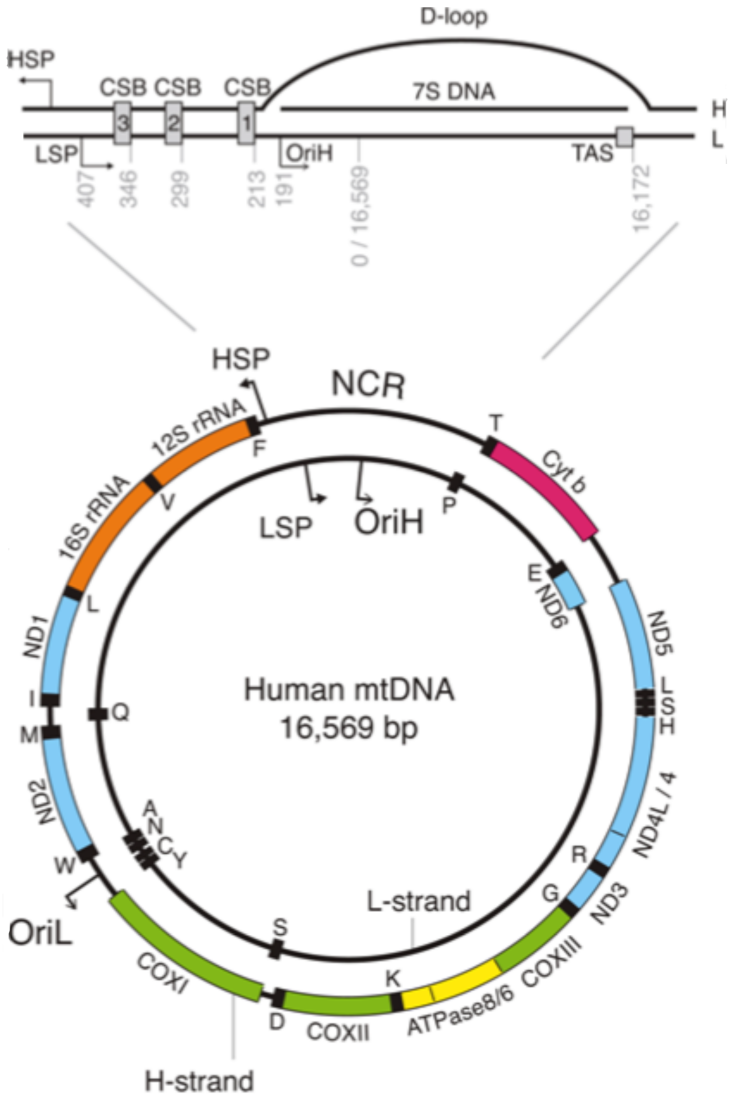

Figure 2. Map of the human mitochondrial genome. The major non-coding regions are the NCR (non-coding region), and OriL (origin of replication for the light strand). The outer and inner circles are the heavy (H) and light (L) strands, respectively. The NCR (enlargement shown above genome; nucleotide positions indicated in grey) contains the H- and L-strand promoters (HSP, LSP), three conserved sequence boxes (CSB1-3), the H-strand origin of replication (OriH) and the termination-associated sequence (TAS). Gene colour coding: complex III cytochrome b (Cyt b)—pink; complex I NADH dehydrogenase (ND) genes—blue; complex IV cytochrome c oxidase (COX) genes— green; complex V ATP synthase (ATPase) genes—yellow; ribosomal RNA (rRNA)—orange; transfer RNA genes—black boxes. From Uhler et al, 2015 [10].

A region between OriH and the termination-associated sequence (TAS) at the end of the NCR can form a displacement-loop (D-loop), so-called because it forms a triple-stranded structure created by prematurely terminated replication from OriH. The pre-terminated nascent H-strand, called 7S DNA (~650 nt), remains annealed to the template strand, though its function remains largely unknown [11]. The core factors required for mitochondrial primer formation and DNA replication are distinct from those in the nucleus. POLRMT, a single subunit RNA polymerase, is responsible for overall mitochondrial transcription including primers needed for mtDNA replication. POLγ, the only known replicative DNA polymerase in mitochondria, comprises the catalytic A subunit and two accessory B subunits. In addition to its polymerase activity, POLγA also harbours 3'–5' exonuclease activity and lyase activity [12]. The duplex DNA at the replication fork is unwound by the hexameric 5'-3' TWINKLE helicase, while mitochondrial single stranded DNA binding protein (mtSSB) protects the single stranded DNA created in its wake (Figure 3) [9]. The replication of mtDNA is independent from the cell cycle; the mechanism of its replication is not well established, and actually, three different models have been proposed to explain how mtDNA is primed and replicated (for review, see [9]). Nucleotides and deoxynucleotides pools required for mtDNA transcription and replication are formed within mitochondria through the *salvage pathway* whereas the *de novo pathway* takes place outside mitochondria. All mtDNA coding sequences

are contiguous to each others, with no introns; since mtDNA has a different codon usage from the universal genetic code, the expression of mitochondrial genes depends on an organelle-specific protein synthesis apparatus that comprises nuclear-encoded transcription and translation factors, as well as mitochondrially encoded tRNAs and rRNAs.

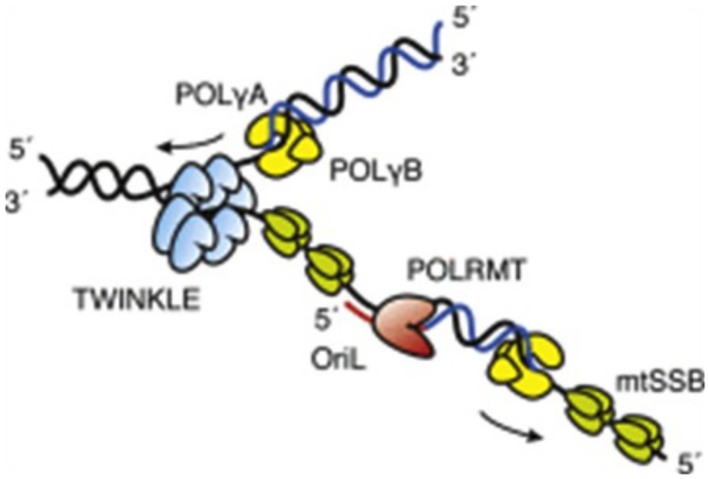

Figure 3. The mtDNA replication fork. TWINKLE helicase (blue) unwinds the dsDNA in a 5′–3′ direction. POLRMT (orange) is shown synthesizing the RNA primer (red) at OriL. The DNA polymerase POLγ (yellow) is made of one A subunit and two B subunits. Tetrameric mtSSB (green) stabilizes single stranded DNA. Template DNA: black: nascent DNA: blue. From Uhler et al, 2015 [10].

Therefore, the mitochondrial DNA of vertebrates includes two rRNAs (12S and 16S), 22 tRNAs and 13 protein coding genes: seven subunits of Complex I, three subunits of Complex IV, two subunits of Complex V, as well as cytochrome b, that is part of Complex III (Figure 4) [13]. MtDNA is exclusively maternally inherited in sexuate organisms [14], probably because sperm

mtDNA is tagged with ubiquitin and actively degraded in the early pre-implantation embryo [15]. There are several copies of mtDNA in each mitochondrion, and approximately 10^3–10^6 copies/cell. On every cellular division, mitochondria, and consequently mtDNA, are randomly distributed into daughter cells. In normal individuals, a single mitochondrial DNA haplotype is present in the whole cell population of the organism, a condition known as homoplasmy. However, the intrinsic propensity of mtDNA to mutate can generate a mixed population of wild type and mutant mtDNA coexisting in the same individual/cell population, a condition termed heteroplasmy [13].

3. Mitochondrial biology

Mitochondria convert energy stored in nutrients into a cell-spendable form, i.e. ATP (adenosine triphosphate) through a process termed oxidative phosphorylation (OXPHOS). The main constituents of oxidative phosphorylation are four large membrane multiheteromeric protein complexes embedded within the inner mitochondrial membrane (cI-IV). These complexes, plus two electron shuttles, Coenzyme Q (ubiquinone) and cytochrome c, carry out mitochondrial respiration. A fifth complex, ATP synthase (or complex V), exploits the energy derived from the electron transport chain and stored in the proton gradient across the IM, to convert ADP into ATP (Figure 4, top). NADH reducing equivalents derived from glycolysis, Krebs' cycle and fatty acid oxidation enter the

mitochondrial electron transport chain (mtETC) through complex I, whereas $FADH_2$ reducing equivalents enter the mtETC through complex II or other dehydrogenases such as electron-transferring-flavoprotein dehydrogenase (ETF-DH). The electrons are then passed via ubiquinone/ubiquinol to the respiratory chain complex III (ubiquinone-cytochrome c oxidoreductase) and, in the final step, from cytochrome c to cytochrome c oxidase (complex IV), which catalyzes the reduction of molecular oxygen to water. This process is coupled with proton pumping across the inner mitochondrial membrane, associated with complex I, III and IV. These complexes move protons out of the mitochondrial matrix, thus generating an electrochemical membrane potential (ΔP) formed by a chemical gradient (ΔpH) and an electrostatic gradient (ΔΨ) across the inner mitochondrial membrane. The last complex of the oxidative phosphorylation system, the ATP synthase, uses the energy derived from the proton gradient to produce ATP from ADP and phosphate [16, 17].

3.1. Complex I

Mammalian complex I is composed of 44 subunits, has an approximate molecular weight of 1MDa and it is the biggest enzyme among mitochondrial respiratory chain complexes [18]. Seven subunits are encoded by mitochondrial DNA (ND1, ND2, ND3, ND4, ND4L, ND5 and ND6), while nuclear DNA encodes the remaining subunits. Complex I subunits can be divided into “core subunits” and “accessory subunits”.

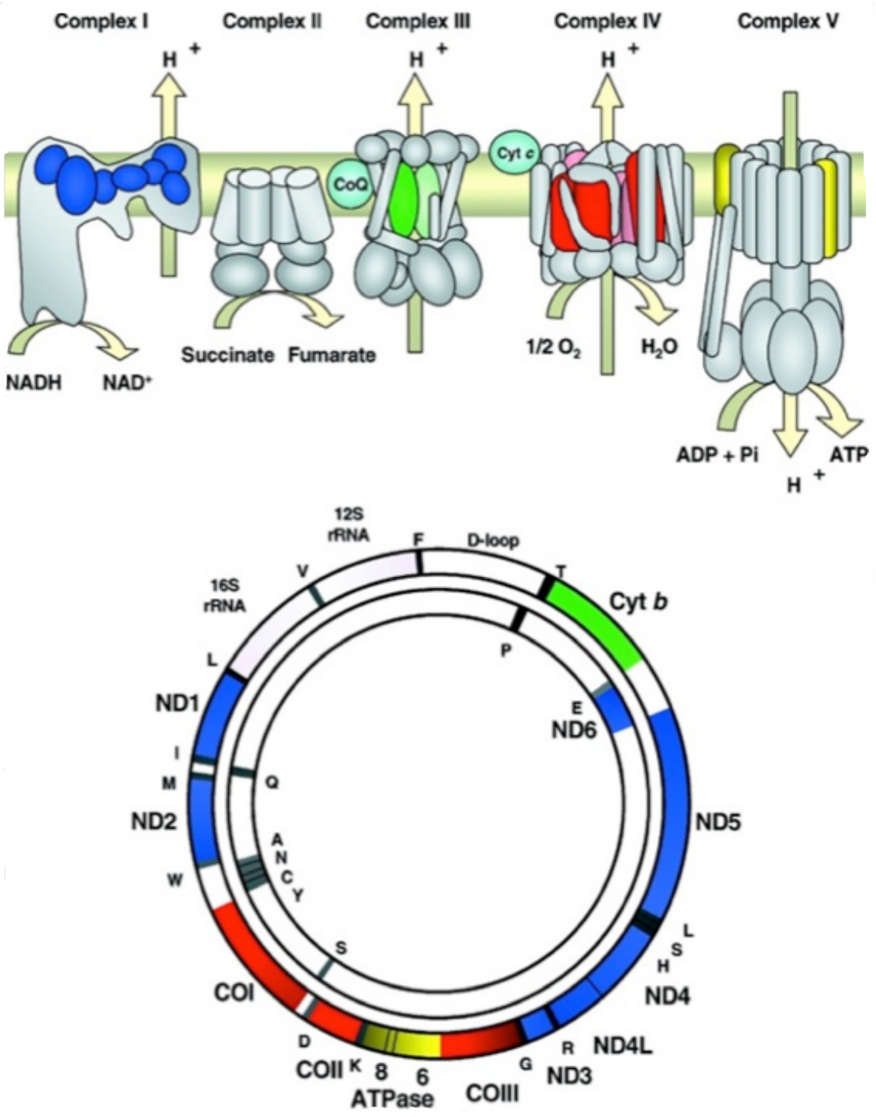

Figure 4. Mitochondrial respiratory chain and human mitochondrial DNA. Top: mitochondrial respiratory chain complexes; the subunits encoded by mitochondrial genome are represented with different colours: complex I subunits = blue; complex III subunits = green; complex IV subunits = red and complex V subunits = yellow. Bottom: human mitochondrial DNA. Genes encoding for mitochondrial respiratory chain complex subunits retain the same colour code. From Zeviani and Di Donato, 2004 [19].

There are 14 “core subunits” (including the seven mitochondrial-encoded plus additional seven nuclear-encoded

subunits) that contain the redox centers, i.e. flavin mononucleotide (FMN), and seven iron-sulfur clusters; these central subunits are sufficient to perform all bioenergetic functions [20]. The remaining 30 “accessory subunits” of mammalian complex I have no direct role in catalysis and their functions are mostly unknown, but they may be involved in assembly, stability, or regulation of the complex [21-23]. The mitochondrial complex I is “L-shaped”, with a hydrophilic peripheral arm extended into the matrix and a hydrophobic membrane arm embedded into the inner mitochondrial membrane [24]. The flavin mononucleotide (FMN) molecule is located on the tip of the hydrophilic arm [25, 26]. The electrons are donated as a hydride to the FMN molecule and then transferred via a chain of seven iron-sulfur (Fe-S) clusters to ubiquinone (Q) bound at the interface between the hydrophilic and the membrane arms. Three functional modules of complex I have been identified: the electron input module or N module, which oxidizes NADH; the electron output module or Q module, which reduces ubiquinone; and the P module, which translocates the protons across the membrane [18, 27, 28].

3.2. Complex II

Mitochondrial Complex II, also known as mitochondrial succinate:ubiquinone oxidoreductase, is a key membrane complex in the Krebs cycle. Complex II catalyzes the oxidation/dehydration of succinate to fumarate in the mitochondrial matrix. The structure contains four proteins, all

encoded by nuclear DNA: the catalytic subunits SDHA and SDHB, and two hydrophobic membrane-anchor proteins SDHC and SDHD. The overall structure is shaped like the letter “q,” with a hydrophilic head and a hydrophobic multipass transmembrane-anchor tail [29]. Succinate oxidation is coupled to reduction of ubiquinone to ubiquinol at the mitochondrial inner membrane, as part of the respiration electron transfer chain. Electrons are transferred from succinate to ubiquinone through the following prosthetic groups: flavin-adenine dinucleotide (FAD); a chain composed of three Fe clusters, [2Fe-2S], [4Fe-4S], and [3Fe-4S] clusters; and heme b, which forms an integral part of the complex [29, 30]. Complex II does not translocate protons, and therefore it only feeds electrons to the electron transport chain [30].

3.3. Complex III

Complex III or cytochrome bc1 complex forms the central part of the mitochondrial respiratory chain, oxidizing coenzyme Q and reducing cytochrome c while pumping protons from the matrix to the intermembrane space through the so-called Q-cycle [31]. Mammalian cIII is a multiheteromeric enzyme of approximately 480KDa composed of eleven different subunits [32, 33], one encoded by mitochondrial DNA (cytochrome b) and ten by nuclear genes. These eleven subunits constitute the monomeric module of a symmetric dimer ($cIII_2$), which is the functionally active form of the enzyme. The mammalian crystal structure [34] differs from that of yeast [35] only because it

contains one additional subunit. This extra subunit (Subunit 9) is just the mitochondrial targeting sequence peptide of the Rieske Fe-S protein, which is incorporated into the complex after its cleavage during import into the mitochondria [36]. Three of the 11 subunits contain the catalytic centers: cytochrome b (MT-CYB), cytochrome c1 (CYC1) and the Rieske protein (UQCRFS1). Cytochrome b contains two heme moieties, the low potential (bL) and the high potential (bH) heme b as prosthetic groups; CYC1 binds a c-type heme group and the Rieske iron-sulfur protein contains a 2Fe-2S cluster. The exact function of the other eight supernumerary subunits (UQCRC1, UQCRC2, UQCRH, UQCRB, UQCRQ, Subunit 9, UQCR10 and UQCR11) remains to be established [37].

3.4. Complex IV

In humans, complex IV is composed of 14 subunits, with the core inner-membrane subunits COI, COII and COIII encoded by mitochondrial DNA. The enzyme contains two iron-containing heme moieties (heme a and a3) and two copper centers (CuA and CuB), all coordinated by COI and COII and operating the electron transfer reactions. Cytochrome c oxidase is the terminal oxidase of the mitochondrial respiratory chain. It catalyzes the oxidation of cytochrome c with the consequent reduction of molecular oxygen to water. Electron transfer occurs from ferrocytochrome c to the CuA center (which acts as a single-electron receptor), then to heme a onto the heme a3/CuB center, and finally to oxygen bound to heme a3. H+/e−

cooperative linkage at Fe(a3)/CuB is envisaged to be involved in proton-pump mechanisms confined to the binuclear center [38]. COI-COII-COIII subunits form the catalytic core of the enzyme responsible of the electron transfer. Since none of the nuclear-encoded subunits is associated with the active site, it was formerly assumed that they were not important in the functional mechanism of the enzyme. However, it is now demonstrated that some of those additional subunits are involved in the stabilization of a dimer state of the oxidase [39] and might participate in the interaction of complex IV with its partner complexes within the respiratory supercomplexes.

3.5. Complex V

The mammalian mitochondrial complex V, or ATP synthase, is the last multi subunit complex of the oxidative phosphorylation system. It synthesizes ATP from ADP in the mitochondrial matrix using the energy provided by the proton electrochemical gradient [19, 40]. ATP synthase consists of two well-defined protein entities: the F_1 sector, a soluble portion situated in the mitochondrial matrix, and the F_0 sector, bound to the inner mitochondrial membrane. F_1 is composed of three copies of each of subunits α and β, and one each of subunits γ, δ and ε. F_1 subunits γ, δ and ε constitute the central stalk of complex V. F_0 consists of a subunit c-ring (probably comprising eight copies in humans) [41] and one copy each of subunits a, b, d, F6 and the oligomycin sensitivity-conferring protein (OSCP). Subunits b, d, F6 and OSCP form the peripheral stalk which lies to one

side of the complex. A number of additional subunits (e, f, g, and A6L), all spanning the membrane, are associated with F0 [42]. Two of the F_0 subunits, subunit a and subunit A6L are encoded by the mtDNA *ATP6* and *ATP8* genes, respectively [43, 44]. The function of ATP synthase is to synthesize ATP from ADP and inorganic phosphate in the F_1 sector. This is made possible by exploiting the energy derived from the proton gradient formed by mitochondrial respiration; protons accumulated in the IMS cross the inner mitochondrial membrane into the matrix through a channel largely formed by subunit a, associated with the F_0 portion of the enzyme. The proton gradient establishes a proton-motive force, composed of $\Delta pH+\Delta\psi$ [45]. The released energy causes the rotation of two rotary motors: the ring of c subunits in F_0 (relative to subunit a), along with subunits γ, δ and ε in F_1 to which it is connected through a central asymmetric stalk. Protons pass F_0 via subunit a to the c-ring [46, 47]. Rotation of subunit γ within the F_1 α3β3 hexamer provides energy for ATP synthesis. This is called “rotary catalysis” [48]. In humans, each complete rotation is carried out by the translocation of 8 protons (one for each c subunit) and leads to the synthesis of 3 molecules of ATP.

3.6. Mitochondria Respiratory Chain Supercomplexes

The organization of respiratory complexes in the inner membrane has been a matter of intense debate. Two models of organization have been hypothesized so far: the *Solid Model* and the *Random Diffusion Model* (Figure 5, A-B). According to

the former model, the respiratory components are closely packed to guarantee accessibility and thus high efficiency in electron transport [49, 50]. Conversely, the *Random Diffusion Model* or *Fluid Model* [51] proposes that the complexes are randomly moving within the inner mitochondrial membrane and that electrons flow between them, being connected by the mobile carriers CoQ and cytochrome c. The latter model gained general acceptance mainly based on kinetic studies and the demonstration that the different respiratory complexes can be purified individually, retaining their enzymatic activity [51]. However, this model was gradually replaced because several indications supported a permanent interaction of complexes, for example the stoichiometric association of complexes I and III after detergent removal from a mixture of isolated complexes [52, 53] and isolation of NADH cytochrome c reductase (complex I+III, [54]). Nowadays, it is generally accepted that respiratory complexes are organized in a dynamic array of states (*Plasticity Model*), from isolated complexes to larger structures (respiratory supercomplexes) (Figure 5, C). The main lines of evidence supporting the existence of supercomplexes are the specific co-migration of respiratory complexes on blue native electrophoresis and their co-purification by sucrose gradient centrifugation [50, 55]. In particular, the complexes involved in supramolecular association are the three proton-translocating enzymes: Complex I (NADH:Coenzyme Q reductase), Complex III (ubiquinol:cytochrome c reductase) and Complex IV (cytochrome c oxidase) [50, 56-58].

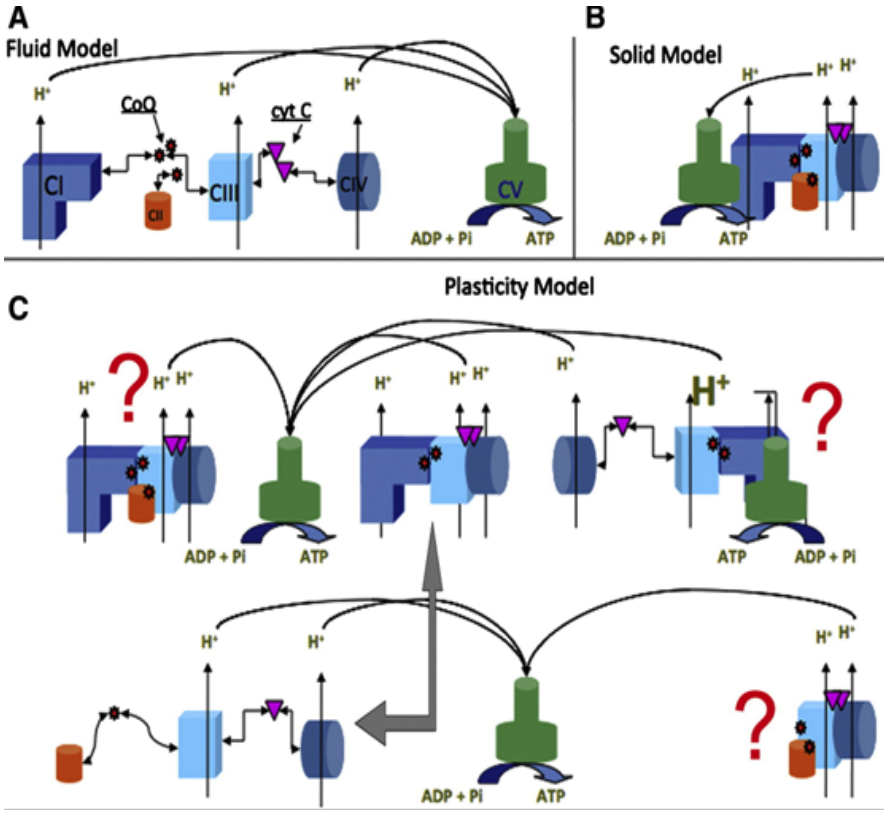

Figure 5. Schematic representation of the different models proposed to explain the organization of the OXPHOS system. (A) Random-collision model or fluid model, (B) the solid model, and (C) the plasticity model. The shape and colour code for representing the individual complexes can be seen in panel A; coenzyme Q is represented as small red-filled stars and cytochrome c as red-filled triangles. The question mark indicates putative associations or supercomplexes which existence is not fully confirmed. From Acin-Perez and Enriquez, 2014 [59].

The association of complex II in supercomplexes has never been established reliably [49]. Although their function is still controversial, Lapuente-Brunn and colleagues discovered that the product of the gene Cox7a2l, named Supercomplex Assembly Factor I (Scafi), specifically modulates assembly of respiratory complexes into supercomplexes, thus supporting their existence as real entities rather than artefacts due to the

specific procedures developed for mitochondrial solubilisation [58].

4. Mitochondrial disorders

Mitochondrial diseases are a clinically heterogeneous group of disorders that arise as a result of dysfunction of the mitochondrial respiratory chain, the essential final pathway for aerobic metabolism, or by mutations in genes involved in additional mitochondrial functions including heme synthesis and iron/sulphur metabolism among others. Tissues and organs that are highly dependent on aerobic metabolism are preferentially involved in mitochondrial disorders [60]. A genetic classification of mitochondrial diseases is based on which genome, nuclear or mitochondrial, is mutated.

4.1. Mutations in mtDNA

Mitochondrial DNA has a higher mutational rate than nuclear DNA; this is because of multiple factors, including absence of protective histones, the lack of homologous recombination, and its proximity to the inner mitochondrial membrane where ROS are generated. Mutations in mtDNA become symptomatic when the amount of mutated molecules offsets a critical threshold. The threshold is lower in tissues that are more dependent on oxidative metabolism. Different thresholds exist for different types of mtDNA mutations. Recent epidemiological studies confirm that pathogenic mtDNA mutations are a major cause of human disease, affecting at least 1 in 5000 of the population [61]. Pathogenic alleles are present in >1 out of 200 live births,

and occur *de novo* at least every 1000 births [62]. As already mentioned, mtDNA is exclusively maternally inherited in vertebrates [14]. Therefore, a mother carrying an mtDNA mutation can transmit it to her children, but only her daughters can further transmit it to the next generation. Due to the polyplasmic, multicopy organisation of mtDNA, a pathogenic mutation could be present in all (homoplasmy) or just in a fraction (heteroplasmy) of mtDNA molecules. Mutations of mtDNA are divided into (I) large-scale rearrangements (i.e. partial deletions or duplications) and (II) inherited point mutations. Whilst large-scale rearrangements are usually sporadic, point mutations are usually maternally inherited. Large-scale rearrangements include several genes and are invariably heteroplasmic. In contrast, point mutations may be heteroplasmic or, albeit more rarely, homoplasmic [19].

4.1.1. Large-scale rearrangements of mtDNA

Single, large-scale rearrangements of mtDNA can be single partial deletions, or partial duplications. The majority of single large-scale rearrangements of mtDNA are sporadic and are therefore believed to be the result of the clonal amplification of a single mutational event, occurring in the maternal oocyte or early during the development of the embryo [63]. Three main clinical phenotypes are associated with these mutations: adult-onset progressive external ophthalmoplegia (PEO), juvenile-onset Kearns-Sayre syndrome (KSS) and congenital Pearson syndrome. PEO is defined as progressive limitation of eye movements caused by impaired "extrinsic" eye muscles, with

normal function of the intrinsic muscles, and ptosis of the eyelids caused by weakness of the elevator palpebrae superioris muscle. KSS is a multisystem disorder of childhood or juvenile onset, characterised by the following symptoms: pigmentary retinopathy, progressive ataxia usually associated with cognitive decline, high protein content in the cerebrospinal fluid, short stature, cardiac conduction blocks and PEO. Pearson syndrome is characterised by severe, usually fatal, congenital pancytopenia with sideroblastic anemia, and, more rarely, exocrine pancreas dysfunction.

4.1.2. Point mutations of mtDNA

In contrast to large-scale rearrangements, mtDNA point mutations are usually maternally inherited. Point mutations involving tRNA genes may impair mitochondrial protein synthesis, leading to combine defects of the mtDNA-dependent respiratory chain complexes. Mutations involving protein-encoding genes affect the function of the individual respiratory chain complexes to which the corresponding protein belongs [64]. The most frequent disorders associated with mtDNA point mutations are termed with the acronyms MELAS, MERRF, NARP and LHON. The syndrome of Mitochondrial Encephalopathy, Lactic Acidosis, and Stroke-like episodes (MELAS) is most commonly caused by a heteroplasmic A-to-G transition mutation at position 3243 of the mitochondrial genome (encoding the mitochondrial- $tRNA^{Leu(UUR)}$). MELAS is characterised by prototypical neurological manifestations including seizures, encephalopathy, and stroke-like episodes,

as well as other frequent secondary manifestations including short stature, cognitive impairment, migraines, depression, cardiomyopathy, cardiac conduction defects, and diabetes mellitus [65]. However, although there are specific mutations typically associated with MELAS (m.3243A>G, m.3271T>C), MELAS is indeed a polygenic disorder associated with at least 29 specific point mutations. In addition to at least seven identified point mutations in the mitochondrial $tRNA^{Leu(UUR)}$ gene, mutations affecting several other mitochondrial tRNA genes (His, Lys, Gln, and Glu) as well as protein-coding genes (MT-ND1, MT-CO3, MT-ND4,MT-ND5, MT-ND6, and MT-CYB) have been associated with the MELAS syndrome [66].

The Myoclonic Epilepsy with Ragged Red Fibers is a rare mitochondrial disorder (MERRF). Diagnostic criteria for MERRF include typical manifestations of the disease: myoclonus, generalized epilepsy, cerebellar ataxia and ragged red fibers (RRF) in muscle biopsy [67]. Clinical features of MERRF are not necessarily uniform in the early stages of the disease, and correlations between clinical manifestations and physiopathology have not been fully elucidated. It is estimated that heteroplasmic point mutations in the $tRNA^{Lys}$ gene of the mtDNA, mainly A8344G, are responsible for almost 90% of MERRF cases [68].

Heteroplasmic mutations in the mitochondrially-encoded *ATP6* gene are responsible of a severe disorder named NARP syndrome (Neurogenic weakness, Ataxia, and Retinitis Pigmentosa). It commonly results from a point mutation at base

pair 8993 of the mitochondrial genome [69]. The clinical phenotype may also include epileptic seizures, sensorineural hearing loss, cognitive impairment, diabetes mellitus, cardiomyopathy, and lactic acidosis.

Leber's Hereditary Optic Neuropathy (LHON) is the most common optic neuropathy caused by a primary mutation in mtDNA [70]. LHON usually presents as painless, subacute, central visual loss in one eye. Weeks to months later, the second eye becomes involved, with a median delay of 6–8 weeks [71, 72]. Loss of vision can be very severe leading to blindness in most cases. Ninety per cent of all cases of LHON are due to one of three point mutations in mtDNA, which are located at nucleotide positions 3460, 11778, and 14484 [70]. All the known mutations occur in genes encoding subunits for complex I in the respiratory chain, particularly in those encoding the ND1 and ND6 subunits [73, 74]. In contrast with the MELAS, MERRF and NARP mutations, LHON mutations are typically homoplasmic. The penetrance is reduced, male individuals being 5-20 fold more prone to develop the disease. Both epidemiological and biochemical studies suggest that environmental factors, e.g. smoking, the mtDNA haplogroup and possibly genomic variants of nuclear DNA clearly influence the penetrance of the disease, although the mechanistic details of these phenomena remain largely unknown.

A summary of these and other mtDNA mutations associated to human disease is reported in Figure 6.

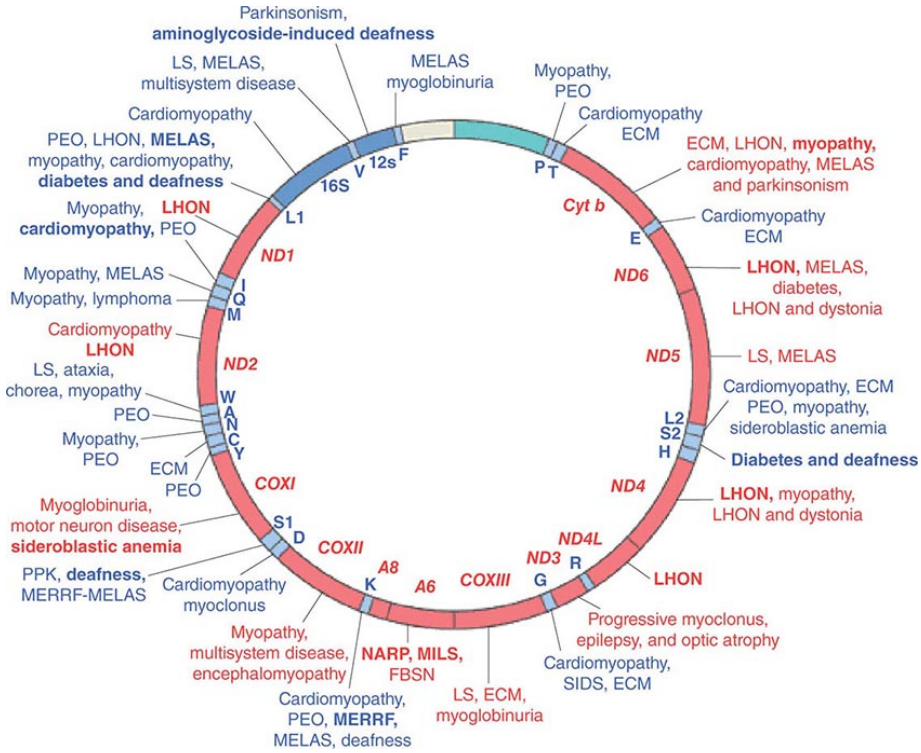

Figure 6. Mutations in the human mitochondrial genome known to cause disease. Disorders that are frequently or prominently associated with mutations in a particular gene are shown in bold. Diseases due to mutations that impair mitochondrial protein synthesis are shown in blue. Diseases due to mutations in protein-coding genes are shown in red. ECM, encephalomyopathy; FBSN, familial bilateral striatal necrosis; LHON, Leber's hereditary optic neuropathy; LS, Leigh syndrome; MELAS, mitochondrial encephalomyopathy, lactic acidosis, and stroke-like episodes; MERRF, myoclonic epilepsy with ragged red fibers; MILS, maternally inherited Leigh syndrome; NARP, neuropathy, ataxia, and retinitis pigmentosa; PEO, progressive external ophthalmoplegia; PPK, palmoplantar keratoderma; SIDS, sudden infant death syndrome (from S Di Mauro et al, 2003 [75]).

4.2. Mutations in nuclear genes

Mutations in nuclear genes responsible of mitochondrial disorders can be classified as follows:

- Genes encoding structural subunits of complexes I-V;
- Genes encoding assembly factors of complexes I-V;

- Genes encoding factors performing or regulating replication, expression and stability of mtDNA;
- Genes encoding mitochondrial proteins related to mitochondrial biogenesis or indirectly associated to oxidative phosphorylation.

4.2.1. Genes encoding structural subunits of complexes I-V

I Structural subunits of Complex I

Complex I deficiency is the most frequent biochemical abnormality found in mitochondrial disorders, together with combine deficiency of Complexes I and IV. Defective complex I can be caused by mutations in one of the seven mtDNA-encoded genes or in one of the 37 nuclear genes encoding complex I structural subunits [75]. Clinical manifestations include Leigh syndrome, neonatal fulminant lactic acidosis, with or without cardiomyopathy or multi-system disorders [76]. Leigh syndrome is a relatively frequent hereditary neuropathological condition, characterised by symmetrical necrotizing lesions along the rostrocaudal structures of the central nervous system, from the basal ganglia to the medulla oblongata; it is an early onset disease, in most cases occurring within the first year of life, with a wide range of clinical manifestations, including severe psychomotor delay, cerebellar and pyramidal signs, dystonia, lactic acidosis, seizures abnormalities of central ventilatory control, incoordination of ocular movements and recurrent vomiting. The pathognomonic focal symmetric lesions,

found at necropsy or by MRI, involve the basal ganglia, particularly putamina, the thalamus, brainstem structures from sub-thalamic nuclei through mesencephalon, pons, medulla oblongata and cerebellum, down to the rostral portion of the spinal cord [77]. The first patient with isolate complex I deficiency was described in 1998 [78], and since then other mutations in 12 different genes encoding for structural subunits have been identified [79]. These subunits are part of the highly conserved "core backbone" of the enzyme, and play a crucial role in the formation of its catalytic structure.

II Structural subunits of Complex II

Complex II (cII) deficiency is an exceptionally rare cause of mitochondrial respiratory chain defects. Different studies have provided different prevalence figures. For instance, Vladutiu and Heffner [80] found 23% of all muscle biopsies with respiratory chain defects to have complex II deficiency, whereas Parfait and co-workers [81] quote cII deficiency in just 2% of their cohort of mitochondrial cases. Ghezzi and co-workers [82] and Scaglia et al [83] found a prevalence of 8% in Italian and US cohorts of infantile mitochondrial disease. Mutations in *SDHA* are rare and typically associated to Leigh syndrome [84-86] whereas an adult-onset presentation is still controversial, having been reported in only one single family. Heterozygous mutations in *SDHC* and *SDHD*, and, albeit more rarely, in *SDHA* and *SDHB* as well, are associated with dominantly inherited or sporadic forms of head and neck paragangliomas and pheochromocytomas [87].

III Structural subunits of Complex III

Complex III defects are rare among OXPHOS patients and are associated to a wide range of neuromuscular, cardiac or multisystem diseases [88, 89]. Mutations in mitochondrial gene *MT-CYB*, which encodes for the subunit cytochrome b, are a well-established cause of complex III defects [90]. Mutations in other complex III structural subunits are exceptionally rare, i.e. in single cases due to mutations in *UQCRB*, *UQCRQ, UQCRC2* and *CYC1* [91-94].

IV Structural subunits of Complex IV

Complex IV defects are, together with those of complex I, the most frequently observed pathologies in mitochondrial patients. While different mutations in mitochondrial-encoded subunits of complex IV have been described, there are a few cases reporting a mutation in a nuclear encoded subunit, COX6B1 [95, 96]. All of these mutations are associated with a combination of early onset leukodystrophic encephalopathy, myopathy and growth retardation or with hydrocephalus and hypertrophic cardiomyopathy.

V Structural subunits of Complex V

Mutations in structural subunits of ATP synthase (complex V) are very rare. Up to now, only two patients with mutations in *ATP5A1* [97] and one patient with mutations in *ATP5E* [98] were reported pointing to the level of rareness of these disorders. These mutations share a similar biochemical

phenotype with pronounced decrease in the content of fully assembled and functional ATP synthase.

4.2.2. Genes encoding assembly factors of complexes I-V

I Assembly factors of Complex I

As complex I is composed of 44 structural subunits of dual genetic origin, its assembly is likely to involve many factors involved in subunit maturation, insertion, addition of cofactor or chaperoning of assembly intermediates [99, 100]. As no complex I is present in a highly exploited model of mitochondrial RC biogenesis, the baker's yeast *Saccharomyces cerevisiae*, identification of complex I assembly factors has largely relied on the identification of informative patients or on mass spectrometry study of complex I assembly intermediates produced by siRNA-based cellular models. Thus far, these studies have been able to identify ten complex I assembly factors: NDUFAF1, Ecsit, ACAD9, NDUFAF2, NDUFAF4 NDUFAF3, C8ORF38, C20ORF7 and FoxRed1. The assembly factor C20ORF7 was identified in 2 families with severe neonatal Complex I deficiency disorder resulting from a homozygous missense mutation in the *C20ORF7* gene [101, 102]. NDUFAF1 was identified in patients with cardioencephalomyopathies with complex I deficiency [103]. NDUFAF1 is imported into mitochondrial matrix and is required for complex I stabilization along with another assembly factor, Ecsit [104]. Null mutations in the gene encoding NDUFAF2 were found in patients suffering from progressive

encephalopathy [105]. Pathogenic mutations in *NDUFAF3* and *NDUFAF4* were identified in cases of fatal neonatal mitochondrial disease with severe complex I deficiency [106]. Mutations in *ACAD9* (Acyl-CoA dehydrogenase family, member 9) were identified in patients suffering from exercise intolerance and cardiomyopathy associated with complex I deficiency [107]. An additional complex I assembly factor is FoxRed1, which has been found mutated in patients with infantile-onset mitochondrial encephalopathy [108].

II Assembly factors of Complex II

Complex II defects are extremely rare, and to date, mutations in only two assembly factors have been reported: mutations in *SDHAF1* gene were associated with an isolated complex II defect and a specific leukoencephalopathic syndrome [82, 109]. *SDH5*, encoding another assembly factor of complex II, was found mutated in a family with hereditary paraganglioma [110].

III Assembly factors of Complex III

Typical to mitochondrial syndromes, complex III defects are associated with a wide range of clinical presentations; the common feature is reduced ubiquinol:cytochrome c oxidoreductase enzymatic activity in patient fibroblasts or skeletal muscle biopsies. Mutations in the nuclear gene *BCS1L* [111] are still the most frequent cause of complex III deficiency, as more than 25 different pathological mutations have been associated with very variable clinical presentations. BCS1L is an assembly factor localized in the IMM belonging to the AAA^+

(ATPases associated with diverse cellular activities) protein family. It is required in the final steps of complex bc1 assembly, where the Rieske protein and the smallest subunit (UQCR11) are incorporated into the pre-cIII$_2$ to complete the process [112-114]. BCS1L operates the transfer of the Rieske Fe-S protein from the matrix to the inner mitochondrial membrane through interaction with the Rip1 N-terminal domain and thanks to ATP hydrolysis [115, 116].

A Scandinavian-specific mutation in *BCS1L* is associated with GRACILE syndrome (Growth Retardation, Aminoaciduria, Cholestasis, Iron overload, Lactic acidosis, and Early death) [117, 118] whereas panoply of other mutations causes early-onset encephalomyopathy [113, 119]. In some patients, BCS1L mutations are associated with Björnstad-Tranenbjaerg syndrome, characterized by deafness, encephalomyopathy and pili torti [120]. Patients with the Björnstad syndrome have mutations that alter residues involved in protein–protein interactions, whereas the GRACILE mutation alters the ATP-binding residues of the BCS1L protein.

Mutations in *TTC19*, encoding the tetratricopeptide repeat domain-containing protein 19, were first described in 2011. *TTC19* is present in animals but absent in other eukaryotes including plants and fungi [89]. Four patients from three unrelated Italian families were investigated: three, including two siblings, had an early-onset, slowly progressive encephalopathy, whereas the fourth patient was affected by a late-onset but rapidly progressive neurological failure [89]. After

these first cases, several other *TTC19* mutations have been published, all consistently associated with isolated complex III deficiency but with different clinical presentations, including progressive neurodegeneration with severe psychiatric signs and cerebellar disease [121], Leigh syndrome [122] and early-onset predominant cerebellar ataxia [123-125]. All these cases carried non-sense or frameshift mutations of the *TTC19* gene predicting the synthesis of a truncated protein and, at least in the first reported patient samples, the levels of TTC19 were undetectable, suggesting mRNA decay and/or protein instability [89]. TTC19 was shown to co-migrate with complex III in Blue-Native Gel Electrophoresis (BNGE) and to co-immunoprecipitate with CORE1, CORE2 and Rieske protein, suggesting a physical interaction with the fully assembled complex III. Although its exact function is currently unknown, a role as a chaperone in the first steps of cIII assembly was proposed, because cIII assembly intermediates containing the early assembled CORE1 and CORE2, but not the late assembled Rieske protein were detected in mutant muscle samples [89]. These authors also suggested an additional role for TTC19, since they found TTC19 cross-reacting material in a high molecular-weight complex of unknown composition, weighing approximately 1MDa. Interestingly, a *Ttc19*-null *Drosophila melanogaster* model showed profound cIII deficiency associated with reduced life span and fertility, and neurological impairment in adult flies but, surprisingly, normal cIII activity in larvae, suggesting a differential developmental

control of cIII assembly in flies [89]. To further investigate the role of TTC19 in complex III biogenesis, a *Ttc19*$^{-/-}$ mouse model was generated from our lab (see Chapter 2).

Human *LYRM7* encodes the LYR (leucine/tyrosine/arginine)-motif protein 7, a member of the Complex1_LYR-like superfamily [126]. The LYR motif has consistently been found in proteins usually containing or delivering Fe-S clusters [127]. The human protein can functionally complement the respiratory defect of a yeast strain lacking Mzm1, the *LYRM7* orthologue in *Saccharomyces cerevisiae* [128]. Mzm1 acts as a chaperone for the incorporation of the Rieske protein; however, the insertion of the Fe–S cluster into the Rieske protein was not affected by this assembly factor [115, 129], suggesting a later-step intervention. The same results have recently been obtained for the human LYRM7/Mzm1L protein [128]. RNAi experiments in HeLa cells showed that, similar to the Mzm1 deletion yeast strain [129], low levels of LYRM7/Mzm1L caused a decrease in the total amount of the Rieske protein, but only in stress conditions [130]. Similar to Mzm1-deficient yeast [129], the phenotype is thermo-sensitive, probably because at high temperatures the unassembled Rieske protein is more prone to degradation and/or aggregation [115]. This could explain why the clinical course drastically worsened in the *LYRM7* mutant patient after a febrile episode [131]. A human Complex III assembly model constructed with these and other observations is represented in Figure 7.

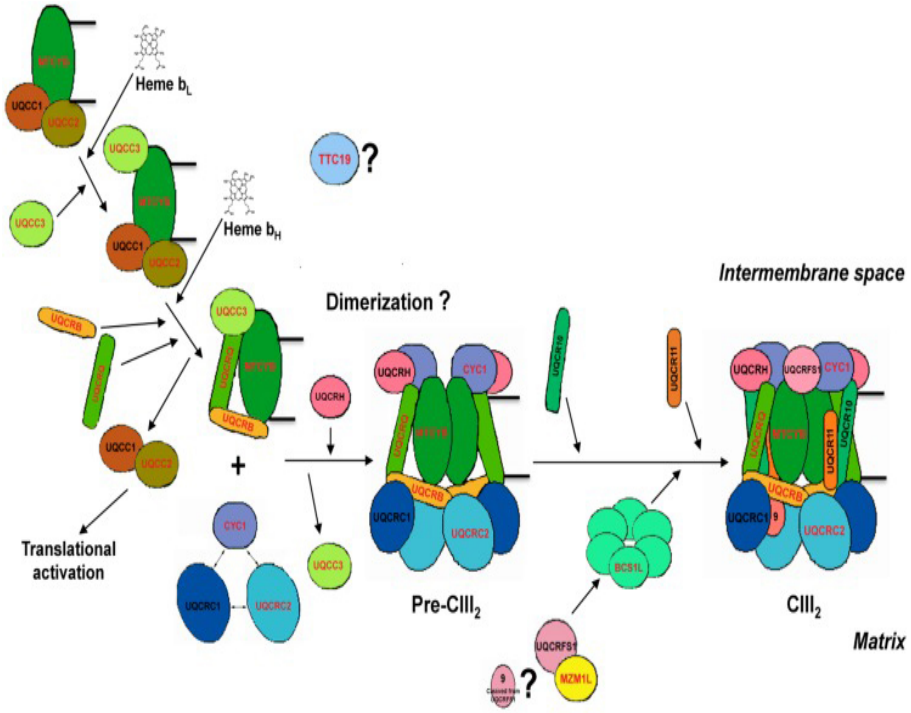

Figure 7. Human complex III assembly model. The model is constructed by homology with the available data for *Saccharomyces cerevisiae*. First, *MT-CYB* is translated in the mitochondrial ribosomes to which UQCC1 and UQCC2 are bound to the exit tunnel, activating its synthesis. The UQCC1-UQCC2 complex remains bound to MT-CYB once it is completely synthesized and incorporated to the mitochondrial inner membrane. Once low-potential heme b (bL) is inserted into the catalytic center of cytochrome b, UQCC3 binds to it and then the high potential heme b (bH) is incorporated. The UQCC1-UQCC2 dimer is released when UQCRB and UQCRQ bind to MT-CYB, to form the early-stage cIII intermediary, so that UQCC1-UQCC2 dimer becomes available to activate translation of new MT-CYB by binding to the mitoribosome. After the formation of the early intermediate MT-CYB+UQCRB+UQCRQ, additional subunits, i.e., UQCRC1, UQCRC2, and CYC1 are incorporated, followed by UQCRH and later UQCR10, to form pre-complex III (pre-$cIII_2$). At this point, the complex is already dimeric, but the precise stage at which dimerization occurs is currently unknown. Finally, UQCRFS1 is translocated from the matrix into the inner mitochondrial membrane and is incorporated into pre-$cIII_2$. In the matrix, UQCRFS1 is bound and stabilized by MZM1L. Finally the last subunit (UQCR11) joins the nascent complex, so that assembly is completed. TTC19 is necessary for the correct biogenesis of $cIII_2$ in human mitochondria, but the step in which it intervenes is not known yet. From Fernandez-Vizarra et al, 2015 [130].

IV Assembly factors of Complex IV

The most frequent clinical manifestation of complex IV deficiency in childhood is Leigh syndrome, although several other phenotypes have been reported, including leukoencephalopathy, cardiomyopathy or encephalo-cardiomyopathy [132]. Most of complex IV defects are due to mutations in COX-assembly factors, such as SURF1 [133-137], SCO1 [138-140], SCO2 [141-144], COX10 [145, 146], COX15 [147-150], COA6 (c1orf31), [151, 152], COX20 (FAM36A) [153, 154], C2orf64 [155].

SURF1 is a small hydrophobic protein of 30kDa embedded within the inner mitochondrial membrane; mutations in *SURF1* gene are the most frequent cause of Leigh syndrome with cytochrome c oxidase deficiency [137]. *SCO1* and *SCO2* are nuclear genes encoding copper binding proteins, with cooperative, non-overlapping functions in CuA site formation [156]. Mutations in these genes cause fatal early onset cardio-encephalo-myopathy with isolated Complex IV deficiency [142, 143]. The gene product of *COX10*, which maps on chromosome 17p13 as *SCO2*, plays a crucial role in the maturation of cytochrome c oxidase. *COX10* encodes a heme A farnesyl transferase that catalyses the first step of the conversions of proto-heme A into heme A, the prosthetic group [157]. Similar to COX10, COX15 is also involved in heme A synthesis; mutations in this gene were reported to cause fatal, hypertrophic cardiomyopathy [158] and atypic, slowly progressive Leigh syndrome [159]. In human mitochondria, COA6 selectively

interacts with SCO2 in a COX2-dependent manner. A loss of COA6 leads to fast turnover of COX2, explaining the reduction in cytochrome c oxidase levels [160]. Mutations in *COA6* are associated with neonatal hypertrophic cardiomyopathy and isolated complex IV deficiency [152]. Recently, mutations in *FAM36A* were reported as a cause of ataxia and muscle hypotonia in one patient, and of cerebellar ataxia, dystonia, and sensory axonal neuropathy in two affected brothers, with reduced complex IV activity [153, 154]. Finally, a homozygous mutation in C2orf64 was described in 2011 in two siblings affected by fatal neonatal cardiomyopathy, with accumulations of complex IV subassemblies in patient's fibroblasts [155]. Recently, deleterious mutations in *APOPT1* gene were described in three individuals from independent cohorts of subjects with isolated Complex IV deficiency and subsequently in three additional unrelated children. The clinical features varied widely from acute neurometabolic decompensation in late infancy to subtle neurological signs presenting in adolescence [161]. Although complex IV deficiency was present in all described patients, the role of the mitochondrial protein APOPT1 in biogenesis or stability of Complex IV still remains elusive.

V Assembly factors of Complex V

A few cases of complex V deficiency have been attributed to mutations in the assembly factor ATP12. Lactic acidosis was present immediately after birth, together with dysmorphic features, and methyl-glutaconic aciduria [162]. Mutations in

another gene, *TMEM70*, were found in individuals with isolated deficiency of ATP synthase, mostly of Gipsy ethnic origin. This prevalent mutation results in hypertrophic cardiomyopathy of variable severity [163, 164].

4.2.3. Genes encoding factors affecting mtDNA maintenance, replication and protein synthesis

In principle, any proteins involved in mtDNA replication, stability and maintenance, if mutated can cause mtDNA instability, with accumulation of multiple mtDNA deletions or depletion as a consequence. Mutations in *POLG* and *POLG2* (encoding the catalytic and accessory subunits of DNA polymerase gamma, respectively) [165], *PEO1* (the mitochondrial helicase Twinkle) [166], and *SLC25A4* (ANT1, the adenine nucleotide translocator) [167] have been associated to the accumulation of multiple mtDNA deletions genes in patients with autosomal dominant progressive external ophthalmoplegia (PEO); these proteins are involved in mtDNA replication and transcription, and their functional loss results in the secondary accumulation of mtDNA carrying different deletion species. Mitochondrial Neurogastrointestinal Encephalomyopathy (MNGIE) is a rare autosomal recessive disorder characterised by multiple deletions and depletion of mtDNA. The mutated gene (*TYMP*) responsible of the disease was identified in 1999 [168] and encodes thymidine phosphorylase TP, a cytosolic enzyme controlling the levels of pyrimidine nucleosides through phosphorolytic catabolism of thymidine to thymine and 2-deoxy-d-ribose-1-phosphate [169]. Mutations in *TYMP* cause an

accumulation of thymidine and deoxyuridine [170, 171], imbalance of nucleotide pools and, as a consequence, mtDNA depletions, multiple deletions and accumulation of point mutations [172, 173]. Alpers syndrome is a progressive neurodegenerative disorder of infancy characterized by diffuse degeneration of cerebral grey matter. While mutations in *POLG* have been associated with Alpers syndrome with liver failure (Alpers-Huttenlocher syndrome) [174-176], mutations in *NARS2* and *PARS2*, the genes encoding the mitochondrial asparaginyl- and prolyl-tRNA synthetases, were recently identified in two additional Alpers patients [177]. MtDNA depletion syndromes (MDSs) are a heterogeneous group of autosomal recessive disorders, characterized by low mtDNA levels in specific tissues. MDSs are rare, usually severe, early onset conditions, usually tissue specific (isolated myopathy, cerebro-hepatic failure) but sometimes manifesting as multisystem entities [178, 179]. These syndromes are a consequence of defects in mtDNA maintenance caused by recessive mutations in nuclear genes involved in either nucleotide synthesis (*TK2, SUCLA2, SUCLG1, RRM2B, DGUOK, MPV17* and *TYMP*) or mtDNA replication (*POLG*, C10orf2). For instance, mutations in *TK2* and *RRMB2* are associated with early onset myopathic disease [180-182]. *SUCLA2* encodes the β subunit of succinyl-coenzyme A synthase, the enzyme that reversibly synthesises succinyl-coenzyme A and ATP from succinate, coenzyme A and ADP in the Krebs cycle. Disruption of *SUCLA2* function can lead to severe encephalomyopathy with mitochondrial DNA

depletion, mild methylmalonic aciduria and infantile lactic acidosis, [183, 184]. Mutations in *SUCLG1*, encoding the α subunit of the enzyme, are less frequent [185].

Mutations in *PEO1* [186, 187], *POLG*, *DGUOK* and *MPV17* are associated with hepatocerebral forms of mtDNA depletions. *DGUOK* encodes the mitochondrial deoxyguanosine kinase, a member of the deoxyribonucleoside kinase family involved in phosphorylation of deoxyribonucleosides. The human dGK protein is highly specific for purine substrates [188]. Patients with mutations in *DGUOK* gene typically present liver dysfunction at birth or within a few months, with or without neurological impairment, and most of them die before four years of age due to liver failure [189]. For a detailed description of *MPV17*-associated disease, see paragraph 5.

4.2.4. Genes encoding mitochondrial proteins indirectly involved in oxidative phosphorylation

Mitochondrial neurological disorders can also be generated by mutations in nuclear genes indirectly related to cellular respiration and energy production [190]. For example, mutations in the *SPG7* gene, encoding a mitochondrial metalloprotease termed paraplegin, are responsible for a recessive form of hereditary spastic paraparesis [191]; likewise, mutations in *ABC7*, encoding a mitochondrial half-type ATP Binding Cassette transporter involved in iron homeostasis, are associated to a X-linked cerebellar ataxia and sideroblastic anaemia [192]. Friedreich's ataxia is an autosomal recessive, degenerative disease involving the central and peripheral

nervous systems and the heart; it is caused by reduced synthesis of the mitochondrial protein frataxin, a subunit of the core Fe−S assembly complex (called SDUF and composed of NFS1, ISD11, ISCU2, and frataxin) [193]. Defective expression of otherwise normal frataxin is caused by an unstable GAA trinucleotide expansion in the first intron of the gene [194].

The X-linked Mohr-Tranebjaerg syndrome (MTS/DFN-1) or deafness/dystonia syndrome results from a mutation in deafness/dystonia protein 1/translocase of mitochondrial inner membrane 8a (*DDP1/TIMM8a*). *DDP1/TIMM8a* is similar to a family of yeast proteins in the mitochondrial intermembrane space, which mediate the import, and insertion of inner membrane proteins. The mutation C66W in the gene *DDP1* avoids the formation of the 70KDa hetero-hexameric protein complex with Timm13 [195].

Finally, Barth syndrome is a rare X-linked genetic disorder first described by Dr Peter G. Barth in 1983 [196]. It is caused by mutations in the *TAZ* gene, encoding for the protein tafazzin. Tafazzin plays an important role in remodelling of cardiolipin, a component of the mitochondrial membrane necessary for maintaining mitochondrial structure as well as for mitochondrial apoptosis and functioning of the electron transport chain [197]. Cardiolipin accounts for 20% of the molecules of the inner mitochondrial membrane and is responsible of the strong impermeability of the inner mitochondrial membrane [198, 199]. It plays critical roles in mitochondrial biogenesis, fusion and fission, respiration, and protein import [200]. Heart failure is the

most common and earliest clinical feature, being the leading cause of death in infants with Barth syndrome. The cardiac features include dilated cardiomyopathy, left ventricular non-compaction, endocardial fibroelastosis, and serious disturbances of heart rhythm such as ventricular tachycardia leading to fibrillation [201].

5. The MDDS due to mutations in MPV17 gene and the animal models used to study the disease

As my studies on MPV17 are central for this thesis, the physiology and pathophysiology of this protein will be addressed more extensively here. In humans, mutations in the *MPV17* gene are responsible of a fatal hepatocerebral form of mitochondrial DNA depletion syndrome [202]; typically, the disease begins at birth or within 8 months with liver failure, hepatomegaly, elevations in aminotransferases and gamma-GT, hypoglycaemia, lactic acidosis, failure to thrive and death between 1 and 19 months [203, 204]. Dietary control of hypoglycaemia was occasionally effective in maintaining relative metabolic compensation and long-term survival [202, 205]. Although diet can partially control metabolic crises, liver failure invariably occurs and currently, the only treatment is liver transplantation. Patients that survived after liver transplant developed neurological symptoms and multiple brain lesions [203]. Also elevations of plasma methionine and S-adenosylmethionine, plus multifocal hepatocellular carcinomas and hepatic microadenomas on a background of cirrhotic liver

were described [206]. Only two reports described patients with adult-onset neurohepatopathy-plus syndrome with multiple deletions of mtDNA in muscle [207, 208]. More recently, a late-onset patient with *MPV17* mutations was described: a 25-year-old woman presenting initially with secondary amenorrhea, followed by a megaloblastic anemia, lactic acidosis, leukoencephalopathy, progressive peripheral neuropathy, and liver cirrhosis [209].

A peculiar manifestation of the disease was first described in 2006 and was called Navajo neurohepatopathy, because initially limited to this population of Arizona and Utah. The recurrent mutation responsible for this condition is a R50Q substitution in the MPV17 protein [210, 211]. Major clinical features include hepatopathy, failure to thrive, corneal anaesthesia and scarring, acral mutilation, recurrent metabolic acidosis, leukoencephalopathy, and sensory-motor peripheral neuropathy, ataxia and neurogenic arthropathy [212-215]. Mitochondrial DNA depletion was detected in the livers of patients. According to the severity of symptoms and age of onset, Navajo Neurohepatopathy can occur in three forms: neonatal, infantile and juvenile [216]. In the neonatal form, the onset is before 6 months of age with jaundice and failure to thrive followed by progression to liver failure before 2 years of age. The infantile form is characterized by onset between 1 and 5 years of age with liver dysfunction, rapidly progressing to liver failure and death. The juvenile form is characterized by variable onset of liver disease, but progressive neurological

deterioration. Liver histological findings include multinucleated giant cells, macro- and microvesicular steatosis, pseudo-acini, inflammation, cholestasis, bridging fibrosis and cirrhosis. Lifespan is prolonged up to 15-20 years [214].

MPV17 is a small, ubiquitous, highly hydrophobic protein of 19 kDa, organized in 4 transmembrane domains. In contrast with previous studies indicating a peroxisomal localization, the protein is embedded in the inner mitochondrial membrane [203, 204, 217] (Figure 8); the function of MPV17 is still unknown, but it seems to be associated to the formation of a high molecular weight complex of approximately >600kDa, since the re-expression of a tagged version of the protein that is unable to take part into the complex, failed to rescue mtDNA depletion in a *Mpv17*$^{-/-}$ mouse model (see Chapter 3). These findings are identical to those previously obtained on SYM1, the *MPV17*-yeast orthologue [218]. MPV17 is imported into mitochondria through the ΔΨ-dependent TOM-TIM import machinery; and the absence of post-import cleavage is typical of IMM carrier proteins, which are inserted into the IMM by the TIM22 complex [203]. Another group found that in the absence of a ΔΨ, only a partial reduction of MPV17 import was observed, suggesting that a fraction of MPV17 was transported within mitochondria, independently of the membrane potential [219]. Recently, Antonenkov and co-workers demonstrated that reconstitution of a recombinant MPV17 into lipid bilayer and subsequent electrophysiological measurements indicated that this protein forms a non-selective channel with a pore diameter of 1.8 nm,

with a weak cation-selectivity and several subconductance states [220].

MPV17 belongs to a family of integral membrane proteins consisting of four members (PXMP2, MPV17, MPV17L, and FKSG24 (MPV17L2)) in mammals and two members (Sym1 and Yor292) in yeast [220]. Mouse Pxmp2 is an abundant peroxisomal protein acting as a non-selective channel transferring small solutes across the membrane [221, 222]. The 1.4 nm pore of Pxmp2 channel showed weak cation selectivity and no voltage dependence at low holding potentials [221]. In contrast to the peroxisomal localization of Pxmp2, the MPV17, MPV17L, and MPV17L2 proteins were detected in the inner mitochondrial membrane [203, 223-225]. A recent paper from Dalla Rosa and co-workers suggests that MPV17L2 interacts with the large subunit of the mitochondrial ribosome and the monosome, and when its expression is reduced by RNA interference, the ribosome is disrupted and translation in the mitochondria is impaired, indicating MPV17L2 plays an important role in ribosomal biogenesis in the organelle [224]. MPV17L exists in two different isoforms: a 20-kDa isoform (l-Mpv17l) has been characterized as a peroxisomal protein with three transmembrane domains, whereas a 10-kDa isoform (s-Mpv17l) has been localized in the cytosol. Both isoforms are involved in ROS metabolism [226-228]. The localisation is controversial, since another paper suggested a mitochondrial localisation for both isoforms in homeostatic conditions [225], where they form of a protein complex with HtrA2. This complex

is suggested to be critical for sensing mitochondrial oxidative stress, and protects against ROS-induced mitochondrial dysfunction [225].

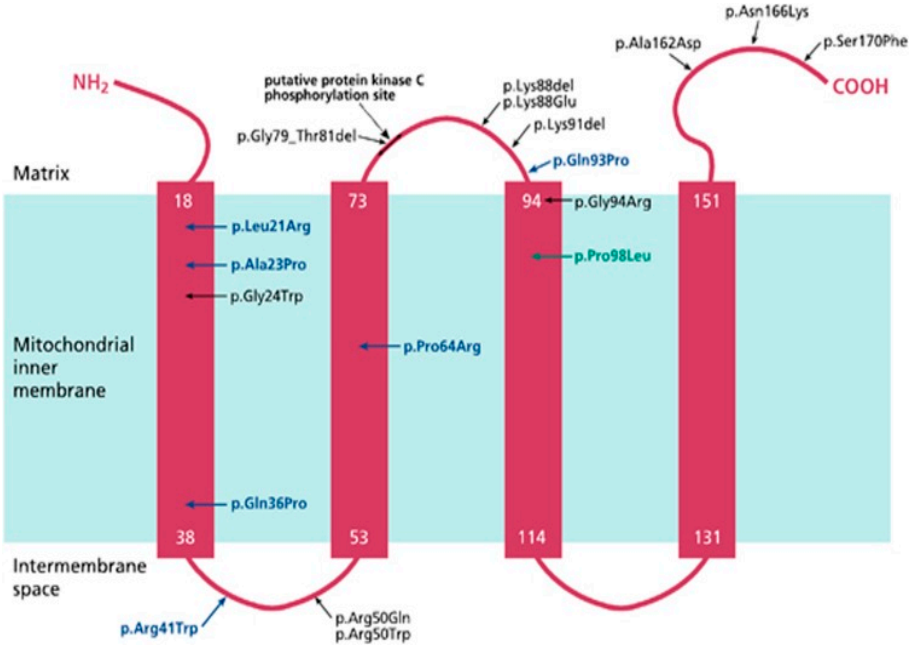

Figure 8. Schematic representation of the MPV17 protein, which is localized to the inner mitochondrial membrane; the 4 α-helical transmembrane spanning domains are indicated by red rectangles, and the number of the first and last amino acids of each of these domains is annotated in white. The missense mutations found in human patients are represented (From Uusimaa et al. 2014) [232].

HtrA2 is a protease acting as an essential regulator of mitochondrial function, protecting mitochondria from stress and preventing apoptosis [229, 230]. A very recent paper reported that Mpv17l interacts H2A histone family, member X (H2AX), ribosomal protein S14 (RPS14), ribosomal protein S3 (RPS3) and B-cell receptor-associated protein 31 (Bap31), and that silencing of Mpv17l caused increase of mtDNA damage and reduced expression of mtDNA-encoded genes [231].

5.1. The Mpv17$^{-/-}$ mouse model

The *Mpv17* gene was initially identified in laboratory mice created by random insertional mutagenesis [233]. The main clinical phenotype of these mice was the development of focal glomerulosclerosis and nephrotic syndrome at a young age [233, 234]. Glomerular damage was related to overproduction of oxygen radicals and accumulation of lipid peroxidation adducts in isolated glomeruli of *Mpv17*$^{-/-}$ mice. The development of the glomerular disease was inhibited by scavengers of oxygen radicals (dithiomethylurea) and lipid peroxidation (probucol), suggesting that the increase in ROS production has a relevant role in the onset of the disease [235]. The human Mpv17 protein rescued the murine phenotype [234]. Mice showed also degeneration of the *stria vascularis* and spiral ligament, loss of cochlear neurons and degeneration of the organ of Corti, similarly to Alports syndrome, an X-linked inherited disorder characterized by progressive nephritis and neurosensory deafness [236]. *Mpv17*$^{-/-}$ mice suffered from severe sensorineural hearing loss as well [237], they also developed significant systemic hypertension and tachycardia between 4 weeks and 5 months of age, accompanied by polyuria and elevated natriuresis [238].

A different strain with milder phenotype was later described by O'Bryan and colleagues: by 52 weeks of age, the mutant strain developed proteinuria, albuminuria and hypoalbuminemia, but neither arterial hypertension nor renal failure. Glomerular sclerosis was widespread, being preceded by mesangiolysis

and microaneurysms, while tubulointerstitial disease was absent. [239].

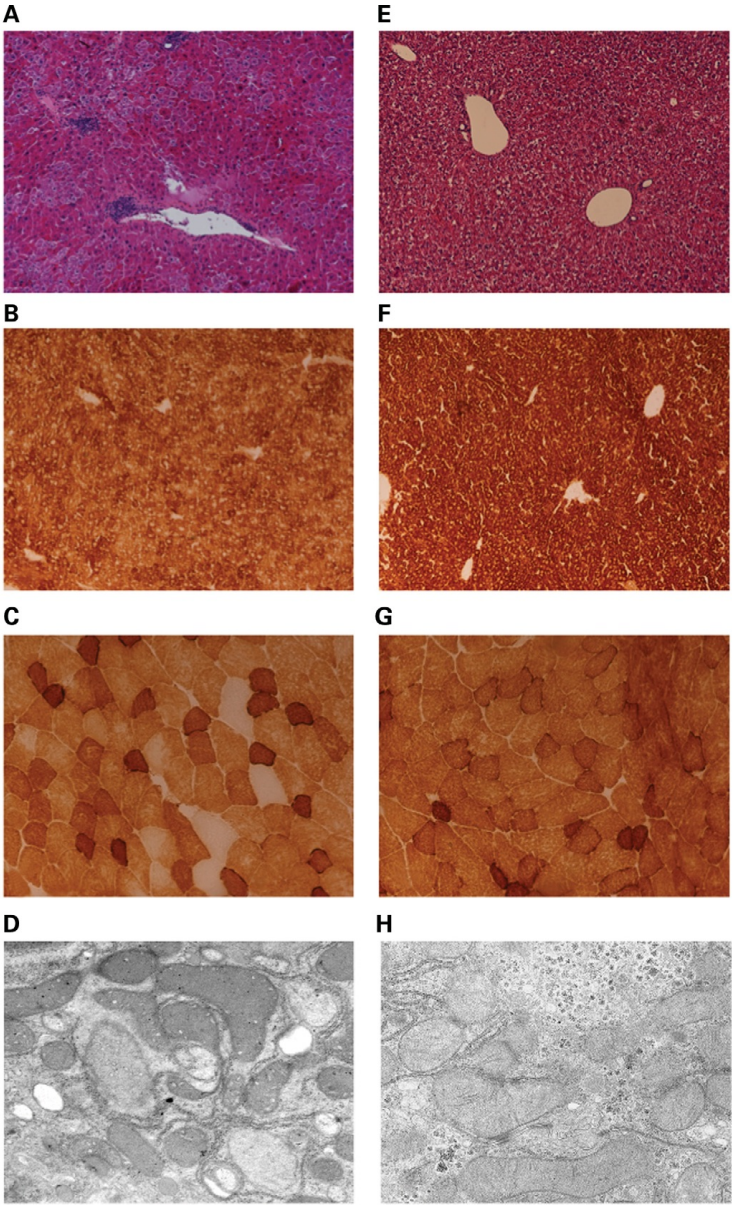

Figure 9 Histological and histochemical analysis. (**A**–**D**) Refer to *Mpv17*$^{-/-}$ mice; (**E**–**H**) refer to *Mpv17*$^{+/+}$ mice. (A and E) Liver H&E (×20): 2 years of age; (B and F) liver COX (×20): 1 year of age; (C and G) muscle COX (×20): 1 year of age; (D and H) electron microscopy ultrastructure of liver hepatocytes (×10400): 1 year of age. From Viscomi et al, 2006 [242].

In contrast to what is observed in *MPV17* mutant patients, the *Mpv17*$^{-/-}$ mice did not develop overt hepatic failure at any age, neither massive necrosis nor cirrhosis in mice as old as 2 years. However, morphological alterations were present in the liver parenchyma starting from 5 months of age, consisting of swelling of hepatocytes with collapse of sinusoidal spaces, scattered nuclear piknosis, scattered degeneration of discrete areas of hepatic lobules, and inflammatory infiltrates concentrated in the portal triads (Figure 9) [240]. AST, ALT and CK enzyme levels were constantly high in blood of knockout mice. Mitochondrial ballooning and disappearance of the internal cristae was consistently observed in *Mpv17*$^{-/-}$ liver, with proliferation of membranes surrounding the altered organelles, suggesting autophagy (Figure 9, D and H). Although infant patients develop hypoglycaemic episodes after 3–4 hours of fasting, 48 hours of fasting failed to induce hypoglycaemia in knockout mice; prolonged exposure to low temperature (a stress condition stimulating the activation of heat production by mitochondrial respiration) did not revealed any differences between wild type and knockout animals [240]. To date, only ketogenic diet, composed of 90% fat, 10% protein and virtually no sugar, caused liver cirrhosis and death in *Mpv17*$^{-/-}$ mice, resembling the human disease (see chapter 3) [241]. Interestingly, *Mpv17*$^{-/-}$ mice on a C57B/6 strain background invariably turn grey at 5–6 months (Figure 10) [240]. Mice show the presence of massive proteinuria from 18 months of age

onwards, but creatinine and urea levels in blood remained within the normal range [240].

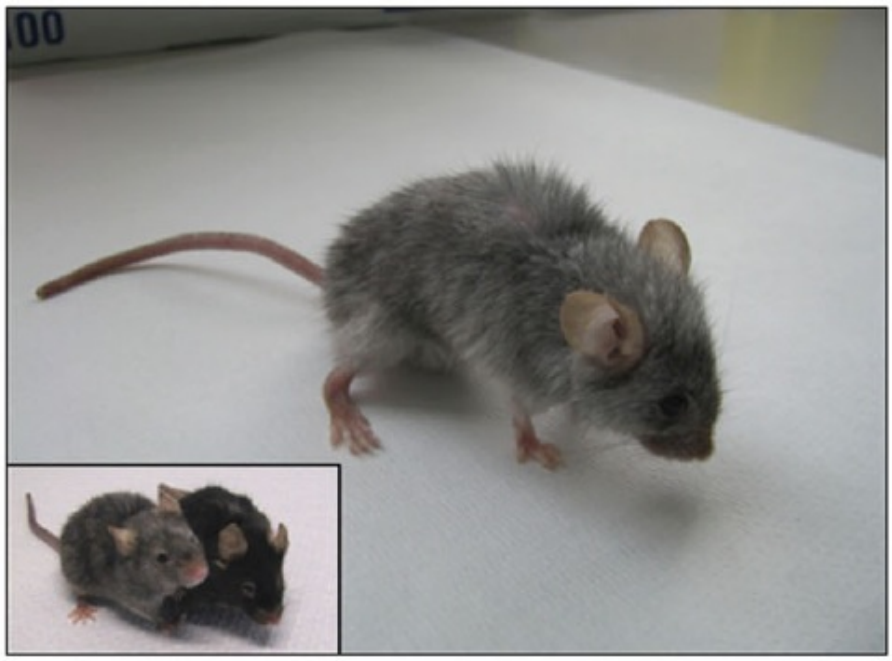

Figure 10 A 2-year-old Mpv17−/− individual. The inset shows −/− (grey) and $^{+/+}$ (black) littermates at 1 year of age. From Viscomi et al, 2006 [242].

Aged *Mpv17*$^{-/-}$ mice display severe atrophy of the skin layers, with thinning of the epidermis, loss of subcutaneous fat, and disorganization of the muscle layer; the hair follicles were also severely hypotrophic [240]. Similar to human patients, mtDNA depletion is present in liver (5% or less than control), muscle (25%), and absent or slightly reduced down to 70% in brain and kidney. Marked reduction in mtDNA is also observed in confluent (non-proliferating) mouse embryonic fibroblasts cultured in serum deprivation. MtDNA depletion can occur in MEFs by inducing aging or stress conditions that require an efficient oxidative phosphorylation system [240]. MtDNA

depletion is associated to complex I, III and IV deficiency in the liver (see chapter 3). In 2010, Papeta and co-workers produced and characterised double mutant *Prkdc*$^{-/-}$*Mpv17*$^{-/-}$ mice [243].Prkdc encodes the catalytic subunit of the trimeric DNA-dependent protein kinase (DNA-PKcs) and has essential roles in DNA repair, signal transduction, and transcriptional activation. Genetic defects in the Prkdc or the Ku70 and Ku80 genes (encoding the regulatory subunits of DNA-PK) result in immunodeficiency, radiosensitivity, and premature aging, which are generally attributed to the requirement for DNA-PK in non-homologous end-joining double strand break repair, the primary mode of DNA repair in non-replicating cells [244]. Prkdc has also been implicated as an essential coactivator of multiple transcription factors, including NRF1. While mice with mutations in either single gene were asymptomatic up to 12 months of age, Prkdc/Mpv17 double-mutant mice developed significant cardiac and renal mtDNA depletion and spontaneous liver, heart, and kidney disease, resulting in excess mortality by 16 weeks of age. These findings suggest that Prkdc genetically interacts with the same pathway of Mpv17.

5.2. Sym1, the yeast orthologue of Mpv17

Sym1 is localised in the IMM and it is required for growth on the non-fermentable carbon source ethanol under thermal stress (37°C). Wild type and Δ-sym1 cells grow equally well on glucose or ethanol at 30°C and on glucose at 37°C, but the Δ-sym1 strain is unable to grow on ethanol-containing medium at

37°C; this is a reversible growth arrest. Mammalian Mpv17 rescues the phenotype. The Sym1 gene is heat shock induced and the Sym1 protein exhibited increased expression during respiratory growth on ethanol; Δ-sym1 cells showed a marked downregulation in the expression of metabolic genes in ethanol at 37°C. In addition, the up regulation of both cytosolic and mitochondrial Hsp70 molecular chaperone genes, both known to be involved in mitochondrial protein translocation, suggests that sym1 cells may be experiencing some form of organellar stress [245].

MtDNA instability in *Saccharomyces cerevisiae* is associated with increased segregation of respiratory-deficient '*petite'* mutants. Growth at 37°C was reduced or impaired with ethanol, acetate, lactate, glycerol and a limited concentration (0.01%) of glucose on a rich medium (YP). This phenotype worsened when these carbon sources were added to a minimal medium (YNB) [218]. Supplementation with glutamate, aspartate, glutamine or asparagine did partially restore aerobic oxidative growth, whereas other non-essential amino acids had no effect. In both stringent and permissive growth conditions, the morphology of Δ-sym1 mutant mitochondria was profoundly altered, with organellar ballooning, flattening of cristae and accumulation of electron-dense particles, similar to what was described in knockout mice. In cells grown at 28°C, Sym1 expression was repressed by glucose and robustly induced by aerobic oxidative carbon sources, including ethanol, as typically observed for genes associated with respiratory metabolism.

However, glucose repression was abolished at 37°C, suggesting for Sym1 a role in the heat response, independent of its role in aerobic oxidative metabolism. The highest expression occurred in cells grown on ethanol at 37°C, suggesting an additive effect of two stressing conditions in Sym1 induction [218]. *In silico* analysis of the Sym1 genomic region revealed the presence of potential transcription factor binding sites including a GTCAC motif specific to Rtg1/Rtg3 located 693 bp upstream from the Sym1 ORF start codon. Rtg1/Rtg3 are transcription factors involved in the mitochondrion-nucleus retrograde response (RTG), a homeostatic control that induces adaptive responses in nuclear gene expression when mitochondrial activities, such as respiration or biogenesis, are failing.

The genes YMC1 and ODC1 were able to rescue the Δ-sym1 OXPHOS growth phenotype. Ymc1 is a mitochondrial carrier protein involved in the coordination of metabolite trafficking between peroxisomes and mitochondria, with a probable role in the transport of tricarboxylic acid (TCA) cycle intermediates. It also completely abolished mtDNA instability. ODC1 encodes an oxodicarboxylate carrier, which transports α-ketoadipate, α-ketoglutarate and other TCA cycle intermediates such as citrate, by a counter-exchange mechanism through the inner mitochondrial membrane. Finally, 2D-BNGE WB analysis using a strain expressing an HA-tagged Sym1 recombinant variant showed that Sym1 takes part in a high molecular–weight complex (>600 kDa) [218]. Purification of Sym1 and

reconstitution into lipid bilayer demonstrated that Sym1 constitutes a rectifying high-conductance cation-selective ion channel, which is voltage regulated; this channel is closed at the physiological IMM potential. This voltage sensitivity would prevent ion leakage across the inner membrane [219].

5.3. The mutant transparent zebrafish

The zebrafish *Danio rerio* has regular pattern of horizontal dark blue stripes covering the flanks of the adult animal. This pattern is composed of three chromatophore types: black melanophores, yellow xanthophores and reflective iridophores (Figure 11). In 2013, the adult viable and fertile mutant transparent (*tra*) was reported, which shows loss or strong reduction of iridophores throughout larval and adult stages [246]. In addition, in adults the number of melanophores is strongly reduced, and stripes break up into spots. The *tra* mutant phenotype is caused by a small deletion in Mpv17. Iridophores produce large amounts of crystals mainly consisting of guanine, located subcellularly in iridosomes (“reflecting platelets”). Interestingly, other zebrafish models have similar phenotype; pigment synthesis is compromised due to dysfunctional biosynthesis of guanosine-derivatives, which serve as intermediates in the formation of guanine. The affected genes encode Paics and Gart, two enzyme complexes involved in the synthesis of inosine monophosphate (IMP), a precursor of the purine nucleotides adenosine monophosphate (AMP) and guanosine monophosphate (GMP). In contrast to Mpv17 mutant

mice and patients, no depletion in mitochondrial DNA content is present in liver, muscle and brain tissues isolated from *tra* mutant adult animals [246].

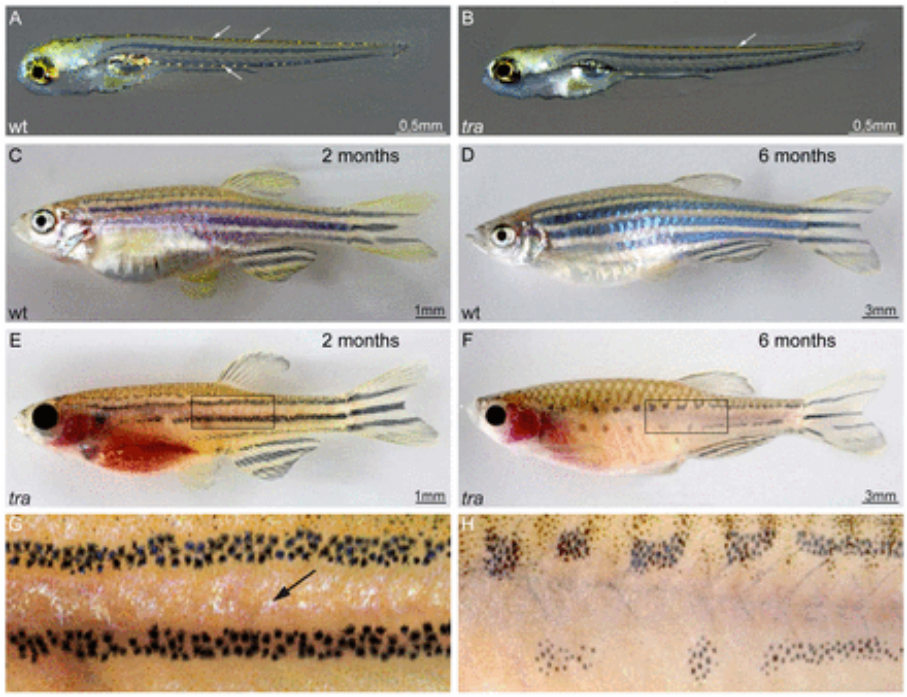

Figure 11. The *tra* mutant zebrafish. Transparent mutants show a reduction in iridophore pigmentation. (A,C,D) Wild type and (B,E–H) tra mutants. Arrows in panels A and B highlight the appearance and position of iridophores in larvae (G-H) Close-up of the region boxed in panel E-F. Scale bars: 0.5 mm (A,B); 1 mm (C,E), 3 mm (D,F).From Krauss et al, 2013 [246].

5.4. What is the lesson learned by studying different species?

In human, mitochondrial DNA depletion syndromes are caused by mutations in genes associated with mtDNA replication machinery or in mitochondrial deoxyribonucleoside triphosphate pools [247]. However, MPV17 plays a so-far unknown role in mtDNA maintenance. A high degree of conservation has been determined between MPV17 and its mouse, zebrafish and

yeast homologs, respectively, whereby mutants in these genes cause very different phenotypes. While dysfunction in human gene causes fatal liver disease, kidney pathology and hair greying are induced in mice, although mtDNA depletion is present but apparently with no consequence in liver functioning, at least in normal conditions. Moreover, the zebrafish inactivation of the Mpv17 homolog was detected as a viable discolouration mutant. Knock out of the yeast orthologue results in a temperature-sensitive metabolic growth phenotype. Actually, the most reliable hypothesis is that the Mpv17 protein forms a channel in the inner mitochondrial membrane, allowing small molecules to pass. These molecules are supposed to be TCA cycle intermediates in yeast, and nucleotides in vertebrates. Moreover, a function modifying the pathologic manifestations of Mpv17-related disease in mice has been identified. This signalling pathway remarkably involves the non-mitochondrial catalytic subunit of DNA-dependent protein kinase (PRKDC), important in double-strand break repair resistance against reactive oxygen-induced genotoxic stress.

6. Treatment of mitochondrial diseases

Given the extreme clinical, biochemical and genetic heterogeneity and the complexity of mitochondrial disease, neither universal nor effective therapies currently exist. Therapeutic options for mitochondrial diseases still remain focused on supportive interventions aimed at relieving complications. However, new therapeutic strategies have

recently been emerging, some of which have shown potential efficacy at the pre-clinical level [248], as follows:

- Activation of mitochondrial biogenesis;
- Modulation of autophagy;
- Inhibition of apoptosis;
- Scavenging of ROS;
- Endurance training;
- Dietary manipulation;
- Scavenging of toxic compounds;
- Supplementation of nucleotides;
- AAV-mediated gene therapy.

Since all these strategies are reviewed in Chapter 4, only AAV mediated gene therapy, the tool used in the work described in Chapter 3, is presented in this section.

6.1. Adeno-associated virus

Adeno-associated virus (AAV) is a non-pathogenic dependent parvovirus that requires helper functions from adenovirus or members of the herpes virus family for efficient replication [249, 250]. Human AAV was discovered in 1965 as a contaminant of adenovirus preparations [251]. The icosahedric, 22-nm in diameter viral capsid has no envelope, and therefore directly mediates many critical host–vector interactions. Because a co-infecting helper virus is usually required for a productive infection to occur, AAV serotypes are ascribed to a separate genus in the Parvoviridae family designated Dependovirus. Despite the high seroprevalence of AAV in the human

population (approximately 80% of humans are seropositive for AAV2) the virus has not been linked to any human illness. To date, more than 100 human and non-human primate AAV serotypes have been identified, including 12 serotypes with 51% and 99% identity in capsid amino acid sequence [252]; the great majority of the sequence variability is located in the surface-exposed regions of the capsid [253], that play a critical role in host–vector interactions. The wild-type AAV genome consists of a linear single-stranded DNA molecule of approximately 4.7 kb; both sense and antisense ssDNA strands are packaged into separate virions with equivalent efficiency [254]. The viral genome contains two open reading frames encoding the viral non-structural (Rep) and capsid (Cap) proteins necessary for virion biosynthesis, flanked by inverted terminal repeats (ITRs, Figure 12, top) [255]. Three promoters, mapping at positions 5, 19, and 40, are used to regulate the expression of these two ORFs [256, 257]. The p5 and p19 promoters direct the expression of the Rep ORF and generate four proteins through a splice variant mechanism termed Rep78, Rep68, Rep52 and Rep40 on basis of their apparent molecular weights [258]. The four Rep proteins are crucial for genome replication, transcription, integration and encapsidation. The p40 promoter directs the expression of the viral capsid proteins VP1, VP2, and VP3 [259, 260]. The three structural capsid proteins assembly together at a VP1:VP2:VP3 ratio of 1:1:10 to form a 60-subunit icosahedric capsid. The inverted terminal repeats have multipalindromic sequences at

their terminal 125 bases, and therefore can fold on themselves via complementary base pairing, to form a characteristic T-shaped hairpin structure (Figure 13) [255]. According to the AAV DNA replication model [261] this secondary structure provides a free 3' hydroxyl group for the initiation of viral DNA replication via a self-priming strand-displacement mechanism involving leading-strand synthesis and double-stranded replicative intermediates. The virus does not encode a polymerase, using instead that of the host cell [262]. The interaction between AAV vector and the target host cell depends on the interplay between the viral capsid with cell surface receptors, but knowledge of these interactions is far from complete. AAV vectors are thus classified in several different serotypes based on their tropism. The most extensively studied AAV serotype, AAV2, uses heparan sulphate proteoglycan as its primary receptor, but also binds several co-receptors including integrins and growth factor receptors [264]. Similar findings hold for other serotypes, which utilize a primary receptor together with one or more co-receptors for optimal attachment and internalization. Since the ITRs contain the necessary *cis-acting* sequences for replication and packaging, the wild-type genome can be engineered by removal of all viral coding sequences and be adapted for gene delivery by placing heterologous DNA sequences of choice between flanking ITRs, and replication and assembly of recombinant AAV (rAAV) virions are then achieved by supplying the AAV Rep and Cap proteins in *trans* along with the

necessary adenoviral helper functions.

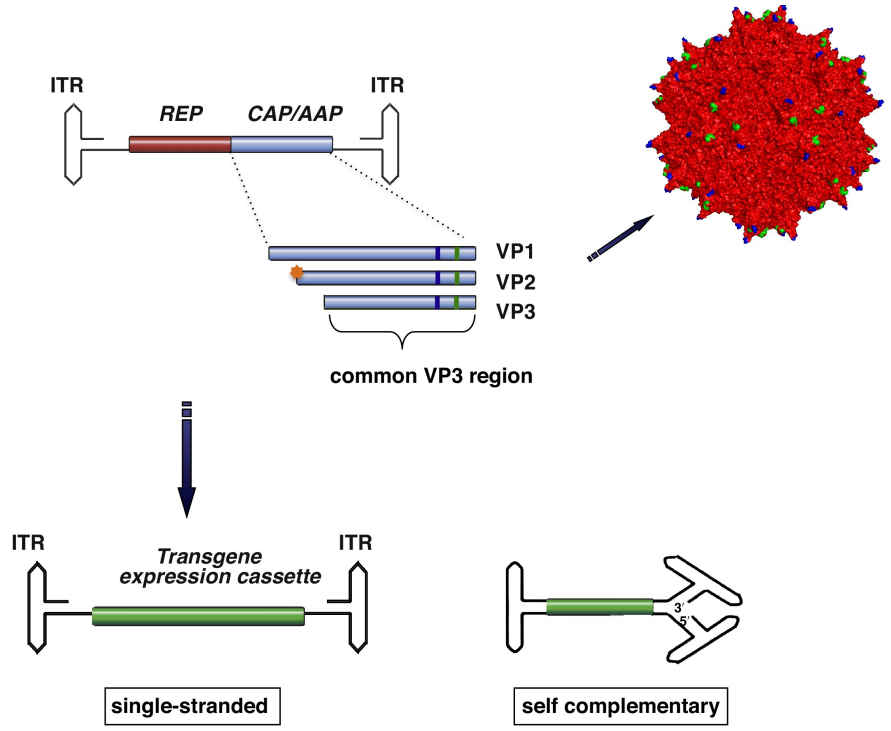

Figure 12 Schematic representation of AAV using AAV2 as example. From Buning et al, 2015 [263].

During the production of rAAV vectors, the transgene cassette is incorporated between the ITR containing plasmid whereas the rep-cap is supplied *in trans* along with the helper function genes in a triple plasmid transfection protocol [265]. This generates replication defective vectors. Following transduction of target cells, the single-stranded recombinant AAV genomes must be converted to double-stranded transcriptionally active forms to facilitate transgene expression; transcriptionally competent dsDNA can form by annealing the sense with the antisense strands in cells transducing at high multiplicity [266], or alternatively, by second strand synthesis [267].

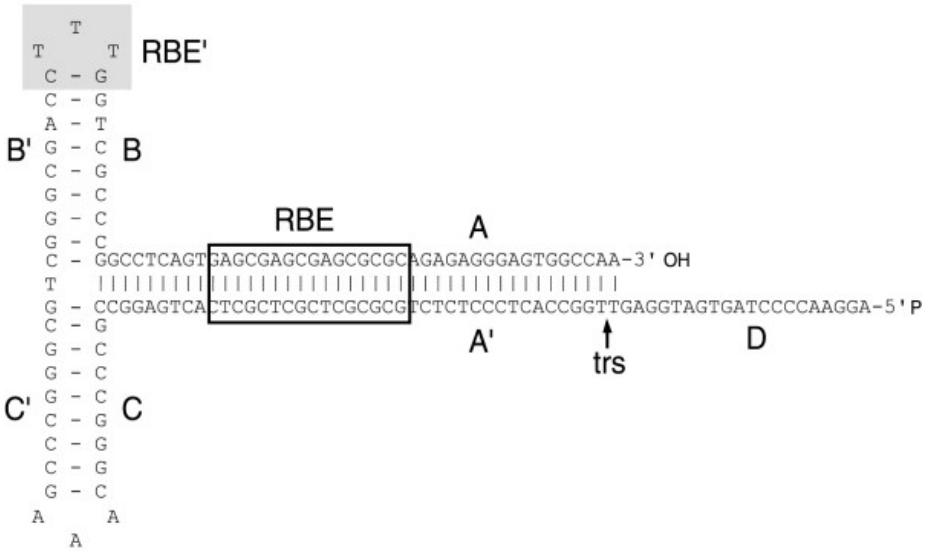

Figure 13. Secondary structure of the AAV2 ITR. The AAV2 ITR serves as origin of replication and is composed of two arm palindromes (B-B' and C-C') embedded in a larger stem palindrome (A-A'). The D sequence is present only once at each end of the genome thus remaining single-stranded. The boxed motif corresponds to the Rep-binding element (RBE) where the AAV Rep78 and Rep68 proteins bind. From Goncalves, 2005 [268].

This process requires host cell activities and is a rate-limiting step in the functional transduction of some post mitotic cell types. Self-complementary AAV (scAAV, Figure 12, bottom) is a viral vector engineered from the naturally occurring AAV vectors, in which the coding region has been designed to form an intra-molecular double-stranded DNA template. Upon infection, rather than waiting for cell mediated synthesis of the second strand, the two complementary halves of scAAV will associate to form one double stranded DNA (dsDNA) unit that is ready for immediate replication and transcription, thus giving faster kinetics and higher overall levels of expression [269]. In transduced cells, vector genomes are maintained

predominantly as episomal circular monomers and concatamers, but can also undergo random genomic integration. In actively replicating cell populations, episomal vector genomes are rapidly lost leaving stable long-term expression dependent on the subset of genomes that have undergone genomic integration [270].

7. Scope of the thesis

The purpose of the experimental work I carried out during my DIMET course has been focused on the generation and characterization of a mouse model of mitochondrial disease, and on the evaluation of adeno-associated virus (AAV)-therapy aimed to cure a severe form of mtDNA depletion syndrome. Although relatively rare as individual genetic diseases, taken as a group primary mitochondrial disorders are now recognized as one of the major health issue among inborn errors of metabolism, with a prevalence >1 in 5.000. The expanding identification of new genes affecting OXPHOS sustains the idea that these disorders are far more common than previously thought. These devastating diseases are complex, with highly variable presentations. Importantly, rational, evidence-based effective treatment is lacking for most of them. Understanding the role of the mutated protein involved in the pathology is the first step to better understand and eventually treat the disease. To this aim, during my DIMET course I have generated and characterised the *Ttc19*$^{-/-}$ mouse model. TTC19 is a protein recently identified as responsible of a severe form of

mitochondrial disease with complex III deficiency. As different as they appear, humans and mice are surprisingly similar. We share more than 95% of our genomes and get most of the same diseases, for many of the same genetic reasons. Therefore, the results of mouse experiments often correlate to human biology; a mouse with a specific disease or condition can serve as a model for a human patient with that same disease or condition. This can lead to better diagnosis and treatment of many diseases. Chapter 2 describes the characterisation of the *Ttc19*$^{-/-}$ mouse model: knockout mice have mitochondrial complex III deficiency with associated increased ROS production, muscle weakness, reduction of spontaneous locomotor activity and energy metabolism, and clear neurological impairments, similarly to human patients. Additional experiments carried out on cellular models suggested that TTC19 interacts with pre-cIII$_2$ before UQCRFS1 incorporation, remaining attached to the complex after its maturation and facilitating its incorporation.

The second part of my work was focused on the evaluation of a gene therapy approach on a mouse model of mitochondrial disease. Successful pre-clinical trials have been reported in the last few years using gene replacement therapy for a number of genetic disorders. The most relevant results have been obtained by recombinant Adeno-associated viral (AAVs) vectors carrying a therapeutic gene, specifically targeted to the affected tissues and organs. Whilst replacement of genes through the whole body is still an unachievable goal, gene replacement in

smaller-size organs is nowadays feasible. Chapter 3 reports the application of this strategy on a mouse model of severe mtDNA depletion syndrome predominantly affecting the liver. Finally, Chapter 4 reviews currently available therapeutic approaches for mitochondrial disease.

References

1. McBride, H.M., M. Neuspiel, and S. Wasiak, Mitochondria: more than just a powerhouse. Curr Biol, 2006. 16(14): p. R551-60.
2. Margulis, L., Symbiosis and evolution. Sci Am, 1971. 225(2): p. 48-57.
3. Mannella, C.A., M. Marko, and K. Buttle, Reconsidering mitochondrial structure: new views of an old organelle. Trends Biochem Sci, 1997. 22(2): p. 37-8.
4. Frey, T.G. and C.A. Mannella, The internal structure of mitochondria. Trends Biochem Sci, 2000. 25(7): p. 319-24.
5. Vogel, F., et al., Dynamic subcompartmentalization of the mitochondrial inner membrane. J Cell Biol, 2006. 175(2): p. 237-47.
6. Benard, G. and R. Rossignol, Ultrastructure of the mitochondrion and its bearing on function and bioenergetics. Antioxid Redox Signal, 2008. 10(8): p. 1313-42.
7. Bogenhagen, D.F., Mitochondrial DNA nucleoid structure. Biochim Biophys Acta, 2012. 1819(9-10): p. 914-20.
8. Rajala, N., et al., Replication factors transiently associate with mtDNA at the mitochondrial inner membrane to facilitate replication. Nucleic Acids Res, 2014. 42(2): p. 952-67.
9. Falkenberg, M., N.G. Larsson, and C.M. Gustafsson, DNA replication and transcription in mammalian mitochondria. Annu Rev Biochem, 2007. 76: p. 679-99.
10. Uhler, J.P. and M. Falkenberg, Primer removal during mammalian mitochondrial DNA replication. DNA Repair (Amst), 2015. 34: p. 28-38.
11. Nicholls, T.J. and M. Minczuk, In D-loop: 40 years of mitochondrial 7S DNA. Exp Gerontol, 2014. 56: p. 175-81.
12. Longley, M.J., et al., Identification of 5'-deoxyribose phosphate lyase activity in human DNA polymerase gamma and its role in mitochondrial base excision repair in vitro. Proc Natl Acad Sci U S A, 1998. 95(21): p. 12244-8.
13. Taylor, R.W. and D.M. Turnbull, Mitochondrial DNA mutations in human disease. Nat Rev Genet, 2005. 6(5): p. 389-402.
14. Giles, R.E., et al., Maternal inheritance of human mitochondrial DNA. Proc Natl Acad Sci U S A, 1980. 77(11): p. 6715-9.

15. Sutovsky, P., et al., Ubiquitin tag for sperm mitochondria. Nature, 1999. 402(6760): p. 371-2.
16. Letts, J.A. and L.A. Sazanov, Gaining mass: the structure of respiratory complex I-from bacterial towards mitochondrial versions. Curr Opin Struct Biol, 2015. 33: p. 135-145.
17. Lenaz, G. and M.L. Genova, Structure and organization of mitochondrial respiratory complexes: a new understanding of an old subject. Antioxid Redox Signal, 2010. 12(8): p. 961-1008.
18. Carroll, J., et al., Analysis of the subunit composition of complex I from bovine heart mitochondria. Mol Cell Proteomics, 2003. 2(2): p. 117-26.
19. Zeviani, M. and S. Di Donato, Mitochondrial disorders. Brain, 2004. 127(Pt 10): p. 2153-72.
20. Brandt, U., Energy converting NADH:quinone oxidoreductase (complex I). Annu Rev Biochem, 2006. 75: p. 69-92.
21. Walker, J.E., The NADH:ubiquinone oxidoreductase (complex I) of respiratory chains. Q Rev Biophys, 1992. 25(3): p. 253-324.
22. Abdrakhmanova, A., et al., Subunit composition of mitochondrial complex I from the yeast Yarrowia lipolytica. Biochim Biophys Acta, 2004. 1658(1-2): p. 148-56.
23. Andrews, B., et al., Assembly factors for the membrane arm of human complex I. Proc Natl Acad Sci U S A, 2013. 110(47): p. 18934-9.
24. Grigorieff, N., Structure of the respiratory NADH:ubiquinone oxidoreductase (complex I). Curr Opin Struct Biol, 1999. 9(4): p. 476-83.
25. Baradaran, R., et al., Crystal structure of the entire respiratory complex I. Nature, 2013. 494(7438): p. 443-8.
26. Sazanov, L.A. and P. Hinchliffe, Structure of the hydrophilic domain of respiratory complex I from Thermus thermophilus. Science, 2006. 311(5766): p. 1430-6.
27. Chomyn, A., et al., The site of synthesis of the iron-sulfur subunits of the flavoprotein and iron-protein fractions of human NADH dehydrogenase. J Biol Chem, 1988. 263(31): p. 16395-400.
28. Galante, Y.M. and Y. Hatefi, Resolution of complex I and isolation of NADH dehydrogenase and an iron--sulfur protein. Methods Enzymol, 1978. 53: p. 15-21.

29. Sun, F., et al., Crystal structure of mitochondrial respiratory membrane protein complex II. Cell, 2005. 121(7): p. 1043-57.
30. Hagerhall, C., Succinate: quinone oxidoreductases. Variations on a conserved theme. Biochim Biophys Acta, 1997. 1320(2): p. 107-41.
31. Crofts, A.R., et al., The Q-cycle reviewed: How well does a monomeric mechanism of the bc(1) complex account for the function of a dimeric complex? Biochim Biophys Acta, 2008. 1777(7-8): p. 1001-19.
32. Schagger, H., et al., Isolation of the eleven protein subunits of the bc1 complex from beef heart. Methods Enzymol, 1986. 126: p. 224-37.
33. Link, T.A., H. Schagger, and G. von Jagow, Analysis of the structures of the subunits of the cytochrome bc1 complex from beef heart mitochondria. FEBS Lett, 1986. 204(1): p. 9-15.
34. Xia, D., et al., Crystal structure of the cytochrome bc1 complex from bovine heart mitochondria. Science, 1997. 277(5322): p. 60-6.
35. Hunte, C., et al., Structure at 2.3 A resolution of the cytochrome bc(1) complex from the yeast Saccharomyces cerevisiae co-crystallized with an antibody Fv fragment. Structure, 2000. 8(6): p. 669-84.
36. Brandt, U., et al., The mitochondrial targeting presequence of the Rieske iron-sulfur protein is processed in a single step after insertion into the cytochrome bc1 complex in mammals and retained as a subunit in the complex. J Biol Chem, 1993. 268(12): p. 8387-90.
37. Xia, D., et al., Structural analysis of cytochrome bc1 complexes: implications to the mechanism of function. Biochim Biophys Acta, 2013. 1827(11-12): p. 1278-94.
38. Wikstrom, M., M.I. Verkhovsky, and G. Hummer, Water-gated mechanism of proton translocation by cytochrome c oxidase. Biochim Biophys Acta, 2003. 1604(2): p. 61-5.
39. Fontanesi, F., et al., Assembly of mitochondrial cytochrome c-oxidase, a complicated and highly regulated cellular process. Am J Physiol Cell Physiol, 2006. 291(6): p. C1129-47.
40. Capaldi, R.A., F1-ATPase in a spin. Nat Struct Biol, 1994. 1(10): p. 660-3.

41. Watt, I.N., et al., Bioenergetic cost of making an adenosine triphosphate molecule in animal mitochondria. Proc Natl Acad Sci U S A, 2010. 107(39): p. 16823-7.
42. Walker, J.E. and V.K. Dickson, The peripheral stalk of the mitochondrial ATP synthase. Biochim Biophys Acta, 2006. 1757(5-6): p. 286-96.
43. Anderson, S., et al., Sequence and organization of the human mitochondrial genome. Nature, 1981. 290(5806): p. 457-65.
44. Jonckheere, A.I., J.A. Smeitink, and R.J. Rodenburg, Mitochondrial ATP synthase: architecture, function and pathology. J Inherit Metab Dis, 2012. 35(2): p. 211-25.
45. Campanella, M., et al., IF(1): setting the pace of the F(1)F(o)-ATP synthase. Trends Biochem Sci, 2009. 34(7): p. 343-50.
46. Cox, G.B., et al., Hypothesis. The mechanism of ATP synthase. Conformational change by rotation of the beta-subunit. Biochim Biophys Acta, 1984. 768(3-4): p. 201-8.
47. Wittig, I. and H. Schagger, Structural organization of mitochondrial ATP synthase. Biochim Biophys Acta, 2008. 1777(7-8): p. 592-8.
48. Devenish, R.J., M. Prescott, and A.J. Rodgers, The structure and function of mitochondrial F1F0-ATP synthases. Int Rev Cell Mol Biol, 2008. 267: p. 1-58.
49. Lenaz, G. and M.L. Genova, Kinetics of integrated electron transfer in the mitochondrial respiratory chain: random collisions vs. solid state electron channeling. Am J Physiol Cell Physiol, 2007. 292(4): p. C1221-39.
50. Schagger, H. and K. Pfeiffer, Supercomplexes in the respiratory chains of yeast and mammalian mitochondria. EMBO J, 2000. 19(8): p. 1777-83.
51. Hackenbrock, C.R., B. Chazotte, and S.S. Gupte, The random collision model and a critical assessment of diffusion and collision in mitochondrial electron transport. J Bioenerg Biomembr, 1986. 18(5): p. 331-68.
52. Fowler, L.R. and S.H. Richardson, Studies on the electron transfer system. L. On the mechanism of reconstitution of the mitochondrial electron transfer system. J Biol Chem, 1963. 238: p. 456-63.
53. Ragan, C.I. and C. Heron, The interaction between mitochondrial NADH-ubiquinone oxidoreductase and ubiquinol-

cytochrome c oxidoreductase. Evidence for stoicheiometric association. Biochem J, 1978. 174(3): p. 783-90.
54. Hatefi, Y. and D.L. Stiggall, Preparation and properties of NADH: cytochrome c oxidoreductase (complex I--III). Methods Enzymol, 1978. 53: p. 5-10.
55. Eubel, H., J. Heinemeyer, and H.P. Braun, Identification and characterization of respirasomes in potato mitochondria. Plant Physiol, 2004. 134(4): p. 1450-9.
56. Acin-Perez, R., et al., Respiratory active mitochondrial supercomplexes. Mol Cell, 2008. 32(4): p. 529-39.
57. Dudkina, N.V., et al., Structure of a mitochondrial supercomplex formed by respiratory-chain complexes I and III. Proc Natl Acad Sci U S A, 2005. 102(9): p. 3225-9.
58. Lapuente-Brun, E., et al., Supercomplex assembly determines electron flux in the mitochondrial electron transport chain. Science, 2013. 340(6140): p. 1567-70.
59. Acin-Perez, R. and J.A. Enriquez, The function of the respiratory supercomplexes: the plasticity model. Biochim Biophys Acta, 2014. 1837(4): p. 444-50.
60. Wallace, D.C. and W. Fan, Energetics, epigenetics, mitochondrial genetics. Mitochondrion, 2010. 10(1): p. 12-31.
61. Chinnery, P.F., et al., The epidemiology of pathogenic mitochondrial DNA mutations. Ann Neurol, 2000. 48(2): p. 188-93.
62. Elliott, H.R., et al., Pathogenic mitochondrial DNA mutations are common in the general population. Am J Hum Genet, 2008. 83(2): p. 254-60.
63. Schon, E.A., et al., A direct repeat is a hotspot for large-scale deletion of human mitochondrial DNA. Science, 1989. 244(4902): p. 346-9.
64. Mariotti, C., et al., Defective respiratory capacity and mitochondrial protein synthesis in transformant cybrids harboring the tRNA(Leu(UUR)) mutation associated with maternally inherited myopathy and cardiomyopathy. J Clin Invest, 1994. 93(3): p. 1102-7.
65. Sproule, D.M. and P. Kaufmann, Mitochondrial encephalopathy, lactic acidosis, and strokelike episodes: basic concepts, clinical phenotype, and therapeutic management of MELAS syndrome. Ann N Y Acad Sci, 2008. 1142: p. 133-58.
66. Wong, L.J., Pathogenic mitochondrial DNA mutations in protein-coding genes. Muscle Nerve, 2007. 36(3): p. 279-93.

67. Fukuhara, N., et al., Myoclonus epilepsy associated with ragged-red fibres (mitochondrial abnormalities): disease entity or a syndrome? Light-and electron-microscopic studies of two cases and review of literature. J Neurol Sci, 1980. 47(1): p. 117-33.
68. Hammans, S.R., et al., Mitochondrial encephalopathies: molecular genetic diagnosis from blood samples. Lancet, 1991. 337(8753): p. 1311-3.
69. Holt, I.J., et al., A new mitochondrial disease associated with mitochondrial DNA heteroplasmy. Am J Hum Genet, 1990. 46(3): p. 428-33.
70. Newman, N.J., Hereditary optic neuropathies: from the mitochondria to the optic nerve. Am J Ophthalmol, 2005. 140(3): p. 517-23.
71. Yu-Wai-Man, P., P.G. Griffiths, and P.F. Chinnery, Mitochondrial optic neuropathies - disease mechanisms and therapeutic strategies. Prog Retin Eye Res, 2011. 30(2): p. 81-114.
72. Yu-Wai-Man, P., et al., Inherited mitochondrial optic neuropathies. J Med Genet, 2009. 46(3): p. 145-58.
73. Valentino, M.L., et al., The ND1 gene of complex I is a mutational hot spot for Leber's hereditary optic neuropathy. Ann Neurol, 2004. 56(5): p. 631-41.
74. Chinnery, P.F., et al., The mitochondrial ND6 gene is a hot spot for mutations that cause Leber's hereditary optic neuropathy. Brain, 2001. 124(Pt 1): p. 209-18.
75. DiMauro, S. and E.A. Schon, Mitochondrial respiratory-chain diseases. N Engl J Med, 2003. 348(26): p. 2656-68.
76. Morris, A.A., et al., Deficiency of respiratory chain complex I is a common cause of Leigh disease. Ann Neurol, 1996. 40(1): p. 25-30.
77. Leigh, D., Subacute necrotizing encephalomyelopathy in an infant. J Neurol Neurosurg Psychiatry, 1951. 14(3): p. 216-21.
78. Loeffen, J., et al., The first nuclear-encoded complex I mutation in a patient with Leigh syndrome. Am J Hum Genet, 1998. 63(6): p. 1598-608.
79. Ugalde, C., et al., Mitochondrial disorders due to nuclear OXPHOS gene defects. Adv Exp Med Biol, 2009. 652: p. 85-116.

80. Vladutiu, G.D. and R.R. Heffner, Succinate dehydrogenase deficiency. Arch Pathol Lab Med, 2000. 124(12): p. 1755-8.
81. Parfait, B., et al., Compound heterozygous mutations in the flavoprotein gene of the respiratory chain complex II in a patient with Leigh syndrome. Hum Genet, 2000. 106(2): p. 236-43.
82. Ghezzi, D., et al., SDHAF1, encoding a LYR complex-II specific assembly factor, is mutated in SDH-defective infantile leukoencephalopathy. Nat Genet, 2009. 41(6): p. 654-6.
83. Scaglia, F., et al., Clinical spectrum, morbidity, and mortality in 113 pediatric patients with mitochondrial disease. Pediatrics, 2004. 114(4): p. 925-31.
84. Bourgeron, T., et al., Mutation of a nuclear succinate dehydrogenase gene results in mitochondrial respiratory chain deficiency. Nat Genet, 1995. 11(2): p. 144-9.
85. Horváth, R., et al., Leigh syndrome caused by mutations in the flavoprotein (Fp) subunit of succinate dehydrogenase (SDHA). J Neurol Neurosurg Psychiatry, 2006. 77(1): p. 74-6.
86. Parfait, B., et al., Compound heterozygous mutations in the flavoprotein gene of the respiratory chain complex II in a patient with Leigh syndrome. Hum Genet, 2000. 106(2): p. 236-43.
87. Astuti, D., et al., Investigation of the role of SDHB inactivation in sporadic phaeochromocytoma and neuroblastoma. Br J Cancer, 2004. 91(10): p. 1835-41.
88. Borisov, V.B., Defects in mitochondrial respiratory complexes III and IV, and human pathologies. Mol Aspects Med, 2002. 23(5): p. 385-412.
89. Ghezzi, D., et al., Mutations in TTC19 cause mitochondrial complex III deficiency and neurological impairment in humans and flies. Nat Genet, 2011. 43(3): p. 259-63.
90. Andreu, A.L., et al., Exercise intolerance due to mutations in the cytochrome b gene of mitochondrial DNA. N Engl J Med, 1999. 341(14): p. 1037-44.
91. Haut, S., et al., A deletion in the human QP-C gene causes a complex III deficiency resulting in hypoglycaemia and lactic acidosis. Hum Genet, 2003. 113(2): p. 118-22.
92. Barel, O., et al., Mitochondrial complex III deficiency associated with a homozygous mutation in UQCRQ. Am J Hum Genet, 2008. 82(5): p. 1211-6.

93. Miyake, N., et al., Mitochondrial complex III deficiency caused by a homozygous UQCRC2 mutation presenting with neonatal-onset recurrent metabolic decompensation. Hum Mutat, 2013. 34(3): p. 446-52.
94. Gaignard, P., et al., Mutations in CYC1, encoding cytochrome c1 subunit of respiratory chain complex III, cause insulin-responsive hyperglycemia. Am J Hum Genet, 2013. 93(2): p. 384-9.
95. Massa, V., et al., Severe infantile encephalomyopathy caused by a mutation in COX6B1, a nucleus-encoded subunit of cytochrome c oxidase. Am J Hum Genet, 2008. 82(6): p. 1281-9.
96. Abdulhag, U.N., et al., Mitochondrial complex IV deficiency, caused by mutated COX6B1, is associated with encephalomyopathy, hydrocephalus and cardiomyopathy. Eur J Hum Genet, 2015. 23(2): p. 159-64.
97. Jonckheere, A.I., et al., A complex V ATP5A1 defect causes fatal neonatal mitochondrial encephalopathy. Brain, 2013. 136(Pt 5): p. 1544-54.
98. Mayr, J.A., et al., Mitochondrial ATP synthase deficiency due to a mutation in the ATP5E gene for the F1 epsilon subunit. Hum Mol Genet, 2010. 19(17): p. 3430-9.
99. Lazarou, M., et al., Assembly of mitochondrial complex I and defects in disease. Biochim Biophys Acta, 2009. 1793(1): p. 78-88.
100. McKenzie, M. and M.T. Ryan, Assembly factors of human mitochondrial complex I and their defects in disease. IUBMB Life, 2010. 62(7): p. 497-502.
101. Gerards, M., et al., Defective complex I assembly due to C20orf7 mutations as a new cause of Leigh syndrome. J Med Genet, 2010. 47(8): p. 507-12.
102. Sugiana, C., et al., Mutation of C20orf7 disrupts complex I assembly and causes lethal neonatal mitochondrial disease. Am J Hum Genet, 2008. 83(4): p. 468-78.
103. Dunning, C.J., et al., Human CIA30 is involved in the early assembly of mitochondrial complex I and mutations in its gene cause disease. EMBO J, 2007. 26(13): p. 3227-37.
104. Vogel, R.O., et al., Identification of mitochondrial complex I assembly intermediates by tracing tagged NDUFS3 demonstrates the entry point of mitochondrial subunits. J Biol Chem, 2007. 282(10): p. 7582-90.

105. Ogilvie, I., N.G. Kennaway, and E.A. Shoubridge, A molecular chaperone for mitochondrial complex I assembly is mutated in a progressive encephalopathy. J Clin Invest, 2005. 115(10): p. 2784-92.
106. Saada, A., et al., C6ORF66 is an assembly factor of mitochondrial complex I. Am J Hum Genet, 2008. 82(1): p. 32-8.
107. Haack, T.B., et al., Exome sequencing identifies ACAD9 mutations as a cause of complex I deficiency. Nat Genet, 2010. 42(12): p. 1131-4.
108. Fassone, E., et al., FOXRED1, encoding an FAD-dependent oxidoreductase complex-I-specific molecular chaperone, is mutated in infantile-onset mitochondrial encephalopathy. Hum Mol Genet, 2010. 19(24): p. 4837-47.
109. Ohlenbusch, A., et al., Leukoencephalopathy with accumulated succinate is indicative of SDHAF1 related complex II deficiency. Orphanet J Rare Dis, 2012. 7: p. 69.
110. Hao, H.X., et al., SDH5, a gene required for flavination of succinate dehydrogenase, is mutated in paraganglioma. Science, 2009. 325(5944): p. 1139-42.
111. de Lonlay, P., et al., A mutant mitochondrial respiratory chain assembly protein causes complex III deficiency in patients with tubulopathy, encephalopathy and liver failure. Nat Genet, 2001. 29(1): p. 57-60.
112. Cruciat, C.M., et al., Bcs1p, an AAA-family member, is a chaperone for the assembly of the cytochrome bc(1) complex. EMBO J, 1999. 18(19): p. 5226-33.
113. Fernandez-Vizarra, E., et al., Impaired complex III assembly associated with BCS1L gene mutations in isolated mitochondrial encephalopathy. Hum Mol Genet, 2007. 16(10): p. 1241-52.
114. Nobrega, F.G., M.P. Nobrega, and A. Tzagoloff, BCS1, a novel gene required for the expression of functional Rieske iron-sulfur protein in Saccharomyces cerevisiae. EMBO J, 1992. 11(11): p. 3821-9.
115. Cui, T.Z., et al., Late-stage maturation of the Rieske Fe/S protein: Mzm1 stabilizes Rip1 but does not facilitate its translocation by the AAA ATPase Bcs1. Mol Cell Biol, 2012. 32(21): p. 4400-9.

116. Wagener, N., et al., A pathway of protein translocation in mitochondria mediated by the AAA-ATPase Bcs1. Mol Cell, 2011. 44(2): p. 191-202.
117. Fellman, V., The GRACILE syndrome, a neonatal lethal metabolic disorder with iron overload. Blood Cells Mol Dis, 2002. 29(3): p. 444-50.
118. Visapää, I., et al., GRACILE syndrome, a lethal metabolic disorder with iron overload, is caused by a point mutation in BCS1L. Am J Hum Genet, 2002. 71(4): p. 863-76.
119. de Lonlay, P., et al., A mutant mitochondrial respiratory chain assembly protein causes complex III deficiency in patients with tubulopathy, encephalopathy and liver failure. Nat Genet, 2001. 29(1): p. 57-60.
120. Hinson, J.T., et al., Missense mutations in the BCS1L gene as a cause of the Bjornstad syndrome. N Engl J Med, 2007. 356(8): p. 809-19.
121. Nogueira, C., et al., Novel TTC19 mutation in a family with severe psychiatric manifestations and complex III deficiency. Neurogenetics, 2013. 14(2): p. 153-60.
122. Atwal, P.S., Mutations in the Complex III Assembly Factor Tetratricopeptide 19 Gene TTC19 Are a Rare Cause of Leigh Syndrome. JIMD Rep, 2014. 14: p. 43-5.
123. Morino, H., et al., Exome sequencing reveals a novel TTC19 mutation in an autosomal recessive spinocerebellar ataxia patient. BMC Neurol, 2014. 14: p. 5.
124. Ardissone, A., et al., Mitochondrial Complex III Deficiency Caused by TTC19 Defects: Report of a Novel Mutation and Review of Literature. JIMD Rep, 2015. 22: p. 115-20.
125. Kunii, M., et al., A Japanese case of cerebellar ataxia, spastic paraparesis and deep sensory impairment associated with a novel homozygous TTC19 mutation. J Hum Genet, 2015. 60(4): p. 187-91.
126. Angerer, H., The superfamily of mitochondrial Complex1_LYR motif-containing (LYRM) proteins. Biochem Soc Trans, 2013. 41(5): p. 1335-41.
127. Maio, N., et al., Cochaperone binding to LYR motifs confers specificity of iron sulfur cluster delivery. Cell Metab, 2014. 19(3): p. 445-57.
128. Sanchez, E., et al., LYRM7/MZM1L is a UQCRFS1 chaperone involved in the last steps of mitochondrial Complex

III assembly in human cells. Biochim Biophys Acta, 2013. 1827(3): p. 285-93.
129. Atkinson, A., et al., The LYR protein Mzm1 functions in the insertion of the Rieske Fe/S protein in yeast mitochondria. Mol Cell Biol, 2011. 31(19): p. 3988-96.
130. Fernandez-Vizarra, E. and M. Zeviani, Nuclear gene mutations as the cause of mitochondrial complex III deficiency. Front Genet, 2015. 6: p. 134.
131. Invernizzi, F., et al., A homozygous mutation in LYRM7/MZM1L associated with early onset encephalopathy, lactic acidosis, and severe reduction of mitochondrial complex III activity. Hum Mutat, 2013. 34(12): p. 1619-22.
132. Shoubridge, E.A., Cytochrome c oxidase deficiency. Am J Med Genet, 2001. 106(1): p. 46-52.
133. Piekutowska-Abramczuk, D., et al., High prevalence of SURF1 c.845_846delCT mutation in Polish Leigh patients. Eur J Paediatr Neurol, 2009. 13(2): p. 146-53.
134. Rahman, S., et al., A SURF1 gene mutation presenting as isolated leukodystrophy. Ann Neurol, 2001. 49(6): p. 797-800.
135. Santoro, L., et al., A novel SURF1 mutation results in Leigh syndrome with peripheral neuropathy caused by cytochrome c oxidase deficiency. Neuromuscul Disord, 2000. 10(6): p. 450-3.
136. Zhu, Z., et al., SURF1, encoding a factor involved in the biogenesis of cytochrome c oxidase, is mutated in Leigh syndrome. Nat Genet, 1998. 20(4): p. 337-43.
137. Tiranti, V., et al., Loss-of-function mutations of SURF-1 are specifically associated with Leigh syndrome with cytochrome c oxidase deficiency. Ann Neurol, 1999. 46(2): p. 161-6.
138. Leary, S.C., et al., Novel mutations in SCO1 as a cause of fatal infantile encephalopathy and lactic acidosis. Hum Mutat, 2013. 34(10): p. 1366-70.
139. Stiburek, L., et al., Loss of function of Sco1 and its interaction with cytochrome c oxidase. Am J Physiol Cell Physiol, 2009. 296(5): p. C1218-26.
140. Valnot, I., et al., Mutations of the SCO1 gene in mitochondrial cytochrome c oxidase deficiency with neonatal-onset hepatic failure and encephalopathy. Am J Hum Genet, 2000. 67(5): p. 1104-9.

141. Leary, S.C., et al., A hemizygous SCO2 mutation in an early onset rapidly progressive, fatal cardiomyopathy. Mol Genet Metab, 2006. 89(1-2): p. 129-33.
142. Papadopoulou, L.C., et al., Fatal infantile cardioencephalomyopathy with COX deficiency and mutations in SCO2, a COX assembly gene. Nat Genet, 1999. 23(3): p. 333-7.
143. Salviati, L., et al., Cytochrome c oxidase deficiency due to a novel SCO2 mutation mimics Werdnig-Hoffmann disease. Arch Neurol, 2002. 59(5): p. 862-5.
144. Tarnopolsky, M.A., et al., Novel SCO2 mutation (G1521A) presenting as a spinal muscular atrophy type I phenotype. Am J Med Genet A, 2004. 125A(3): p. 310-4.
145. Coenen, M.J., et al., Cytochrome c oxidase biogenesis in a patient with a mutation in COX10 gene. Ann Neurol, 2004. 56(4): p. 560-4.
146. Valnot, I., et al., A mutation in the human heme A:farnesyltransferase gene (COX10) causes cytochrome c oxidase deficiency. Hum Mol Genet, 2000. 9(8): p. 1245-9.
147. Alfadhel, M., et al., Infantile cardioencephalopathy due to a COX15 gene defect: report and review. Am J Med Genet A, 2011. 155A(4): p. 840-4.
148. Bugiani, M., et al., Novel mutations in COX15 in a long surviving Leigh syndrome patient with cytochrome c oxidase deficiency. J Med Genet, 2005. 42(5): p. e28.
149. Glerum, D.M., et al., COX15 codes for a mitochondrial protein essential for the assembly of yeast cytochrome oxidase. J Biol Chem, 1997. 272(30): p. 19088-94.
150. Oquendo, C.E., et al., Functional and genetic studies demonstrate that mutation in the COX15 gene can cause Leigh syndrome. J Med Genet, 2004. 41(7): p. 540-4.
151. Stroud, D.A., et al., COA6 is a mitochondrial complex IV assembly factor critical for biogenesis of mtDNA-encoded COX2. Hum Mol Genet, 2015. 24(19): p. 5404-15.
152. Baertling, F., et al., Mutations in COA6 cause cytochrome c oxidase deficiency and neonatal hypertrophic cardiomyopathy. Hum Mutat, 2015. 36(1): p. 34-8.
153. Doss, S., et al., Recessive dystonia-ataxia syndrome in a Turkish family caused by a COX20 (FAM36A) mutation. J Neurol, 2014. 261(1): p. 207-12.

154. Szklarczyk, R., et al., A mutation in the FAM36A gene, the human ortholog of COX20, impairs cytochrome c oxidase assembly and is associated with ataxia and muscle hypotonia. Hum Mol Genet, 2013. 22(4): p. 656-67.
155. Huigsloot, M., et al., A mutation in C2orf64 causes impaired cytochrome c oxidase assembly and mitochondrial cardiomyopathy. Am J Hum Genet, 2011. 88(4): p. 488-93.
156. Leary, S.C., et al., Human SCO1 and SCO2 have independent, cooperative functions in copper delivery to cytochrome c oxidase. Hum Mol Genet, 2004. 13(17): p. 1839-48.
157. Valnot, I., et al., A mutation in the human heme A:farnesyltransferase gene (COX10) causes cytochrome c oxidase deficiency. Hum Mol Genet, 2000. 9(8): p. 1245-9.
158. Antonicka, H., et al., Mutations in COX15 produce a defect in the mitochondrial heme biosynthetic pathway, causing early-onset fatal hypertrophic cardiomyopathy. Am J Hum Genet, 2003. 72(1): p. 101-14.
159. Bugiani, M., et al., Novel mutations in COX15 in a long surviving Leigh syndrome patient with cytochrome c oxidase deficiency. J Med Genet, 2005. 42(5): p. e28.
160. Pacheu-Grau, D., et al., Cooperation between COA6 and SCO2 in COX2 maturation during cytochrome c oxidase assembly links two mitochondrial cardiomyopathies. Cell Metab, 2015. 21(6): p. 823-33.
161. Melchionda, L., et al., Mutations in APOPT1, encoding a mitochondrial protein, cause cavitating leukoencephalopathy with cytochrome c oxidase deficiency. Am J Hum Genet, 2014. 95(3): p. 315-25.
162. De Meirleir, L., et al., Respiratory chain complex V deficiency due to a mutation in the assembly gene ATP12. J Med Genet, 2004. 41(2): p. 120-4.
163. Cizkova, A., et al., TMEM70 mutations cause isolated ATP synthase deficiency and neonatal mitochondrial encephalocardiomyopathy. Nat Genet, 2008. 40(11): p. 1288-90.
164. Spiegel, R., et al., TMEM70 mutations are a common cause of nuclear encoded ATP synthase assembly defect: further delineation of a new syndrome. J Med Genet, 2011. 48(3): p. 177-82.

165. Van Goethem, G., et al., Mutation of POLG is associated with progressive external ophthalmoplegia characterized by mtDNA deletions. Nat Genet, 2001. 28(3): p. 211-2.
166. Spelbrink, J.N., et al., Human mitochondrial DNA deletions associated with mutations in the gene encoding Twinkle, a phage T7 gene 4-like protein localized in mitochondria. Nat Genet, 2001. 28(3): p. 223-31.
167. Kaukonen, J., et al., Role of adenine nucleotide translocator 1 in mtDNA maintenance. Science, 2000. 289(5480): p. 782-5.
168. Nishino, I., A. Spinazzola, and M. Hirano, Thymidine phosphorylase gene mutations in MNGIE, a human mitochondrial disorder. Science, 1999. 283(5402): p. 689-92.
169. Brown, N.S. and R. Bicknell, Thymidine phosphorylase, 2-deoxy-D-ribose and angiogenesis. Biochem J, 1998. 334 (Pt 1): p. 1-8.
170. Spinazzola, A., et al., Altered thymidine metabolism due to defects of thymidine phosphorylase. J Biol Chem, 2002. 277(6): p. 4128-33.
171. Martí, R., et al., Definitive diagnosis of mitochondrial neurogastrointestinal encephalomyopathy by biochemical assays. Clin Chem, 2004. 50(1): p. 120-4.
172. Ferraro, P., et al., Mitochondrial deoxynucleotide pools in quiescent fibroblasts: a possible model for mitochondrial neurogastrointestinal encephalomyopathy (MNGIE). J Biol Chem, 2005. 280(26): p. 24472-80.
173. Pontarin, G., et al., Mitochondrial DNA depletion and thymidine phosphate pool dynamics in a cellular model of mitochondrial neurogastrointestinal encephalomyopathy. J Biol Chem, 2006. 281(32): p. 22720-8.
174. Naviaux, R.K. and K.V. Nguyen, POLG mutations associated with Alpers' syndrome and mitochondrial DNA depletion. Ann Neurol, 2004. 55(5): p. 706-12.
175. Davidzon, G., et al., POLG mutations and Alpers syndrome. Ann Neurol, 2005. 57(6): p. 921-3.
176. Ferrari, G., et al., Infantile hepatocerebral syndromes associated with mutations in the mitochondrial DNA polymerase-gammaA. Brain, 2005. 128(Pt 4): p. 723-31.
177. Sofou, K., et al., Whole exome sequencing reveals mutations in NARS2 and PARS2, encoding the mitochondrial asparaginyl-tRNA synthetase and prolyl-tRNA synthetase, in

patients with Alpers syndrome. Mol Genet Genomic Med, 2015. 3(1): p. 59-68.
178. Nogueira, C., et al., Infantile-onset disorders of mitochondrial replication and protein synthesis. J Child Neurol, 2011. 26(7): p. 866-75.
179. Spinazzola, A. and M. Zeviani, Disorders of nuclear-mitochondrial intergenomic communication. Biosci Rep, 2007. 27(1-3): p. 39-51.
180. Bourdon, A., et al., Mutation of RRM2B, encoding p53-controlled ribonucleotide reductase (p53R2), causes severe mitochondrial DNA depletion. Nat Genet, 2007. 39(6): p. 776-80.
181. Bornstein, B., et al., Mitochondrial DNA depletion syndrome due to mutations in the RRM2B gene. Neuromuscul Disord, 2008. 18(6): p. 453-9.
182. Saada, A., et al., Mutant mitochondrial thymidine kinase in mitochondrial DNA depletion myopathy. Nat Genet, 2001. 29(3): p. 342-4.
183. Elpeleg, O., et al., Deficiency of the ADP-forming succinyl-CoA synthase activity is associated with encephalomyopathy and mitochondrial DNA depletion. Am J Hum Genet, 2005. 76(6): p. 1081-6.
184. Ostergaard, E., et al., Deficiency of the alpha subunit of succinate-coenzyme A ligase causes fatal infantile lactic acidosis with mitochondrial DNA depletion. Am J Hum Genet, 2007. 81(2): p. 383-7.
185. Liu, Y., et al., Five novel SUCLG1 mutations in three Chinese patients with succinate-CoA ligase deficiency noticed by mild methylmalonic aciduria. Brain Dev, 2015.
186. Sarzi, E., et al., Twinkle helicase (PEO1) gene mutation causes mitochondrial DNA depletion. Ann Neurol, 2007. 62(6): p. 579-87.
187. Hakonen, A.H., et al., Recessive Twinkle mutations in early onset encephalopathy with mtDNA depletion. Brain, 2007. 130(Pt 11): p. 3032-40.
188. Johansson, K., et al., Structural basis for substrate specificities of cellular deoxyribonucleoside kinases. Nat Struct Biol, 2001. 8(7): p. 616-20.
189. Haudry, C., et al., Maternal uniparental disomy of chromosome 2 in a patient with a DGUOK mutation associated

with hepatocerebral mitochondrial DNA depletion syndrome. Mol Genet Metab, 2012. 107(4): p. 700-4.
190. Zeviani, M., The expanding spectrum of nuclear gene mutations in mitochondrial disorders. Semin Cell Dev Biol, 2001. 12(6): p. 407-16.
191. Arnoldi, A., et al., A clinical, genetic, and biochemical characterization of SPG7 mutations in a large cohort of patients with hereditary spastic paraplegia. Hum Mutat, 2008. 29(4): p. 522-31.
192. Maguire, A., et al., X-linked cerebellar ataxia and sideroblastic anaemia associated with a missense mutation in the ABC7 gene predicting V411L. Br J Haematol, 2001. 115(4): p. 910-7.
193. Schmucker, S., et al., Mammalian frataxin: an essential function for cellular viability through an interaction with a preformed ISCU/NFS1/ISD11 iron-sulfur assembly complex. PLoS One, 2011. 6(1): p. e16199.
194. Campuzano, V., et al., Friedreich's ataxia: autosomal recessive disease caused by an intronic GAA triplet repeat expansion. Science, 1996. 271(5254): p. 1423-7.
195. Roesch, K., et al., Human deafness dystonia syndrome is caused by a defect in assembly of the DDP1/TIMM8a-TIMM13 complex. Hum Mol Genet, 2002. 11(5): p. 477-86.
196. Barth, P.G., et al., An X-linked mitochondrial disease affecting cardiac muscle, skeletal muscle and neutrophil leucocytes. J Neurol Sci, 1983. 62(1-3): p. 327-55.
197. Takeda, A., et al., Eponym: Barth syndrome. Eur J Pediatr, 2011. 170(11): p. 1365-7.
198. Valianpour, F., et al., Cardiolipin deficiency in X-linked cardioskeletal myopathy and neutropenia (Barth syndrome, MIM 302060): a study in cultured skin fibroblasts. J Pediatr, 2002. 141(5): p. 729-33.
199. Schlame, M., et al., Deficiency of tetralinoleoyl-cardiolipin in Barth syndrome. Ann Neurol, 2002. 51(5): p. 634-7.
200. Joshi, A.S., et al., Cellular functions of cardiolipin in yeast. Biochim Biophys Acta, 2009. 1793(1): p. 212-8.
201. Garratt, V., et al., What is Barth syndrome? Midwives, 2011. 14(4): p. 32-3.
202. Spinazzola, A., et al., MPV17 encodes an inner mitochondrial membrane protein and is mutated in infantile

hepatic mitochondrial DNA depletion. Nat Genet, 2006. 38(5): p. 570-5.
203. Spinazzola, A., et al., MPV17 encodes an inner mitochondrial membrane protein and is mutated in infantile hepatic mitochondrial DNA depletion. Nat Genet, 2006. 38(5): p. 570-5.
204. Wong, L.J., et al., Mutations in the MPV17 gene are responsible for rapidly progressive liver failure in infancy. Hepatology, 2007. 46(4): p. 1218-27.
205. Parini, R., et al., Glucose metabolism and diet-based prevention of liver dysfunction in MPV17 mutant patients. J Hepatol, 2009. 50(1): p. 215-21.
206. Mudd, S.H., et al., Two patients with hepatic mtDNA depletion syndromes and marked elevations of S-adenosylmethionine and methionine. Mol Genet Metab, 2012. 105(2): p. 228-36.
207. Garone, C., et al., MPV17 Mutations Causing Adult-Onset Multisystemic Disorder With Multiple Mitochondrial DNA Deletions. Arch Neurol, 2012. 69(12): p. 1648-51.
208. Blakely, E.L., et al., MPV17 mutation causes neuropathy and leukoencephalopathy with multiple mtDNA deletions in muscle. Neuromuscul Disord, 2012. 22(7): p. 587-91.
209. Mendelsohn, B.A., et al., Adult-Onset Fatal Neurohepatopathy in a Woman Caused by MPV17 Mutation. JIMD Rep, 2014. 13: p. 37-41.
210. Karadimas, C.L., et al., Navajo neurohepatopathy is caused by a mutation in the MPV17 gene. Am J Hum Genet, 2006. 79(3): p. 544-8.
211. Spinazzola, A., et al., Lack of founder effect for an identical mtDNA depletion syndrome (MDS)-associated MPV17 mutation shared by Navajos and Italians. Neuromuscul Disord, 2008. 18(4): p. 315-8.
212. Holve, S., et al., Liver disease in Navajo neuropathy. J Pediatr, 1999. 135(4): p. 482-93.
213. Cheema, T.A. and S. Swanson, Hand involvement in Navajo neurohepatopathy: a case report. Hand (N Y), 2011. 6(2): p. 217-9.
214. Karadimas, C.L., et al., Navajo neurohepatopathy is caused by a mutation in the MPV17 gene. Am J Hum Genet, 2006. 79(3): p. 544-8.

215. Vu, T.H., et al., Navajo neurohepatopathy: a mitochondrial DNA depletion syndrome? Hepatology, 2001. 34(1): p. 116-20.
216. Johnsen, S.D., P.C. Johnson, and S.R. Stein, Familial sensory autonomic neuropathy with arthropathy in Navajo children. Neurology, 1993. 43(6): p. 1120-5.
217. Zwacka, R.M., et al., The glomerulosclerosis gene Mpv17 encodes a peroxisomal protein producing reactive oxygen species. EMBO J, 1994. 13(21): p. 5129-34.
218. Dallabona, C., et al., Sym1, the yeast ortholog of the MPV17 human disease protein, is a stress-induced bioenergetic and morphogenetic mitochondrial modulator. Hum Mol Genet, 2010. 19(6): p. 1098-107.
219. Reinhold, R., et al., The channel-forming Sym1 protein is transported by the TIM23 complex in a presequence-independent manner. Mol Cell Biol, 2012. 32(24): p. 5009-21.
220. Antonenkov, V.D., et al., The Human Mitochondrial DNA Depletion Syndrome Gene MPV17 Encodes a Non-selective Channel That Modulates Membrane Potential. J Biol Chem, 2015. 290(22): p. 13840-61.
221. Rokka, A., et al., Pxmp2 is a channel-forming protein in Mammalian peroxisomal membrane. PLoS One, 2009. 4(4): p. e5090.
222. Antonenkov, V.D. and J.K. Hiltunen, Transfer of metabolites across the peroxisomal membrane. Biochim Biophys Acta, 2012. 1822(9): p. 1374-86.
223. Casalena, G., et al., Mpv17 in mitochondria protects podocytes against mitochondrial dysfunction and apoptosis in vivo and in vitro. Am J Physiol Renal Physiol, 2014. 306(11): p. F1372-80.
224. Dalla Rosa, I., et al., MPV17L2 is required for ribosome assembly in mitochondria. Nucleic Acids Res, 2014. 42(13): p. 8500-15.
225. Krick, S., et al., Mpv17l protects against mitochondrial oxidative stress and apoptosis by activation of Omi/HtrA2 protease. Proc Natl Acad Sci U S A, 2008. 105(37): p. 14106-11.
226. Iida, R., et al., M-LP, Mpv17-like protein, has a peroxisomal membrane targeting signal comprising a transmembrane domain and a positively charged loop and up-regulates expression of the manganese superoxide dismutase gene. J Biol Chem, 2003. 278(8): p. 6301-6.

227. Iida, R., et al., A novel alternative spliced Mpv17-like protein isoform localizes in cytosol and is expressed in a kidney- and adult-specific manner. Exp Cell Res, 2005. 302(1): p. 22-30.
228. Iida, R., et al., Human Mpv17-like protein is localized in peroxisomes and regulates expression of antioxidant enzymes. Biochem Biophys Res Commun, 2006. 344(3): p. 948-54.
229. Jones, J.M., et al., Loss of Omi mitochondrial protease activity causes the neuromuscular disorder of mnd2 mutant mice. Nature, 2003. 425(6959): p. 721-7.
230. Martins, L.M., et al., Neuroprotective role of the Reaper-related serine protease HtrA2/Omi revealed by targeted deletion in mice. Mol Cell Biol, 2004. 24(22): p. 9848-62.
231. Iida, R., M. Ueki, and T. Yasuda, Identification of interacting partners of Human Mpv17-like protein with a mitigating effect of mitochondrial dysfunction through mtDNA damage. Free Radic Biol Med, 2015. 87: p. 336-345.
232. Uusimaa, J., et al., Clinical, biochemical, cellular and molecular characterization of mitochondrial DNA depletion syndrome due to novel mutations in the MPV17 gene. Eur J Hum Genet, 2014. 22(2): p. 184-91.
233. Weiher, H., et al., Transgenic mouse model of kidney disease: insertional inactivation of ubiquitously expressed gene leads to nephrotic syndrome. Cell, 1990. 62(3): p. 425-34.
234. Schenkel, J., et al., Functional rescue of the glomerulosclerosis phenotype in Mpv17 mice by transgenesis with the human Mpv17 homologue. Kidney Int, 1995. 48(1): p. 80-4.
235. Binder, C.J., et al., Glomerular overproduction of oxygen radicals in Mpv17 gene-inactivated mice causes podocyte foot process flattening and proteinuria: A model of steroid-resistant nephrosis sensitive to radical scavenger therapy. Am J Pathol, 1999. 154(4): p. 1067-75.
236. Meyer zum Gottesberge, A.M., A. Reuter, and H. Weiher, Inner ear defect similar to Alport's syndrome in the glomerulosclerosis mouse model Mpv17. Eur Arch Otorhinolaryngol, 1996. 253(8): p. 470-4.
237. Muller, M., et al., Loss of auditory function in transgenic Mpv17-deficient mice. Hear Res, 1997. 114(1-2): p. 259-63.

238. Clozel, M., et al., Age-dependent hypertension in Mpv17-deficient mice, a transgenic model of glomerulosclerosis and inner ear disease. Exp Gerontol, 1999. 34(8): p. 1007-15.
239. O'Bryan, T., et al., Course of renal injury in the Mpv17-deficient transgenic mouse. J Am Soc Nephrol, 2000. 11(6): p. 1067-74.
240. Viscomi, C., et al., Early-onset liver mtDNA depletion and late-onset proteinuric nephropathy in Mpv17 knockout mice. Hum Mol Genet, 2009. 18(1): p. 12-26.
241. Bottani, E., et al., AAV-mediated liver-specific MPV17 expression restores mtDNA levels and prevents diet-induced liver failure. Mol Ther, 2014. 22(1): p. 10-7.
242. Viscomi, C., et al., Early-onset liver mtDNA depletion and late-onset proteinuric nephropathy in Mpv17 knockout mice. Hum Mol Genet, 2009. 18(1): p. 12-26.
243. Papeta, N., et al., Prkdc participates in mitochondrial genome maintenance and prevents Adriamycin-induced nephropathy in mice. J Clin Invest, 2010. 120(11): p. 4055-64.
244. Dip, R. and H. Naegeli, More than just strand breaks: the recognition of structural DNA discontinuities by DNA-dependent protein kinase catalytic subunit. FASEB J, 2005. 19(7): p. 704-15.
245. Trott, A. and K.A. Morano, SYM1 is the stress-induced Saccharomyces cerevisiae ortholog of the mammalian kidney disease gene Mpv17 and is required for ethanol metabolism and tolerance during heat shock. Eukaryot Cell, 2004. 3(3): p. 620-31.
246. Krauss, J., et al., transparent, a gene affecting stripe formation in Zebrafish, encodes the mitochondrial protein Mpv17 that is required for iridophore survival. Biol Open, 2013. 2(7): p. 703-10.
247. Copeland, W.C., Defects in mitochondrial DNA replication and human disease. Crit Rev Biochem Mol Biol, 2012. 47(1): p. 64-74.
248. Torres-Torronteras, J., et al., Gene therapy using a liver-targeted AAV vector restores nucleoside and nucleotide homeostasis in a murine model of MNGIE. Mol Ther, 2014. 22(5): p. 901-7.
249. Casto, B.C., R.W. Atchison, and W.M. Hammon, Studies on the relationship between adeno-associated virus type I (AAV-1) and adenoviruses. I. Replication of AAV-1 in certain

cell cultures and its effect on helper adenovirus. Virology, 1967. 32(1): p. 52-9.
250. Buller, R.M., et al., Herpes simplex virus types 1 and 2 completely help adenovirus-associated virus replication. J Virol, 1981. 40(1): p. 241-7.
251. Atchison, R.W., B.C. Casto, and W.M. Hammon, Adenovirus-Associated Defective Virus Particles. Science, 1965. 149(3685): p. 754-6.
252. Lisowski, L., et al., Selection and evaluation of clinically relevant AAV variants in a xenograft liver model. Nature, 2014. 506(7488): p. 382-6.
253. Xie, Q., et al., The atomic structure of adeno-associated virus (AAV-2), a vector for human gene therapy. Proc Natl Acad Sci U S A, 2002. 99(16): p. 10405-10.
254. Berns, K.I. and S. Adler, Separation of two types of adeno-associated virus particles containing complementary polynucleotide chains. J Virol, 1972. 9(2): p. 394-6.
255. Koczot, F.J., et al., Self-complementarity of terminal sequences within plus or minus strands of adenovirus-associated virus DNA. Proc Natl Acad Sci U S A, 1973. 70(1): p. 215-9.
256. Green, M.R. and R.G. Roeder, Transcripts of the adeno-associated virus genome: mapping of the major RNAs. J Virol, 1980. 36(1): p. 79-92.
257. Green, M.R. and R.G. Roeder, Definition of a novel promoter for the major adenovirus-associated virus mRNA. Cell, 1980. 22(1 Pt 1): p. 231-42.
258. Mendelson, E., J.P. Trempe, and B.J. Carter, Identification of the trans-acting Rep proteins of adeno-associated virus by antibodies to a synthetic oligopeptide. J Virol, 1986. 60(3): p. 823-32.
259. Becerra, S.P., et al., Synthesis of adeno-associated virus structural proteins requires both alternative mRNA splicing and alternative initiations from a single transcript. J Virol, 1988. 62(8): p. 2745-54.
260. Becerra, S.P., et al., Direct mapping of adeno-associated virus capsid proteins B and C: a possible ACG initiation codon. Proc Natl Acad Sci U S A, 1985. 82(23): p. 7919-23.
261. Berns, K.I., Parvovirus replication. Microbiol Rev, 1990. 54(3): p. 316-29.

262. Ni, T.H., et al., Cellular proteins required for adeno-associated virus DNA replication in the absence of adenovirus coinfection. J Virol, 1998. 72(4): p. 2777-87.
263. Buning, H., et al., Engineering the AAV capsid to optimize vector-host-interactions. Curr Opin Pharmacol, 2015. 24: p. 94-104.
264. Asokan, A., D.V. Schaffer, and R.J. Samulski, The AAV vector toolkit: poised at the clinical crossroads. Mol Ther, 2012. 20(4): p. 699-708.
265. Wright, J.F., Transient transfection methods for clinical adeno-associated viral vector production. Hum Gene Ther, 2009. 20(7): p. 698-706.
266. Nakai, H., T.A. Storm, and M.A. Kay, Recruitment of single-stranded recombinant adeno-associated virus vector genomes and intermolecular recombination are responsible for stable transduction of liver in vivo. J Virol, 2000. 74(20): p. 9451-63.
267. Ferrari, F.K., et al., Second-strand synthesis is a rate-limiting step for efficient transduction by recombinant adeno-associated virus vectors. J Virol, 1996. 70(5): p. 3227-34.
268. Goncalves, M.A., Adeno-associated virus: from defective virus to effective vector. Virol J, 2005. 2: p. 43.
269. McCarty, D.M., P.E. Monahan, and R.J. Samulski, Self-complementary recombinant adeno-associated virus (scAAV) vectors promote efficient transduction independently of DNA synthesis. Gene Ther, 2001. 8(16): p. 1248-54.
270. Cunningham, S.C., et al., Gene delivery to the juvenile mouse liver using AAV2/8 vectors. Mol Ther, 2008. 16(6): p. 1081-8.

Chapter 2

Ttc19 is an assembly factor of respiratory complex III leading to slowly progressive neurodegeneration

Emanuela Bottani[1], Carla Giordano[2], Raffaele Cerutti[1], Ian Fearnly[1], Giulia d'Amati[2], Carlo Viscomi[1], Erika Fernandez-Vizarra[1,2], Massimo Zeviani[1,2]

[1]MRC Mitochondrial Biology Unit, Wellcome Trust/MRC Building Hills Road, Cambridge, CB2 0XY, UK

[2] Department of Radiological, Oncological and Pathological Sciences, Sapienza University of Rome, 00161 Rome, Italy

In preparation

Abstract

Tetratricopeptide 19 (TTC19) is a putative new assembly factor for respiratory complex III (ubiquinol:cytochrome c oxidoreductase, cIII). Mutations in *TTC19* have been associated with different neurological phenotypes, ranging from early-onset, slowly progressive neurodegeneration to late-onset, rapidly progressive neurological failure, as well as cerebellar hypoplasia, bilateral basal ganglia lesions, and spinocerebellar ataxia. Here we used a multidisciplinary strategy to investigate the pathogenetic mechanism of TTC19-related diseases and to dissect the role of TTC19 in cIII assembly. First, we developed and characterized a *Ttc19*$^{-/-}$ mouse showing a mainly neurological phenotype, similar to what is observed in the patients. Astrogliosis and accumulation of ubiquitinated proteins were consistently observed in the thalamus of *Ttc19*$^{-/-}$ brains, although we did not find obvious signs of neurodegeneration. Increased production of reactive oxygen species (ROS) was found in several tissues of *Ttc19*$^{-/-}$ animals, and may contribute to the neurological phenotype. Complex III was analyzed by 2D-Blue Native Gel Electrophoresis (BNGE) on mitochondria isolated from different tissues and showed an altered migration pattern in those from *Ttc19*$^{-/-}$ animals. In addition, the levels of UQCRFS1 (also known as Rieske protein or RISP) incorporated in the fully assembled cIII were reduced. These findings suggest a role for TTC19 in the insertion of UQCRFS1 in cIII. A SILAC-based proteomic approach sowed that TTC19 is associated to cIII before the incorporation of UQCRFS1 and

either facilitates or stabilizes its incorporation into nascent cIII. Our work sheds new light on the molecular function of TTC19 and suggests a possible mechanism by which the disease arises, indicating new avenues for the therapy.

1. Introduction

Complex III (cIII), or ubiquinol:cytochrome c oxidoreductase is a mitochondrial respiratory chain enzyme formed by 11 different subunits, presenting a dimeric structure of approximately 480 kDa [1]. It catalyzes the transfer of electrons from Coenzyme Q to cytochrome c, while pumping protons from the matrix to the intermembrane space. Cytochrome b (MT-CYB), the only cIII subunit encoded by mtDNA, is one of the three catalytic subunits of cIII, containing a low potential (b_L) and a high potential (b_H) heme b moieties as prosthetic groups. Among the other ten subunits, all encoded by nine nuclear genes, two play a catalytic role: the Fe_2S_2 cluster-containing Rieske protein (encoded by *UQCRFS1*), and cytochrome c1 (encoded by *CYC1*), which contains a c-type heme group. The role of the other eight 'supernumerary' subunits still remains unclear.

Although cIII assembly has been less intensively investigated compared to other respiratory complexes, in the last few years the study of yeast mutant models has provided some insight into this process [1-5]. The study of cIII-associated human diseases has confirmed that some of cIII assembly steps are similar to yeast, especially the late ones. Accordingly, cIII

assembly starts with MT-CYB still bound to chaperones UQCC1 and UQCC2, being these released through the progressive incorporation of additional subunits into an inactive dimeric pre-cIII, which is eventually activated by the incorporation of UQCRFS1. This is mediated by BCS1L, the most extensively characterized cIII assembly factor [6]. Pathogenetic mutations have been found in some of the assembly factors including BCS1L [7], TTC19 [8], LYRM7 [9], UQCC2 [10] and UQCC3 [11]. In particular, mutations in *TTC19* have been found in patients with heterogeneous phenotypes, including early-onset, slowly progressive encephalomyopathy, adult-onset, rapidly progressive neurological failure or spincerebellar ataxia, and childhood or juvenile spinocerebellar ataxia with psychosis (OMIM: 613814). *TTC19* encodes the tetratricopeptide repeat domain 19 protein, consisting of 380 amino acids with no known orthologues in yeast and plants. Unlike other assembly factors, TTC19 has been found to bind mature dimeric cIII ($cIII_2$), whereas its absence leads to accumulation of cIII-subassembly species in mutant fibroblasts [8]. The mechanistic role of TTC19 in cIII assembly or stability is still unclear.

In an attempt to clarify TTC19 function in relation with cIII biogenesis and the pathogenetic mechanisms underlying its defects, we have used cell and mouse models. First, we have phenotypically characterized a constitutive *Ttc19* knockout mouse (*Ttc19*$^{-/-}$). Second, we have investigated the interaction

of TTC19 with $cIII_2$ using mass spectrometry applied on recombinant cellular models.

2. Results

I Neurological and metabolic characterization of Ttc19$^{-/-}$ mice

We first generated a constitutive *Ttc19*$^{-/-}$ mouse by gene targeting (Supplementary Figure 1).

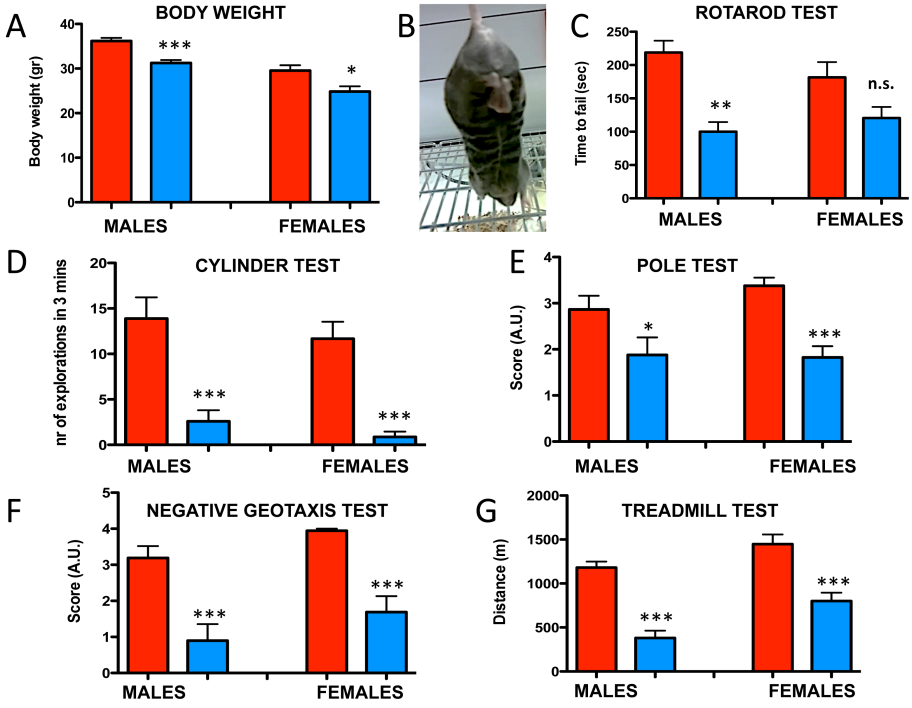

Figure 1: clinical characterization of 6 month-old T*tc19*$^{-/-}$ mice. (A) Body weights of *Ttc19*$^{-/-}$ vs. *Ttc19*^{wt} littermates, n= 8-11 per group, (B) feet clasping reflex, (C) rotarod test, n = 6 – 8 animals/group, average of 3 trials/mouse. (D) cylinder test, n = 6 – 9 animals/group, average of 2 trials/mouse, (E) pole test, n = 6 – 9 animals/group, average of 5 trials/mouse, (F) negative geotaxis test, n = 6 – 9 animals/group, average of 2 trials/mouse, (G) treadmill test, n = 6-11 animals/group. Error bars represent SEM * $p < 0.05$, ** $p < 0.01$ ***$p < 0.005$. Red bars: *Ttc19*^{wt}; blue bars: *Ttc19*$^{-/-}$.

Both *Ttc19*$^{-/-}$ males and females showed a slight but statistically significant reduced body weight at 6 months compared to wild-type littermates (Figure 1A). No differences were observed between *Ttc19*$^{+/+}$ and *Ttc19*$^{+/-}$ animals for any of the studied parameters, and both genotypes were used as controls (*Ttc19*^{wt}). Several tests were used to assess neurological, behavioural and metabolic features. At 6 months of age, *Ttc19*$^{-/-}$ mice showed a pathological feet-clasping reflex (Figure 1B), and scored significantly less than their wild-type littermates in rotarod, cylinder, negative geotaxis and pole tests, which measure motor coordination, exploratory behaviour, general proprioception, and basal ganglia motor planning, respectively (Figure 1C-F). Motor endurance assessed by standard treadmill test was also reduced in *Ttc19*$^{-/-}$ vs. *Ttc19*^{wt} animals (Figure 1G). Some of these features were already present at 3 months of age (Supplementary Figure 2) but worsened at 6 months. No differences in lifespan were observed up to 21 months (not shown).

To study whole-body metabolism, we used a Comprehensive Lab Animals Monitoring System (CLAMS). *Ttc19*$^{-/-}$ females showed reduced food and water consumption compared to *Ttc19*^{wt} littermates (Figure 2A, B); VO_2 consumption and VCO_2 production were significantly reduced in *Ttc19*$^{-/-}$ vs. *Ttc19*^{wt} animals (Figure 2C, D); accordingly the Energy Expenditure (i.e. the heat rate normalized to body weight) was decreased (Figure 2E), although statistical significance was achieved in females but not males. RER was significantly reduced in

females but not males (Figure 2F). Total, ambulatory and rearing movements were significantly decreased in *Ttc19*$^{-/-}$ vs. *Ttc19*^{wt} littermates (Figure 2G). These data indicate an overall reduction of energy metabolism in *Ttc19*$^{-/-}$ mice.

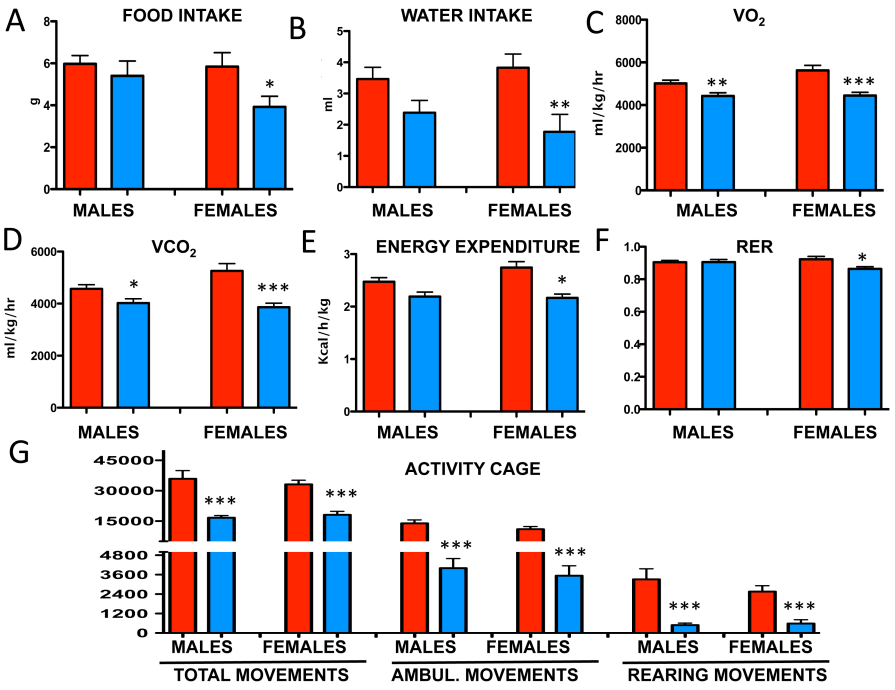

Figure 2: CLAMS analysis during the dark phase. (A) Food intake over 36 hours, (B) water intake over 36 hours (C) VO_2 consumption, average of 2 experiments (D) VCO_2 production, average of 2 experiments (E) energy expenditure/body weight, average of 2 experiments (F) RER, average of 2 experiments (G) total, ambulatory and rearing movements, average of 2 experiments; n = 8-12 animals/group. Error bars represent SEM *p < 0.05, ** p < 0.01 ***p < 0.005. Red bars: *Ttc19*^{wt}; blue bars: *Ttc19*$^{-/-}$.

II Neuropathological characterization of Ttc19$^{-/-}$ *mice*

Next, we analysed the neuropathological features of *Ttc19*$^{-/-}$ mice. Extensive astrogliosis, most often surrounding dilated vascular structures (Figure 3A,C), and accumulation of ubiquitinated proteins (Figure 3E) were detected in the thalamus of all *Ttc19*$^{-/-}$ mice analysed (n=6), suggesting an

ongoing brain injury. These features were not observed in wild-type littermates (n=4) (Figure 3B,D,F). No abnormalities were detected in skeletal muscle by H&E (not shown). Light microscopy of brain sections stained with either hematoxylin-eosin (not shown) or Nissl (Figure 3G,H) did not reveal obvious neuronal damage or loss. These findings were confirmed by immunostaining for NeuN and CD68, as well as by staining with fluorojade C, TUNEL, and anti caspase 3 antibody, which were similar to controls. Neurons from *Ttc19*$^{-/-}$ mice brain failed to show abnormal deposits of NF-H, Amyloid Aβ, and Phospho-Tau neurofilaments (not shown).

III Biochemical analysis of Ttc19$^{-/-}$ *tissues*

The activities of single respiratory complexes were analysed by spectrophotometric and histochemical assays. At three and six months of age, cIII/CS activity was significantly reduced (approx 50%, $p<0.01$) in brain, liver and skeletal muscle from *Ttc19*$^{-/-}$ vs. *Ttc19*^{wt} (Figure 4A), with no differences between males and females (not shown); the residual activity being further reduced (approx 40%) at 18 months (Supplementary Figure 3A-B). Surprisingly, also SDH/CS and cII/CS activities were slightly but significantly ($p<0.05$) decreased in brain (Figure 4A), and even more in brain and skeletal muscle from 18 month-old females (Supplementary Figure 3A-B). This result was also confirmed by SDH staining of skeletal muscle (Supplementary Figure 3C), although we do not have an obvious explanation for the reduced cII activity.

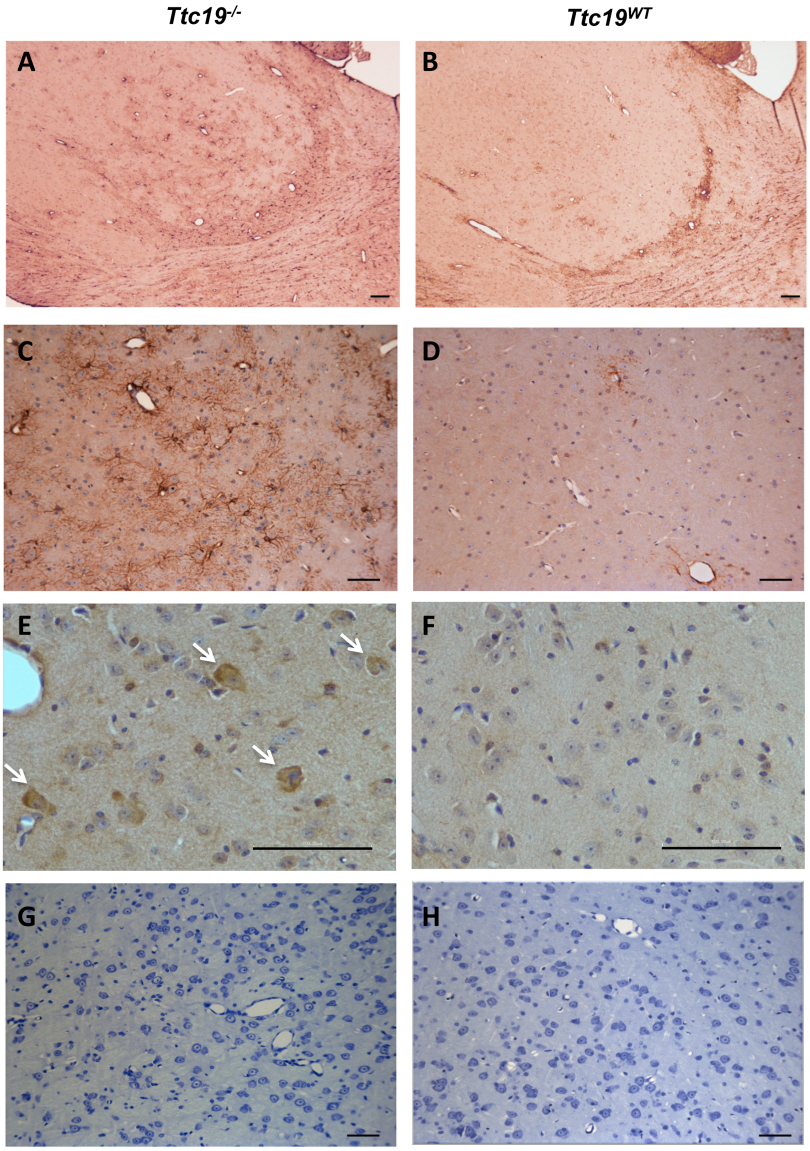

Figure 3. Histology and immunohistochemistry of brains from *Ttc19*$^{-/-}$ mice. A prominent perivascular astrocytic gliosis is evident in the thalamus of *Ttc19*$^{-/-}$ mice (A-C) as compared with their wild-type littermates (B-D), as marked by immunoperoxidase staining for glial fibrillary acidic protein (GFAP). Ubiquitin-positive neurons (arrows) were detected in *Ttc19*$^{-/-}$ but not in *Ttc19*^{wt} brains (E-F). No rarefaction of neurons was observed by Nissl stain (G, H) both in *Ttc19*$^{-/-}$ and *Ttc19*^{wt} mice. The brains were examined in whole-hemisphere sagittal sections of 6-months-old *Ttc19*$^{-/-}$ (n=6) and *Ttc19*$^{+/+}$ (n=6) mice. Scale bars = 25 μm (A-D and G-H) and 100 μm (E-F).

Since cIII is one of the main sites of ROS generation along the respiratory chain [12], we measured H_2O_2 production *in vitro* by a fluorometric assay on isolated mitochondria from liver, heart and skeletal muscle from *Ttc19*$^{-/-}$ vs. *Ttc19*^{wt} mice. We found that *Ttc19*$^{-/-}$ had significantly higher ROS levels compared to wild-type littermates (Figure 4B-D).

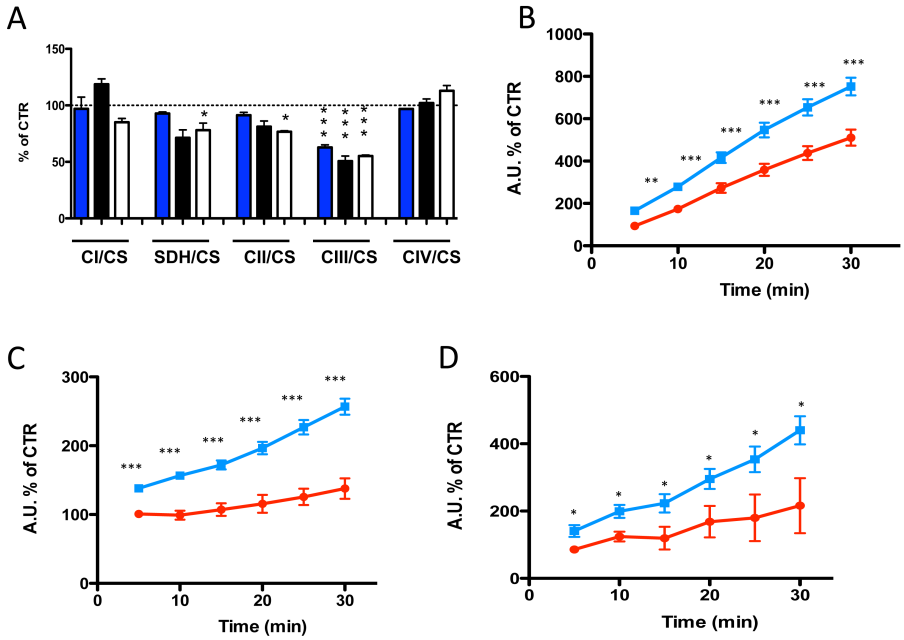

Figure 4. Biochemical analysis of *Ttc19*$^{-/-}$ tissues. (A) Spectrophotometric analysis of biochemical activities of mitochondrial respiratory chain complexes normalised to CS activity and expressed as percentage compared to control values. Blue bars: liver; black bars: skeletal muscle; white bars: brain. N= 4 mice/group, age = 3 month-old. H_2O_2 quantification in isolated mitochondria over time: B liver, C heart, D skeletal muscle. Blue lines: *Ttc19*$^{-/-}$ samples, red lines: *Ttc19*^{wt} samples. N= 3 tissues/group in duplicate. Error bars represent SEM; * $p < 0.05$, ** $p < 0.01$, ***$p < 0.005$

IV Analysis of cIII$_2$ assembly status in Ttc19$^{-/-}$ *tissues*

We then investigated the assembly status of cIII in mitochondria isolated from brain, liver and skeletal muscle of *Ttc19*$^{-/-}$ and *Ttc19*^{wt} mice by BNGE. 1D-BNGE revealed an altered

electrophoretic pattern in the *Ttc19*$^{-/-}$ samples from all tissues (Figure 5A), as cIII$_2$ migrated more slowly and appeared as a blurred multiband pattern. This phenomenon was observed using both digitonin and dodecylmaltoside (Figure 5B).

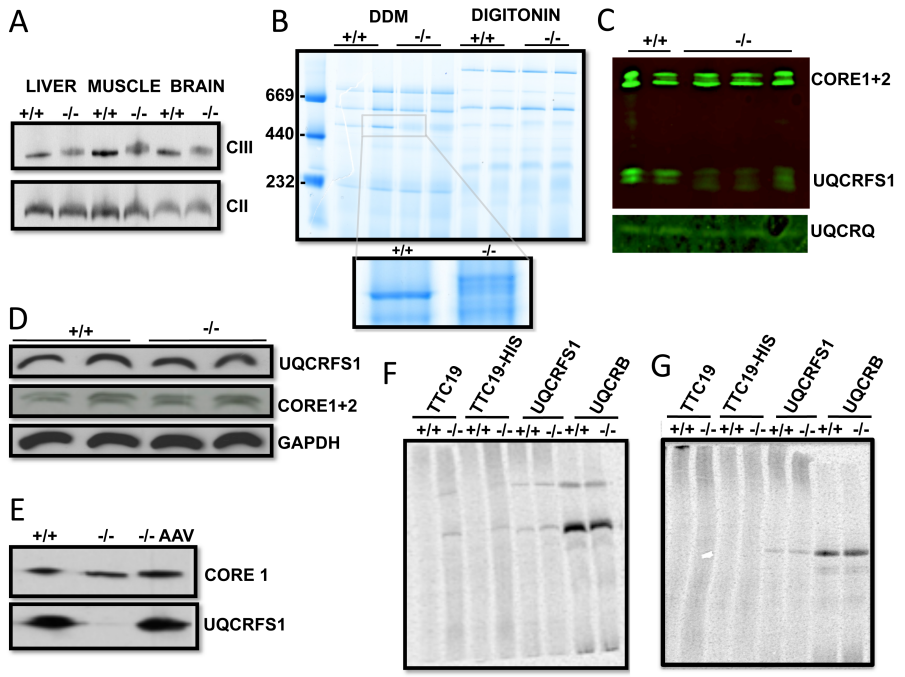

Figure 5. Characterization of cIII$_2$ in *Ttc19*$^{-/-}$ tissues. (A) Immunovisualisation of cIII in BNGE of mitochondria extracted from liver, muscle and brain. Anti-CORE1 and anti-SDH70 were used for cIII and cII visualisation respectively. (B) Top: BNGE of *Ttc19*^{wt} and *Ttc19*$^{-/-}$ mitochondria, solubilised with DDM or Digitonin. Bottom: an enlargement of cIII band. (C) WB of the subunits in cIII bands cut from 1D-BNGE and run on SDS-PAGE. (D) WB on total homogenates. No obvious differences in UQCRFS1 level were detected. (E) WB on complex III band denatured and run on SDS-PAGE. The re-expression of TTC19-HIS mediated by AAV in the liver of *Ttc19*$^{-/-}$ mice restored the incorporation of UQCRFS1 in cIII. (F, G) *In organello* import of ^{35}S-labelled hTTC19, hTTC19-6HIS, UQCRFS1 and Uqcrb. *Ttc19*^{wt} and *Ttc19*$^{-/-}$ mitochondria were solubilised in digitonin (F) or DDM (G) and run on a BNGE. UQCRFS1 and UQCRB were used for cIII visualisation.

However, high resolution clear native gel electrophoresis (hCNE), which omits Coomassie Brilliant Blue G from the preparation, or BNGE on highly pure mitochondria obtained by sucrose gradient revealed no differences in $cIII_2$ migration pattern in *Ttc19*$^{-/-}$ vs. *Ttc19*^{wt} mice (Supplementary Figure 4A). Interestingly, the expression of a 6xHis tagged *hTTC19* (hTtc19-6xHis) by using a hepatotropic adeno-associated viral vector (AAV2/8) restored the wild-type $cIII_2$ migration pattern in the liver mitochondria (Supplementary Figure 4B), demonstrating the specificity of this phenomenon. These data suggest a conformational abnormality of the $cIII_2$ in the absence of TTC19, resulting in an alteration in the interaction of $cIII_2$ with the Coomassie dye and/or the lipid environment.

No accumulation of $cIII_2$ sub-assemblies was detected in mitochondria from *Ttc19*$^{-/-}$ mouse tissues by denaturing 2D-BNGE using antibodies against several subunits of cIII (Supplementary Figure 4C). Nevertheless, SDS-PAGE of the native BNGE band corresponding to $cIII_2$ showed a clear reduction of incorporated UQCRFS1 in *Ttc19*$^{-/-}$ vs. *Ttc19*^{wt} mouse samples (Figure 5C), despite normal levels of UQCRFS1 mRNA (Supplementary Fig 4D), and total (free + bound) UQCRFS1 protein (Figure 5D). Taken together, these results demonstrate a role for TTC19 in the incorporation/stabilisation of the Rieske protein in $cIII_2$. Interestingly, the levels of incorporated UQCRFS1 into $cIII_2$ were restored by expressing hTTC19 with the AAV8-hTTC19 vector (Figure 5E).

In order to further characterise the interaction with $cIII_2$ [8], we performed *in organello* import experiments using *in vitro* translated ^{35}S-labelled TTC19 followed by BNGE. We found the ^{35}S-TTC19 in bands compatible with $cIII_2$ and $cIII_2$-containing supercomplexes when the samples were solubilised with the mild detergent digitonin. However, the signal was not detectable when mitochondria were treated with dodecylmaltoside (DDM), suggesting a labile interaction. Notably, TTC19 was only incorporated in $cIII_2$ in *Ttc19*$^{-/-}$ mitochondria, indicating that the exogenous protein cannot outcompete the endogenous one (Figure 5 F,G).

V TTC19 co-purifies with $cIII_2$ in HEK cells

To have mechanistic proof of the physical interaction of TTC19 with $cIII_2$, we then performed a Stable Isotope Labelling by Amino acids in Cell culture (SILAC) analysis using a cell line carrying a recombinant human TTC19-FLAG construct. We initially showed that hTTC19-FLAG protein was robustly expressed in these cells upon doxycycline induction (Figure 6A) and coimmunoprecipitated with UQCRFS1 and UQCRC2 (Figure 6B), thus confirming its interaction with the fully assembled $cIII_2$.

Next, the protein interactions of hTTC19-FLAG were analysed by SILAC method in parental and recombinant HEK cells. Sixty-four proteins were quantitatively different in the hTTC19-FLAG pull-down in comparison with the native cell line, in both 'forward' and 'reverse' experiments (Figure 6C and Supplementary Table I). We found that 51/64 protein species

were components of the respiratory chain, including 8 subunits of cIII, as well as numerous subunits of cI and cIV (Supplementary Table I), likely as a consequence of the known interactions between $cIII_2$ and both cI and cIV in the formation of supercomplexes. As for the eight pulled-down cIII subunits, all clustered together in similar amount, with the exception UQCRFS1 that was clearly less abundant.

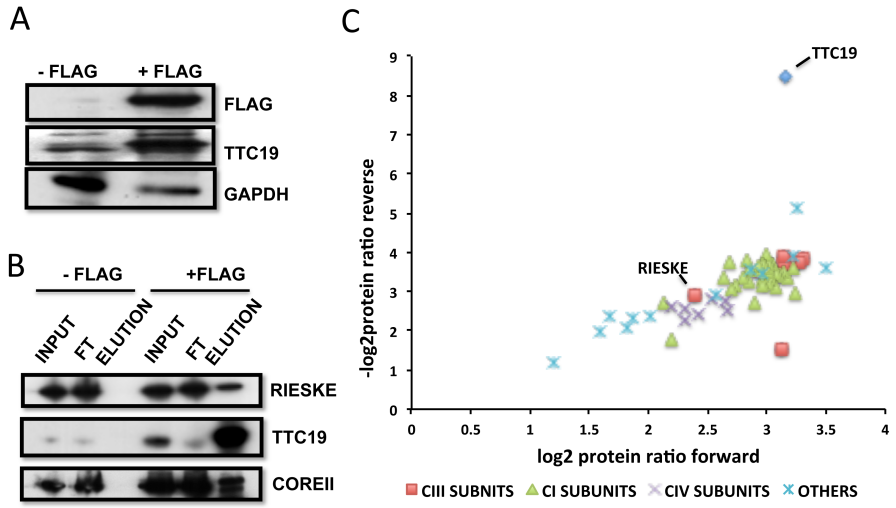

Figure 6. TTC19 interacts with cIII. (A) WB on total protein extracts from parental (-FLAG) and recombinant (+ FLAG) cell lines showed robust expression of hTTC19-FLAG upon doxycycline induction. (B) Pull-down of hTTC19-FLAG with agarose beads confirmed interaction with cIII subunits. (C) Proteins interacting with hTTC19-FLAG. The data were obtained by mass spectrometric analysis of fraction eluted via the FLAG tag in a SILAC experiment conducted with HEK cells expressing hTTC19-FLAG, combined with parental cells in 1:1 ratio. The upper right quadrant of the scatter plot is shown. The data points come from forward- and reverse-labeled samples.

This suggests that TTC19 interacts first with pre-$cIII_2$, i.e. before UQCRFS1 incorporation, but remains attached to the complex after its maturation. MT-CYB, UQCR11 and subunit 9 failed to be detected, probably due to the extreme hydrophobicity of the

first and to the very small sizes of the other two. Notably, other cIII assembly factors, which do not interact with mature $cIII_2$, were also undetected, including BCS1L, LYRM7/MZM1L, UQCC1, 2 and 3.

3. Discussion

Mutations in *TTC19* have been found in patients with mitochondrial cIII deficiency associated with heterogeneous neurological syndromes [8, 13-19].

TTC19 ablation in *D. melanogaster* caused cIII deficiency and a neurological phenotype in adult flies [8]. Similarly, *Ttc19*$^{-/-}$ mice show compromised whole body metabolism with reduced cIII activities in all the tested tissues. In addition, signs of neurological impairment were displayed by *Ttc19*$^{-/-}$ animals in a panel of *in vivo* tests, which may be related to the alterations observed in the thalamus.

The pathogenetic mechanisms in TTC19-associated diseases might at least in part involve oxidative stress since cIII is one of the main sites of ROS production within mitochondria [12] when electron transfer to cytochrome c cannot proceed normally as, for example, when UQCRFS1 fails to be incorporated in BCS1L mutated cells [20, 21]. *Ttc19*$^{-/-}$ tissues did produce more hydrogen peroxide, suggesting oxidative stress as a component of the pathophysiological mechanisms underlying the neuromuscular defect found in TTC19-less mice and humans.

Our molecular analyses of cIII assembly in mouse mitochondria showed that TTC19 is physically associated with $cIII_2$, it is

necessary to maintain the proper conformation of the enzyme and to let UQCRFS1 be efficiently incorporated within the nascent complex. Unlike other assembly factors (for instance BCS1L and MZM1L/LYRM7), TTC19 seems to act as a chaperone that binds pre-$cIII_2$ early but remains in contact with the complex until late assembly stages of assembly, in fact up to the fully assembled $cIII_2$ dimer and possibly, according to our SILAC and *in vitro* import data, even during the formation of $cIII_2$ containing supercomplexes.

The results previously reported by Ghezzi et al, showed an accumulation of early assembly intermediates of cIII in homogenates from patients' muscle. We were unable to show similar patterns in *Ttc19*$^{-/-}$ mouse mitochondria. However, the data from Ghezzi et al, do not rule out the possibility that the observed accumulation of subcomplexes containing CORE1 and 2 is due to instability of the pre-$cIII_2$ rather than to a defect in their incorporation. In addition, partially assembled species were found in mutant cultured fibroblasts rather than solid tissues, which may have different turnover of the respiratory complexes or quality control mechanisms to dispose partially assembled or misfolded proteins. Studies on mutant MEFs should help address this issue. In mouse mitochondria we observed different migration and lesser focalization of the $cIII_2$ band that could reflect changes in the complex structure or interaction with the lipid milieu, which could hamper the stability of the complex. In addition, Ghezzi et al. reported that TTC19 was detected in a very high molecular weight complex (>1MDa)

in DDM solubilized samples from Hela and 143B cells, after BNGE and immunodetection. Using a ^{35}S-labelled TTC19 and an *in organello* import assay we only detected a specific signal corresponding to $cIII_2$ and $cIII_2$-containing supercomplexes, similar to those observed with UQCRB and UQCRFS1, two structural subunits of $cIII_2$. In addition, the signal was only detected in digitonin, but not DDM-solubilized *Ttc19*$^{-/-}$ mitochondria, suggesting a relatively loose binding of TTC19 with $cIII_2$. This interaction was however stable enough to prevent the endogenous protein from being dislodged by the exogenous one. The association of TTC19 with pre-$cIII_2$ and $cIII_2$ was also confirmed by SILAC analysis. In these experiments the pulled-down material included cI, cIII and cIV structural subunits, in agreement with the proposed interaction between cI, cIV and cIII to form supercomplexes or respirasomes [22, 23]. The amount of pulled-down UQCRFS1 was lower that for the other cIII subunits, again supporting a role for TTC19 in the stabilisation/assembly of the pre-$cIII_2$, before the later incorporation of UQCRFS1 as a final step in the maturation of $cIII_2$.

4. Methods

Reagents and materials: Antibodies (anti-CORE1, CORE2, UQCRB, UQCRQ, CYC1, UQCRFS1, CD68, Ubiquitin, amyloid precursor protein, heavy molecular weight neurofilament, phosphorylated tau) were from Mitoscience, anti-GAPDH, Caspase-3, and NeuN were from Millipore, anti-FLAG was from

Sigma, anti-TTC19 from Atlas Antibodies, anti-alpha synuclein phospho specific was from Covance, anti-glial fibrillary acidic protein (GFAP) was from Dako. Primary antibodies were visualized using horseradish peroxidase-conjugated secondary antibodies (Dako, Glostrup, Denmark).

Plasmid preparation: Human complementary DNA (cDNA) encoding TTC19 was introduced into Flp-In T-REx human embryonic kidney cells (HEK293T, Life Technologies) to establish inducible, transgenic cell lines. The transgene carried a carboxy-terminal octapeptide (DYKDDDDK) (FLAG)

Cell culture and transfection: Human embryonic kidney cells were grown in Dulbecco's Modified Eagle's Medium (Life Technologies) supplemented with 10% fetal bovine serum, penicillin (100 units/mL), and streptomycin (0.1 mg/mL), 15 µg/ml Blasticidin^{S} and 100 µg/ml Zeocin (Biosciences), under 5% (vol/vol) CO_2. For the generation of inducible transgenic TTC19-FLAG cell lines, transfection was mediated using Lipofectamine 2000 (Life Technologies) according to manufacturer's instructions. Following transfection, cells underwent selection in DMEM supplemented with 10% tetracycline-free FBS, penicillin (100 units/mL), streptomycin (0.1 mg/mL), 15 µg/ml Blasticidin^{S} and 100 µg/ml hygromycin^{B} (Sigma). Gene expression was induced by adding doxycycline (Sigma) to the culture medium with a final concentration of 10 ng/ml for 24 h.

Real-Time PCR: Transcripts analysis was carried out by SYBR Green real- time PCR, as described in Viscomi et al [24].

Construction of AAV2/8 vector: AAV2/8-TBG-hTTC19-HIS vectors was produced by the AAV Vector Core of the Telethon Institute of Genetics and Medicine (Naples, Italy) by triple transfection of 293T cells and purified by CsCl gradients [25] Physical titers of the viral preparations (genome copies per ml) were determined by real-time PCR [26] (Applied Biosystems, Foster City, CA) and dot-blot analysis.

Western blot: Cells were counted and lyzed on ice in TG buffer (Tris.HCl 20 mM pH 7.5, NaCl 500 mM, EDTA 2 mM, Triton-X-100 1%, Glycerol 10%) supplemented with protease inhibitors (Roche). Lysate was centrifuged at 13000×g and supernatant transferred to fresh pre-chilled 1.5 mL tubes. Tissues total homogenates were prepared in RIPA buffer (50 mM Tris HCl [pH 8], 150 mM NaCl, 1% NP-40, 0.5% sodium deoxycholate, 0.1% SDS) with the addition of a protease inhibitor cocktail (Roche). Protein concentration was determined by the Lowry method. Aliquots were run through a 4-12% polyacrylamide SDS-PAGE (Life Technologies) and electroblotted onto a nitrocellulose membrane, which was then immunodecorated with different antibodies.

BNGE and hrCNE: Blue-Native Gel Electrophoresis (BNGE) was performed on mitochondria from mouse tissues as

described [27]. Mitochondria were solubilized either with n-dodecyl-β-d-maltoside (DDM) 1% or digitonin 4mg/mg of proten. Equal amounts of protein or were separated on 4–12% or 12% Bis-Tris NuPAGE gels (Life Technologies). For 2D-BNGE, each gel slice was cut, denatured with a solution containing 1% SDS and 1% β-mercaptoehanol for 1hour and then run through a 4-12% polyacrylamide SDS-PAGE (Life Technologies). hrCNE was performed as described [28].

In organello import of radiolabeled proteins: human TTC19, TTC196His, UQCRFS1 and UQCRB radiolabelled proteins were obtained via coupled transcription and translation (TNT) in a reticulocyte system in the presence of ^{35}S-methionine. Mitochondria were isolated from livers by differential centrifugation and the *in vitro import* assay was then carried out as described [29]. Mitochondria were then solubilized and run on a non-denaturing, 1D-BNGE as described above.

Generation of Ttc19$^{-/-}$ mice. All procedures were conducted under the UK Animals (Scientific Procedures) Act, 1986, approved by Home Office license (PPL: 7538) and local ethical review. C57BL/6N-A/a targeted ES cells (agouti) were obtained from the EUCOMM consortium. The targeting vector was produced using a KO first allele (reporter-tagged insertion with conditional potential) strategy [30], with loxP sites surrounding exon 7, encoding the second tetratricopeptide domain, and whose deletion was predicted to lead to no protein expression

by non-sense mediated decay. ES cells were injected into C57Bl/6N blastocysts, and two 90-100% chimeric males were obtained. Germ line transmission assessed by backcrossing to C57Bl/6N wild type females was obtained at the 4th litter. The LacZ and Neomycin resistence cassette were removed by crossing with a general deleter Cre strain. The animals were maintained on a C57Bl/6N background. The animals were maintained in a temperature- and humidity-controlled animal-care facility with a 12 hr light/dark cycle and free access to water and food and were sacrificed by cervical dislocation.

Behavioural and locomotor analysis. Mice were monitored weekly for onset of postural abnormalities, weight loss and general health. Neurological and metabolic phenotype was evaluated further with a set of different coordination and sensorimotor tests, as described below.

Treadmill: A treadmill apparatus (Columbus Instruments) was used to measure motor exercise endurance according to the number of falls in the motivational grid during a gradually accelerating program with speed initially at 6.5 m/min and increasing by 0.5 m/min every 3 min. The test was terminated by exhaustion, defined as >10 falls/min into the motivational grid.

Rotarod: to measure coordination skills, a Rotarod (Ugo Basile, Italy) apparatus was set with a starting velocity of 4 rpm and an

acceleration of 20 rpm/min. All of the animals received 3 days of training consisting of three trials for each session. On the test day, animals received 3 trials and the time of latency to fall was calculated for each mouse.

Cylinder Test: to measure rearing activity, animals were placed in a clear Plexiglas cylinder (13.5 cm inside diameter x 17.6 cm height). While in the cylinder, animals typically rear and engage in exploratory behavior by placing their forelimbs along the wall of the cylinder. Activity was measured by counting the number of rears made by each animal in a 3-min period without recording specific limb use.

Pole test: Animals were placed head upwards on top of a vertical plastic pole 50 cm in length (diameter, 0.5 cm). The base of the pole was placed in the home cage. Once placed on the pole, normal animals orientate themselves downward and descend the length of the pole back into their home cage. All of the animals received 2 days of training consisting of three trials for each session. On the test day, animals received 5 trials and the time to orientate downward and descend the pole was scored as follows: 0 = Falls off; 1 = Turns, but falls off; 2 = Turns and climbs down within 25s; 3 = Turns and climbs down within 15s; 4 = Turns and climbs down within 10s.

Negative geotaxis test: this test assesses the ability of the mouse to turn on a vertically positioned grid from being in the

head-down position to the head-up position by rotating the body by 180°. Some mice may not be able to maintain their position on the grid at all (scored as 0), or may freeze for the duration of the 30 s test (1), move slightly but do not turn (2), turn and freeze (3) or turn and climb the grid (4).

Comprehensive laboratory animal monitoring system (CLAMS): the Comprehensive Laboratory Animal Monitoring System (CLAMS™, Columbus Instruments, Columbus, OH) is a set of live-in cages for automated, non-invasive and simultaneous monitoring of horizontal and vertical activity, feeding and drinking, O_2 consumption and CO_2 production. *Ttc19*$^{-/-}$ mice and control littermates were individually placed in CLAMS™ cages and monitored over a 36 hr period. Food and water consumption are measured directly as accumulated data. The following parameters were measured: VO_2 (volume of oxygen consumed, mL/Kg/hr), VCO_2 (volume of carbon dioxide produced, mL/Kg/hr), RER (respiratory exchange ratio), heat (Kcal/hr), XYZ total activity (all horizontal beam breaks in counts); data were collected every 10-minutes.

Morphological analysis. For histochemical analysis, tissues were frozen in liquid-nitrogen pre-cooled isopentane. Eight µm-thick sections were stained for COX and SDH, as described [31]. For histological and immunohistochemical analyses, mice were anesthetized with an overdose of pentobarbital and perfused with PBS followed by 4% PFA. Brains were dissected

and post fixed in 4% PFA. Whole brains were cut along the sagittal plane and embedded in paraffin. Six µm-thick sections were used for analysis. Hematoxylin-eosin and Nissl staining were performed by standard methods. Immunohistochemistry was performed using antibodies against amyloid precursor protein (1:200), heavy molecular weight neurofilament (1:2000); ubiquitin (1:50), phosphorylated tau (1:50), alpha synuclein phospho specific (1:200), NeuN (1:500), CD68 (1: 500), glial fibrillary acidic protein (1:100) and Caspase-3 (1:500). Primary antibodies were visualized using horseradish peroxidase-conjugated secondary antibodies (Dako, Glostrup, Denmark).
Tunel assay (Promega) was performed to label apoptotic cells and Fluoro Jade B stain (Millipore) to label degenerating neurons.

Biochemical Analysis of MRC Complexes. Brain and skeletal muscle samples were snap-frozen in liquid nitrogen and homogenized in 10 mM phosphate buffer (pH 7.4). The spectrophotometric activity of CI, CII, CIII, and CIV, as well as CS, was measured as described [32].

ROS measurement: ROS production in isolated mitochondria was detected by fluorimetric assay using Amplex Red Hydrogen Peroxide/Peroxidase Assay Kit (Invitrogen) according to manufacture's instructions.

Proteomics: SILAC experiments were performed as described

[33]. Cells were grown in either “heavy” DMEM containing arginine and lysine isotopically labeled with ^{15}N and ^{13}C, or in “light” DMEM containing ^{14}N and ^{12}C arginine and lysine (Sigma-Aldrich). These media were supplemented with proline (200 mg/L) to suppress the conversion of arginine to proline, and with dialyzed FBS (Life Technologies) to prevent dilution of heavy isotopes. To ensure maximal incorporation, the cells were doubled at least eight times in media containing heavy isotopes. The analysis was based on two SILAC experiments, one in which the parental cells were labelled in heavy medium and the recombinant cells in light medium (“forward exp”), and the second vice versa (“reverse exp”). Cells (15 mg protein) were solubilized in PBS with complete EDTA-free protease inhibitor mixture (Roche) and enriched for mitoplasts with digitonin. Mitoplasts were solubilized in digitonin, 4mg/mg of protein, in PBS containing protease inhibitor (Roche), glycerol (10% vol/vol), and a mixture artificial phospholipid stock: 0.09 mg/ml 1-hexadecanoyl-2--(9Z-octadecenoyl)-sn-glycero-3-phosphocholine; 0.03 mg/ml 1-palmitoyl-2-oleoyl-sn-glycero-3-phosphoethanolamine, and 1-hexadecanoyl-2-(9Z-octadecenoyl) -sn-glycero-3-phospho- (1'-rac-glycerol)) (Avanti Polar Lipids). Insoluble material was filtered off. hTTC19-FLAG was purified at 4 °C with M2 FLAG agarose (Sigma-Aldrich). Bound proteins were eluted with 3× FLAG peptide (125 ng/μL). Each lane of the Comassie blue-stained gel was cut into 14 slices and each of these was subjected to analysis using an LTQ OrbiTrap XL mass spectrometer. Each sample for mass

spectrometric analysis consisted of a 1:1 mixture of proteins immunopurified from mitoplasts from control and hTTC19-FLAG cells. They were reduced, alkylated, and fractionated by SDS/PAGE on 10–20% acrylamide gradient gels in Tris-glycine buffer (Life Technologies), and proteins in gel slices were digested with trypsin. Peptides were dissolved in 5% (vol/vol) aqueous acetonitrile containing 0.1% (vol/vol) formic acid. They were fractionated in a Thermo Easy-nLC with a reverse-phase column (75 μm i.d. × 100 mm; Nanoseparations) with a gradient of 0–40% buffer B over 84 min with a flow rate of 300 nL/min (buffers A and B, 5% and 95% aqueous acetonitrile, respectively, each containing 0.1% formic acid). The effluent was passed into an LTQ OrbiTrap XL mass spectrometer (Thermo Fisher) operating in data-dependent MS/MS mode, with a mass scan range of 400–2,000 Da for precursor ions and MS/MS of the top 10 highest abundance ions selected from the full scan. Each tryptic peptide produced a peptide ion pair differing by either 10.01 or 8.01 Da for peptides with C-terminal arginine or lysine, respectively. Peptide pairs were located by MaxQuant and identified with Andromeda by comparison of fragment ion masses in tandem mass spectra and the human UniProt database [34]. A heavy:light ratio was calculated with MaxQuant. The median peptide ratio was taken to be the protein ratio, using at least two ratios for each protein. The ratios from each experiment were plotted on horizontal and vertical axes, respectively, of a “scatter plot” as the log base 2 value. Thus, a fourfold change in the abundance of a protein in

both experiments becomes 2 on each axis, and the protein is represented by a point in the top right quadrant of the scatter plot. The horizontal and vertical axes represent 2 raised to the power of zero, a ratio of 1, and no changes in abundance. Proteins unaffected by experimental conditions cluster around the origin, and those with consistent increases or decreases in abundance occur in the top right or bottom left quadrants, respectively. A diagonal line from the top right to bottom left represents a perfect correlation between the two experiments. Statistically significant proteins in both orientations of labeling were identified with Perseus [35] ($P < 0.05$). Points in the two other quadrants represent proteins where the differences are irreproducible in the replicate experiments. Those in the top left quadrant contain exogenous contaminants.

Statistical Analysis. All numerical data are expressed as mean ± SEM. Student's unpaired two-tail t test was used for statistical analysis. Differences were considered statistically significant for $p < 0.05$.

5. Supplemental information

Supplementary Figure 1

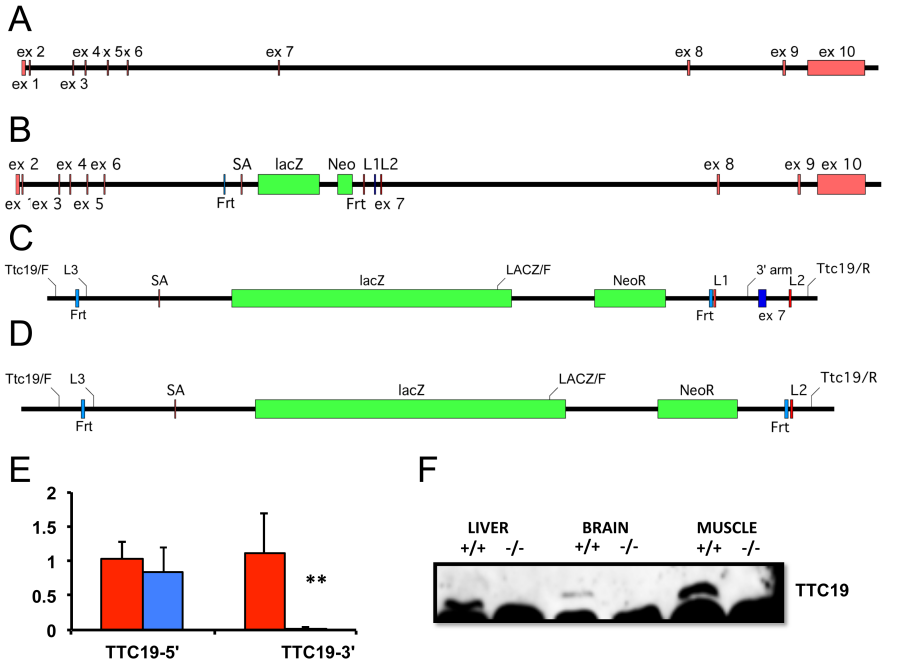

Knockout strategy: (A) WT Ttc19 allele (B) Recombinant allele obtained by homologous recombination. Hexon 7 is surrounded by two LoxP sites (L1 and L2); the LacZ and Neo cassettes are surrounded by two Frt sites. Note the presence of splicing acceptor (SA) before the LacZ cassette. (C) Detail of recombinant allele. Note the position of the oligos used for genotypying (D) Recombinant allele after Cre recombinase. (E) Transcript level of Ttc19 at 5' and 3' of the deleted exon 7 in mouse livers. Red bars: *Ttc19*^{wt}, blue bars: *Ttc19*$^{-/-}$. Error bars represent SD, ** p< 0.005, n=3. (F) WB on total homogenates in several tissues confirmed the ablation of Ttc19.

Supplementary Figure 2

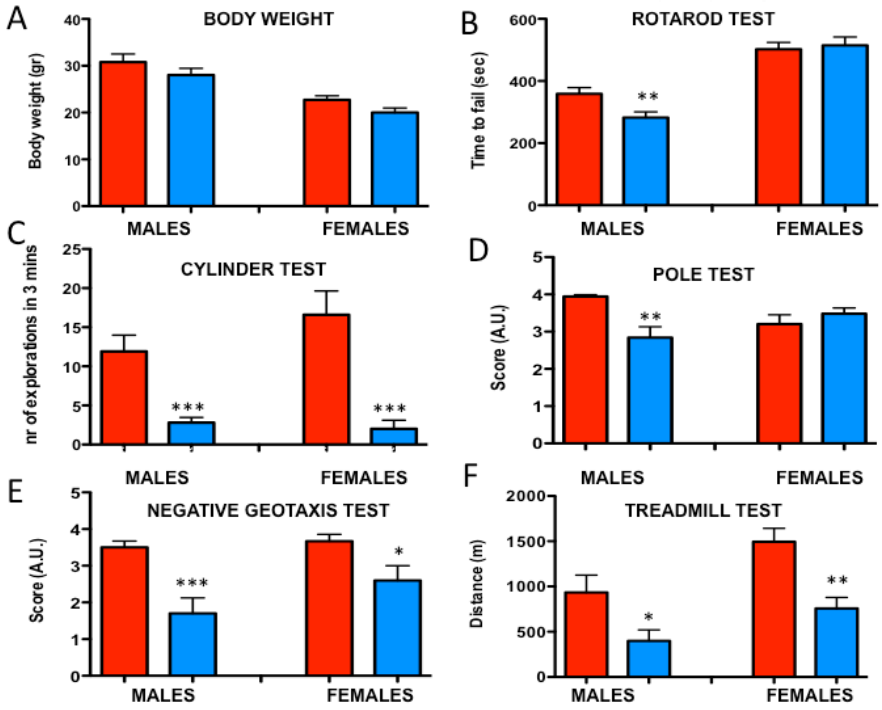

Supplementary Figure 2: clinical characterization of 3 month-old *Ttc19*$^{-/-}$ mice. (A) body weights of 3 month-old *Ttc19*$^{-/-}$ (blue bar) vs.*Ttc19*$^{+/+}$ (red bar) littermates, n= 8-11 per group, (B) rotarod test, n = 6 – 8 animals/group, average of 3 trials/mouse (C) cylinder test, n = 6 – 9 animals/group, average of 2 trials/mouse (D) pole test, n = 6 – 9 animals/group, average of 5 trials/mouse (E) negative geotaxis test, n = 6 – 9 animals/group, average of 2 trials/mouse (F) treadmill test, n = 6-11 animals/group. Colour code as in (A). Error bars represent SEM * $p < 0.05$, ** $p < 0.01$ ***$p < 0.005$.

Supplementary Figure 3

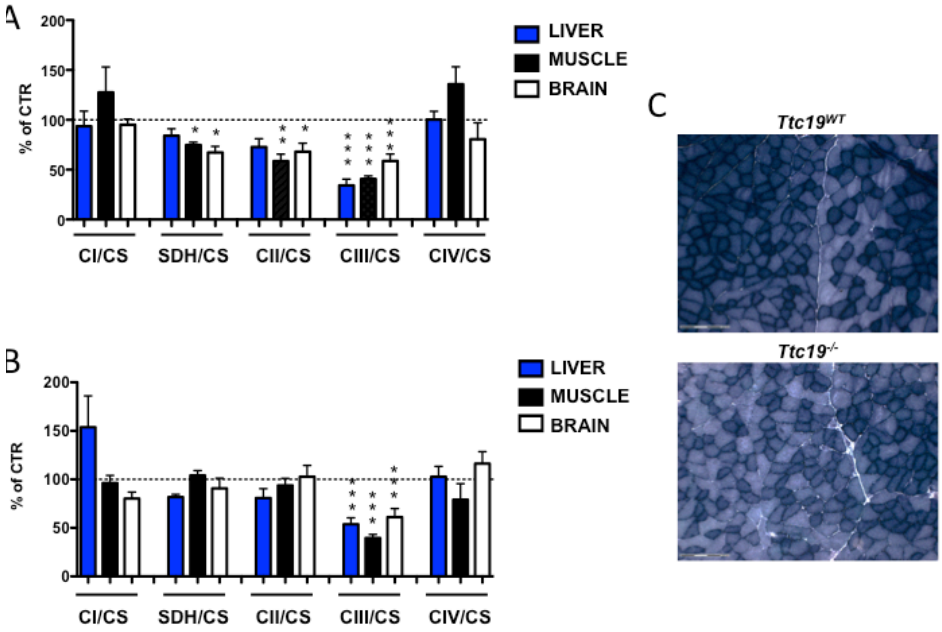

Supplementary Figure 3. Biochemical analysis of *Ttc19*$^{-/-}$ tissues. (A) Spectrophotometric analysis of biochemical activities of mitochondrial respiratory chain complexes normalised to CS activity and expressed as percentage compared to control values. N= 4 mice/group, age = 18 month-old, females (B) Spectrophotometric analysis of biochemical activities of mitochondrial respiratory chain complexes normalised to CS activity and expressed as percentage compared to control values. N= 4 mice/group, age = 18 month-old, males C: SDH staining, Females, 18month-old, bar = 150um. Error bars represent SEM * $p < 0.05$, ** $p < 0.01$, ***$p < 0.005$

Supplementary Figure 4

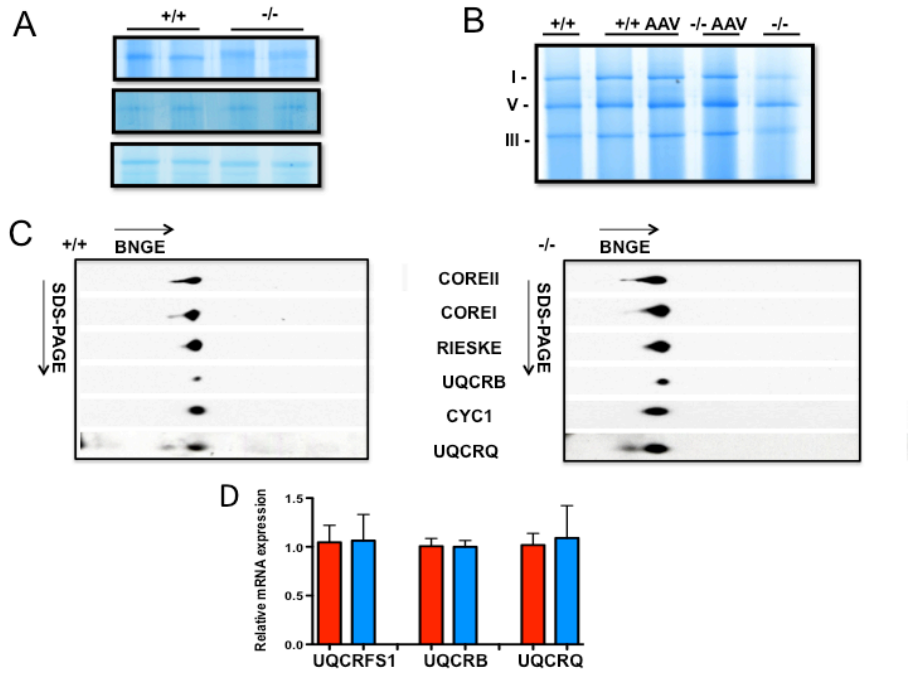

Characterisation of cIII migration and composition. (A) Migration pattern of cIII band from mitochondria extracted from tissues and run in different experimental procedures: 1D-BNGE (top), 1D-hrCNE (middle) and 1D-BNGE with previously sucrose-gradient purified mitochondria (bottom). (B) the expression of hTTC19 mediated by AAV2/8 in the liver corrects the migration pattern and/or structure of cIII. (C) 2D-BNGE of control (+/+) and knockout (-/-) mitochondria revealed no accumulations of cIII-subassemblies. (D) No changes of UQCRFS1 mRNA were detected in tissues (liver).

Supplemetary Table 1

Protein names	Gene name	Ratio H/L normalized forward exp	Ratio H/L normalized reverse exp
Tetratricopeptide repeat protein 19, mitochondrial	TTC19	3.161581	8.487382
Cytochrome b-c1 complex subunit 7	UQCRB	3.306452	3.835409
Cytochrome c1, heme protein, mitochondrial	CYC1	3.276288	3.73685
Cytochrome b-c1 complex subunit 1, mitochondrial	UQCRC1	3.198211	3.729675
Cytochrome b-c1 complex subunit 9	UQCR10	2.968552	3.514161
Cytochrome b-c1 complex subunit Rieske, mitochondrial	UQCRFS1	2.387032	2.932581
Cytochrome b-c1 complex subunit 8	UQCRQ	3.143818	3.707774
Cytochrome b-c1 complex subunit 2, mitochondrial	UQCRC2	3.138569	3.90485
Cytochrome b-c1 complex subunit 6, mitochondrial	UQCRH	3.119439	1.506558
NADH dehydrogenase [ubiquinone] iron-sulfur protein 6, mitochondrial	NDUFS6	2.635313	3.373626
NADH dehydrogenase [ubiquinone] 1 beta subcomplex subunit 5, mitochondrial	NDUFB5	3.1772	3.342078
NADH-ubiquinone oxidoreductase chain 5	MT-ND5	2.199719	1.800877
NADH dehydrogenase [ubiquinone] 1 beta subcomplex subunit 6	NDUFB6	3.149081	3.486473
NADH dehydrogenase [ubiquinone] 1 beta subcomplex subunit 9	NDUFB9	3.108491	3.466273
NADH dehydrogenase [ubiquinone] 1 beta subcomplex subunit 7	NDUFB7	3.098504	3.407256
NADH-ubiquinone oxidoreductase chain 4	MT-ND4	3.081715	3.460179
NADH dehydrogenase [ubiquinone] 1 alpha subcomplex subunit 5	NDUFA5	3.069582	3.112662

Protein names	Gene name	Ratio H/L normalized forward exp	Ratio H/L normalized reverse exp
NADH-ubiquinone oxidoreductase 75 kDa subunit, mitochondrial	NDUFS1	3.044044	3.695835
NADH dehydrogenase [ubiquinone] 1 alpha subcomplex subunit 11	NDUFA11	3.041085	3.711871
NADH-ubiquinone oxidoreductase chain 1	MT-ND1	3.033758	3.37716
NADH-ubiquinone oxidoreductase chain 3	MT-ND3	3.033018	3.319622
NADH dehydrogenase [ubiquinone] 1 alpha subcomplex subunit 13	NDUFA13;	3.015087	3.547864
NADH dehydrogenase [ubiquinone] 1 alpha subcomplex subunit 2	NDUFA2	3.012569	3.729062
NADH dehydrogenase [ubiquinone] 1 beta subcomplex subunit 10	NDUFB10	3.011567	3.21317
NADH dehydrogenase [ubiquinone] 1 subunit C2	NDUFC2	3.010494	3.525779
NADH dehydrogenase [ubiquinone] 1 beta subcomplex subunit 3	NDUFB3	3.008021	3.588487
NADH dehydrogenase [ubiquinone] flavoprotein 2, mitochondrial	NDUFV2	3.003314	3.679014
NADH dehydrogenase [ubiquinone] flavoprotein 1, mitochondrial	NDUFV1	2.988376	3.926448
NADH dehydrogenase [ubiquinone] 1 beta subcomplex subunit 8, mitochondrial	NDUFB8	2.983404	3.6694
NADH dehydrogenase [ubiquinone] iron-sulfur protein 5	NDUFS5	2.969307	3.312008
NADH dehydrogenase [ubiquinone] 1 alpha subcomplex subunit 6	NDUFA6	3.226555	3.605016
NADH dehydrogenase [ubiquinone] 1 alpha subcomplex subunit 10, mitochondrial	NDUFA10	2.964657	3.688525

Protein names	Gene name	Ratio H/L normalized forward exp	Ratio H/L normalized reverse exp
NADH dehydrogenase [ubiquinone] 1 beta subcomplex subunit 1	NDUFB1	2.95745	3.165402
NADH dehydrogenase [ubiquinone] 1 beta subcomplex subunit 4	NDUFB4	2.936233	3.550735
NADH dehydrogenase [ubiquinone] iron-sulfur protein 4, mitochondrial	NDUFS4	2.93446	3.627485
NADH dehydrogenase [ubiquinone] iron-sulfur protein 8, mitochondrial	NDUFS8	2.890953	2.71293
NADH dehydrogenase [ubiquinone] 1 alpha subcomplex subunit 8	NDUFA8	3.24618	2.963982
NADH dehydrogenase [ubiquinone] iron-sulfur protein 3, mitochondrial	NDUFS3	2.846654	3.253051
NADH dehydrogenase [ubiquinone] 1 alpha subcomplex subunit 9, mitochondrial	NDUFA9	2.841369	3.568632
NADH dehydrogenase [ubiquinone] 1 alpha subcomplex subunit 12	NDUFA12	2.827169	3.789701
NADH dehydrogenase [ubiquinone] iron-sulfur protein 2, mitochondrial	NDUFS2	2.798362	3.342459
NADH dehydrogenase [ubiquinone] 1 beta subcomplex subunit 11, mitochondrial	NDUFB11	2.72694	3.159847
NADH dehydrogenase [ubiquinone] iron-sulfur protein 7, mitochondrial	NDUFS7	2.70896	3.06927
NADH dehydrogenase [ubiquinone] 1 alpha subcomplex subunit 7	NDUFA7	2.682101	3.759434
NADH dehydrogenase [ubiquinone] 1 alpha subcomplex subunit 4	NDUFA4	2.127567	2.731685
Cytochrome c oxidase subunit 6C	COX6C	2.669027	2.522758
Cytochrome c oxidase subunit 5B, mitochondrial	COX5B	2.65908	2.776355

Protein names	Gene name	Ratio H/L normalized forward exp	Ratio H/L normalized reverse exp
Cytochrome c oxidase subunit 2	MT-CO2	2.536998	2.825619
Cytochrome c oxidase subunit 4 isoform 1, mitochondrial	COX4I1	2.415678	2.42523
Cytochrome c oxidase subunit 5A, mitochondrial	COX5A	2.314812	2.286093
Cytochrome c oxidase protein 20 homolog	COX20	2.31098	2.569351
Cytochrome c oxidase subunit 7A2, mitochondrial	COX7A2	2.18973	2.613432
Cytochrome c oxidase subunit 7A-related protein, mitochondrial	COX7A2L	2.963178	3.45272
Apoptosis-inducing factor 1, mitochondrial	AIFM1	2.02219	2.385111
Growth hormone-inducible transmembrane protein	GHITM	1.874167	2.342634
ATP-dependent zinc metalloprotease YME1L1	YME1L1	1.817173	2.049487
Coiled-coil-helix-coiled-coil-helix domain-containing protein 2, mitochondrial;	CHCHD2;	1.674325	2.380972
Mitochondrial import inner membrane translocase subunit TIM50	TIMM50	1.594692	1.964095
Sideroflexin-1	SFXN1	1.194844	1.195484
Presenilins-associated rhomboid-like protein, mitochondrial;P-beta	PARL	3.507287	3.593337
Stomatin-like protein 2, mitochondrial	STOML2	2.565256	2.911044
HCLS1-associated protein X-1	HAX1	3.250855	5.146422
Caseinolytic peptidase B protein homolog	CLPB	3.22711	3.87326
Myeloid leukemia factor 2	MLF2	2.868489	3.555799

References

1. Iwata, S., et al., Complete structure of the 11-subunit bovine mitochondrial cytochrome bc1 complex. Science, 1998. 281(5373): p. 64-71.
2. Gruschke, S., et al., The Cbp3-Cbp6 complex coordinates cytochrome b synthesis with bc(1) complex assembly in yeast mitochondria. J Cell Biol, 2012. 199(1): p. 137-50.
3. Hildenbeutel, M., et al., Assembly factors monitor sequential hemylation of cytochrome b to regulate mitochondrial translation. J Cell Biol, 2014. 205(4): p. 511-24.
4. Smith, P.M., J.L. Fox, and D.R. Winge, Biogenesis of the cytochrome bc(1) complex and role of assembly factors. Biochim Biophys Acta, 2012. 1817(2): p. 276-86.
5. Zara, V., L. Conte, and B.L. Trumpower, Biogenesis of the yeast cytochrome bc1 complex. Biochim Biophys Acta, 2009. 1793(1): p. 89-96.
6. Fernandez-Vizarra, E. and M. Zeviani, Nuclear gene mutations as the cause of mitochondrial complex III deficiency. Front Genet, 2015. 6: p. 134.
7. Fernandez-Vizarra, E., et al., Impaired complex III assembly associated with BCS1L gene mutations in isolated mitochondrial encephalopathy. Hum Mol Genet, 2007. 16(10): p. 1241-52.
8. Ghezzi, D., et al., Mutations in TTC19 cause mitochondrial complex III deficiency and neurological impairment in humans and flies. Nat Genet, 2011. 43(3): p. 259-63.
9. Invernizzi, F., et al., A homozygous mutation in LYRM7/MZM1L associated with early onset encephalopathy, lactic acidosis, and severe reduction of mitochondrial complex III activity. Hum Mutat, 2013. 34(12): p. 1619-22.
10. Tucker, E.J., et al., Mutations in the UQCC1-interacting protein, UQCC2, cause human complex III deficiency associated with perturbed cytochrome b protein expression. PLoS Genet, 2013. 9(12): p. e1004034.
11. Wanschers, B.F., et al., A mutation in the human CBP4 ortholog UQCC3 impairs complex III assembly, activity and cytochrome b stability. Hum Mol Genet, 2014. 23(23): p. 6356-65.
12. Brand, M.D., The sites and topology of mitochondrial superoxide production. Exp Gerontol, 2010. 45(7-8): p. 466-72.

13. Ardissone, A., et al., Mitochondrial Complex III Deficiency Caused by TTC19 Defects: Report of a Novel Mutation and Review of Literature. JIMD Rep, 2015.
14. Atwal, P.S., Mutations in the Complex III Assembly Factor Tetratricopeptide 19 Gene TTC19 Are a Rare Cause of Leigh Syndrome. JIMD Rep, 2014. 14: p. 43-5.
15. Kunii, M., et al., A Japanese case of cerebellar ataxia, spastic paraparesis and deep sensory impairment associated with a novel homozygous TTC19 mutation. J Hum Genet, 2015. 60(4): p. 187-91.
16. Melchionda, L., et al., A novel mutation in TTC19 associated with isolated complex III deficiency, cerebellar hypoplasia, and bilateral basal ganglia lesions. Front Genet, 2014. 5: p. 397.
17. Mordaunt, D.A., et al., Phenotypic variation of TTC19-deficient mitochondrial complex III deficiency: a case report and literature review. Am J Med Genet A, 2015. 167(6): p. 1330-6.
18. Morino, H., et al., Exome sequencing reveals a novel TTC19 mutation in an autosomal recessive spinocerebellar ataxia patient. BMC Neurol, 2014. 14: p. 5.
19. Nogueira, C., et al., Novel TTC19 mutation in a family with severe psychiatric manifestations and complex III deficiency. Neurogenetics, 2013. 14(2): p. 153-60.
20. Hinson, J.T., et al., Missense mutations in the BCS1L gene as a cause of the Bjornstad syndrome. N Engl J Med, 2007. 356(8): p. 809-19.
21. Moran, M., et al., Cellular pathophysiological consequences of BCS1L mutations in mitochondrial complex III enzyme deficiency. Hum Mutat, 2010. 31(8): p. 930-41.
22. Genova, M.L. and G. Lenaz, Functional role of mitochondrial respiratory supercomplexes. Biochim Biophys Acta, 2014. 1837(4): p. 427-43.
23. Acin-Perez, R. and J.A. Enriquez, The function of the respiratory supercomplexes: the plasticity model. Biochim Biophys Acta, 2014. 1837(4): p. 444-50.
24. Viscomi, C., et al., Early-onset liver mtDNA depletion and late-onset proteinuric nephropathy in Mpv17 knockout mice. Hum Mol Genet, 2009. 18(1): p. 12-26.
25. Xiao, W., et al., Gene therapy vectors based on adeno-associated virus type 1. J Virol, 1999. 73(5): p. 3994-4003.

26. Gao, G., et al., Purification of recombinant adeno-associated virus vectors by column chromatography and its performance in vivo. Hum Gene Ther, 2000. 11(15): p. 2079-91.
27. Nijtmans, L.G., N.S. Henderson, and I.J. Holt, Blue Native electrophoresis to study mitochondrial and other protein complexes. Methods, 2002. 26(4): p. 327-34.
28. Wittig, I.,, Karas, M., and Schagger, H. High Resolution Clear Native Electrophoresis for In-gel Functional Assays and Fluorescence Studies of Membrane Protein Complexes. Molecular and Cellular proteomics, 6:1215–1225, 2007
29. Petruzzella, V., et al., Identification and characterization of human cDNAs specific to BCS1, PET112, SCO1, COX15, and COX11, five genes involved in the formation and function of the mitochondrial respiratory chain. Genomics, 1998. 54(3): p. 494-504.
30. Skarnes, W.C., et al., A conditional knockout resource for the genome-wide study of mouse gene function. Nature, 2011. 474(7351): p. 337-42.
31. Sciacco, M. and E. Bonilla, Cytochemistry and immunocytochemistry of mitochondria in tissue sections. Methods Enzymol, 1996. 264: p. 509-21.
32. Bugiani, M., et al., Clinical and molecular findings in children with complex I deficiency. Biochim Biophys Acta, 2004. 1659(2-3): p. 136-47.
33. Andrews, B., et al., Assembly factors for the membrane arm of human complex I. Proc Natl Acad Sci U S A, 2013. 110(47): p. 18934-9.
34. Cox, J., et al., Andromeda: a peptide search engine integrated into the MaxQuant environment. J Proteome Res, 2011. 10(4): p. 1794-805.
35. Cox, J. and M. Mann, Quantitative, high-resolution proteomics for data-driven systems biology. Annu Rev Biochem, 2011. 80: p. 273-99.

Acknowledgments

This work was supported by: the Pierfranco and Luisa Mariani Foundation Italy, Telethon-Italy GGP11011, the Core Grant from the MRC, ERC FP7-322424 (to M.Z), GR-2010-2306-756 from the Italian Ministry of Health (to C.V.)

Chapter 3

AAV-mediated liver-specific MPV17 expression restores mtDNA levels and prevents diet-induced liver failure

Emanuela Bottani[1], Carla Giordano[2], Gabriele Civiletto[1], Ivano Di Meo[1], Alberto Auricchio[3], Emilio Ciusani[4], Silvia Marchet[1], Costanza Lamperti[1], Giulia d'Amati[2], Carlo Viscomi[1,] and Massimo Zeviani[1,5]

[1]Unit of Molecular Neurogenetics, The Foundation "Carlo Besta" Institute of Neurology IRCCS, Milan, Italy
[2]Department of Radiological, Oncological and Pathological Sciences, Sapienza University, Roma, Italy
[3]Telethon Institute of Genetics and Medicine (TIGEM) and Division of Medical Genetics, Department of Pediatrics, "Federico II" University, Naples, Italy
[4]Laboratory of Clinical Pathology and Medical Genetics, The Foundation "Carlo Besta" Institute of Neurology IRCCS, Milan, Italy
[5]present address: MRC-Mitochondrial Biology Unit, Cambridge, UK

Molecular Therapy 2014 Jan;22(1):10-7

Abstract

Mutations in human MPV17 cause a hepato-cerebral form of mitochondrial DNA depletion syndrome (MDS) hallmarked by early-onset liver failure, leading to premature death. Liver transplantation and frequent feeding using slow-release carbohydrates are the only available therapies, although surviving patients eventually develop slowly progressive peripheral and central neuropathy. The physiological role of Mpv17, including its functional link to mtDNA maintenance, is still unclear. We show here that Mpv17 is part of a high molecular weight complex of unknown composition, which is essential for mtDNA maintenance in critical tissues, i.e. liver, of a Mpv17 knockout mouse model. On a standard diet, *Mpv17*$^{-/-}$ mouse shows hardly any symptom of liver dysfunction, but a ketogenic diet leads these animals to liver cirrhosis and failure. However, when expression of human MPV17 is carried out by AAV-mediated gene replacement, the *Mpv17*$^{-/-}$ mice are able to reconstitute the Mpv17-containing supramolecular complex, restore liver mtDNA copy number and OXPHOS proficiency, and prevent liver failure induced by the ketogenic diet. These results open new therapeutic perspectives for the treatment of MPV17-related liver specific MDS.

1. Introduction

The term mitochondrial DNA depletion syndrome (MDS) indicates a heterogeneous group of diseases characterized by profound reduction in mitochondrial DNA (mtDNA) copy number in one or several tissues[1]. Myopathic, encephalomyopathic and hepatocerebral forms of MDS are known, due to mutations in gene products involved in mtDNA maintenance, either by controlling the supply of deoxynucleotides for, or by carrying out the, synthesis of mtDNA. MDS is considered rare, with an estimated prevalence of 1:100000[2], although the number of genes associated with this condition is rapidly expanding, and a systematic diagnostic screening is hampered by tissue specificity. For instance, thymidine kinase 2 (TK2)[3], and guanosine kinase (dGK)[4] are two enzymes involved in deoxynucleotide recycling in mitochondria; p53-ribonucleotide reductase subunit 2 (p53-R2)[5] and thymidine phosphorylase (TP)[6] are two cytosolic enzymes controlling the de novo biosynthesis of deoxynucleotides (p53-R2), and the catabolism of nucleotides (TP), respectively; polymerase gamma (POLG)[7] is the mitochondrion-specific DNA polymerase, and Twinkle, the mtDNA helicase. MPV17[9-16] a small protein of the inner mitochondrial membrane, is a prominent cause of hepatocerebral MDS, accounting for about 50% of the cases. More than 20 different MPV17 mutations in >70 patients have been reported so far. However, the functional and mechanistic links between Mpv17 and mtDNA maintenance are still missing. Nevertheless, studies on SYM1, the MPV17 yeast ortholog,

suggest a role for this protein in controlling the flux of Krebs cycle intermediates across the inner mitochondrial membrane. How this functional data relates to mtDNA maintenance and integrity is unknown. In addition, studies based on Blue-Native Gel Electrophoresis have demonstrated that SYM1 is present within a high molecular weight complex of approximately 600 kDa, the composition of which is, however, unknown[17]. Liver involvement associated with severe hypoglycemic crises, and rapidly progressive deterioration of hepatic function, leading to liver cirrhosis and failure, are early and predominant features of MPV17-dependent MDS. Unlike other MDS, neurological involvement in MPV17-associated hepatocerebral MDS is generally mild or absent at disease onset, but progressive peripheral neuropathy and cerebellar degeneration appear later in those MPV17 mutant patients who survive fatal, early onset metabolic impairment and liver failure. Although no cure is currently available for MPV17-related MDS, therapeutic interventions based on liver transplantation or on frequent meals of a corn-starch based diet[18] have been attempted, to delay disease progression or protect patients from fatal hypoglycemia. Liver transplantation has been carried out in 10 patients, but five of them died early thereafter of multiorgan failure or sepsis[14]. Prompt-release carbohydrates, such as corn-starch, seem to be effective in preventing fatal hypoglycaemic accidents, but the surviving patients invariably progress to hepatic, and eventually neurological, degeneration. Central and peripheral neuropathy is a predominant feature in subjects

affected by Navajo neurohepatopathy (NNH), a well-known disease of Navajo people from south-east US, recently shown to be caused by a specific mutation in the MPV17 gene[19]. Clinical features of NNH/MPV17 syndrome include sensory motor neuropathy with ataxia, leukoencephalopathy, corneal ulcerations, acral mutilation, poor somatic development with sexual infantilism, serious systemic infections, and, of course, liver derangement. The knockout mouse for Mpv17 (*Mpv17*$^{-/-}$) is characterized by profound, early-onset mtDNA depletion in liver[10], degeneration of the inner ear structures, particularly of the organ of Corti and *stria vascularis*, determining profound hearing loss[20], and late onset, fatal kidney dysfunction, dominated by proteinuria due to focal segmental glomerulosclerosis (FSGS)[10]. Although the molecular and biochemical features in the liver of *Mpv17*$^{-/-}$ mice closely resemble those of human patients, including severe mtDNA depletion, these animals show hardly any sign of hepatic dysfunction in standard captivity conditions and live well beyond the first year of life, with neither obvious neurological impairment nor neuropathological abnormalities. However, we show here that *Mpv17*$^{-/-}$ mice fed with a high-fat ketogenic diet rapidly develop liver cirrhosis and failure. Importantly, treatment with liver-specific an adeno-associated viral vector (serotype 2/8, AAV2/8) expressing human MPV17 (hMPV17) restores mtDNA copy number and prevents liver degeneration. This effect is linked to the formation of the 600 kDa complex containing Mpv17, since Mpv17 variants that do not allow this

structure to be formed cannot rescue the liver phenotype *in vivo*.

2. Results

I Mpv17 is part of a high molecular weight complex

In order to investigate the physical status of Mpv17 in vivo, we analyzed isolated mitochondria from *Mpv17*$^{+/-}$ and *Mpv17*$^{-/-}$ livers by Blue Native Gel Electrophoresis (BNGE) immunoblot, using an antibody specific against the mammalian Mpv17 protein (αMpv17). Although the antibody did not work in the (native) first dimension, in the (denaturing) second dimension the αMpv17 was able to visualize Mpv17 cross-reacting material (CRM) in control, but not knockout, mitochondria.

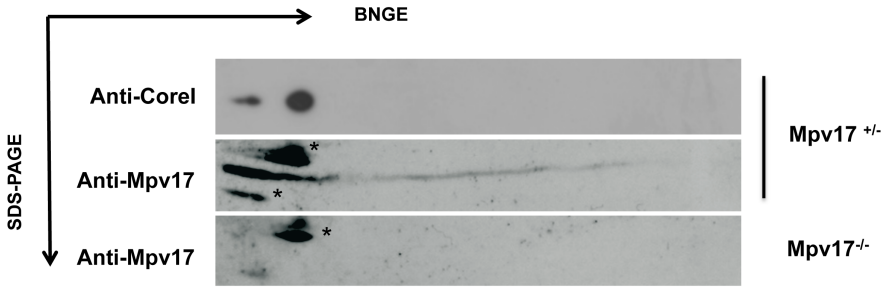

Figure 1. Characterization of the Mpv17-containing macromolecular complex. Liver mitochondria from (A) *Mpv17*$^{+/-}$ and (B) *Mpv17*$^{-/-}$ mice were analyzed by 2-D BNGE. The blots were immunostained with an αMPV17 antibody; the filter was then stripped and re-stained with an αCore 1 antibody to determine the molecular weight of the complex. The asterisks mark unspecific bands.

Most of the 20kDa Mpv17 protein was in fact present in a spot corresponding to a complex of >600kDa, as suggested by re-staining with an αCORE1 antibody marking the mitochondrial

complex III dimer (Fig 1). These findings are identical to those previously obtained on SYM1[17].

II AAV2/8-mediated hMPV17 expression rescues the Mpv17$^{-/-}$ mouse liver phenotype

We constructed an AAV2/8 viral vector expressing the hMPV17 cDNA to the liver, under the control of the liver-specific thyroxine-binding globulin (TBG) promoter. The hMPV17 protein is almost identical to the mouse (m)Mpv17 protein, displaying fourteen changes, none of which was in highly conserved residues or was predicted to have deleterious consequences by SIFT analysis[21] (Supplemental Information Figure S1). AAV2/8-hMPV17 was administered to groups of two-month old *Mpv17*$^{-/-}$ and *Mpv17*$^{+/-}$ mice (n=4 each) by retro-orbital injection at a concentration of 4 x 10^{12} viral genomes (vg)/Kg. The mice were sacrificed three weeks later. Blood samples drawn before AAV-treatment and again just before the sacrifice, showed that AST and ALT enzymes, two markers of hepatocyte leakage, were high before AAV-administration in *Mpv17*$^{-/-}$ mice, whereas they were normalized after AAV administration (Fig 2A), suggesting correction of liver damage. No change was observed in control animals upon AAV injection, suggesting that AAV has no hepatotoxicity *per se*. Viral DNA was detected by PCR in liver, but not in kidney, skeletal muscle, heart and brain (not shown), confirming the specific hepato-tropism of AAV2/8[22]; similar amounts of viral DNA/cell were found in *Mpv17*$^{+/-}$ and *Mpv17*$^{-/-}$ livers (0.9±0.3 vs. 1.2±0.5) (Fig 2B). Next, we measured MPV17 mRNA

expression by RT-qPCR. Since human and mouse MPV17 sequences are almost identical, we were unable to design primers suitable to distinguish endogenous from AAV-mediated expression. However, in both AAV-treated *Mpv17*$^{-/-}$ and *Mpv17*$^{+/-}$ mice, Mpv17 mRNA levels were much higher than the levels found in untreated *Mpv17*$^{+/-}$ mice (Fig 2F). Accordingly, western blot immunovisualization with αMpv17 showed that the amount of Mpv17-CRM in AAV-treated *Mpv17*$^{-/-}$ liver homogenates (not shown) and isolated mitochondria (Fig 2D) was much higher than that found in control mice. Analysis by 2D-BNGE immunoblotting demonstrated that hMPV17 was integrated into a high molecular weight complex similar to that detected in control mitochondria (Fig 2E). The mtDNA copy number was markedly increased in livers from AAV-treated *Mpv17*$^{-/-}$ mice (1282±372 copies/cell) compared to untreated *Mpv17*$^{-/-}$ littermates (95±34 copies/cell) (Whitney-Mann test: $p<0.0001$), and similar to that of untreated wild type livers (1402±192; $p=0.90$) (Fig 2C). Intriguingly, the AAV-treated *Mpv17*$^{+/-}$ mice had slightly increased levels of mtDNA as well (1857±144) compared to untreated littermates ($p<0.0001$) (Fig 2C). Notably, an AAV expressing hMPV17 tagged with a HA epitope, was neither able to enter the complex (Supporting Information Fig S2A) nor to complement the mtDNA depletion (Supporting Information Fig S2B) in spite of high viral content in liver (Supporting Information Fig S2C), suggesting that the HA epitope hampers the function of MPV17, possibly by interfering

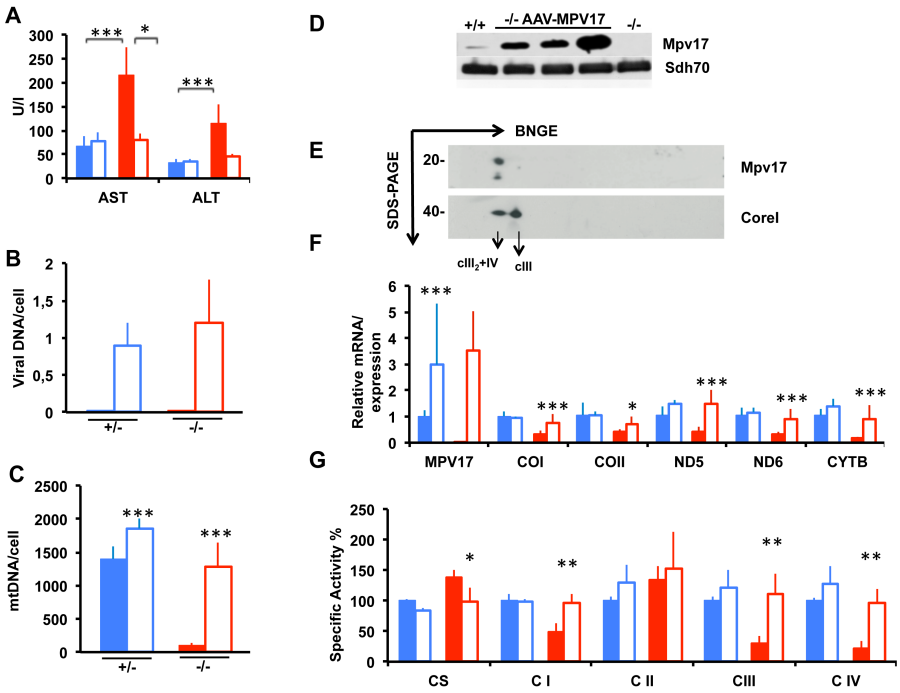

Figure 2. Molecular and clinical characterization of AAV2/8-TBG-h.MPV17-treated mice. A single retro-orbital injection of 4x1012 vg/Kg was performed in two-month old *Mpv17*$^{+/-}$ and *Mpv17*$^{-/-}$ mice. A) Analysis of AST and ALT plasma levels in mice before and after AAV administration. The asterisks indicate significance (p), calculated by either the Wilcoxon test to compare mice pre- and post-AAV treatment, or the Mann-Whitney test to compare different groups of animals: *p < 0.05; ***p<0.0001 B) Viral DNA content in livers from *Mpv17*$^{+/-}$ and *Mpv17*$^{-/-}$ mice. No amplification was obtained in AAV-untreated mice. Color codes: solid blue: untreated *Mpv17*$^{+/-}$; blue outline: AAV-treated *Mpv17*$^{+/-}$; solid red: *Mpv17*$^{-/-}$; red outline: AAV-treated *Mpv17*$^{-/-}$. Bars indicate the standard deviation (SD). C) MtDNA content in livers from AAV-treated and untreated *Mpv17*$^{+/-}$ and *Mpv17*$^{-/-}$ mice. Note that mtDNA content in AAV-treated animals is comparable to that of naïve *Mpv17*$^{+/-}$ animals, and that a slight, but significant, increase is also present in the AAV-treated vs. untreated controls. Color codes: solid blue: untreated *Mpv17*$^{+/-}$; blue outline: AAV-treated *Mpv17*$^{+/-}$; solid red: *Mpv17*$^{-/-}$; red outline: AAV- treated *Mpv17*$^{-/-}$. Bars indicate the standard deviation (SD). Asterisks indicate significance (p) calculated by the Mann-Whitney test: *p < 0.05; **p < 0.01; ***p < 0.0001. D) Western blot analysis of the hMPV17 protein: the amount detected in isolated liver mitochondria from three AAV-treated *Mpv17*$^{-/-}$ mice is higher than that detected in Mpv17-/+ littermates, whereas the protein is absent in a mitochondrial sample from a *Mpv17*$^{-/-}$ naïve individual. E) 2D-BNGE on liver mitochondria from AAV-treated *Mpv17*$^{-/-}$ mice. Note that the spot has a molecular weight similar to the cIII2+cIV supercomplex, as determined by staining with an αCORE1 antibody. F) mRNA expression analysis. Note AAV-treated *Mpv17*$^{-/-}$ mice

show normal levels of transcripts. All values are normalized to the untreated control. Color codes: solid blue: untreated *Mpv17*$^{+/-}$; blue outline: AAV-treated *Mpv17*$^{+/-}$; solid red: *Mpv17*$^{-/-}$; red outline: AAV- treated *Mpv17*$^{-/-}$. Bars indicate the standard deviation (SD). Asterisks indicate significance (p) calculated by the Mann-Whitney test: *p < 0.05; ***p < 0.0001. G) MRC activities in treated vs. untreated *Mpv17*$^{+/-}$ and *Mpv17*$^{-/-}$ mice. cI, cIII, and CIV activities are normalized in AAV-treated *Mpv17*$^{-/-}$ animals. Note that CS activity, which is increased in *Mpv17*$^{-/-}$ mice, is normal in the AAV-treated group. Color codes: solid blue: untreated *Mpv17*$^{+/-}$; blue outline: AAV-treated *Mpv17*$^{+/-}$; solid red: *Mpv17*$^{-/-}$; red outline: AAV- treated *Mpv17*$^{-/-}$. Bars indicate the standard deviation (SD). Asterisks indicate significance (p) calculated by the Mann-Whitney test: *p < 0.05; **p < 0.01.

with the formation of the supramolecular complex, which appears as necessary for mtDNA maintenance. As expected, the mtDNA copy number in skeletal muscle was similar in treated vs. untreated *Mpv17*$^{-/-}$ individuals (not shown). The increase in mtDNA copy number in AAV-treated vs. untreated *Mpv17*$^{-/-}$ livers, was paralleled by an increase in mtDNA-encoded transcripts (COI, COII, ND5, ND6, cyt b), and in the enzymatic activities of complexes I, III, and IV (Fig 2F,G). Mitochondrial respiratory chain (MRC) activities were not increased in mice treated with hMPV17-HA recombinant AAV vectors (Supporting Information Fig S2D), and in fact transaminases levels were as high as those found in untreated naïve *Mpv17*$^{-/-}$ littermates (Supporting Information Fig S2E).

III Ketogenic diet induces severe cirrhosis in Mpv17$^{-/-}$ *mice*

Ketogenic diet (KD) supplies ≈80% of the energy from fat. Although KD has been suggested to induce mitochondrial biogenesis in skeletal muscle[23], it seems to act detrimentally in OXPHOS defective mouse models unable to consume the excess of NADH derived from fat metabolism[24]. We

investigated the effects of KD administered for two months to two-month old groups of *Mpv17*$^{-/-}$ and *Mpv17*$^{+/-}$ mice (n. 4 individuals each). Both *Mpv17*$^{-/-}$ and *Mpv17*$^{+/-}$ KD-treated animals showed initial weight loss, which was progressively recovered by *Mpv17*$^{+/-}$ but not *Mpv17*$^{-/-}$ individuals (Supporting Information Fig S3A). After 2 months, KD-treated mice showed marked increase of plasma ALT and AST levels, which was much higher in the *Mpv17*$^{-/-}$ than in the *Mpv17*$^{+/-}$ group (Supporting Information Fig S3B). At necroscopy, the *Mpv17*$^{-/-}$ livers were markedly enlarged and yellowish (Supporting Information Fig S3C). Histological examination revealed diffuse micro and macrovacuolar steatosis, hepatocellular necrosis with inflammatory infiltrates and lipogranulomas. In addition, picrosirius red, which selectively stains collagen fibers, showed fibrous septa surrounding nodules of regenerating hepatocytes, consistent with cirrhosis (Fig 3A, B). Contrariwise, *Mpv17*$^{+/-}$ livers displayed only a mild, albeit variable, micro- and macrovacuolar steatosis and peri-sinusoidal collagen deposition (Fig 3C, D), as expected by prolonged exposure to a high-fat diet. The mtDNA content was unchanged in both KD-fed genotypes compared to standard diet (SD)-fed littermates, indicating that KD failed to induce mitochondrial biogenesis in liver (Supporting Information Fig S4A), as confirmed by histochemical staining for COX (Supporting Information Fig S4B). Indeed, transcript analysis showed a reduction of some MRC subunits in KD- vs. SD-fed mice (Supporting Information Fig S4C, D). Massive steatosis prevented us to perform

spectrophotometric assays of MRC activities in liver homogenates.

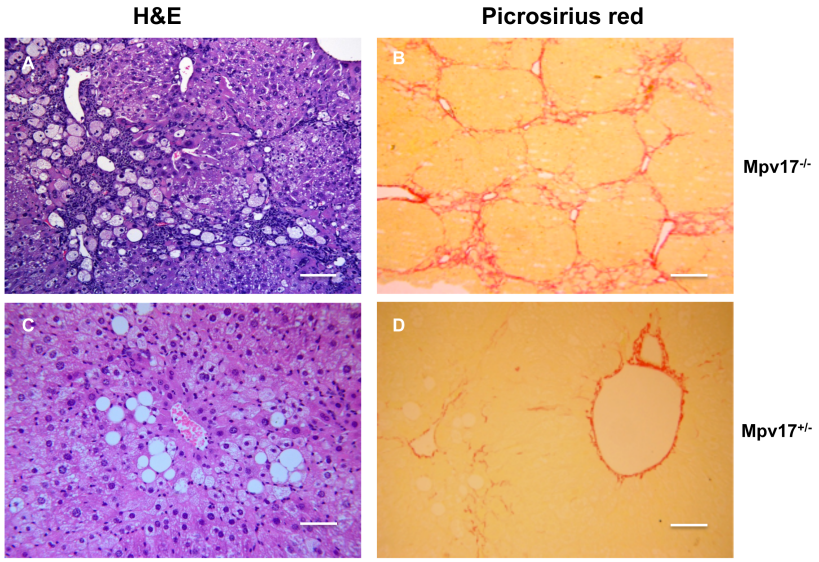

Figure 3. Histological analysis of livers from KD-fed mice. Hematoxylin-eosin (A and C), and picrosirius red (B and D) staining in KD-fed *Mpv17*$^{-/-}$ and *Mpv17*$^{+/-}$ livers. See text for details. Scale bars: 150 μm (A-C); 300μm (B-D).

IV AAV-mediated Mpv17 expression corrects liver damage of ketogenic diet

We next investigated whether treatment by AAV2/8-hMPV17 was able to (i) prevent and/or (ii) correct the severe liver derangement induced in *Mpv17*$^{-/-}$ mice by KD. In a first protocol, aiming at preventing damage, KD administration for two months was started three weeks after the injection of $4x10^{12}$ (n=4) or $4x10^{13}$ (n=3) vg/Kg AAV2/8-hMPV17 into 2 month old *Mpv17*$^{+/-}$ and *Mpv17*$^{-/-}$ mice. Here, we show data referred to the higher viral dose, but similar results were also obtained using the lower dose (Supporting Information Fig S5).

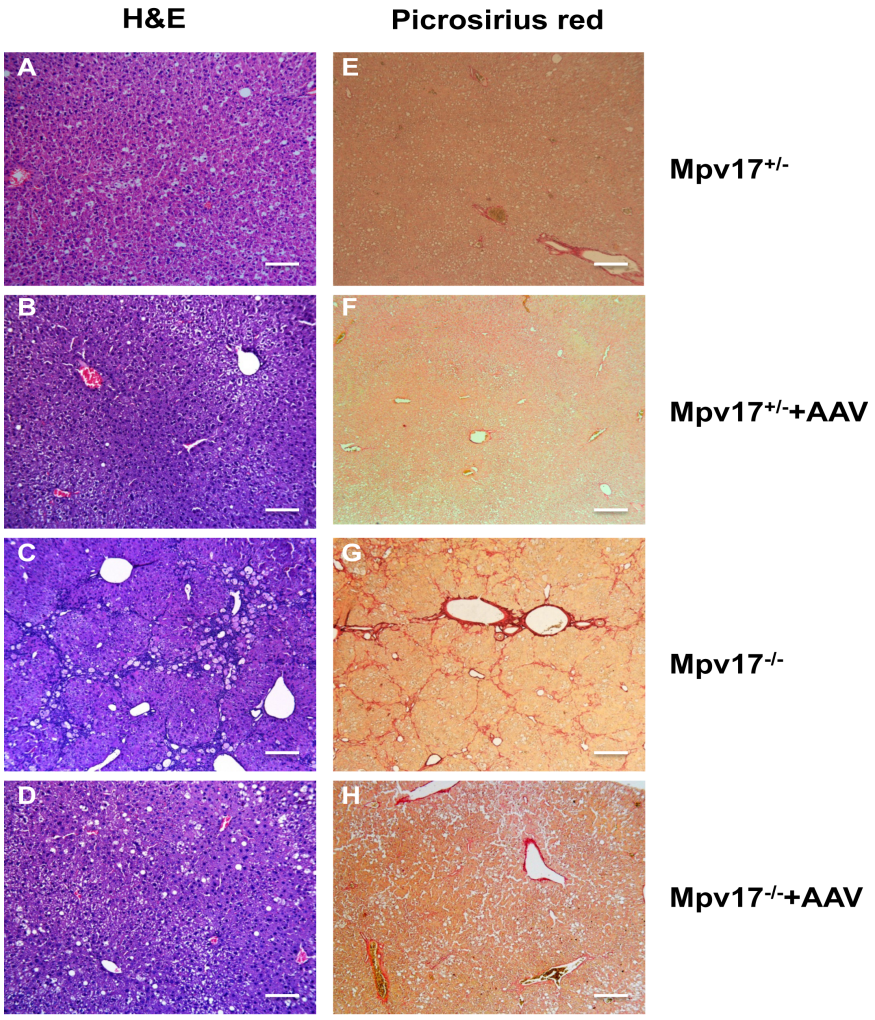

Figure 4. Histological analysis of livers from KD-fed mice pre-treated with AAV. A single retro-orbital injection of $4x10^{13}$ vg/Kg was performed in two months old *Mpv17*$^{+/-}$ and *Mpv17*$^{-/-}$ mice. KD was started three weeks later. Hematoxylin-eosin (A-D); picrosirius red (E-H) staining. A-E: Untreated *Mpv17*$^{+/-}$. B-F: AAV-treated *Mpv17*$^{+/-}$. C-G: Untreated *Mpv17*$^{-/-}$. D-H: AAV-treated *Mpv17*$^{-/-}$. See text for details. Scale bars: A-D: 150 µm, E-H: 300µm.

Body weights were monitored throughout the experiment and hepatic enzyme levels were measured at the end of the treatment. As mentioned before, untreated *Mpv17*$^{-/-}$ mice

showed progressive loss of body weight, whereas AAV-treated *Mpv17*$^{-/-}$ individuals recovered their starting weight after initial loss, and gained weight over time with a trend similar to that of AAV-treated and untreated *Mpv17*$^{+/-}$ animals (Supporting Information Fig S6A). In contrast to untreated KD-fed *Mpv17*$^{-/-}$ mice, AAV-treated KD-fed *Mpv17*$^{-/-}$ mice showed plasmatic levels of hepatic enzymes similar to those of control littermates in KD (Supporting Information Fig S6B). Livers from KD-fed AAV-treated *Mpv17*$^{-/-}$ animals were significantly less enlarged (9.9±2.6 vs. 7.0±1.0; Mann-Whitney test $p<0.01$; Supporting Information Fig S6C), and remarkably less damaged upon histological examination than those from untreated *Mpv17*$^{-/-}$ littermates (Fig 4). Eventually, whilst AAV-untreated *Mpv17*$^{-/-}$ individuals invariably developed overt cirrhosis and necrosis by two months of KD, AAV-treated *Mpv17*$^{-/-}$ animals showed only variable degrees of steatosis and some inflammatory infiltrates, comparable to those of control animals exposed to the same diet (Fig 4). These results clearly indicate that AAV2/8-hMPV17 treatment prevents KD-induced liver damage in *Mpv17*$^{-/-}$ mice. We observed that the viral DNA content was much lower in KD-fed than in SD-fed livers (1.2±0.2 vs. 12.8±2.3 in *Mpv17*$^{+/-}$, $p<0.05$; 0.4±0.3 vs. 14.8±1.0 copies/cell in *Mpv17*$^{-/-}$, $p<0.05$) (Fig 5A), suggesting that KD induced strong dilution of viral DNA. Since the DNA of recombinant AAV vectors remains episomal[25] and is replication defective, a possible explanation for this phenomenon is increased cell proliferation.

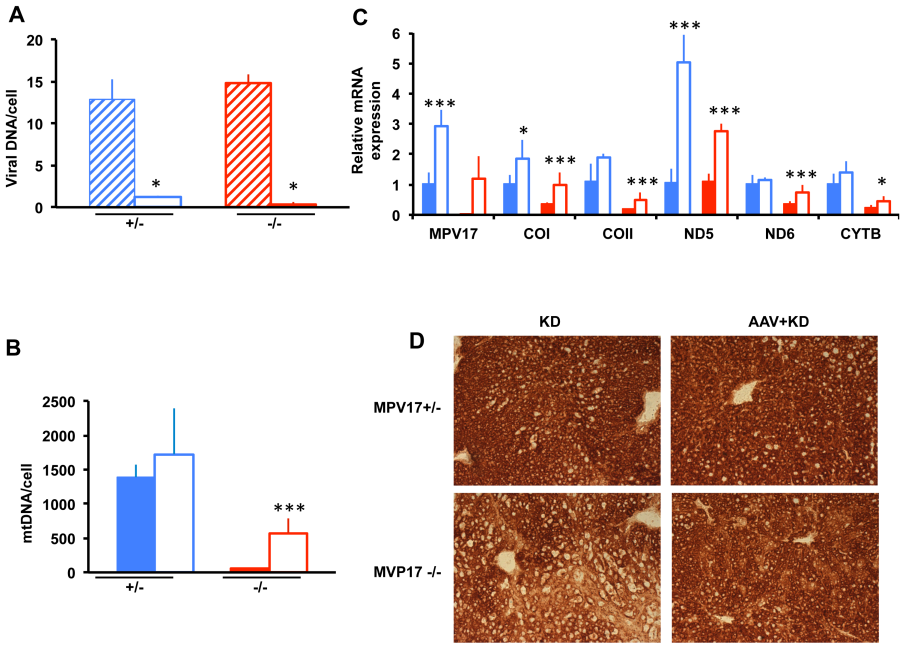

Figure 5. Molecular and biochemical characterization of KD-fed mice pretreated with AAV A) Viral DNA content in livers from AAV-treated *Mpv17*$^{+/-}$ and *Mpv17*$^{-/-}$ mice in Standard Diet (SD) vs. Ketogenic Diet (KD). Blue stripes: AAV-treated *Mpv17*$^{+/-}$ mice in SD; blue outline: AAV-treated *Mpv17*$^{+/-}$ mice in KD; red stripes: AAV-treated *Mpv17*$^{-/-}$ mice in SD; red outline: AAV-treated *Mpv17*$^{-/-}$ mice in KD. Bars indicate the standard deviation (SD). B) MtDNA analysis in AAV-treated vs. untreated, KD-fed mice. Note that mtDNA content is AAV-treated *Mpv17*$^{-/-}$ is higher than in untreated littermates, but remains lower than in control littermates. C) Mitochondrial transcripts analysis in AAV-treated vs. untreated, KD-fed mice. All values are normalized to the KD-fed untreated controls. D) COX histochemical staining.

To confirm this hypothesis, we performed quantitative analysis of proliferating vs. non-proliferating hepatocytes by measuring proliferating cell nuclear antigen (PCNA), a marker of cell proliferation[26]. The nuclear staining index for PCNA was 18.2±13.6% in SD vs. 74.2±7.7% in KD in *Mpv17*$^{+/-}$ and 20.9±15.1% in SD vs. 81.7±12.5 in KD in *Mpv17*$^{-/-}$ mice (Student t test: $p<0.005$ for both groups; Supporting Information Fig S7A). Similar results were obtained in AAV-treated mice

(Supporting Information Fig S7B). This result highlights the effect of KD in promoting hepatocyte proliferation in mouse liver, and may explain the decrease of viral content observed during the KD treatment. Nevertheless, the mtDNA content increased from 49±8 copies/cell in naïve *Mpv17*$^{-/-}$ to 576±211 copies/cell in AAV-treated *Mpv17*$^{-/-}$ littermates (Fig 5B). This increase was paralleled by robust expression of mtDNA transcripts, becoming quantitatively comparable to that of untreated KD-fed *Mpv17*$^{+/-}$ littermates (Fig 5C), and led to significant recovery of COX histochemical activity (Fig 5D). In a second protocol, aiming at correcting damage, we tested whether AAV-based hMPV17 gene replacement therapy can stop or reverse an already ongoing liver derangement, as typically found in patients. We first KD-fed for one month two groups of two-month old *Mpv17*$^{-/-}$ and *Mpv17*$^{+/-}$ mice. This treatment caused liver damage, as clearly indicated by increased hepatic-enzyme levels in plasma of both groups (Supporting Information Fig S8A). We then administered $4x10^{13}$ vg/Kg of AAV-hMPV17 to both groups of animals, while KD was continued for one additional month before sacrifice, so that this group of mice was overall exposed to KD as long as the first group. Livers from *Mpv17*$^{-/-}$ animals showed a statistically non-significant trend towards reduced hepatomegaly compared to untreated littermates, whereas livers from *Mpv17*$^{+/-}$ mice were unaffected (Supporting Information Fig S8B). Again, the livers from *Mpv17*$^{-/-}$ mice were protected from developing extensive KD-induced liver damage, showing moderate hepatocyte

steatosis, in absence of necrosis and fibrosis (Fig 6A,B), while livers from *Mpv17*$^{+/-}$ exposed to this protocol displayed only mild and focal steatosis (Fig 6C, D).

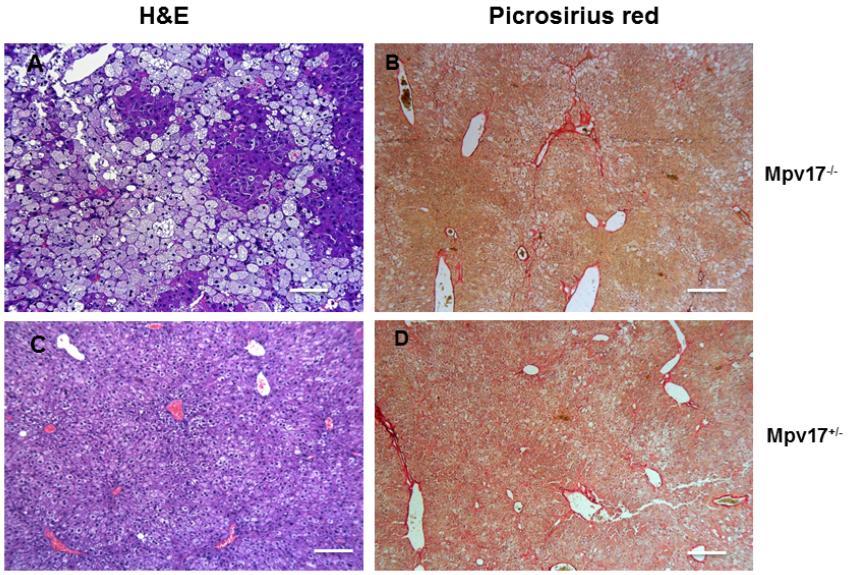

Figure 6. Histological analysis of livers from AAV post-treated, KD-fed mice A single retro-orbital injection of 4x1013 vg/Kg was performed in two-month old *Mpv17*$^{+/-}$ and *Mpv17*$^{-/-}$ mice one month after starting KD. Hematoxylin-Eosin (A and C), and Picrosirius red (B and D) staining in AAV post treated *Mpv17*$^{-/-}$ and *Mpv17*$^{+/-}$ livers. See text for details. Scale bars: A-C: 150µm, BD: 300µm.

Viral DNA quantification showed 5.6±3.1 vg/cell in *Mpv17*$^{-/-}$ and 5.0±2.5 vg/cell in *Mpv17*$^{+/-}$ mice (Fig 7A), leading to high levels of MPV17 mRNA in both *Mpv17*$^{-/-}$ and *Mpv17*$^{+/-}$ livers (Fig 7B). The mtDNA copy number was significantly increased in AAV-treated vs. untreated *Mpv17*$^{-/-}$ individuals (501±263 vs. 49±8, Mann-Whitney test: $p<0.01$) although remained lower than in treated (1387±331 copies/cell) and untreated (1384±194 copies/cell) *Mpv17*$^{+/-}$ littermates (Fig 7C).

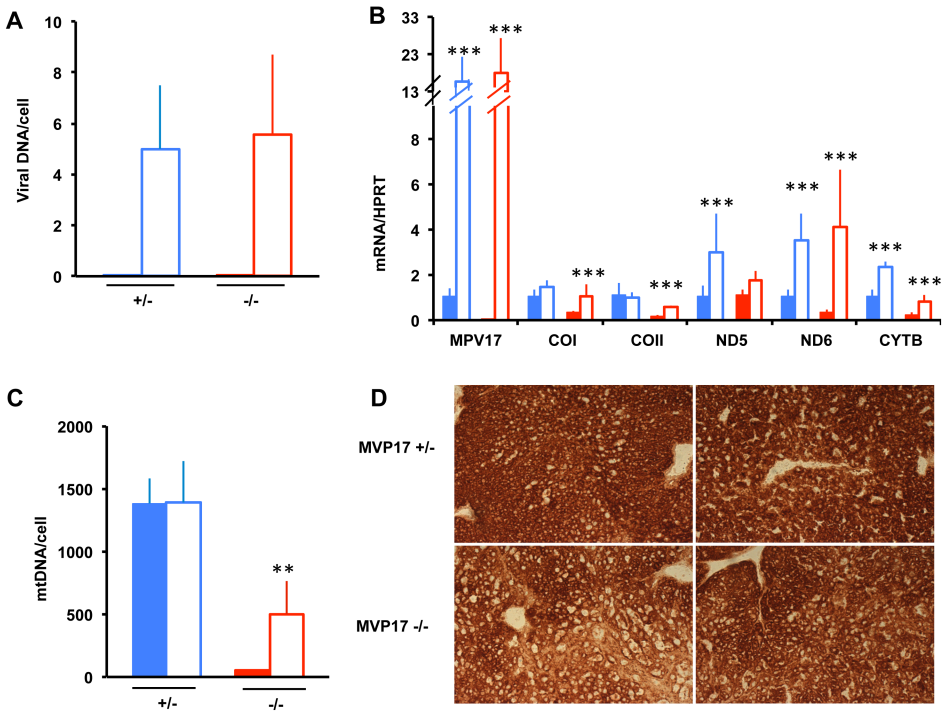

Figure 7. Molecular and biochemical characterization of livers from AAV post treated, KD-fed mice A) Viral DNA content in livers. B) MtDNA analysis. Note that mtDNA content is AAV-treated *Mpv17*$^{-/-}$ is higher than in untreated littermates, but remains lower than in control littermates. C) Mitochondrial transcripts analysis. D) COX histochemical staining. The asterisks indicate significance (p) calculated by the Mann-Whitney test for independent samples: **p < 0.001; ***p < 0.001. Color codes: solid blue: untreated *Mpv17*$^{+/-}$; blue outline: AAV-treated Mpv17+/; solid red: *Mpv17*$^{-/-}$; red outline: AAV-treated *Mpv17*$^{-/-}$. Bars indicate the standard deviation (SD).

In parallel, mitochondrial transcripts were significantly increased in the *Mpv17*$^{-/-}$ livers, up to levels comparable to KD-fed control littermates (Fig 7B), and COX histochemical activity was increased as well (Fig 7D). Nevertheless, the overall clinical conditions were clearly worse in post-KD AAV-treated than in pre-KD AAV treated *Mpv17*$^{-/-}$ mice. The hepatic enzyme levels increased, whereas the body-weight decreased (Supporting Information Fig S8C,D), suggesting that our “late” AAV

treatment can possibly slow the evolution of pre-existing liver damage, but is unable to reverse the downhill clinical progression of the disease.

3. Discussion

We provide here novel information on the connection between MPV17 and mtDNA maintenance, although the complete elucidation of the physiological role of this elusive, medically relevant and biologically intriguing protein is still missing. First, we have demonstrated that, like the yeast ortholog SYM1, mammalian MPV17 forms a high molecular weight complex in both cell cultures and mouse tissues. By reconstitution into lipid bilayers, Sym1 has recently been shown to aggregate as a high molecular complex to form a functional pore possibly a cation channel[27]. Similar to mitochondrial carrier proteins, both Mpv17 and SYM1 are imported into the inner mitochondrial membrane via the TIM23 complex without cleavage of a leader peptide. A channel activity has not been (yet) demonstrated for the mammalian Mpv17, but we have shown here that Mpv17 participates in a high molecular weight complex necessary for its function, since variants that fail to be incorporated do not rescue the liver phenotype of *Mpv17*$^{-/-}$ mice, including mtDNA depletion. A second goal of our work consisted in the development of therapeutic strategies for liver-specific MDS. Although many mitochondrial abnormalities cause multisystem disorders, some affect only or predominantly a single organ, being thus amenable to treatment by tissue-specific gene

replacement. Most of the MPV17 mutant cases are characterized by early onset, often fatal liver failure, associated with profound tissue specific mtDNA depletion, whereas other tissues are relatively (e.g. skeletal muscle), or completely (e.g. heart) spared. We used recombinant AAV vectors to target the therapeutic gene to the liver, because this approach is relatively safe, non invasive and translatable to humans We clearly showed that AAV-mediated expression of human MPV17 in *Mpv17*$^{-/-}$ mouse livers can correct the molecular phenotype, i.e. severe mtDNA depletion, in standard conditions, thus normalizing the MRC defects. We then showed that ketogenic diet (KD) cause *Mpv17*$^{-/-}$ mice to rapidly develop severe hepatomegaly and macrovacuolar steatosis, which evolves into cirrhosis and overt liver failure within two months. By contrast, *Mpv17*$^{+/-}$ littermates exposed to the same diet displayed only mild steatosis, mostly of the microvacuolar type. Administration of AAV2/8-hMPV17 before starting KD effectively protected *Mpv17*$^{-/-}$ mice from liver derangement. Partial protection from KD-induced liver failure was also obtained in mice exposed to KD before AAV treatment that is when liver damage was already ongoing, as indicated by elevated plasma levels of hepatic enzymes. However, in this case AAV-treatment was able to halt the progression of the disease, but not to revert already established liver damage. This result is in agreement with the evidence that the AAV1 serotype is able to efficiently transduce both normal and cirrhotic livers[28], with no significant dilution of the viral load over time. We propose AAV2/8-based

therapy as a realistic strategy to prevent liver failure in patients with mutations in MPV17 and eventually in other forms of liver MDS. AAV2/8 serotype can remain for a long time in the liver of mice[29-31], cats[32], and humans[33], with no significant side effects. Whilst targeting of AAV-mediated therapeutic protein is still challenging for large-size tissues such as skeletal muscle, or impermeable organs such as the brain, this approach is becoming a realistic option for gene conditions affecting a single, compliant organ, such as the liver in case of hepatic MDS, for proteins that are secreted by a targetable organ, such as the liver again for factor IX, the circulating enzyme missing in Haemophilia B[33], or in disorders that can be effectively cured by using liver to clear the bloodstream from toxic substances by making liver competent for clearing the bloodstream from toxic compounds. The latter strategy has proven successful for Ethylmalonic Encephalopathy, a mitochondrial disease due to the accumulation of toxic free sulphide, and can in principle be applied to mitochondrial neuro-gastro-intestinal encephalomyopathy MNGIE, due to accumulation of thymidine to toxic levels in plasma and tissues.

4. Materials and Methods

Construction of AAV2/8 vectors. AAV2/8-TBG-h.MPV17 and AAV2/8-TBG-h.MPV17HA vectors were produced by the AAV Vector Core of the Telethon Institute of Genetics and Medicine (TIGEM, Naples, Italy) by triple transfection of 293 cells and purified by CsCl gradients[34]. Physical titers of the viral

preparations (genome copies/ml) were determined by real-time PCR35 (Applied Biosystems, Foster City, CA, USA) and dot-blot analysis. Genomic DNA extraction, PCR and quantitative PCR Total DNA was extracted from frozen tissues using the Maxwell apparatus (Promega) following the instructions of the manufacturer. AAV-derived DNA was detected by standard PCR amplification using primer pairs specific to the hMPV17 gene. SYBRGREEN based real-time quantitative PCR was carried out for mtDNA and AAV-copy number analysis as previously described[10,22]; the RNAseP gene was used as a reference. Total RNA was extracted from liquid nitrogen snap frozen liver by Total RNA Mini Kit (tissue), according to the manufacturer's instructions (Geneaid). Of total RNA, 2µg was treated with RNase free-DNase and retrotranscribed using the GoTaq 2-Step RT-qPCR System (Promega). Approximately 25 ng of cDNA was used for real-time PCR assay using primers specific for amplification of several genes[36]. Oligonucleotide sequences are available on request.

Biochemical Analysis of MRC Complexes. Liver samples stored in liquid nitrogen were homogenized in 10 mM phosphate buffer (pH 7.4), and the spectrophotometric activity of cI, cII, cIII and cIV, as well as CS, was measured as described[37].

Morphological Analysis. Histochemical analyses were performed as described38. Hematoxylin and eosin, and picrosirius red staining were performed according to standard

protocols. Livers were formalin-fixed and paraffin embedded. Consecutive sections (5-6μm thick) were stained with hematoxylin-eosin and Picrosirius red for histological examination. Immunostaining with anti- proliferating cell nuclear antigen (PCNA) monoclonal antibodies (Abcam, Cambridge UK, dilution 1:6000) was performed for quantitative evaluation of proliferating hepatocytes. Two hundred cells per slide were manually counted in four high-power fields (original magnification: 40x) and the number of proliferating hepatocytes (in all cell cycle stages) was expressed as a ratio over the total cell number.

Immunoblotting. Ten percent w/v homogenates in 10mM phosphate buffer pH 7.4 were prepared from liver and centrifuged at 800g for 10 min to eliminate cellular debris. Total protein extracts were run through a 12% SDS–polyacrylamide gel (40μg/sample), and electroblotted onto nitrocellulose filters. The filters were immunostained with specific antibodies against MPV17 (Proteintech), CORE1 and the 70kDa subunit of SDH (Molecular probes, Invitrogen) and protein bands were visualized using the ECL chemioluminscence kit (Amersham). Twenty microgram of proteins from isolated liver mitochondria[39] were run on a 12% SDS–polyacrylamide gel. BNGE was performed isolated liver mitochondria as described40. Fifteen microliters of sample were run through a 5–13% non-denaturating gradient (1D-BNGE). For denaturing two-dimensional BNGE electrophoresis, the one-dimensional BNGE

lane was excised, treated for 1 h at room temperature (20°C) with 1% SDS and 1% β-mercapto-ethanol and then run through a 16.5% tricine-SDS–polyacrylamide gel using a 10% spacer gel.

Analysis of body fluids. AST and ALT were determined in blood samples by standard methods.

Experimental ethics policy. Animal studies were approved by the Ethics Committee of the Foundation 'Carlo Besta' Neurological Institute, in accordance with the guidelines of the Italian Ministry of Health. The use and care of animals followed the Italian Law D.L. 116/1992 and the EU directive 86/609/CEE. The mice were kept on a C57Bl6/129Sv mixed background, and wt littermates were used as controls. Standard food and water were given ad libitum. Ketogenic diet was administered for two months (SSNIFF, Germany) ad libitum. Body weight and food consumption were monitored twice a week.

5. Supplemental Information

Supplemental Figure 1

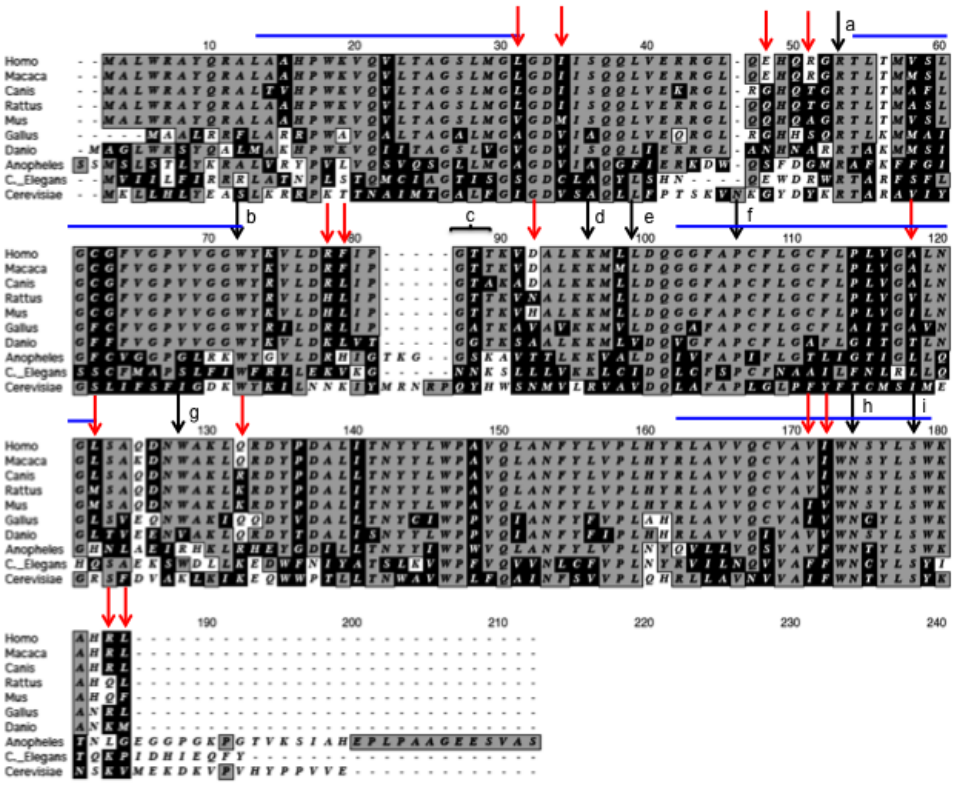

Alignment of eukaryotic Mpv17 orthologues. The blue lines indicate the transmembrane domains predicted with TMpred. *Shaded grey*: identities; *letters on black background:* similarities; *letters on white background:* mismatches. Note that none of the mismatches between humans and mice was predicted to be deleterious in humans, suggesting preservation of protein function. The *red arrows* show the differences between human and murine proteins. The black arrows and the bracket show the position of residues mutated in patients (note that the numbers in the alignment are NOT referred to the position in humans):

a) R50Q8
b) W69X: Wong et al, 2007
c) G79_T81Del10
d) K88E; K88Del13
e) L91Del13
f) P98L13
g) W120X8
h) N166K8

Supplemental Figure 2

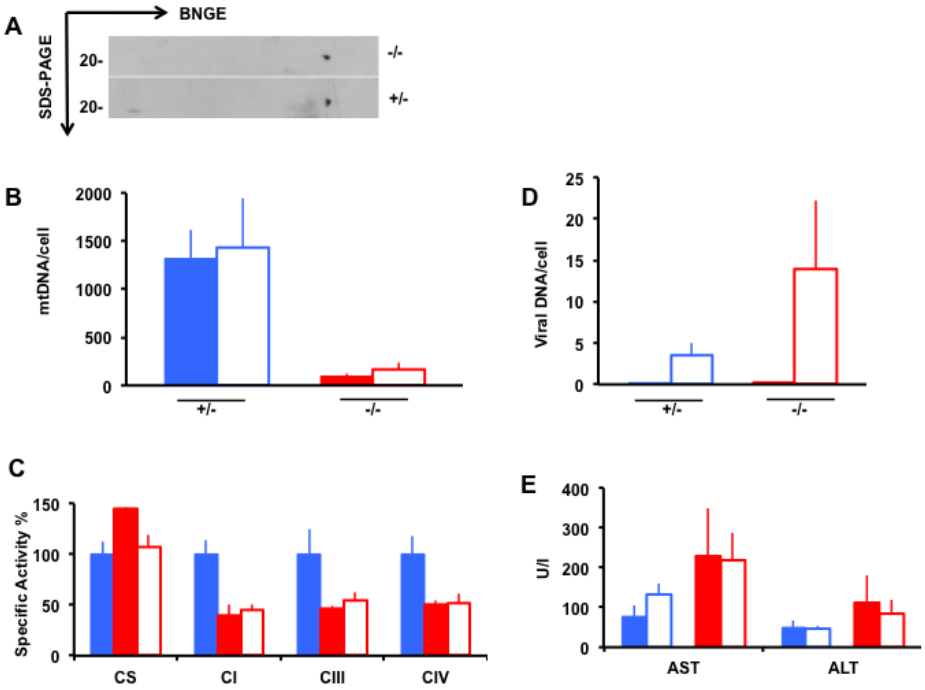

AAV-mediated expression of hMPV17-HA in *Mpv17*$^{-/-}$ mice. A) 2D-BNGE using anti-HA in *Mpv17*$^{-/-}$ and *Mpv17*$^{+/-}$ mice B) mtDNA analysis. Note that there is no significant difference between AAVh.MPV17-HA treated vs. untreated samples. C) Biochemical analysis D) Viral DNA content E) AST and ALT transaminases levels in plasma Colour codes: *solid blue*: untreated *Mpv17*$^{+/-}$ mice; *blue outline*: AAV-treated *Mpv17*$^{+/-}$ mice; *solid red*: untreated *Mpv17*$^{-/-}$ mice; *red outline*: AAV-treated *Mpv17*$^{-/-}$ mice. Bars indicate the standard deviation (SD).

Supplemental Figure 3

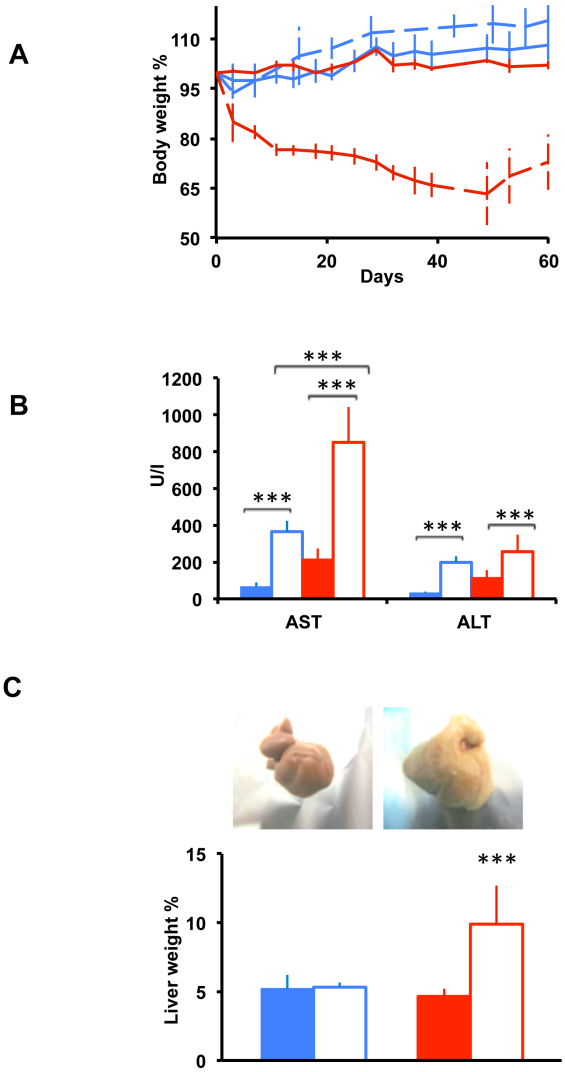

Effects of KD on *Mpv17*$^{-/-}$ and control littermates. A) Body weight changes during 2-months of SD and KD. Solid blue: SD-fed *Mpv17*$^{+/-}$; dashed blue: KD-fed *Mpv17*$^{+/-}$; solid red: SD-fed *Mpv17*$^{-/-}$; dashed red: KD-fed *Mpv17*$^{-/-}$. B) AST and ALT transaminases levels in plasma C) Liver weight (as a percentage of body weight). Note that *Mpv17*$^{-/-}$ liver is yellowish and hugely increased. Asterisks indicate significance (p) calculated by Mann-Whitney test for unpaired samples: *p < 0.05; **p < 0.01; ***p < 0.0001. Colour codes: solid blue: SD-fed *Mpv17*$^{+/-}$ mice; blue outline: KD-fed *Mpv17*$^{+/-}$ mice; solid red: SD-fed *Mpv17*$^{-/-}$ mice; red outline: KD-fed *Mpv17*$^{-/-}$ mice. Bars indicate the standard deviation (SD).

Supplemental Figure 4

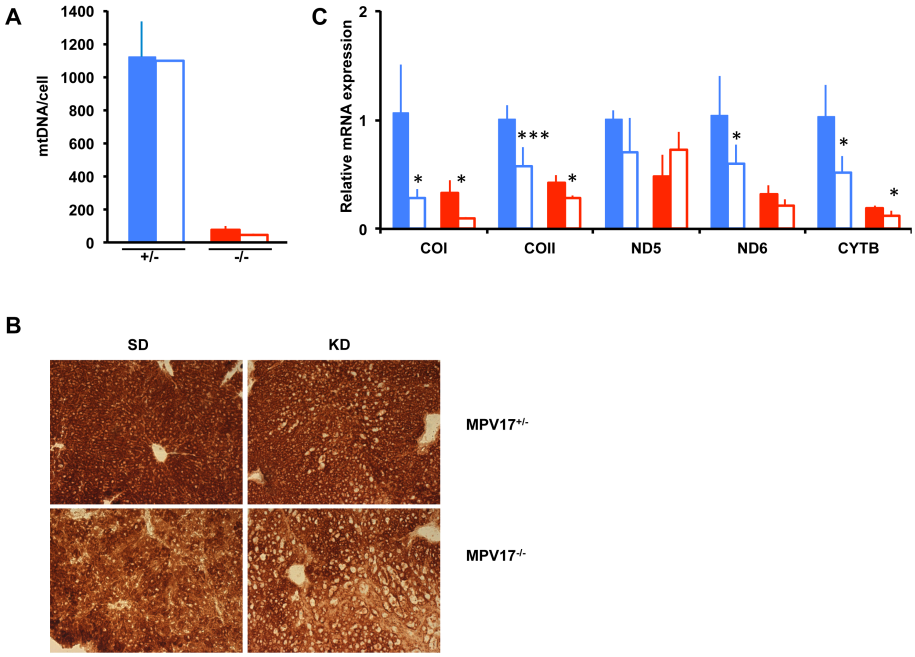

KD does not induce mitochondrial biogenesis in liver. A) MtDNA content analysis in SD- and KD-fed *Mpv17*$^{+/-}$ and *Mpv17*$^{-/-}$ mice. B) COX histochemical staining. Note that COX activity is as much reduced in KD- as in SD-fed animals. C) mRNA transcription analysis. Note that some of the mitochondrial transcripts are significantly reduced in both control and knockout KD-fed mice. Asterisks indicate significance (p) calculated by Mann-Whitney test for unpaired samples: *$p < 0.05$; ***$p < 0.0001$ Colour codes: solid blue: SD-fed *Mpv17*$^{+/-}$ mice; blue outline: KD-fed *Mpv17*$^{+/-}$ mice; solid red: SD-fed *Mpv17*$^{-/-}$ mice; red outline: KD-fed *Mpv17*$^{-/-}$ mice. Bars indicate the standard deviation (SD).

Supplemental Figure 5

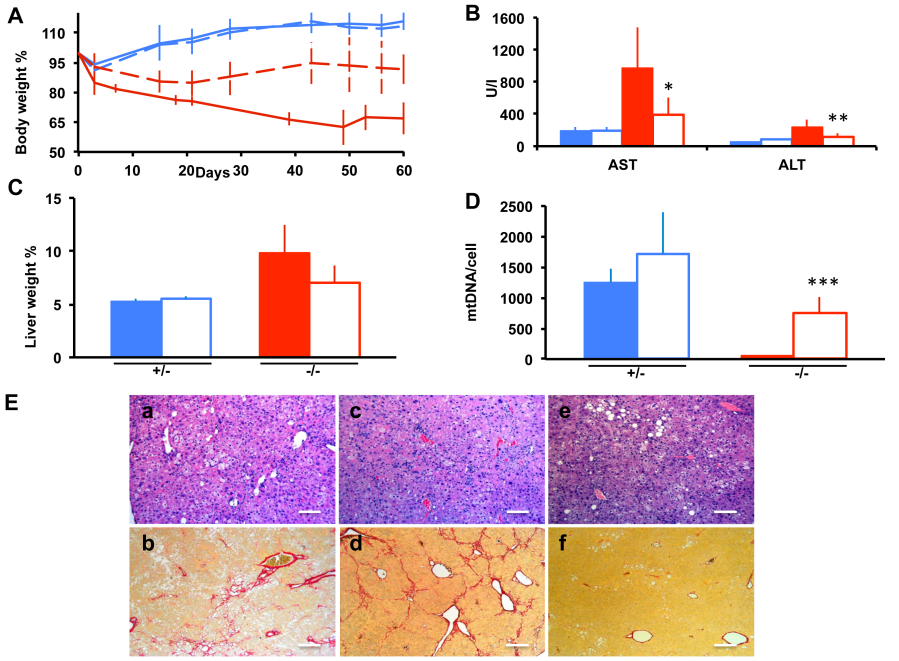

AAV2/8-hMPV17 4x10^{12} vg/Kg partially rescues KD-induced liver damage in *Mpv17*$^{-/-}$ mice. A single retro-orbital injection of 4x10^{12} vg/Kg was performed in two-month old *Mpv17*$^{+/-}$ and *Mpv17*$^{-/-}$ mice. KD was started three weeks later. A) Body weight changes during 2 months of KD in AAV-treated and untreated mice. Solid blue: untreated *Mpv17*$^{+/-}$; dashed blue: AAV-treated *Mpv17*$^{+/-}$; solid red: untreated *Mpv17*$^{-/-}$; dashed red: AAV-treated *Mpv17*$^{-/-}$. B) AST and ALT transaminases levels in plasma. C) Liver weight (% of body weight). Note the non-significant reduction in AAV-treated *Mpv17*$^{-/-}$ mice. D) MtDNA analysis. Note that mtDNA content is AAV-treated *Mpv17*$^{-/-}$ is higher than in untreated littermates, but remains lower than in control littermates. Asterisks indicate significance (p) calculated by the Mann-Whitney test for unpaired samples: *p < 0.05; **p < 0.01; ***p < 0.0001 Colour codes: solid blue: SD-fed *Mpv17*$^{+/-}$ mice; blue outline: KD-fed *Mpv17*$^{+/-}$ mice; solid red: SD-fed *Mpv17*$^{-/-}$ mice; red outline: KD-fed *Mpv17*$^{-/-}$ mice. Bars indicate the standard deviation (SD). E) Histological features on hematoxylin-eosin (a, c, e); picrosirius red (b, d, f) staining. a,b: AAV-treated *Mpv17*$^{-/-}$ show liver steatosis and focal inflammatory infiltrates. There is only a mild increase in fibrosis, without overt cirrhosis. c,d: untreated *Mpv17*$^{-/-}$ with liver steatosis, moderate inflammatory infiltrates and cirrhosis. e,f: Untreated *Mpv17*$^{+/-}$ show only hepatocyte steatosis, in absence of cirrhosis. Scale bars: a, c, e: 150µm, b, d, f: 300µm.

Supplemental Figure 6

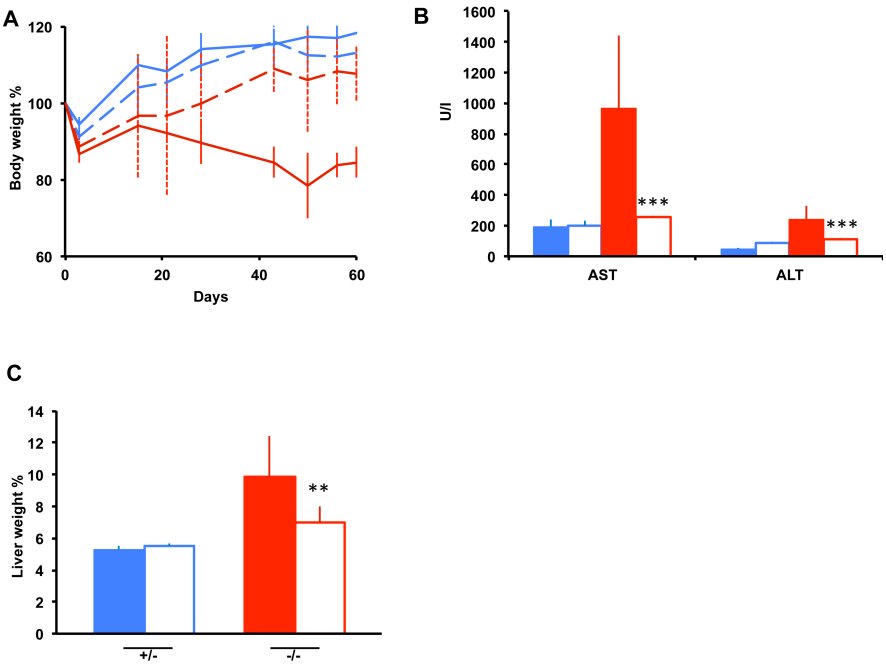

AAV2/8-hMPV17 4 x 10^{13} vg/Kg rescues KD-induced liver damage in *Mpv17*$^{-/-}$ mice. A single retro-orbital injection of 4x1013 vg/Kg was performed in two months old *Mpv17*$^{+/-}$ and *Mpv17*$^{-/-}$ mice. KD was started three weeks later. A) Body weight changes during 2-months of KD in AAV-treated and untreated mice. Solid blue: untreated *Mpv17*$^{+/-}$; dashed blue: AAV-treated *Mpv17*$^{+/-}$; solid red: untreated *Mpv17*$^{-/-}$; dashed red: AAV-treated *Mpv17*$^{-/-}$. B) AST and ALT levels in plasma in AAV-treated and untreated groups. C) Liver weight (% of body weight). Asterisks indicate significance (p) calculated by the Mann-Whitney test for unpaired samples: **p < 0.01; ***p < 0.0001. Colour codes: solid blue: untreated *Mpv17*$^{+/-}$; blue outline: AAV-treated *Mpv17*$^{+/-}$; solid red: untreated *Mpv17*$^{-/-}$; red outline: AAV-treated *Mpv17*$^{-/-}$. Bars indicate the standard deviation (SD).

Supplemental Figure 7

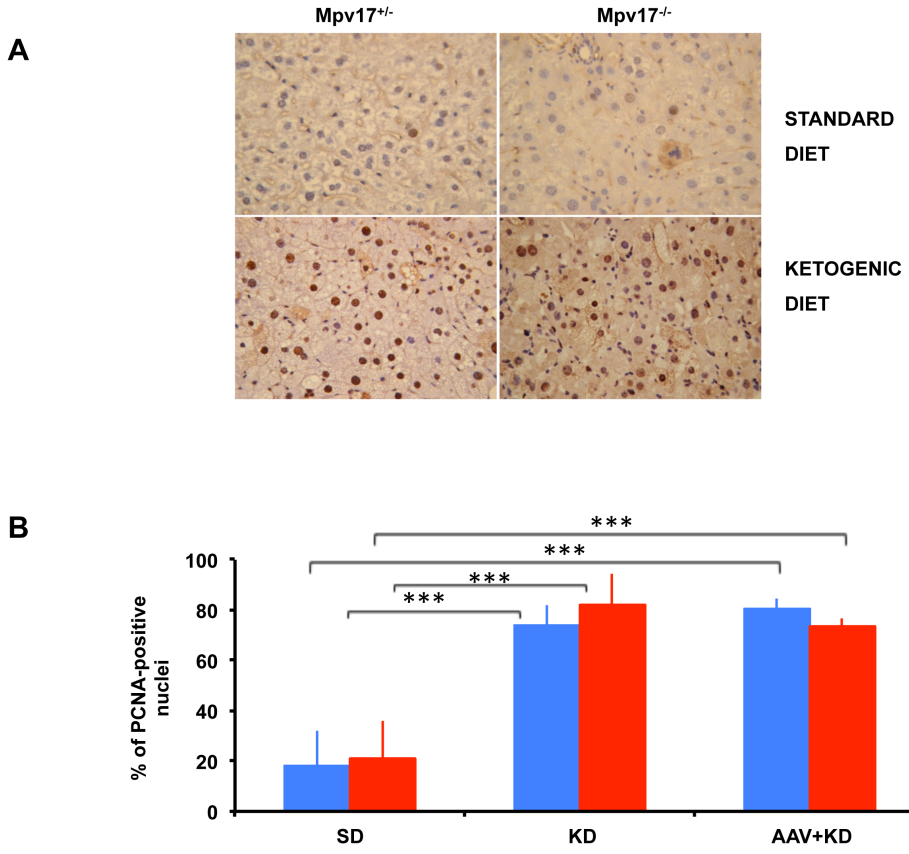

Effect of KD on hepatocytes proliferation. A) PCNA immuno-histochemical staining of SD and KD fed livers. B) quantitation of PCNA-positive nuclei. Colour codes: Solid blue: *Mpv17*$^{+/-}$ mice; solid red: *Mpv17*$^{-/-}$ mice. The bars represent the standard deviation (SD). Asterisks indicate significance (p) calculated by unpaired Student's two-tailed t test: ***p < 0.005.

Supplemental Figure 8

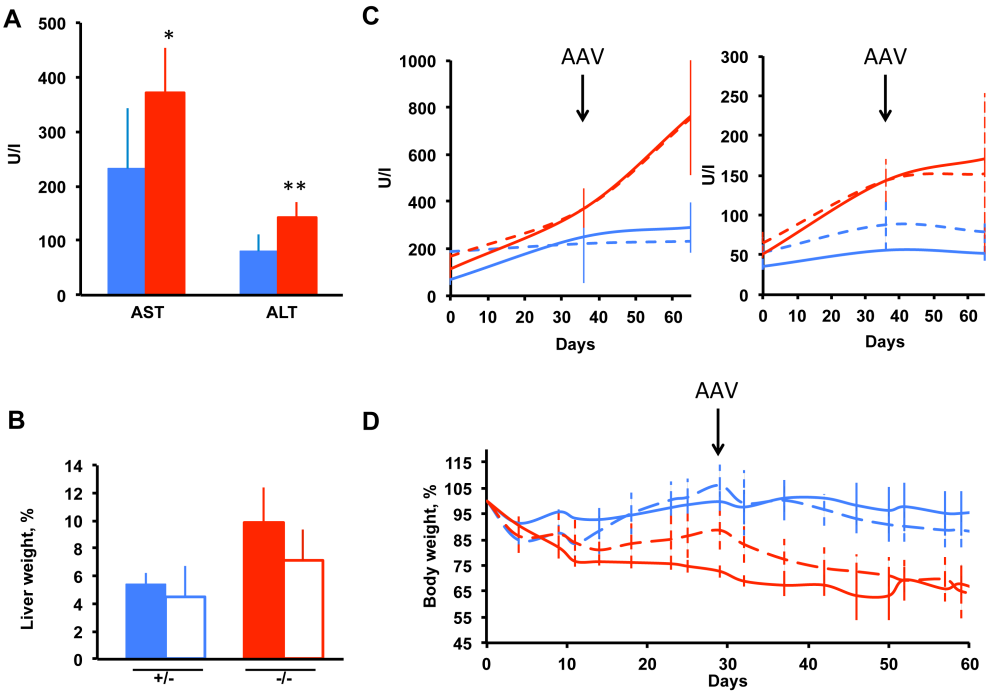

Effects of administration of AAV-hMPV17 in mice pre-treated with KD. A) AST and ALT levels in plasma of *Mpv17*$^{+/-}$ and *Mpv17*$^{-/-}$ animals after one month of KD, just before AAV administration. Asterisks indicate significance (p) calculated by the Mann-Whitney test for unpaired samples: **p < 0.01; ***p < 0.0001. B) Liver weight (% of body weight). Solid blue: untreated *Mpv17*$^{+/-}$, blue outline: AAV-treated *Mpv17*$^{+/-}$, solid red: untreated *Mpv17*$^{-/-}$, red outline: AAV-treated *Mpv17*$^{-/-}$. C) AST (left) and ALT (right) trend during the experimental protocol. The arrow indicates the time point of AAV administration. D) Body weight changes during 2-months of KD in AAV-treated and untreated mice. The arrow indicates the time point of AAV administration. Solid blue: untreated *Mpv17*$^{+/-}$; dashed blue: AAV-treated *Mpv17*$^{+/-}$; solid red: untreated *Mpv17*$^{-/-}$; dashed red: AAV-treated *Mpv17*$^{-/-}$.

References

1. Suomalainen A, Isohanni P (2010) Mitochondria DNA depletion syndromes –many genes, common mechanisms. Neuromusc Disorders 20: 429-437
2. Cohen BH, Naviaux RK (2010) The clinical diagnosis of POLG disease and other mitochondrial DNA depletion syndromes. Methods 51: 364-373
3. Saada A, Shaag A, Mandel H, Nevo Y, Eriksson S, Elpeleg, O (2001) Mutant mitochondrial thymidine kinase in mitochondrial DNA depletion myopathy. Nat Genet 29: 342-344
4. Mandel H, Szargel R, Labay V, Elpeleg O, Saada A, Shalata A et al. (2001). The deoxyguanosine kinase gene is mutated in individuals with depleted hepatocerebral mitochondrial DNA. Nat Genet 29: 337-341
5. Bourdon A, Minai L, Serre V, Jais JP, Sarzi E, Aubert S et al. (2007). Mutation of RRM2B, encoding p53-controlled ribonucleotide reductase (p53R2), causes severe mitochondrial DNA depletion. Nat Genet 39: 776-780
6. Nishino I, Spinazzola A, Hirano M. (1999). Thymidine phosphorylase gene mutations in MNGIE, a human mitochondrial disorder. Science 283: 689-692
7. Ferrari G, Lamantea E, Donati A, Filosto M, Briem E, Carrara F, et al. (2005). Infantile hepatocerebral syndromes associated with mutations in the mitochondrial DNA polymerase-gammaA. Brain 128: 723-731
8. Hakonen AH, Isohanni P, Paetau A, Herva R, Suomalainen A and Lonnqvist T. (2007). Recessive Twinkle mutations in early onset encephalopathy with mtDNA depletion. Brain 130: 3032-3040
9. Spinazzola A, Viscomi C, Fernandez-Vizarra E, Carrara F, D'Adamo P, Calvo S et al. (2006). MPV17 encodes an inner mitochondrial membrane protein and is
mutated in infantile hepatic mitochondrial DNA depletion. Nat Genet 38: 570-575
10. Viscomi C, Spinazzola A, Maggioni M, Fernandez-Vizarra E, Massa V, Pagano
C, et al. (2009). Early-onset liver mtDNA depletion and late-onset proteinuric nephropathy in Mpv17 knockout mice. Hum Mol Genet 18:12-26
11. Wong LJ, Brunetti-Pierri N, Zhang Q, Yazigi N, Bove KE,

Dahms BB et al. (2007) Mutations in the MPV17 gene are responsible for rapidly progressive liver failure in infancy. Hepatology 46: 1218-1227
12. Navarro-Sastre A, Martin-Hernandez E, Campos Y, Quintana E, Medina E, de Las Heras RS et al. (2008). Lethal hepatopathy and leukodystrophy caused by a novel mutation in MPV17 gene: description of an alternative MPV17 spliced form. Mol Genet Metab 94: 234-239
13. Spinazzola A, Santer R, Akman OH, Tsiakas K, Schaefer H, Ding X et al. (2008). Hepatocerebral form of mitochondrial DNA depletion syndrome. Arch Neurol 65: 1-6
14. El-Hattab AW, Li FY, Schmitt E, Zhang S, Craigen WJ, Wong LJ. (2010). MPV17-associated hepatocerebral mitochondrial DNA depletion syndrome: new patients and novel mutations. Mol Genet Metab 99: 300-308
15. Nogueira C, de Souza CF, Husny A, Derks TG, Santorelli FM, Vilarinho L. (2012). MPV17: fatal hepatocerebral presentation in a Brazilian infant. Mol Genet Metab 107: 764
16. AlSaman A, Tomoum H, Invernizzi F, Zeviani M. (2012). Hepatocerebral form of mitochondrial DNA depletion syndrome due to mutation in MPV17 gene. Saudi J Gastroenterol 18: 285-289
17. Dallabona C, Marsano RM, Arzuffi P, Ghezzi D, Mancini P, Zeviani M et al. (2010). Sym1, the yeast ortholog of the MPV17 human disease protein, is a stress induced bioenergetic and morphogenetic mitochondrial modulator. Hum Mol Genet 19: 1098-1107
18. Parini R, Furlan F, Notarangelo L, Spinazzola A, Uziel G, Strisciuglio P, et al. (2009). Glucose metabolism and diet-based prevention of liver dysfunction in MPV17 mutant patients. J Hepatol 50: 215-21
19. Karadimas CL, Vu TH, Holve SA, Chronopoulou P, Quinzii C, Johnsen SD et
al. (2006). Navajo neurohepatopathy is caused by a mutation in the MPV17 gene. Am J Hum Genet 79: 544-548
20. Meyer zum Gottesberge AM, Reuter A, Weiher H. (1996). Inner ear defect similar to Alport's syndrome in the glomerulosclerosis mouse model Mpv17. Eur Arch Otorhinolaryngol 253: 470-474
21. Ng PC, Henikoff S. (2003). SIFT: Predicting amino acid changes that affect protein function. Nucleic Acids Res 31:

3812-3814
22. Di Meo I, Auricchio A, Lamperti C, Burlina A, Viscomi C, Zeviani M (2012) Effective AAV-mediated gene therapy in a mouse model of ethylmalonic encephalopathy. EMBO Mol Med 4:1008-1014
23. Ahola-Erkkilä S, Carroll CJ, Peltola-Mjösund K, Tulkki V, Mattila I, Seppänen-
Laakso T et al. (2010). Ketogenic diet slows down mitochondrial myopathy progression in mice. Hum Mol Genet 19: 1974-1984
24. Wenz T, Luca C, Torraco A, Moraes CT. (2009). mTERF2 regulates oxidative
phosphorylation by modulating mtDNA transcription. Cell Metab 9: 499-511
25. Nakai H, Yant SR, Storm TA, Fuess S, Meuse L, Kay MA. (2001). Extrachromosomal recombinant adeno-associated virus vector genomes are primarily responsible for stable liver transduction in vivo. J Virol 75: 6969-6976
26. Pritchard MT, Malinak RN, Nagy LE. (2011). Early growth response (EGR)-1 is required for timely cell-cycle entry and progression in hepatocytes after acute carbon tetrachloride exposure in mice. Am J Physiol Gastrointest Liver Physiol 300: 1124-1131
27. Reinhold R, Krüger V, Meinecke M, Schulz C, Schmidt B, Grunau SD et al. (2012). The channel-forming Sym1 protein is transported by the TIM23 complex in a presequence-independent manner. Mol Cell Biol 32:5009-21.
28. Sobrevals L, Enguita M, Rodriguez C, Gonzalez-Rojas J, Alzaguren P, Razquin N et al. (2012). AAV vectors transduce hepatocytes in vivo as efficiently in cirrhotic as in healthy rat livers. Gene Ther 19: 411-417
29. Tessitore A, Faella A, O'Malley T, Cotugno G, Doria M, Kunieda T et al. (2008) Biochemical, pathological, and skeletal improvement of mucopolysaccharidosis VI after gene transfer to liver but not to muscle. Mol Ther 16:30-37
30. Chandler RJ, Venditti CP. (2010). Long-term rescue of a lethal murine model of methylmalonic acidemia using adeno-associated viral gene therapy. Mol Ther. 1: 11-16
31. Moscioni D, Morizono H, McCarter RJ, Stern A, Cabrera-Luque J, Hoang A et al. (2006). Long-term correction of ammonia metabolism and prolonged survival in ornithine transcarbamylase-deficient mice following liver-directed

treatment with adeno-associated viral vectors. Mol Ther 14: 25-33
32. Cotugno G, Annunziata P, Tessitore A, O'Malley T, Capalbo A, Faella A et al. (2011). Long-term amelioration of feline Mucopolysaccharidosis VI after AAV mediated liver gene transfer. Mol Ther 19: 461-469
33. Nathwani AC, Tuddenham EG, Rangarajan S, Rosales C, McIntosh J, Linch DC et al. (2012). N Engl J Med 365: 2357-2365
34. Xiao W, Chirmule N, Berta SC, McCullough B, Gao G, Wilson JM. (1999). Gene therapy vectors based on adeno-associated virus type 1. J Virol 73: 3994- 400
35. Gao G, Qu G, Burnham MS, Huang J, Chirmule N, Joshi B et al. (2000). Purification of recombinant adeno-associated virus vectors by column chromatography and its performance in vivo. Hum Gene Ther 11: 2079-2091
36. Viscomi C, Bottani E, Civiletto G, Cerutti R, Moggio M, Fagiolari G et al. (2011). In vivo correction of COX deficiency by activation of the AMPK/PGC-1α axis. Cell Metab 14:80-90
37. Bugiani M, Invernizzi F, Alberio S, Briem E, Lamantea E, Carrara F et al. (2004) Clinical and molecular findings in children with complex I deficiency. Biochim Biophys Acta 1659: 136-147
38. Sciacco M, Bonilla E. (1996). Cytochemistry and immunocytochemistry of mitochondria in tissue sections. Methods Enzymol 264:509-521
39. Fernández-Vizarra E, López-Pérez MJ, Enriquez JA. (2002). Isolation of biogenetically competent mitochondria from mammalian tissues and cultured cells. Methods 26: 292-297
40. Schägger H, von Jagow G. (1987). Tricine-sodium dodecyl sulfatepolyacrylamide gel electrophoresis for the separation of proteins in the range from 1 to 100 kDa. Anal Biochem 166: 368-379

Acknowledgments

This work was supported by the Pierfranco and Luisa Mariani Foundation Italy, Telethon-Italy GPP10005 and GGP11011 (to MZ), Cariplo 2011-0526 (to MZ), European Research Council Grant ERC-322424 (to MZ), and The Italian Ministry of Health Research Grant, GR-2010-2306-756 (to CV). We wish to thank dr Daniele Ghezzi for helpful discussion.

Chapter 4

Emerging concepts in the therapy of mitochondrial disease

Review

Carlo Viscomi[a,b,], **Emanuela Bottani[b]**, Massimo Zeviani[a,b,]

[a]Unit of Molecular Neurogenetics, The Foundation "Carlo Besta" Institute of Neurology IRCCS, 20133 Milan, Italy

[b] MRC-Mitochondrial Biology Unit, Cambridge CB20XY, UK

Biochimica et Biophysica Acta 1847 (2015) 544–557

Abstract

Mitochondrial disorders are an important group of genetic conditions characterized by impaired oxidative phosphorylation. Mitochondrial disorders come with an impressive variability of symptoms, organ involvement, and clinical course, which considerably impact the quality of life and quite often shorten the lifespan expectancy. Although the last 20 years have witnessed an exponential increase in understanding the genetic and biochemical mechanisms leading to disease, this has not resulted in the development of effective therapeutic approaches, amenable of improving clinical course and outcome of these conditions to any significant extent. Therapeutic options for mitochondrial diseases still remain focused on supportive interventions aimed at relieving complications. However, new therapeutic strategies have recently been emerging, some of which have shown potential efficacy at the pre-clinical level. This review will present the state of the art on experimental therapy for mitochondrial disorders.

1. Introduction

1.1. Basic concepts of mitochondrial biology and medicine

Mitochondria are semi-autonomous double-membrane organelles, the inner membrane being folded to form mitochondrial cristae, where respiratory chain (RC) complexes reside. The main role of mitochondria is to extract energy from nutrients through respiration, and convert it into heat, or store it as ATP, the energy currency of cells. This is ultimately carried out by the respiratory chain (RC), through a process termed oxidative phosphorylation (OXPHOS). Respiration is performed by four multiheteromeric RC complexes, CI–IV, that transfer the electrons stripped off from nutrient-derived substrates as hydrogen atoms, to molecular oxygen. Electrons are conveyed to the RC through redox shuttle moieties, NADH + H+ for complex I, $FADH_2$ for complex II. This electron flow is coupled with the translocation of protons across the inner mitochondrial membrane from the matrix to the intermembrane space, operated by complexes I, III and IV, generating an electrochemical gradient which is then exploited by RC complex V (or ATP synthase) to carry out the condensation of ADP and Pi into ATP [1]. Mitochondria have their own DNA (mtDNA), a maternally inherited, double-stranded circular molecule of 16.5 kb in mammals, encoding 13 subunits of the RC complexes I, III, IV and V (complex II is composed of four nucleus-encoded subunit with no contribution from mtDNA). In addition, mtDNA contains 22 tRNAs, and 2 rRNA genes, which form the RNA

apparatus serving the in situ translation of the 13 mtDNA-encoded respiratory chain subunits. MtDNA is present in hundreds to thousands of copies in the different cell types in an individual. In normal individuals, mtDNAs are all identical to each other, a condition termed homoplasmy. However, pathogenic mtDNA mutations are frequently co-existing in variable amount with wild-type mtDNA molecules, a condition termed heteroplasmy. The rest of the mitochondrial proteome, which is estimated to consist of approximately 1500 polypeptides, is encoded by nuclear genes, translated in the cytosol into proteins, which are eventually targeted to and imported into the organelles by an active process.

Complex I (NADH-ubiquinone oxidoreductase) contains seven mtDNA-encoded subunits (ND1–ND6 and ND4L) and at least 37 nucleus-encoded subunits of complex I; electrons are transferred from NADH, the main redox shuttle of pyruvate dehydrogenase and TCA cycle, onto a hydrophobic mobile electron carrier, ubiquinone (coenzyme Q, CoQ). Complex II (succinate-ubiquinone oxidoreductase) is composed of only four subunits, all encoded by the nuclear genome and transfers electrons from $FADH_2$, mainly derived from beta-oxidation of fatty acids, to CoQ. Complex III (ubiquinol-ferricytochrome c oxidoreductase) has a single mtDNA-encoded subunit, apocytochrome b, and 10 subunits encoded by the nuclear genome. Complex III transfers electrons from CoQ to another electron shuttle, cytochrome c, which in turn transfers them to complex IV. Complex IV (cytochrome c oxidase, COX), which is

composed of three mtDNA-encoded and 11 nucleus-encoded subunits, transfers electrons to molecular oxygen, with the formation of water. Complex V (oligomycin-sensitive ATP synthase), which utilizes the energy potential of the electrochemical gradient to carry out ATP synthesis, is composed of two mtDNA-encoded subunits (ATPase 6 and 8), and at least 13 nuclear DNA-encoded subunits. These subunits are arranged to form two distinct particles. The membrane-embedded F0 particle constitutes a rotor operated by protons flowing through it. The rotation of this structure is transmitted to the matrix-protruding F1 particle, which catalyses the biosynthesis of ATP [2].

Numerous specific assembly factors and chaperons are needed to assemble the protein backbone, insert suitable prosthetic groups and metal-containing reactive centres and form each holocomplex [3].

Other components of the mitochondrial proteome are required for a huge array of biological processes, including replication, transcription, and translation of the mtDNA, formation and assembly of the respiratory chain complexes, fission–fusion of the mitochondrial network, signalling and execution pathways (e.g. ROS production and apoptosis), scavenging of toxic compounds, and many other metabolic processes, as diverse as fatty acid oxidation, biosynthesis of pyrimidines, heme, and Fe–S clusters, etc.

From a genetic standpoint, primary mitochondrial diseases can be classified into two major categories, depending on which

genome, mitochondrial or nuclear, carries the responsible mutations. MtDNA mutations include point mutations, either homo- or heteroplasmic, and (invariably heteroplasmic) large-scale rearrangements. Heteroplasmic point mutations have been found in all mitochondrial genes, and lead to different clinical phenotypes, including some canonical syndromes such as mitochondrial encephalomyopathy with lactic acidosis and stroke-like episodes (MELAS) [4], myoclonic epilepsy with ragged red fibres (MERRF) [5], neurogenic weakness, ataxia and retinitis pigmentosa (NARP) [6], and Leigh syndrome (LS). The main disease entity associated with homoplasmic mtDNA mutations is Leber's hereditary optic neuropathy (LHON) [7]. Rearrangements (single deletions or duplications) of mtDNA are responsible for sporadic progressive external ophthalmoplegia (PEO) [8], Kearns–Sayre syndrome (KSS) [8], and Pearson's syndrome [9].

Nuclear mutations have been found in a huge number of genes directly or indirectly related to the respiratory chain, encoding, for instance, (i) proteins involved in mtDNA maintenance and/or replication machinery; (ii) structural subunits of the respiratory chain complexes; (iii) assembly factors of the respiratory complexes; (iv) components of the translation apparatus; and (v) proteins of the execution pathways, such as fission/fusion and apoptosis (see [10] for an exhaustive list).

Mitochondrial diseases are hallmarked by huge clinical, biochemical and genetic heterogeneity, which hampers the collection of homogeneous cohorts of patients to establish the

efficacy of a treatment. For instance, clinical outcomes in primary coenzyme Q deficiency span from encephalomyopathy, multisystem disease, cerebellar ataxia, isolated myopathy and nephrotic syndrome [11]. For unknown reasons only 20% of the patients respond to CoQ_{10}, the only available therapy [11]. Studies in cellular models suggest that the slow pharmacokinetics of CoQ_{10} can explain the different responses observed in humans, but more studies are needed to clarify this issue. Similarly, riboflavin is effective in some cases of mitochondrial disease due to mutations in genes encoding FMN- or FAD-dependent proteins such as NDUFV1 (the FMN binding subunit of complex I), AIFM1, ACAD9 [12,13], and SDHA (the FAD binding subunit of complex II). However, not all patients respond to riboflavin supplementation [14].

1.2. Experimental therapeutic strategies

Remarkable progress has been made in recent years on understanding both the fundamental pathogenic processes underlying mitochondrial disease, and the mechanisms of mitochondrial biogenesis and signalling. Based on this knowledge, sensible therapeutic strategies have recently been proposed to combat mitochondrial disorders, for which experimental evidence is accumulating in cellular and animal models. These can be broadly divided in “generalist” strategies, which could in principle be applied to a wide spectrum of different disease conditions, and “disease-tailored” strategies, applicable to a single disease (Table 1). The first group

includes: (i) regulation/activation of mitochondrial biogenesis; (ii) regulation/activation of mitochondrial autophagy; (iii) inhibition of mitochondrial apoptosis; (iv) scavenging of toxic compounds; (v) bypass of electron transfer chain defects; and (vi) nuclear transfer. The second group includes (i) scavenging of specific toxic compounds in specific diseases, (ii) supplementation of nucleotides, and (iii) gene- and cell-replacement therapies. Each of these strategies can be pursued by different approaches, such as pharmacological treatments, gene transfer to express the missing or a therapeutic protein, stem-cell/organ transplantation.

Table 1: Summary of the experimental therapies for mitochondrial diseases.

	Strategy	**Method**
Generalist	Activation of mitochondrial biogenesis Modulation of autophagy Inhibition of apoptosis Scavenging of ROS Endurance training Dietary manipulation	Pharmacology
	By-passing RC block ZFNs orTALENs to shift heteroplasmy Overexpressing aaRSs to stabilize mutated mt-RNA Somatic nuclear transfer	AAV-mediated gene therapy
Disease-tailored	Scavenging of toxic compounds Supplementation of nucleotides	Pharmacology
	Replacement of the missing gene	AAV-mediated gene therapy

This review will focus on emerging experimental (i.e. pre-clinical) therapies for mitochondrial disease. Ongoing clinical trials have recently been reviewed elsewhere [15].

2. Pharmacological and metabolic interventions

2.1. Increasing mitochondrial biogenesis

Mitochondrial diseases are hallmarked by bioenergetics defects, ultimately leading to decreased ATP synthesis. Thus, therapeutic interventions aimed at increasing the ATP levels available to cells may be beneficial. Importantly, mitochondrial disease become manifest when the residual activity of the defective gene product, either mitochondrial or nuclear encoded, falls below a critical threshold, suggesting that even partial restoration of the activity may be sufficient to rescue or at least ameliorate the phenotype. The idea that mitochondrial biogenesis is critical to determine the phenotypic outcome of disease has been boosted by the recent observation that increased mitochondrial content protects non-manifesting carriers of the LHON mutations. This can partly explain the incomplete penetrance of the disease and opens the possibility to stimulate mitochondrial biogenesis as a therapeutic strategy for LHON [16].

Increased mitochondrial biogenesis is a physiological response to stress conditions (e.g.: cold, exercise, nutritional status), which is activated to meet the energetic requirements of tissues [17].

The pathways controlling mitochondrial biogenesis (Figure 1) have mainly been investigated in skeletal muscle and brown adipose tissue, and shown to rely, in most of the cases, on the peroxisome proliferator-activated receptor gamma (PPARγ)

coactivators 1α and β (the PGC family). PGC proteins interact with and activate several transcription factors, including the Nuclear Respiratory Factors (NRF1 and 2), and the Peroxisomal Proliferator Activator receptors (PPAR α, β, and γ) among others. NRFs and PPARs in turn increase the transcription of genes related to oxidative phosphorylation (OXPHOS) and fatty acid oxidation (FAO) pathways, respectively. PGC-1α is the best characterized PGC protein. Its activity is inhibited by acetylation, which in turn is controlled by the acetylase GCN5 and deacetylase SIRT1, and is increased by phosphorylation, which depends on the activities of several kinases, including p38 MAPK, glycogen synthase kinase 3b (GSK3b) and AMP-dependent kinase (AMPK) [18,19]. Importantly, as AMPK and SIRT1 are druggable enzymes, they have been exploited in several pre-clinical experiments to activate PGC-1α and induce mitochondrial biogenesis.

The idea that increasing the amount and/or function of mitochondria could be beneficial in mitochondrial disease was tested by treating fibroblasts from patients with different mitochondrial diseases with bezafibrate [19], a pan-PPAR agonist widely used to treat metabolic syndrome and diabetes. This treatment led to an improvement in the defective activities of the respiratory chain complexes, dependent on the induction of PGC-1α activity. These findings were subsequently reinforced by in vivo observations reported by Wenz et al. [20], who used both a muscle-specific PGC-1α transgenic mouse and bezafibrate to improve the motor performance of a muscle-

specific knockout mouse for Cox10, a farnesyltransferase involved in the biosynthesis of COX-specific heme a. Notably, this effect was not due to restoration of COX activity in isolated mitochondria but to increased mitochondrial content, which determined an overall increase in ATP availability in the muscle fibers. It is unclear why the stimulation of mitochondrial biogenesis caused by genetic or pharmacological induction of PGC-1α seems more effective than that spontaneously occurring in pathological conditions such as for instance, ragged-red fibers. One hypothesis is that while the mitochondriogenic pathway is activated only in highly mutated, bioenergetically spent mitochondria clustering in ragged red fibers, the mitochondrial biogenetic activation through pharmacological modulation of PGC-1α is generalized and involves also OXPHOS proficient mitochondria, which can then exert effective functional complementation along the entire muscle fiber [20]. A second beneficial effect of PGC-1α activation is the switch towards oxidative fiber types, which increases the energetic efficiency of the tissue [21].

Beneficial effects of bezafibrate were also reported in cybrids harbouring pathological tRNA mutations [22] and in the nervous tissue of a brain-specific Cox10 knockout mouse [23]. However, these results failed to be confirmed in subsequent studies, including bezafibrate treatment of three mouse models of COX deficiency [24–26].

The reason(s) of these discrepant results are unclear. PGC-1α seems to act predominantly upstream of the PPAR receptors,

i.e. as a co-activator of the PPAR-dependent pathways, rather than being induced by PPARs, although work in a reporter-gene system in cultured cells has shown that overexpressed PPARs can indeed bind to a PPAR-responsive element in the promoter of PGC-1α gene, and increase the reporter gene transcription [27]. However, these results are based on highly engineered recombinant systems in cells, and have never been confirmed in animal models [28–30].

An alternative pathway to induce PGC-1α dependent mitochondriogenesis is centered on the activation of the AMP-dependent kinase (AMPK). By using the AMPK agonist AICAR Viscomi et al. obtained robust induction of OXPHOS-related gene transcription and increase of respiratory chain complex activities in three models of COX deficiency, a Surf1 constitutive knockout mouse (Surf1$^{-/-}$), a Sco2 knockout/knockin (Sco2KOKI) mouse and a muscle-specific Cox15 (ACTA-Cox15$^{-/-}$) mouse [24]. The increase in the respiratory chain activities resulted in striking improvement of motor endurance in the Sco2KOKI, but not in ACTA- Cox15$^{-/-}$mice. This difference is likely related to the more severe clinical phenotype of the ACTA-Cox15$^{-/-}$mouse model, which could not be corrected in spite of a clear, albeit partial, rescue of COX activity. In keeping with this, we observed a partial but transient increase of the motor performance in muscle-specific KO mice when the treatment with AICAR was started early during the disease course, i.e. at 4 weeks of age. Notably, ACTA-Cox15$^{-/-}$mice overexpressing PGC-1α (TgPGC-1α) also showed improved

motor performance compared to naive ACTA-Cox15$^{-/-}$littermates, but this effect was transient and, at 6 months of age, both ACTA-Cox15$^{-/-}$and ACTA-Cox15$^{-/-}$–Tg-PGC-1α mice were able to run only for a few minutes on a treadmill, suggesting that PGC-1α delayed, but did not arrest, the disease progression (Bottani et al , unpublished). Interestingly, Saada and colleagues [31] found that AICAR was the most effective compound in inducing mitochondrial biogenesis in complex I deficient cells, whereas bezafibrate gave erratic results, as already reported by Bastin et al. [19] and also observed by us in either mutant cells (Bottani et al, unpublished) or mouse models [24]. A single report showed that bezafibrate can rescue the COX-defect of SCO2 mutant fibroblasts [32]. However, analysis of OxPhos activities and Seahorse oxygen consumption carried out in our lab failed to show any beneficial effect of bezafibrate on a fibroblast cell line from a SCO2 mutant patient and in Sco2KOKI MEFs (Bottani et al, unpublished). Finally, Bastin et al. [33] reported an increase of OXPHOS markers in bezafibrate-treated CPT2-mutant patients, but no evidence of efficacy in mitochondrial disease patients has so far been reported.

A further strategy to activate PGC-1α is to promote its deacetylation via Sirtuin 1 (Sirt1). Sirt1 is a nuclear deacetylase that utilizes the NAD^+ moiety to deacetylate acetyl-lysine residues of proteins. Notably, NAD^+ exerts a substrate-dependent activation of Sirt1, which has homeostatic significance, setting up mitochondrial biogenesis to NAD^+

availability. We recently showed that the NAD^+ pool can be increased by diet supplementation with its natural precursor nicotinamide riboside (NR) or by genetic or pharmacological inhibition of poly(ADP) ribosyl-polymerase 1 (Parp1), a NAD^+ consumer and Sirt1 competitor. These treatments lead to activation of Sirt1 (and other sirtuins) and boost mitochondrial respiration by inducing OXPHOS genes via the PGC-1α axis [34]. As a result, Sco2KOKI mice showed improved motor performance up to normal values. NR was also effective in delaying the disease progression of the deletor mouse, another model of mitochondrial myopathy due to expression of a mutant variant of Twinkle, the mtDNA helicase. Also in this model, NR induced robust mitochondrial biogenesis, corrected abnormalities of mitochondrial ultrastructure, and prevented the generation of multiple mtDNA rearrangements [35]. Importantly, both studies showed that NR also induced the mitochondrial unfolded protein response (UPR^{mt}). UPR^{mt} is a stress response that activates transcription of mitochondrial chaperones to preserve protein homeostasis within the organelle (see [36–38] for extensive review). These observations suggest the involvement of UPRmt in the protective effects provided by NR. In addition, we found that PARP-inhibitors partially improved COX deficiency also in the brain, raising the possibility for their use to target neurological defects.

Taken together these findings open the exciting perspective to use a single therapeutic strategy to target a wide spectrum of genetically heterogeneous mitochondrial diseases. However,

more work is warranted to refine and optimize the most effective strategies. For instance, bezafibrate gave highly variable and poorly reproducible results, and AICAR, although highly effective and widely used in experimental work, has a short half-life after intravenous administration (1.4–2.2 h), poor bioavailability after oral ingestion (less than 5%) and causes increased blood levels of lactic acid and uric acid, making it a poor candidate for long-term use [39,40].

Conversely, the possibility to transfer into clinical practice the supplementation with NR (or other NAD^+ precursors) and the administration of PARP inhibitors (PARPi), seem to be more realistic options. NR is a natural compound, in fact part of vitamin B3, enriched in maternal milk, and several PARPis are currently under clinical trial as anticancer therapeutic agents [41]. However, so far the effects of these compounds have been investigated in a limited number of mouse models of mitochondrial disease. Longer-term treatments and studies in different disease models are needed to confirm efficacy and prompt their use in clinical trials. In addition, the potential mutagenic effects of PARPis in non-cancer patients are still to be adequately investigated, although a long-term study in mouse models of diet-induced obesity, and data in patients treated with Olaparib (AZD-2281) [42], both suggest limited genomic toxicity [43]. Resveratrol (RSV) is another compound reported to trigger mitochondrial biogenesis in several animal models, including *Caenorhabditis elegans*, *Drosophila melanogaster* and *Mus musculus*. The mechanism by which

RSV activates mitochondrial biogenesis is still debated. The common idea that RSV operates via direct activation of Sirt1 has been recently challenged by showing that in fact RSV inhibits phosphodiesterase IV [44]. The consequent raise in cAMP levels triggers a Ca^{2+}–calmodulin–kinase–kinase–β-signalling pathway, leading to the activation of AMPK. In addition, Lopes Costa and colleagues [45] have provided some evidence that RSV can correct complex I and IV defects in human fibroblasts via Sirt1- and AMPK-independent mechanisms, which involve estrogen receptor (ER) and estrogen-related receptor alpha (ERRα).

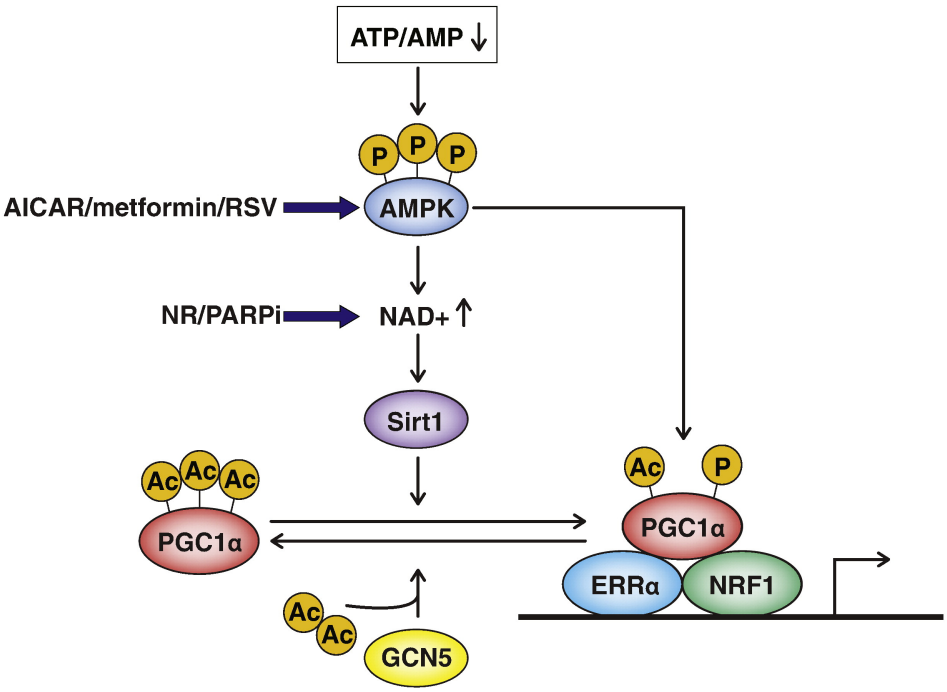

Figure 1: PGC1α-dependent mitochondriogenic pathway and its pharmacological modulation.

These are nuclear receptors co-activated by PGC-1α and β, which upregulate mitochondriogenic pathways [46]. Wenz and colleagues [47] reported that RSV and metformin, a biguanide largely used in diabetes therapy, both stabilize mitochondrial respiratory chain supercomplexes, without increasing mitochondrial protein content in cells.

Finally, the stimulation of the retinoid X receptor-α (RXRα) by retinoic acid has been shown to correct the OXPHOS defects in cybrid cells containing different loads of the 3243A>G MELAS mutation, possibly by increasing the RXRA–PGC-1α interaction [48]. Further work is required to determine whether this also applies to other types of mtDNA or nDNA mutations.

2.2. Endurance training

Endurance training has also been exploited to trigger mitochondrial biogenesis, and shown to delay the effects of aging in mice [22,49]. In addition to PGC-1α activation, endurance training seems to activate PGC-1β, as well as AMPK, p38γ MAPK, and the hypoxia inducible factors (HIFs) [50]. Notably, recent data showed that double PGC-1α and -1β knockout mice had reduced respiration but normal mitochondrial content and morphology, normal muscle fibers composition and normal endurance performance [51]. This work challenges the central role of PGC-1 proteins in regulating mitochondrial content but the decrease of respiratory capacity indicates an effect of the system in setting OxPhos proficiency. Irrespective of the molecular mechanism, endurance exercise

has been reported as beneficial and safe in patients affected by mitochondrial myopathy [52–54], in muscle-specific Cox10 knockout mice [55], and in the mtDNA mutator mice, where it appears to rescue progeroid aging [49]. Importantly, these beneficial effects were not limited to skeletal muscle but also involved other organs, including the brain.

2.3. Scavenging toxic compounds

Pharmacological interventions have been used to modify the course of specific mitochondrial diseases characterized by metabolic blocks in mitochondria, which lead to accumulation of toxic substances. A first example is the use of N-acetylcysteine (NAC) and metronidazole to dump high levels of hydrogen sulfide (H_2S) characteristic of ethylmalonic encephalopathy (EE) [56]. EE is a devastating, multisystem disease of infancy due to mutations in ETHE1, a gene encoding a mitochondrial sulfur dioxygenase (SDO) involved in the disposal of H_2S. H_2S is produced by the catabolism of sulfurated amino acids in tissues and by the anaerobic bacterial flora in the large intestine, and in concentrations above nanomolar is highly toxic, leading to profound inhibition of the terminal segment of fatty acids beta oxidation and, more importantly, COX, and direct damage to endothelial lining of small vessels [57]. Accumulation of H_2S then causes a generalized microvasculopathy and COX deficiency, with multiple organ damage, including brain, skin (with petechial purpura and orthostatic acrocyanosis), skeletal muscle and large intestine. The first step of H_2S metabolism

(Figure 2) is catalyzed by sulfide:quinone oxido-reductase (SQOR) to form thiosulfate (SSO_3^{2-}) using sulfite (SO_3^{2-}) as an acceptor for the sulfur sulfane (HS^-) moiety of H_2S ($H_2S + SO_3^{2-} + 2e^- \rightarrow SSO_3^{2-}$). Thiosulfate is the substrate of thiosulfate:sulfur transferase (TST) [58], which uses reduced glutathione (GSH) to transfer its sulfane sulphur to form glutathione persulfide (GSS^-), whereas the rest of the molecule generates sulfite, which is thus recycled ($SSO_3^{2-} + GS^- \rightarrow GSS^- + SO_3^{2-}$). The GSS−persulfide is then oxidized by the sulfur dioxygenase activity (SDO) encoded by ETHE1 to produce sulfite and reduced glutathione ($GSS^- + O_2 + H2O \rightarrow GS^- + SO_3^{2-}$). SO_3^{2-} can thus be either oxidized to sulfate (SO_4^{2-}) through the sulfite oxidase (SO) (in the liver) or be recycled through SQOR (in extra-hepatic tissues). NAC is a cell-permeable precursor of GSH, which can act as an intracellular H_2S buffer. Metronidazole is an antibiotic specifically active against H_2S-producing anaerobic bacteria and protozoa. Administration of NAC and metronidazole significantly prolonged the lifespan and clinical conditions of an *Ethe1*$^{-/-}$ mouse model, when administered singly or, more effectively, in combination [56]. The same compounds were also effective in a cohort of EE patients, ameliorating some of the clinical hallmarks of the disease, including chronic diarrhea, and diffuse microvasculopathy with acrocyanosis. Some signs of CNS involvement were also improved, leading to increased alertness and wakefulness, and decreased number and duration of epileptic seizures [56].

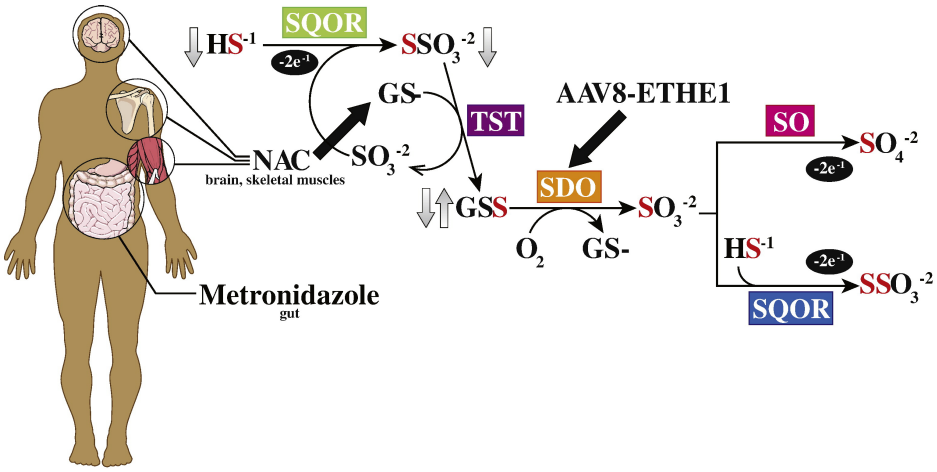

Figure 2. Metabolism of H_2S and therapeutic interventions

Reactive oxygen species (ROS), generated as by-products of mitochondrial respiration, play a double role, as they may be potentially harmful but are also important signalling molecules in a number of pathways including adaptation to hypoxia, regulation of autophagy, control of immunological responses, promotion of cell differentiation, and set-up of longevity (Figure 3) [59,60]. Within mitochondria, highly reactive superoxide (O_2^-) is produced at several sites in the matrix and intermembrane space, including the flavin moiety of complex I, the ubiquinone-binding sites in complex III, glycerol 3-phosphate dehydrogenase, the electron transferring flavoprotein:Q oxidoreductase (ETFQOR) of fatty acids and branched-chain amino acid oxidation, and pyruvate and 2-oxoglutarate dehydrogenases [61]. O_2^- is rapidly converted into the much less harmful hydrogen peroxide (H_2O_2) by the mitochondrial manganese superoxide dismutase (SOD2) [60]. H_2O_2 can

diffuse through both inner and outer mitochondrial membranes and access the cytosol or can be converted to water by mitochondrial glutathione peroxidases (GPX) or peroxiredoxins (PRX) [60]. On the other hand, superoxide produced in the intermembrane space can exit the mitochondria and be converted into hydrogen peroxide in the cytosol by copper superoxide dismutase (SOD1). Cytosolic H_2O_2 is believed to be the main form of ROS with signalling function in the cell as it can oxidize protein thiol residues. Its levels are tightly regulated by reduction to water, operated by cytosolic GPXs and PRXs and peroxisomal catalase [60]. Increased ROS production occurs as a consequence of respiratory chain dysfunction due to, for instance, aging [62] or specific OXPHOS defects [63], and may lead to damage of cellular structures, including proteins, lipids and nucleic acids. These observations constitute the rational basis for the use of antioxidants in the therapy of mitochondrial diseases. At the same time, however, ROS can transduce signals in a number of pathways [59]. Cocktails of antioxidant compounds, including lipoic acid, vitamins C and E, and CoQ, have extensively been used in the therapy of mitochondrial diseases for a long time, but no quantitative studies have been carried out in animal models to validate their use. Likewise, randomized double blind trials are still missing to support their efficacy in patients [1,15]. In addition, although a transgenic mouse overexpressing a mitochondrially-targeted catalase shows increased lifespan and resistance to oxidative damage [64], the efficacy of antioxidants in cellular and/or

animal models of OXPHOS defects is still controversial. However, two recent papers underline the importance of ROS overproduction in the pathogenesis of cI-related Leigh syndrome [65] and a potential therapeutic target in cI-related disorders in cell models [66].

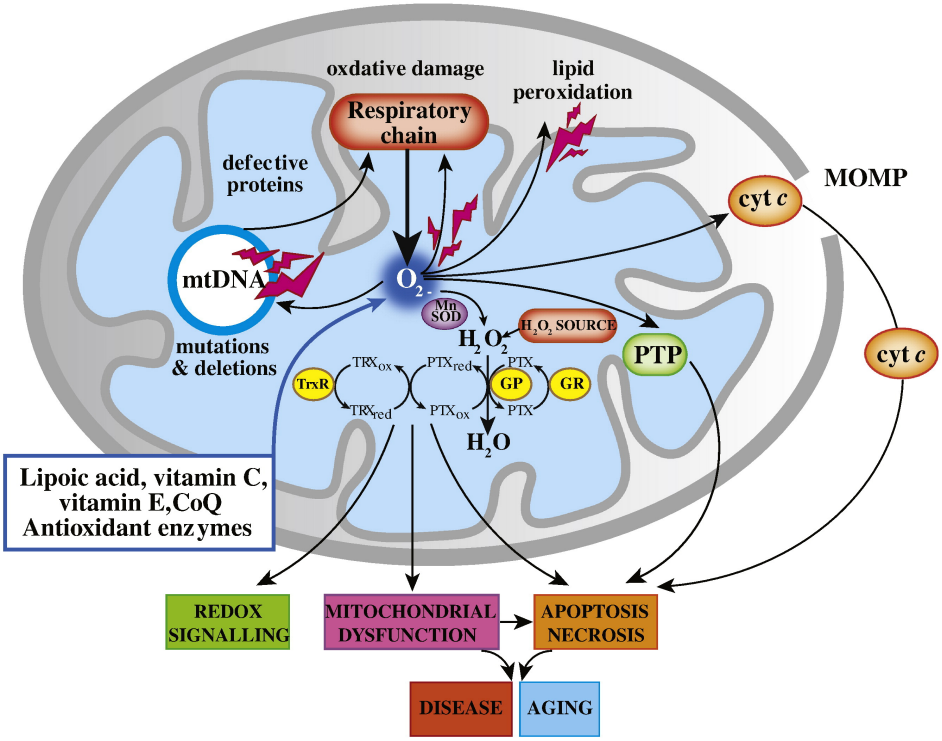

Figure 3. ROS production and detoxification.

2.4. Supplementation of nucleotides

Supplementation of deoxyribonucleotides can effectively correct mtDNA depletion in patients' fibroblasts carrying mutations in enzymes involved in the control of the mitochondrial nucleotide and deoxynucleotide pools (e.g. deoxy-guanosine kinase, dGK,

and thymidine phosphorylase, TP, encoded by the DGUOK and TYMP genes respectively).

Likewise, mtDNA depletion has also been corrected *in vivo*, by treating a Tymp knockout mouse model with either dCtd or tetrahydrouridine, an inhibitor of nucleotide catabolism [67–70]. Mutations in human TYMP1, encoding TP, are responsible of mitochondrial neuro-gastro-intestinal encephalomyopathy, MNGIE [71]. MNGIE is a severe, autosomal recessive mitochondrial disorder of early adulthood, characterized by painful gastrointestinal dysmotility causing chronic diarrhea and leading to cachexia, progressive external ophthalmoplegia with mitochondrial myopathy, and severe sensory-motor peripheral neuropathy. Patients usually die of complications due to their critical nutritional status, with an average age at death of 37 years [72]. TP is a cytosolic enzyme catalyzing the first step of thymidine (dThd) and deoxyuridine (dUrd) catabolism. As a consequence of TP dysfunction, MNGIE patients accumulate dThd and dUrd systemically, which ultimately results in imbalances of the mitochondrial pool of deoxyribonucleoside triphosphates (dNTPs) [73]. In fact, increased deoxythymidine triphosphate (dTTP) and decreased deoxycytidine triphosphate (dCTP) have been measured in vitro and in vivo. This dNTP imbalance is mutagenic for mitochondrial DNA (mtDNA), resulting in depletion, multiple deletions, and point mutations accumulating in post-mitotic organs, notably intestinal smooth muscle, skeletal muscle and the nervous system, and cause progressive mitochondrial deficiency and organ failure.

Although the mouse model has hardly any clinical sign, it is clearly characterized by markedly abnormal dNTP pools, similar to MNGIE patients.

Promising results were also obtained in a Thymidine Kinase 2 (Tk2) H126N knockin mouse reproducing a pathological mutation found in patients. Tk2 encodes the gene for the mitochondrial thymidine kinase, which phosphorylates thymidine and deoxycytidine pyrimidine nucleosides to generate deoxythymidine monophosphate (dTMP) and deoxycytidine monophosphate (dCMP). Absence of Tk2 determines an imbalance of dNTP pools leading to mtDNA instability and depletion. The Tk2 H126N reproduces a human disease characterized by early-onset fatal encephalomyopathy due to mtDNA depletion and multiple RC defects. Treatment with 200 or 400 mg/kg/day leads to increased dNTP concentrations and mtDNA content, rescuing the RC defects, and significantly prolonging lifespan from 13 to 34 days.

2.5. Targeting autophagy

Autophagy (literally “self-eating”) is a physiological pathway aimed at two fundamental and related goals: (i) to recycle energy by degradation of cellular components, and (ii) to warrant quality control of cellular organelles [74–76]. These two goals are achieved through complex processes tailored to selectively eliminate single macromolecules or small organellar portions (microautophagy), or entire organelles that are damaged or supernumerary (macroautophagy), including

peroxisomes (pexophagy), endoplasmic reticulum (ER-phagy) and mitochondria (mitophagy). In macroautophagy, the specific target is ultimately engulfed within a double-membrane vacuole called the autophagosome that eventually gets fused with lysosomes to form the autolysosome, where complete digestion of the organelle components takes place [77]. The specificity of the cargo is determined by specific receptors on the surface of the organelles, targeting them to the pre-autophagosome [78].

Autophagy is regulated by several metabolic sensors, such as growth factors, amino acids and glucose concentrations, and energy status. Anabolic conditions, e.g. high glucose and amino acid availability, activate transduction cascades converging on two main pathways both causing inhibition of autophagy (Figure 4). In the first pathway, the mammalian target of rapamycin complex 1 (mTORC1) is activated and inhibits autophagy. In the second pathway, which acts independently from mTORC1, cyclic AMP (cAMP) levels are increased, leading to increased inositol-1,4,5-trisphosphate (Ins(1,4,5)P3). This causes the release of Ca^{2+} from the ER and inhibition of autophagy via Ca^{2+}-activated calpains. Conversely, catabolic conditions activate pathways such as the AMPK cascade, and the basic helix–loop–helix leucine zipper transcription factor EB (TFEB), which trigger autophagy. In conditions of low energy (e.g. starvation) TFEB is phosphorylated and consequently migrates to the nucleus, where it promotes autophagic and lysosome biogenetic programs. AMPK also inhibits mTORC1 and activates UNC51-like kinase 1 (ULK1) complex, a

serine/threonine protein kinase, which stimulates the autophagic cascade.

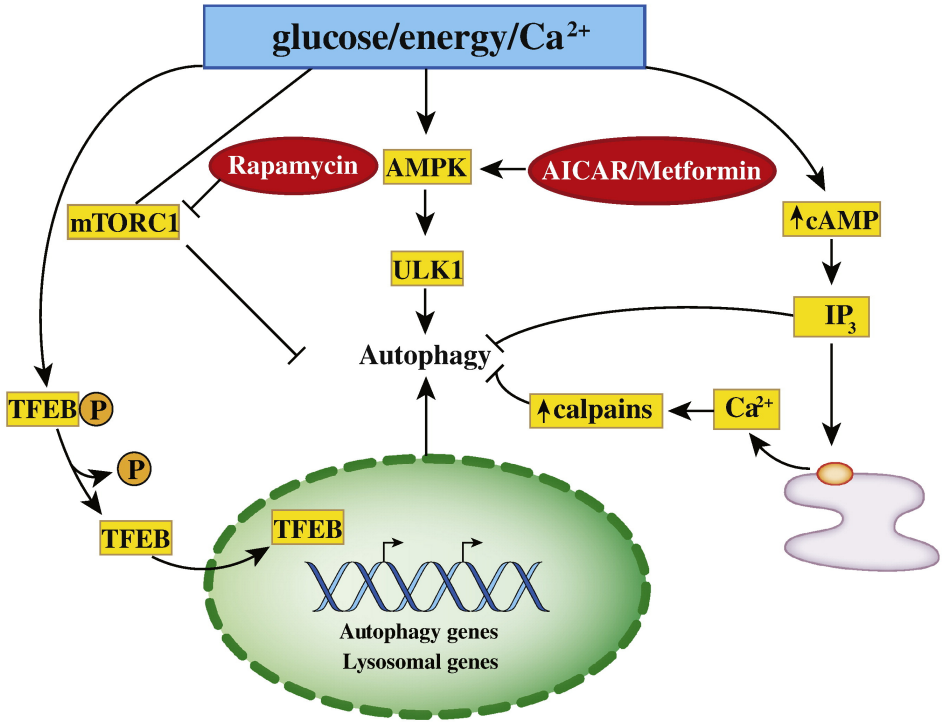

Figure 4. Regulation of autophagy.

Chronic treatment with the mTOR inhibitor rapamycin, which activates autophagy, significantly delayed both disease progression and fatal outcome of a Ndufs4$^{-/-}$mouse which lacks the 18kDa Ndufs4 subunit of complex I. Mutations of NDUFS4 are associated with autosomal recessive, severe infantile Leigh disease in humans and with rapidly progressive, early fatal neurological failure in the Ndufs4$^{-/-}$mouse model [79]. Although the underlying mechanism remains partly unexplained, the effect of rapamycin seems to be exquisitely metabolic, as no

increase in complex I activity or amount was detected in treated vs. untreated mice. In fact, metabolomic analysis of Ndufs4$^{-/-}$brains was hallmarked by accumulation of pyruvate, lactate, and glycolytic intermediates, as well as reduced free amino acids, free fatty acids, nucleotides, and products of nucleotide catabolism, increased oxidative stress markers, and reduced levels of GABA and dopamine. Rapamycin treatment corrected several of these abnormal metabolic biomarkers. However, more investigation is warranted to clarify the underlying mechanism, and to extend it to other models of mitochondrial disease.

2.6. Dietary manipulations

Several approaches based on dietary measures have been attempted, with controversial results. Ketogenic diet (KD), i.e. a high-fat, low- carbohydrate diet, has been proposed to stimulate mitochondrial beta-oxidation, and provide ketones, which constitute an alternative energy source for the brain, heart and skeletal muscle. Ketone bodies are metabolized to acetyl-CoA, which enters the Krebs cycle and is oxidized to feed the RC and ultimately generate ATP via OXPHOS. This pathway partially bypasses complex I via increased synthesis of succinate, which donates electrons to the respiratory chain via complex II. Increased ketone bodies have also been associated with increased expression of OXPHOS genes, possibly via a starvation-like response [80]. Starvation is a stressing condition to the cell, which results in activation of many transcription

factors and cofactors (including SIRT1, AMPK, and PGC-1α) that ultimately increase mitochondrial biogenesis [80]. KD reduced the mutation load of a heteroplasmic mtDNA deletion in a cybrid cell line from a Kearns–Sayre syndrome patient [81], was shown to increase the expression levels of uncoupling proteins and mitochondrial biogenesis in the hippocampus of mice and rats [82,83], and increased mitochondrial GSH levels [84] in rat brain. These phenomena could contribute to explain the anticonvulsant effects of KD. In a preclinical trial on the deletor mouse, KD slowed the progression of mitochondrial myopathy [85]. However, other reports showed that KD can have the opposite effect, and worsens the mitochondrial defect in vivo, for instance in the Mterf2$^{-/-}$ [86], or the Mpv17$^{-/-}$ mouse models [87].

Similar to KD, a high fat diet (HFD) was shown to have a protective effect on fibroblasts with complex I deficiency and be effective in delaying the neurological symptoms of the Harlequin mouse, a model of partial complex I defect associated with a homozygous mutation of AIFM1, encoding the mitochondrial apoptosis inducing factor [88].

Similar results could in principle be achieved using other compounds that release succinate in mitochondria. An example is triheptaoin, an anaplerotic compound inducing a rapid increase of plasmatic C4- and C5-ketone bodies, the latter being a precursor of propionyl-CoA, which is then converted into succinyl-CoA. Treatment with triheptaoin has been reported to dramatically improve cardiomyopathy in patients with VLCAD

deficiency and myopathic symptoms in CPT2 deficiency patients [89,90].

2.7. Targeting the PTP

The permeability transition pore is a transient channel deemed to be formed by ATPase dimers [91], which opens upon stress stimuli, such as excessive mitochondrial Ca^{2+} uptake, increased ROS, decreased mitochondrial membrane potential, and low ATP levels. The opening of the PTP leads to complete dissipation of the mitochondrial membrane potential, osmotic swelling of the organelle and ultimately mitochondrial disruption; as a consequence of the release of cytochrome c and other apoptotic triggers, the cell can eventually die. Substantial cell loss or damage may lead to organ failure and disease. Thus, targeting the PTP is a potentially effective strategy to prolong cell survival, slow disease progression, and diminish symptoms severity [92]. Cyclosporine A (CsA) has for long been known to inhibit the PTP through a cyclophilin-D dependent mechanism. CsA has recently been used in patients with Bethlem/Ullrich congenital muscular dystrophy, which are allelic conditions due to mutations in the gene encoding collagen VI. Mitochondrial dysfunction and proneness to apoptosis in skeletal muscle have been documented in both syndromes, and CsA treatment for one month corrected these phenomena in a cohort of five patients [93]. However, while apoptosis plays well-established roles in several pathologies, its contribution to the pathogenesis of primary mitochondrial diseases is not univocally established.

3. Molecular approaches to treat mitochondrial diseases

3.1. Targeted re-expression of the mutated gene

Correction of a mutation by expressing the wild-type gene in critical organs has for long been envisaged as the definitive cure for genetic diseases. Although we are still far from having achieved a general strategy for gene replacement in the whole body, large-size organs (e.g. skeletal muscle), or impermeable organs (e.g. brain), several successes have been reported in the last years for a number of genetic diseases, in both preclinical models and patients. In fact, while expression of therapeutic genes through the whole body is still unachievable, and quantitative targeting of skeletal muscle is only feasible in small rodents but not in humans, smaller organs can be targeted by exploiting currently available technologies. In particular the introduction of adeno-associated viral (AAVs) vectors has given new stamina to gene therapy. AAVs belong to the parvoviridae family, which are not associated with any disease in humans or animals, and remain episomic in the cells for prolonged time, thus reducing the risk of insertional mutagenesis [94]. In addition, several serotypes with õ- different cellular specificity have been selected, allowing specific targeting of several organs and tissues [95] (Figure 5). In the context of mitochondrial disease models, AAV2 was first administered by local injections to correct the myopathy associated with Ant1$^{-/-}$mice [96]. More recently, we reported that a recombinant construct expressing human Ethe1^{wt} could

be targeted to the liver using a hepatotropic AAV2/8 serotype. When titers > 10^{12} viral genomes/kg were injected in three-week old Ethe1$^{-/-}$ mice, Ethe1-associated SDO activity was completely recovered in liver [57], leading to efficient clearance of H_2S from the bloodstream. This treatment was associated with significant rescue of the profound COX deficiency due to the inhibitory effect of H_2S, correction of the other biomarkers of the disease (e.g. high plasma and urine levels of ethylmalonate, lactate and thiosulfate), remarkable clinical improvement and marked prolongation of the lifespan, from a few weeks in untreated animals to over 8 months in AAV-treated littermates [97]. Notably, preliminary data in the same mouse model suggests that administration of the AAV2/8 construct in two doses at P1 and P21 is even more effective, leading to further prolongation of the lifespan to over 1.5 years (Di Meo et al, unpublished).

The same liver-specific AAV2/8 vector has been exploited to treat a mouse model for MNGIE [98]. Although the Tymp$^{-/-}$ mouse displays hardly any clinical sign, it is characterized by markedly abnormal dNTP pools, similar to MNGIE patients. Intra-venous injection of AAV2/8 particles expressing human wt TYMP (10^{12}–10^{13} viral DNA/kg) normalized dCTP and dTTP levels in plasma and tissues for up to 8 months of age. This encouraging proof-of-principle result supports the transferability of the AAV2/8 treatment to cure MNGIE patients. The current standard treatment for MNGIE relies on bone marrow transplantation [99,100], which is however burdened by a >

50% post-graft mortality due to poor clinical conditions of the recipient patients. A non-invasive and safe procedure like systemic administration of suitably engineered AAV vectors is clearly more acceptable and can lead to substantial improvement of the otherwise ominous prognosis of this extremely invalidating disorder.

Another potential application of AAV2/8-mediated gene therapy is for correcting liver-specific mitochondrial dysfunction. To demonstrate this, we have used the Mpv17$^{-/-}$mouse. Mpv17 is a small protein of unknown function embedded in the inner mitochondrial membrane, which is mutated in patients affected by hepatocerebral forms of severe mtDNA depletion syndrome [101], including Navajo neuro-hepatopathy [102]. Similar to the human disease, the mouse model shows profound decrease of mtDNA copy number in the liver, but, in contrast to humans, hardly any clinical phenotype of hepatopathy is detected in standard conditions [103]. However, liver steatosis evolving into cirrhosis associated with fatal liver failure is produced in Mpv17$^{-/-}$exposed to KD [87]. We showed that an AAV2/8 viral vector expressing human MPV17wt fully rescued the mtDNA depletion and prevented the KD-induced cirrhosis in Mpv17$^{-/-}$mice, when the treatment was initiated before starting the KD regime, whereas the same treatment significantly delayed but not arrested disease progression when initiated after starting KD [87].

Notably, the recent introduction of new serotypes efficiently and selectively targeting the liver, in particular AAV5, opens the

possibility to repeat the injection well after the first administration without incurring in immunological neutralization [104,105].

Finally, an AAV2 vector [106] has also been used to re-express AIF in the eye of the Harlequin mouse, leading to correction of complex I deficiency and long-lasting protection of retinal ganglion cells and optic nerve from degeneration [107].

Taken together, these preclinical results demonstrate the great potential of AAV-mediated gene therapy to combat specific mitochondrial diseases. Nevertheless, a number of issues will need to be addressed in the coming years, including the development of suitable strategies to effectively target extra-hepatic, critical organs such as skeletal muscle, heart and brain. Although some success has been obtained in the treatment of non-mitochondrial myopathies and dystrophies in preclinical models [108–110], their efficacy in humans is still under investigation.

A strategy repeatedly proposed to correcting mtDNA mutations in protein-encoding genes is based on allotopic expression. In this approach, the recoded wild type gene, transfected to the nucleus, expresses a recombinant protein containing a mitochondrial targeting sequence (MTS), to address it to mitochondria. A 3'-UTR signal is usually added, that in yeast serves to target transcripts of mitochondrial proteins to the organelle surface. These transcripts are then translated by a local pool of ribosomes into proteins, which can promptly be imported into the organelle. This approach has been attempted

in fibroblasts carrying mutations in ND1, ND4 and ATP6 genes [111–113] and in a rat model of LHON [114]. Taken together, the results from these experiments are very controversial, as conflicting data have been obtained by different groups on the ability of recoded, mitochondrially targeted mtDNA gene products to be effectively imported and correctly inserted within the respiratory chain complexes [115]. In particular, allotopically expressed ND6 gene, recoded according to the universal genetic code, failed to be imported into mitochondria, remaining stuck onto the OMM. The correction of the complex I defect reported in these experiment was later deemed to be a spurious result due to selection of spontaneous revertants in the cell culture [115]. Nevertheless, two open-label clinical trials based on AAV-mediated allotopic expression of mtDNA genes for LHON are currently recruiting patients (https://clinicaltrial.gov). Likewise, a therapeutic strategy for LHON, based on the use of an AAV2 construct has been proposed to express the wild type ND4 gene in LHON mutant cybrids and in a transgenic rat model of LHON. The AAV2 capsid protein VP2 has been engineered by adding an MTS in order to promote the internalization of the viral particle into mitochondria [116]. Again, convincing demonstration that the full viral particle is in fact translocated within mitochondria and its ability to properly express the therapeutic gene is, in our opinion, lacking; these controversial results have not been replicated by others.

The multiploidy organization of mtDNA, its confinement within an almost impermeable double-membrane barrier, and the

virtual absence of homologous recombination, are formidable hurdles against the direct, controlled manipulation of this genome for therapeutic intervention. Nevertheless, several approaches have been proposed to this aim, and some are giving promising results. A first strategy was based on the use of protein nucleic acids (PNAs) as an “antigenomic” device [117,118]. PNAs are synthetic DNA-like molecules in which the pyrimidine and purine residues are linked to an aminoethyl (pseudopeptide) backbone. Since these molecules are not charged at physiological pH, a PNA binds its complementary DNA with greater affinity than natural nucleic acids, so that PNA–DNA hybrids are more stable than DNA–DNA hybrids. PNAs complementary to either the mtDNA stretch containing the 8344A>G MERRF mutation in mt-tRNA^{Lys} [5], or the breakpoint junction associated with the mtDNA common deletion, were shown to be imported into mitochondria, where they inhibited the replication of mutant but not wild type mtDNA; however no such effect was demonstrated in cell lines [119]. In another approach, a synthetic N-terminal signal was used to introduce oligonucleotides complementary to mtDNA into the mitochondrial matrix. Oligonucleotides were annealed to complementary PNAs and the hybrid molecule was selectively imported into the mitochondrial matrix, but its antigenomic effect was not demonstrated [120].

Recently, an alternative approach has been used to target allotopically expressed tRNAs and mRNAs to the mitochondria. This approach takes advantage from the observation that

RNase P, a ribonucleoprotein involved in the processing of mitochondrial transcripts, is imported into mitochondria through a specialized system (PNPase) that specifically recognizes its RNA component (H1 RNA). By fusing the gene of interest with a 20-ribonucleotide stem-loop sequence from the H1 RNA, some evidence was provided in support of correction of mt-tRNA and COII gene mutations in cell lines [121,122]. These findings deserve further investigation and independent confirmation.

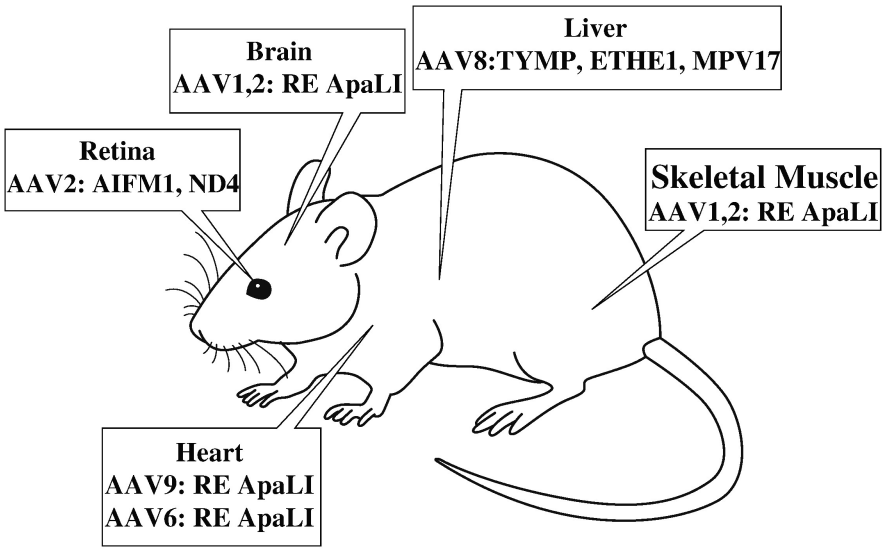

Figure 5. AAV-based gene therapies in mouse models of mitochondrial diseases.

3.2. Manipulating mtDNA heteroplasmy

As pathogenic mutations of mtDNA are often heteroplasmic, and behave as “recessive-like” mutations, suitable therapeutic intervention can be envisaged, aimed at eliminating or reducing the amount of mutated DNA below the threshold at which the disease manifests. This result has been achieved in cellular

models by targeting to mitochondria recombinant restriction endonucleases [123–125], zinc finger-endonucleases [126] or TALENs [127]. Mitochondrially targeted restriction enzymes have been used in a variety of systems to induce a shift in heteroplasmy. For instance, the 8399T>G NARP mutation forms a unique CCCGGG restriction site in mtDNA specific to the restriction endonuclease SmaI (the wild type sequence is CCCGTG). A mitochondrially targeted recombinant SmaI variant was in fact able to substantially decrease the 8399T>G mutation load in heteroplasmic mutant cybrids. This was followed by repopulation of cells with wild-type mtDNA, restoration to normal of mitochondrial membrane potential and increase of intracellular ATP levels [128,129]. The PstI endonuclease, whose restriction site is present in human and mouse but not rat mtDNA, was targeted to human mitochondria, where it degraded mtDNA, and determined a shift towards the rat haplotype in a hybrid cell line harbouring both mouse and rat mtDNA [125]. Subsequent work has demonstrated the efficacy of this approach in NZB/BalbC heteroplasmic mice in which AAV1,2 vectors expressing a mitochondrially-targeted restriction endonuclease ApaLI were injected locally into muscle or brain [130]; other vectors expressing the same endonuclease were administered by i.v. infusion to target specific organs, such as the liver (with adenovirus) or the heart (with AAV6) [123,131]. In addition, an AAV9 vector expressing the mitochondria- targeted ApaLI was also used to markedly shift mtDNA heteroplasmy in skeletal and cardiac muscle of neonate

mice harbouring two mtDNA haplotypes that differed for the presence or absence of a unique ApaLI restriction site (GTGCAC) [124].

In practice, this approach can be used therapeutically only if a unique restriction site is created by an mtDNA mutation, as in the case of the 8993T>G NARP, an exceptionally rare event. However, the recent development of zinc-finger nuclease and TALEN technologies can offset this limitation. Zinc finger nucleases (ZFNs) are chimeric enzymes in which the modular Cys_2His_2 zinc finger DNA-binding domains present in numerous transcription factors are conjugated to the C-terminal catalytic subunit of the type II restriction enzyme FokI [132, 133]. Each zinc finger domain recognizes three nucleotides, so that appropriate arrangements of the zinc finger modules permit to target virtually any DNA sequence for nucleolytic cleavage. ZFN can be targeted to mitochondria by adding a suitable MTS at the N-terminus. Likewise, transcription activator-like effectors nucleases (TALEN) exploit DNA-binding domains of the Xanthomonas bacteria composed of 33–35-amino-acid repeats, each recognizing a single base pair, fused with the FokI nuclease. Again, TALENs can be targeted to mitochondria via an N-terminal MTS (MitoTALENs).

MitoTALENs [127] have been proven to eliminate heteroplasmic mutant mtDNA in cybrid cells carrying either the m.8483_13459del4977 common mtDNA deletion [134–136] or the m.14459G>A LHON/Dystonia mutation in the MT-ND6 gene [137]. In both cases, a transient decrease in total mtDNA levels

occurred followed by repopulation with wild type mtDNA up to normal values.

Likewise, mitochondrially targeted ZFNs (mtZFNs) were successfully used in heteroplasmic cybrids to cleave mtDNA harbouring either the heteroplasmic m.8993T>G NARP mutation [6] or the common deletion. As for TALENS and restriction enzymes, mtZFNs led to a reduction in mutant mtDNA haplotype load, and subsequent repopulation of wild-type mtDNA, associated with restoration of mitochondrial respiration [126].

3.3. Stabilizing mutant mt-tRNA

More than 50% of the mtDNA mutations are localized in tRNA genes, leading to a wide range of syndromes, such as MELAS or MERRF. Aminoacyl-tRNA synthetases (aaRSs) are ubiquitously expressed, essential enzymes performing the attachment of amino acids to their cognate tRNA molecules as the first step of protein synthesis [138]. Several lines of evidence in yeast and human cell lines indicate that overexpressing cognate mt-aaRS can attenuate the detrimental effects of mt-tRNA point mutations [139–142]. For instance, overexpression of mt-leucyl-tRNA synthetase (mt-LeuRS) corrects the respiratory chain deficiency of transmitochondrial cybrids harbouring the MELAS mutation in the mt-tRNA$^{Leu(UUR)}$ gene (MTTL1) [138,141]. Likewise, overexpressing the cognate mt-valyl-tRNA synthetase (mt-ValRS) restored, at least in part, steady-state levels of mutated mt-tRNA^{Val} in cybrid cell lines

[142]. Finally, constitutive high levels of mt-isoleucyl-tRNA synthetase (mt-IleRS) were shown to be associated with reduced penetrance of the homoplasmic m.4277T>C mt-tRNA^{Ile} mutation, which causes hypertrophic cardiomyopathy [143]. In addition, experiments in yeast and human cells have shown that the overexpression of either human mt-LeuRS or mt-ValRS was able of rescuing the pathological phenotype associated with mutations in both the cognate and the non-cognate mt-tRNA. A region in the carboxy-terminal domain of mt-LeuRS was found necessary and sufficient to determine this phenomenon, probably via a chaperone-like stabilizing effect [144,145].

An alternative approach to the same issue was based on the observation that in yeast some tRNAs were encoded in the nuclear genome and imported into the mitochondria. So, tRNA mutations in mtDNA may in principle be complemented by expressing a xenotopic nDNA-encoded yeast mitochondrial tRNA from the mammalian nucleus. This approach has been attempted for the treatment of human cells harbouring the tRNALys nucleotide 8344A>G mutation using the yeast tRNA^{Lys}nDNA gene [122,146,147]. This partially restored the mitochondrial dysfunction associated with the mitochondrial protein-synthesis defect. Similarly, a Leishmania-mitochondrial RNA import complex has been exploited to introduce the human cytosolic tRNA^{Lys} into human cybrids harbouring the tRNA^{Lys} 8344A>G mtDNA mutation by a caveolin-1-dependent pathway, obtaining a significant restoration of mitochondrial

function [148]. These findings, however, are still controversial and need confirmation from independent labs.

3.4. Targeting fission and fusion

Mitochondria are highly dynamic organelles whose shape and mass are finely tuned by the activity of pro-fusion proteins, such as mitofusin 1 (MFN1), MFN2 and optic atrophy protein 1 (OPA1) and pro-fission proteins, such as dynamin-related protein 1 (DRP1) and mitochondrial fission 1 protein (FIS1) [78,149]. Alterations in the genes encoding these complex machineries lead to disease in humans. For instance, mutations in OPA1 are associated with autosomal dominant optic atrophy [150] and mutations in MFN2 cause Charcot–Marie–Tooth disease type 2A [151]. In addition, disruption of Mfn1 and Mfn2 in the skeletal muscle of the $POLG^{D257A}$ mutator mouse leads to striking worsening of the phenotype, due to accumulation of mtDNA mutations, suggesting that the physiological balance between fission and fusion protects the integrity of mtDNA through continuous mixing of mtDNA pools [152]. Two additional observations are relevant in this context. First, overexpression of Opa1, a multitasking GTPase involved in shaping mitochondrial cristae and promoting fusion of the inner mitochondrial membrane, has been shown to increase respiratory efficiency by stabilizing the respiratory chain supercomplexes [153]. Second, some compounds affecting fission and fusion have been identified, such as the Drp1 inhibitor MDIVI-1 and M1-hydrazone that probably promotes

fusion by acting on Mfn or Opa1. However, the therapeutic potential of these compounds for mitochondrial diseases has still to be proved.

3.5. Bypassing the block of the respiratory chain

An emerging concept in mitochondrial medicine is the possibility to by-pass the block of OXPHOS due to mutations affecting the RC complexes by using the “alternative” enzymes NADH dehydrogenase/CoQ reductase (Ndi1) and CoQ/O2 alternative oxidase (AOX).

These are single-peptide enzymes, located in the mitochondrial inner membrane, which transfer electrons to (Ndi1) and from (AOX) CoQ, without pumping protons across the membrane. Ndi1 substitutes complex I in yeast mitochondria. AOX is an alternative electron transport system present in lower eukaryotes, plants and several invertebrates that by-passes the complex III + IV segment of the respiratory chain. Expression of these proteins is well tolerated in mammalian cells [154], flies and mice [155] and has successfully been exploited to by-pass complex I or complex III/IV defects in human cells [156,157] and Drosophila models [158–160]. The therapeutic mechanism is based on the capacity of these enzymes to restore the electron flow through the quinone pool, thus preventing accumulation of reduced intermediates and oxidative damage [161]. However, this is not accompanied by restoration of proton translocation across the inner mitochondrial membrane, and does not directly increase ATP production. Nevertheless, the

restoration of the electron flow can reactivate the unaffected RC complexes, thus indirectly promoting the rebuilding of the proton gradient and the reactivation of OXPHOS. AOX-expressing mice have recently been created and shown to be viable and fertile [155], thus opening the possibility to test whether this approach is amenable in a mammalian organism, using suitable mouse models of complex III or IV deficiency.

3.6. Somatic nuclear transfer

Given the difficulty of manipulating mtDNA and the uncertainties of genetic counselling for mtDNA mutations, prenatal or pre-implantation genetic diagnosis is nowadays the best option available to women carrying pathogenic mtDNA mutations. However, these techniques can only be applied to subjects with low levels of mtDNA mutations in oocytes and are technically challenging. Recent technical improvements in non-human primates [162] and non-viable human embryos [163, 164] have paved the way to replace the mutated maternal mtDNA with that obtained from a healthy woman, by transferring either the spindle-chromosomal complex of mature oocytes, or the pronuclei during the pre-zygotic stage of fertilized egg. Both techniques have been refined in order to minimize the amount of mutant mtDNA carried over into the recipient ooplasm. A child born by these procedures will carry the nuclear genes of the affected mother (and healthy father) but the healthy mitochondrial genes of the donor (see also [165] for a very recent summary of the on-going debate on this important topic).

4. Conclusions

Mitochondrial diseases are amazingly complex and its biology has so far prevented the development of effective therapy for most of them. Nevertheless, the last few years witnessed numerous attempts to significantly modify the phenotype in cellular and animal models by using either disease-specific or wide-spectrum strategies applicable to several disorders. The wealth of knowledge accumulated in over 25 years of intensive studies aimed at elucidating the genetic causes and the pathogenic mechanisms of mitochondrial diseases has driven these first “proof of concept” successes that now need to be translated and tested on patients. In addition, mitochondrial dysfunction is nowadays recognized as central in several medical conditions, including diabetes, inflammation, cancer and neurodegeneration; this will certainly have a synergistic effect to expand our knowledge on the pathomechanisms underlying both primary and secondary mitochondrial impairment and to prompt the development of more effective, evidence-based therapeutic approaches.

References

[1] D.C. Wallace, W.Fan, V.Procaccio, Mitochondrial energetics and therapeutics, Annu. Rev. Pathol. 5 (2010) 297–348.
[2] J.E. Walker, The ATP synthase: the understood, the uncertain and the unknown, Biochem. Soc. Trans. 41 (2013) 1–16.
[3] E.Fernandez-Vizarra, V.Tiranti, M. Zeviani, Assembly of the oxidative phosphorylation system in humans: what we have learned by studying its defects, Biochim. Biophys. Acta 1793 (2009) 200–211.
[4] Y.Goto, I.Nonaka, S.Horai, A mutation in the tRNA(Leu)(UUR) gene associated with the MELAS subgroup of mitochondrial encephalomyopathies, Nature 348 (1990) 651–653.
[5] J.M.Shoffner, M.T.Lott, A.M.Lezza, P.Seibel, S.W.Ballinger, D.C.Wallace, Myoclonic epilepsy and ragged-red fiber disease (MERRF) is associated with a mitochondrial DNA tRNA(Lys) mutation, Cell 61 (1990) 931–937.
[6] I.J.Holt, A.E.Harding, R.K.Petty, J.A.Morgan-Hughes, A new mitochondrial disease associated with mitochondrial DNA heteroplasmy, Am. J. Hum. Genet. 46 (1990) 428–433.
[7] D.C. Wallace, G. Singh, M.T. Lott, J.A. Hodge, T.G. Schurr, A.M. Lezza, L.J. Elsas 2nd, E.K.Nikoskelainen, Mitochondrial DNA mutation associated with Leber's heredi- tary optic neuropathy, Science 242 (1988) 1427–1430.
[8] C.T.Moraes, S.DiMauro, M.Zeviani, A.Lombes, S.Shanske, A.F.Miranda, H.Nakase, E.Bonilla, L.C.Werneck, S.Servidei, et al , Mitochondrial DNA deletions in progressive external ophthalmoplegia and Kearns–Sayre syndrome, N. Engl. J. Med. 320 (1989) 1293–1299.
[9] A.Rotig, M.Colonna, J.P.Bonnefont, S.Blanche, A.Fischer, J.M. Saudubray, A.Munnich, Mitochondrial DNA deletion in Pearson's marrow/pancreas syndrome, Lancet 1 (1989) 902–903.
[10] W.J.Koopman, P.H.Willems, J.A.Smeitink, Monogenic mitochondrial disorders,N. Engl. J. Med. 366 (2012) 1132–1141.
[11] L.C. Lopez, M. Luna-Sanchez, L. Garcia-Corzo, C.M. Quinzii, M. Hirano, Pathomechanisms in coenzyme q10-deficient human fibroblasts, Mol. Syndromol. 5 (2014) 163–169.

[12] D. Ghezzi, I. Sevrioukova, F. Invernizzi, C. Lamperti, M. Mora, P. D'Adamo, F. Novara, O. Zuffardi, G. Uziel, M. Zeviani, Severe X-linked mitochondrial encephalomyopathy associated with a mutation in apoptosis-inducing factor, Am. J. Hum. Genet. 86 (2010) 639–649.
[13] T.B.Haack, K.Danhauser, B.Haberberger, J.Hoser, V.Strecker, D.Boehm, G.Uziel, E. Lamantea, F. Invernizzi, J. Poulton, B. Rolinski, A. Iuso, S. Biskup, T. Schmidt, H.W. Mewes, I. Wittig, T. Meitinger, M. Zeviani, H. Prokisch, Exome sequencing identifies ACAD9 mutations as a cause of complex I deficiency, Nat. Genet. 42 (2010) 1131–1134.
[14] J. Nouws, F. Wibrand, M. van den Brand, H. Venselaar, M. Duno, A.M. Lund, S. Trautner, L. Nijtmans, E. Ostergard, A patient with complex I deficiency caused by a novel ACAD9 mutation not responding to riboflavin treatment, JIMD Rep. 12 (2014) 37–45.
[15] M.Kanabus, S.J.Heales, S.Rahman, Development of pharmacological strategies for mitochondrial disorders, Br. J. Pharmacol. 171 (2014) 1798–1817.
[16] C. Giordano, L. Iommarini, L. Giordano, A. Maresca, A. Pisano, M.L. Valentino, L. Caporali, R. Liguori, S. Deceglie, M. Roberti, F. Fanelli, F. Fracasso, F.N. Ross- Cisneros, P. D'Adamo, G. Hudson, A. Pyle, P. Yu-Wai-Man, P.F. Chinnery, M. Zeviani, S.R. Salomao, A. Berezovsky, R. Belfort Jr , D.F. Ventura, M. Moraes, M. Moraes Filho, P. Barboni, F. Sadun, A. De Negri, A.A. Sadun, A. Tancredi, M. Mancini, G. d'Amati, P. Loguercio Polosa, P. Cantatore, V. Carelli, Efficient mitochondrial biogenesis drives incomplete penetrance in Leber's hereditary optic neuropathy, Brain 137 (2014) 335–353.
[17] R.C. Scarpulla, Transcriptional paradigms in mammalian mitochondrial biogenesis and function, Physiol. Rev. 88 (2008) 611–638.
[18] P.J. Fernandez-Marcos, J. Auwerx, Regulation of PGC-1alpha, a nodal regulator of mitochondrial biogenesis, Am. J. Clin. Nutr. 93 (2011) 884S–890S.
[19] J. Bastin, F. Aubey, A. Rotig, A. Munnich, F. Djouadi, Activation of peroxisome proliferator-activated receptor pathway stimulates the mitochondrial respiratory chain and can correct deficiencies in patients' cells lacking its components, J. Clin. Endocrinol. Metab. 93 (2008) 1433–1441.

[20] T. Wenz, F. Diaz, B.M. Spiegelman, C.T. Moraes, Activation of the PPAR/PGC-1alpha pathway prevents a bioenergetic deficit and effectively improves a mitochondrial myopathy phenotype, Cell Metab. 8 (2008) 249–256.
[21] J. Lin, H. Wu, P.T. Tarr, C.Y. Zhang, Z. Wu, O. Boss, L.F. Michael, P. Puigserver, E. Isotani, E.N. Olson, B.B. Lowell, R. Bassel-Duby, B.M. Spiegelman, Transcriptional co-activatorPGC-1 alpha drives the formation of slow-twitch muscle fibres, Nature 418 (2002) 797–801.
[22] T. Wenz, X. Wang, M. Marini, C.T. Moraes, A metabolic shift induced by a PPAR panagonist markedly reduces the effects of pathogenic mitochondrial tRNA mutations, J. Cell. Mol. Med. 15 (2011) 2317–2325.
[23] N. Noe, L. Dillon, V. Lellek, F. Diaz, A. Hida, C.T. Moraes, T. Wenz, Bezafibrate im- proves mitochondrial function in the CNS of a mouse model of mitochondrial encephalopathy, Mitochondrion 13 (2013) 417–426.
[24] C.Viscomi, E.Bottani, G.Civiletto, R.Cerutti, M.Moggio, G.Fagiolari, E.A.Schon, C. Lamperti, M. Zeviani, In vivo correction of COX deficiency by activation of the AMPK/PGC-1alpha axis, Cell Metab. 14 (2011) 80–90.
[25] S.Yatsuga, A.Suomalainen, Effect of bezafibrate treatment on late-onset mitochondrial myopathy in mice, Hum. Mol. Genet. 21 (2012) 526–535.
[26] L.M. Dillon, A. Hida, S. Garcia, T.A. Prolla, C.T. Moraes, Long-term bezafibrate treat- ment improves skin and spleen phenotypes of the mtDNA mutator mouse, PLoS One 7 (2012) e44335.
[27] E.Hondares, I.Pineda-Torra, R.Iglesias, B.Staels, F.Villarroya, M.Giralt, PPARdelta, but not PPARalpha, activates PGC-1alpha gene transcription in muscle, Biochem. Biophys. Res. Commun. 354 (2007) 1021–1027.
[28] S. Kleiner, V. Nguyen-Tran, O. Bare, X. Huang, B. Spiegelman, Z. Wu, PPAR(delta) agonism activates fatty acid oxidation via PGC-1(alpha) but does not increase mitochondrial gene expression and function, J. Biol. Chem. 284 (2009) 18624–18633.
[29] S.Luquet, J.Lopez-Soriano, D.Holst, A.Fredenrich, J.Melki, M.Rassoulzadegan, P.A. Grimaldi, Peroxisome proliferator-activated receptor delta controls muscle development and oxidative capability, FASEB J. 17 (2003) 2299–2301.

[30] Y.X.Wang, C.L.Zhang, R.T.Yu, H.K.Cho, M.C.Nelson, C.R.Bayuga-Ocampo, J.Ham, H. Kang, R.M. Evans, Regulation of muscle fiber type and running endurance by PPARdelta, PLoS Biol. 2 (2004) e294.
[31] A. Golubitzky, P. Dan, S. Weissman, G. Link, J.D. Wikstrom, A. Saada, Screening for active small molecules in mitochondrial complex I deficient patient's fibroblasts, reveals AICAR as the most beneficial compound, PLoS One 6 (2011) e26883.
[32] A. Casarin, G. Giorgi, V. Pertegato, R. Siviero, C. Cerqua, M. Doimo, G. Basso, S. Sacconi, M. Cassina, R. Rizzuto, S. Brosel, M.D. M, S. Dimauro, E.A. Schon, M. Clementi, E. Trevisson, L. Salviati, Copper and bezafibrate cooperate to rescue cyto- chrome c oxidase deficiency in cells of patients with SCO2 mutations, Orphanet J. Rare Dis. 7 (2012) 21.
[33] F. Djouadi, J. Bastin, Species differences in the effects of bezafibrate as a potential treatment of mitochondrial disorders, Cell Metab. 14 (2011) 715–716 (author reply 717).
[34].Cerutti, E.Pirinen, C.Lamperti, S.Marchet, A.A.Sauve, W.Li, V.Leoni, E.A.Schon, F. Dantzer, J. Auwerx, C. Viscomi, M. Zeviani, NAD-dependent activation of Sirt1 corrects the phenotype in a mouse model of mitochondrial disease, Cell Metab. 19 (2014) 1042–1049.
[35] N.A. Khan, M. Auranen, I. Paetau, E. Pirinen, L. Euro, S. Forsstrom, L. Pasila, V. Velagapudi, C.J. Carroll, J. Auwerx, A. Suomalainen, Effective treatment of mitochondrial myopathy by nicotinamide riboside, a vitamin B3, EMBO Mol. Med.6 (2014) 721–731.
[36] R.D. Martinus, G.P. Garth, T.L. Webster, P. Cartwright, D.J. Naylor, P.B. Hoj, N.J. Hoogenraad, Selective induction of mitochondrial chaperones in response to
loss of the mitochondrial genome, Eur. J. Biochem. FEBS 240 (1996) 98–103.
[37] T. Yoneda, C. Benedetti, F. Urano, S.G. Clark, H.P. Harding, D. Ron, Compartment- specific perturbation of protein handling activates genes encoding mitochondrial chaperones, J. Cell Sci. 117 (2004) 4055–4066.
[38] Q. Zhao, J. Wang, I.V. Levichkin, S. Stasinopoulos, M.T. Ryan, N.J. Hoogenraad, A mitochondrial specific stress response in mammalian cells, EMBO J. 21 (2002) 4411–4419.

[39] L.J. Goodyear, The exercise pill—too good to be true? N. Engl. J. Med. 359 (2008) 1842–1844.
[40] N. Musi, L.J. Goodyear, Targeting the AMP-activated protein kinase for the treatment of type 2 diabetes, Curr. Drug Targets Immune Endocr. Metabol. Disord. 2(2002) 119–127.
[41] N. Yamamoto, H. Nokihara, Y. Yamada, Y. Goto, M. Tanioka, T. Shibata, K.
Yamada, H. Asahina, T. Kawata, X. Shi, T. Tamura, A Phase I,dose-finding and pharmacokinetic study of olaparib (AZD2281) in Japanese patients with advanced solid tumors, Cancer Sci. 103 (2012) 504–509.
[42] N. Bundred, J. Gardovskis, J. Jaskiewicz, J. Eglitis, V. Paramonov, P. McCormack, H. Swaisland, M. Cavallin, T. Parry, J. Carmichael, J.M. Dixon, Evaluation of the pharmacodynamics and pharmacokinetics of the PARP inhibitor olaparib: a phase I multicentre trial in patients scheduled for elective breast cancer surgery, Investig. New Drugs 31 (2013) 949–958.
[43] E. Pirinen, C. Canto, Y.S. Jo, L. Morato, H. Zhang, K.J. Menzies, E.G. Williams, L. Mouchiroud, N. Moullan, C. Hagberg, W. Li, S. Timmers, R. Imhof, J. Verbeek, A. Pujol, B. van Loon, C. Viscomi, M. Zeviani, P. Schrauwen, A.A. Sauve, K. Schoonjans, J. Auwerx, Pharmacological inhibition of poly(ADP-Ribose) polymerases improves fitness and mitochondrial function in skeletal muscle, Cell Metab. 19 (2014) 1034–1041.
[44] S.J. Park, F. Ahmad, A. Philp, K. Baar, T. Williams, H. Luo, H. Ke, H. Rehmann, R. Taussig, A.L. Brown, M.K. Kim, M.A. Beaven, A.B. Burgin, V. Manganiello, J.H. Chung, Resveratrol ameliorates aging-related metabolic phenotypes by inhibiting cAMP phosphodiesterases, Cell 148 (2012) 421–433.
[45] A. Lopes Costa, C. Le Bachelier, L. Mathieu, A. Rotig, A. Boneh, P. De Lonlay, M.A. Tarnopolsky, D.R. Thorburn, J. Bastin, F. Djouadi, Beneficial effects of resveratrol on respiratory chain defects in patients' fibroblasts involve estrogen receptor and estrogen-related receptor alpha signaling, Hum. Mol. Genet. 23 (2014) 2106–2119.
[46] G. Deblois, V. Giguere, Functional and physiological genomics of estrogen-related receptors (ERRs) in health and disease, Biochim. Biophys. Acta 1812 (2011) 1032–1040.

[47] A. Hofer, N. Noe, C. Tischner, N. Kladt, V. Lellek, A. Schauss, T. Wenz, Defining the action spectrum of potential PGC-1alpha activators on a mitochondrial and cellular level in vivo, Hum. Mol. Genet. 23 (2014) 2400–2415.
[48] S. Chae, B.Y. Ahn, K. Byun, Y.M. Cho, M.H. Yu, B. Lee, D. Hwang, K.S. Park, A systems approach for decoding mitochondrial retrograde signaling pathways, Sci. Signal. 6 (2013) rs4.
[49] A. Safdar, J.M. Bourgeois, D.I. Ogborn, J.P. Little, B.P. Hettinga, M. Akhtar, J.E. Thompson, S. Melov, N.J. Mocellin, G.C. Kujoth, T.A. Prolla, M.A. Tarnopolsky, Endurance exercise rescues progeroid aging and induces systemic mitochondrial rejuvenation in mtDNA mutator mice, Proc. Natl. Acad. Sci. U. S. A. 108 (2011) 4135–4140.
[50] G.C. Rowe, R. El-Khoury, I.S. Patten, P. Rustin, Z. Arany, PGC-1alpha is dispensable for exercise-induced mitochondrial biogenesis in skeletal muscle, PLoS One 7 (2012) e41817.
[51] G.C. Rowe, I.S. Patten, Z.K. Zsengeller, R. El-Khoury, M. Okutsu, S. Bampoh, N. Koulisis, C. Farrell, M.F. Hirshman, Z. Yan, L.J. Goodyear, P. Rustin, Z. Arany, Disconnecting mitochondrial content from respiratory chain capacity in PGC-1-deficient skeletal muscle, Cell Rep. 3 (2013) 1449–1456.
[52] T.D. Jeppesen, M. Schwartz, D.B. Olsen, F. Wibrand, T. Krag, M. Duno, S. Hauerslev, J. Vissing, Aerobic training is safe and improves exercise capacity in patients with mitochondrial myopathy, Brain 129 (2006) 3402–3412.
[53] M. Zeviani, Train, train, train! No pain, just gain, Brain 131 (2008) 2809–2811.
[54] J.L. Murphy, E.L. Blakely, A.M. Schaefer, L. He, P. Wyrick, R.G. Haller, R.W. Taylor, D.M. Turnbull, T. Taivassalo, Resistance training in patients with single, large-scale deletions of mitochondrial DNA, Brain 131 (2008) 2832–2840.
[55] T. Wenz, F. Diaz, D. Hernandez, C.T. Moraes, Endurance exercise is protective for mice with mitochondrial myopathy, J. Appl. Physiol. 106 (2009) 1712–1719.
[56] C. Viscomi, A.B. Burlina, I. Dweikat, M. Savoiardo, C. Lamperti, T. Hildebrandt, V. Tiranti, M. Zeviani, Combined treatment with oral metronidazole and N- acetylcysteine is effective in ethylmalonic encephalopathy, Nat. Med. 16 (2010) 869–871.

[57] V. Tiranti, C. Viscomi, T. Hildebrandt, I. Di Meo, R. Mineri, C. Tiveron, M.D. Levitt, A. Prelle, G. Fagiolari, M. Rimoldi, M. Zeviani, Loss of ETHE1, a mitochondrial dioxygenase, causes fatal sulfide toxicity in ethylmalonic encephalopathy, Nat. Med. 15 (2009) 200–205.
[58] S.L. Melideo, M.R. Jackson, M.S. Jorns, Biosynthesis of a central intermediate in hydrogen sulfide metabolism by a novel human sulfur transferase and its yeast ortholog, Biochemistry 53 (2014) 4739–4753.
[59] N. Raimundo, Mitochondrial pathology: stress signals from the energy factory, Trends Mol. Med. 20 (2014) 282–292.
[60] L.A. Sena, N.S. Chandel, Physiological roles of mitochondrial reactive oxygen species, Mol. Cell 48 (2012) 158–167.
[61] M.D. Brand, The sites and topology of mitochondrial superoxide production, Exp. Gerontol. 45 (2010) 466–472.
[62] A. Bratic, N.G. Larsson, The role of mitochondria in aging, J. Clin. Invest. 123 (2013) 951–957.
[63] N. Raimundo, L. Song, T.E. Shutt, S.E. McKay, J. Cotney, M.X. Guan, T.C. Gilliland, D. Hohuan, J. Santos-Sacchi, G.S. Shadel, Mitochondrial stress engages E2F1 apoptotic signaling to cause deafness, Cell 148 (2012) 716–726.
[64] S.E. Schriner, N.J. Linford, G.M. Martin, P. Treuting, C.E. Ogburn, M. Emond, P.E. Coskun, W. Ladiges, N. Wolf, H. Van Remmen, D.C. Wallace, P.S. Rabinovitch, Extension of murine life span by overexpression of catalase targeted to mitochondria, Science 308 (2005) 1909–1911.
[65] L. Liu, K. Zhang, H. Sandoval, S. Yamamoto, M. Jaiswal, E. Sanz, Z. Li, J. Hui, B.H. Graham, A. Quintana, H.J. Bellen, Glial Lipid Droplets and ROS Induced by Mitochondrial Defects Promote Neurodegeneration, Cell 160 (2015) 177–190.
[66] L. Blanchet, J.A. Smeitink, S.E. van Emst-de Vries, C. Vogels, M. Pellegrini, A.I. Jonckheere, R.J. Rodenburg, L.M. Buydens, J. Beyrath, P.H. Willems, W.J. Koopman, Quantifying small molecule phenotypic effects using mitochondrial morpho-functional fingerprinting and machine learning, Sci. Rep. 5 (2015) 8035.
[67] J.W. Taanman, J.R. Muddle, A.C. Muntau, Mitochondrial DNA depletion can be prevented by dGMP and dAMP supplementation in a resting culture of deoxyguanosine kinase-deficient fibroblasts, Hum. Mol. Genet. 12 (2003) 1839–1845.

[68] S. Bulst, A. Abicht, E. Holinski-Feder, S. Muller-Ziermann, U. Koehler, C. Thirion, M.C. Walter, J.D. Stewart, P.F. Chinnery, H. Lochmuller, R. Horvath, In vitro supplementation with dAMP/dGMP leads to partial restoration of mtDNA levels in mitochondrial depletion syndromes, Hum. Mol. Genet. 18 (2009) 1590–1599.
[69] S. Bulst, E. Holinski-Feder, B. Payne, A. Abicht, S. Krause, H. Lochmuller, P.F. Chinnery, M.C. Walter, R. Horvath, In vitro supplementation with deoxynucleoside monophosphates rescues mitochondrial DNA depletion, Mol. Genet. Metab. 107 (2012) 95–103.
[70] Y. Camara, E. Gonzalez-Vioque, M. Scarpelli, J. Torres-Torronteras, A. Caballero, M. Hirano, R. Marti, Administration of deoxyribonucleosides or inhibition of their catabolism as a pharmacological approach for mitochondrial DNA depletion syndrome, Hum. Mol. Genet. 23 (2014) 2459–2467.
[71] I. Nishino, A. Spinazzola, M. Hirano, Thymidine phosphorylase gene mutations in MNGIE, a human mitochondrial disorder, Science 283 (1999) 689–692.
[72] I. Nishino, A. Spinazzola, M. Hirano, MNGIE: from nuclear DNA to mitochondrial DNA, Neuromuscul. Disord. NMD 11 (2001) 7–10.
[73] A. Spinazzola, R. Marti, I. Nishino, A.L. Andreu, A. Naini, S. Tadesse, I. Pela, E. Zammarchi, M.A. Donati, J.A. Oliver, M. Hirano, Altered thymidine metabolism due to defects of thymidine phosphorylase, J. Biol. Chem. 277 (2002) 4128–4133.
[74] L. Galluzzi, F. Pietrocola, B. Levine, G. Kroemer, Metabolic control of autophagy, Cell 159 (2014) 1263–1276.
[75] N. Mizushima, Autophagy: process and function, Genes Dev. 21 (2007) 2861–2873.
[76] D.C. Rubinsztein, P. Codogno, B. Levine, Autophagy modulation as a potential therapeutic target for diverse diseases, Nat. Rev. Drug Discov. 11 (2012) 709–730.
[77] C. Settembre, A. Fraldi, D.L. Medina, A. Ballabio, Signals from the lysosome: a control centre for cellular clearance and energy metabolism, Nat. Rev. Mol. Cell Biol. 14 (2013) 283–296.
[78] P. Mishra, D.C. Chan, Mitochondrial dynamics and inheritance during cell division, development and disease, Nat. Rev. Mol. Cell Biol. 15 (2014) 634–646.

[79] S.C. Johnson, M.E. Yanos, E.B. Kayser, A. Quintana, M. Sangesland, A. Castanza, L. Uhde, J. Hui, V.Z. Wall, A. Gagnidze, K. Oh, B.M. Wasko, F.J. Ramos, R.D. Palmiter, P.S. Rabinovitch, P.G. Morgan, M.M. Sedensky, M. Kaeberlein, mTOR inhibition alle- viates mitochondrial disease in a mouse model of Leigh syndrome, Science 342 (2013) 1524–1528.
[80] J. Nunnari, A. Suomalainen, Mitochondria: in sickness and in health, Cell 148
(2012) 1145–1159.
[81] S. Santra, R.W. Gilkerson, M. Davidson, E.A. Schon, Ketogenic treatment reduces deleted mitochondrial DNAs in cultured human cells, Ann. Neurol. 56 (2004) 662–669.
[82] P.G. Sullivan, N.A. Rippy, K. Dorenbos, R.C. Concepcion, A.K. Agarwal, J.M. Rho, The ketogenic diet increases mitochondrial uncoupling protein levels and activity, Ann. Neurol. 55 (2004) 576–580.
[83] K.J. Bough, J. Wetherington, B. Hassel, J.F. Pare, J.W. Gawryluk, J.G. Greene, R. Shaw, Y. Smith, J.D. Geiger, R.J. Dingledine, Mitochondrial biogenesis in the anticonvulsant mechanism of the ketogenic diet, Ann. Neurol. 60 (2006) 223–235.
[84] S.G. Jarrett, J.B. Milder, L.P. Liang, M. Patel, The ketogenic diet increases
mitochondrial glutathione levels, J. Neurochem. 106 (2008) 1044–1051.
[85] S. Ahola-Erkkila, C.J. Carroll, K. Peltola-Mjosund, V. Tulkki, I. Mattila, T. Seppanen- Laakso, M. Oresic, H. Tyynismaa, A. Suomalainen, Ketogenic diet slows down mitochondrial myopathy progression in mice, Hum. Mol. Genet. 19 (2010) 1974–1984.
[86] T. Wenz, C. Luca, A. Torraco, C.T. Moraes, mTERF2 regulates oxidative phosphorylation by modulating mtDNA transcription, Cell Metab. 9 (2009) 499–511.
[87] E. Bottani, C. Giordano, G. Civiletto, I. Di Meo, A. Auricchio, E. Ciusani, S. Marchet, C. Lamperti, G. d'Amati, C. Viscomi, M. Zeviani, AAV-mediatedliver-specific MPV17 expression restores mtDNA levels and prevents diet-induced liver failure, Mol. Ther. 22 (2013) 10–17.
[88] M. Schiff, P. Benit, R. El-Khoury, D. Schlemmer, J.F. Benoist, P. Rustin, Mouse studies to shape clinical trials for

mitochondrial diseases: high fat diet in Harlequin mice, PLoS One 6 (2011) e28823.
[89] C.R. Roe, L. Sweetman, D.S. Roe, F. David, H. Brunengraber, Treatment of cardiomyopathy and rhabdomyolysis in long-chain fat oxidation disorders using an anaplerotic odd-chain triglyceride, J. Clin. Invest. 110 (2002) 259–269.
[90] N.J. Watmough, L.A. Bindoff, M.A. Birch-Machin, S. Jackson, K. Bartlett, C.I. Ragan, J. Poulton, R.M. Gardiner, H.S. Sherratt, D.M. Turnbull, Impaired mitochondrial beta- oxidation in a patient with an abnormality of the respiratory chain. Studies in skeletal muscle mitochondria, J. Clin. Invest. 85 (1990) 177–184.
[91] V. Giorgio, S. von Stockum, M. Antoniel, A. Fabbro, F. Fogolari, M. Forte, G.D. Glick, V. Petronilli, M. Zoratti, I. Szabo, G. Lippe, P. Bernardi, Dimers of mitochondrial ATP synthase form the permeability transition pore, Proc. Natl. Acad. Sci. U. S. A. 110 (2013) 5887–5892.
[92] A. Rasola, P. Bernardi, The mitochondrial permeability transition pore and its involvement in cell death and in disease pathogenesis, Apoptosis 12 (2007) 815–833.
[93] L. Merlini, A. Angelin, T. Tiepolo, P. Braghetta, P. Sabatelli, A. Zamparelli, A. Ferlini, N.M. Maraldi, P. Bonaldo, P. Bernardi, Cyclosporin A corrects mitochondrial dys- function and muscle apoptosis in patients with collagen VI myopathies, Proc. Natl. Acad. Sci. U. S. A. 105 (2008) 5225–5229.
[94] F. Mingozzi, K.A. High, Therapeutic in vivo gene transfer for genetic disease using AAV: progress and challenges, Nat. Rev. Genet. 12 (2011) 341–355.
[95] G.P. Gao, M.R. Alvira, L. Wang, R. Calcedo, J. Johnston, J.M. Wilson, Novel adeno- associated viruses from rhesus monkeys as vectors for human gene therapy, Proc. Natl. Acad. Sci. U. S. A. 99 (2002) 11854–11859.
[96] A. Flierl, Y. Chen, P.E. Coskun, R.J. Samulski, D.C. Wallace, Adeno-associatedvirus- mediated gene transfer of the heart/muscle adenine nucleotide translocator (ANT) in mouse, Gene Ther. 12 (2005) 570–578.
[97] I. Di Meo, A. Auricchio, C. Lamperti, A. Burlina, C. Viscomi, M. Zeviani, Effective AAV-mediated gene therapy in a mouse model of ethylmalonic encephalopathy, EMBO Mol. Med. 4 (2012) 1008–1014.

[98] J. Torres-Torronteras, C. Viscomi, R. Cabrera-Perez, Y. Camara, I. Di Meo, J. Barquinero, A. Auricchio, G. Pizzorno, M. Hirano, M. Zeviani, R. Marti, Gene therapy using a liver-targetedAAV vector restores nucleoside and nucleotide homeostasis in a murine model of MNGIE, Mol. Ther. 22 (2014) 901–907.
[99] M. Hirano, R. Marti, C. Casali, S. Tadesse, T. Uldrick, B. Fine, D.M. Escolar, M.L. Valentino, I. Nishino, C. Hesdorffer, J. Schwartz, R.G. Hawks, D.L. Martone, M.S. Cairo, S. DiMauro, M. Stanzani, J.H. Garvin Jr., D.G. Savage, Allogeneic stem cell transplantation corrects biochemical derangements in MNGIE, Neurology 67 (2006) 1458–1460.
[100] S. Rahman, I.P. Hargreaves, Allogeneic stem cell transplantation corrects biochem- ical derangements in MNGIE, Neurology 68 (2007) 1872 (author reply 1872; dis- cussion 1872–1873).
[101] A. Spinazzola, C. Viscomi, E. Fernandez-Vizarra, F. Carrara, P. D'Adamo, S. Calvo, R.M. Marsano, C. Donnini, H. Weiher, P. Strisciuglio, R. Parini, E. Sarzi, A. Chan, S. DiMauro, A. Rotig, P. Gasparini, I. Ferrero, V.K. Mootha, V. Tiranti, M. Zeviani, MPV17 encodes an inner mitochondrial membrane protein and is mutated in infantile hepatic mitochondrial DNA depletion, Nat. Genet. 38 (2006) 570–575.
[102] C.L. Karadimas, T.H. Vu, S.A. Holve, P. Chronopoulou, C. Quinzii, S.D. Johnsen, J. Kurth, E. Eggers, L. Palenzuela, K. Tanji, E. Bonilla, D.C. De Vivo, S. DiMauro, M. Hirano, Navajo neurohepatopathy is caused by a mutation in the MPV17 gene, Am. J. Hum. Genet. 79 (2006) 544–548.
[103] C. Viscomi, A. Spinazzola, M. Maggioni, E. Fernandez-Vizarra, V. Massa, C. Pagano, R. Vettor, M. Mora, M. Zeviani, Early-onset liver mtDNA depletion and late-onset proteinuric nephropathy in Mpv17 knockout mice, Hum. Mol. Genet. 18 (2009) 12–26.
[104] A. Paneda, L. Vanrell, I. Mauleon, J.S. Crettaz, P. Berraondo, E.J. Timmermans, S.G. Beattie, J. Twisk, S. van Deventer, J. Prieto, A. Fontanellas, M.S. Rodriguez-Pena, G. Gonzalez-Aseguinolaza, Effect of adeno-associated virus serotype and genomic structure on liver transduction and biodistribution in mice of both genders, Hum. Gene Ther. 20 (2009) 908–917.

[105] C. Unzu, A. Sampedro, I. Mauleon, M. Alegre, S.G. Beattie, R.E. de Salamanca, J. Snapper, J. Twisk, H. Petry, G. Gonzalez-Aseguinolaza, J. Artieda, M.S. Rodriguez- Pena, J. Prieto, A. Fontanellas, Sustained enzymatic correction by rAAV-mediated liver gene therapy protects against induced motor neuropathy in acute porphyria mice, Mol. Ther. 19 (2011) 243–250.
[106] A. Bouaita, S. Augustin, C. Lechauve, H. Cwerman-Thibault, P. Benit, M. Simonutti, M. Paques, P. Rustin, J.A. Sahel, M. Corral-Debrinski, Downregulation of apoptosis-inducing factor in Harlequin mice induces progressive and severe optic atrophy which is durably prevented by AAV2-AIF1 gene therapy, Brain 135 (2012) 35–52.
[107] J.A. Klein, C.M. Longo-Guess, M.P. Rossmann, K.L. Seburn, R.E. Hurd, W.N. Frankel, R.T. Bronson, S.L. Ackerman, The Harlequin mouse mutation downregulates apoptosis-inducing factor, Nature 419 (2002) 367–374.
[108] M.K. Childers, R. Joubert, K. Poulard, C. Moal, R.W. Grange, J.A. Doering, M.W. Lawlor, B.E. Rider, T. Jamet, N. Daniele, S. Martin, C. Riviere, T. Soker, C. Hammer, L. Van Wittenberghe, M. Lockard, X. Guan, M. Goddard, E. Mitchell, J. Barber, J.K. Williams, D.L. Mack, M.E. Furth, A. Vignaud, C. Masurier, F. Mavilio, P. Moullier, A.H. Beggs, A. Buj-Bello, Gene therapy prolongs survival and restores function in murine and canine models of myotubular myopathy, Sci. Transl. Med. 6 (2014) 220ra210.
[109] J.P. Greelish, L.T. Su, E.B. Lankford, J.M. Burkman, H. Chen, S.K. Konig, I.M. Mercier, P.R. Desjardins, M.A. Mitchell, X.G. Zheng, J. Leferovich, G.P. Gao, R.J. Balice-Gordon, J.M. Wilson, H.H. Stedman, Stable restoration of the sarcoglycan complex in dystro- phic muscle perfused with histamine and a recombinant adeno-associated viral vector, Nat. Med. 5 (1999) 439–443.
[110] P. Gregorevic, M.J. Blankinship, J.M. Allen, R.W. Crawford, L. Meuse, D.G. Miller, D.W. Russell, J.S. Chamberlain, Systemic delivery of genes to striated muscles using adeno-associated viral vectors, Nat. Med. 10 (2004) 828–834.
[111] C. Bonnet, V. Kaltimbacher, S. Ellouze, S. Augustin, P. Benit, V. Forster, P. Rustin, J.A. Sahel, M. Corral-Debrinski, Allotopic mRNA localization to the mitochondrial surface

rescues respiratory chain defects in fibroblasts harboring mitochondrial DNA mutations affecting complex I or v subunits, Rejuvenation Res. 10 (2007) 127–144.
[112] V. Kaltimbacher, C. Bonnet, G. Lecoeuvre, V. Forster, J.A. Sahel, M. Corral
Debrinski, mRNA localization to the mitochondrial surface allows the efficient translocation inside the organelle of a nuclear recoded ATP6 protein, RNA 12 (2006) 1408–1417.
[113] C. Bonnet, S. Augustin, S. Ellouze, P. Benit, A. Bouaita, P. Rustin, J.A. Sahel, M. Corral- Debrinski, The optimized allotopic expression of ND1 or ND4 genes restores respiratory chain complex I activity in fibroblasts harboring mutations in these genes, Biochim. Biophys. Acta 1783 (2008) 1707–1717.
[114] S. Ellouze, S. Augustin, A. Bouaita, C. Bonnet, M. Simonutti, V. Forster, S. Picaud, J.A. Sahel, M. Corral-Debrinski, Optimized allotopic expression of the human mitochondrial ND4 prevents blindness in a rat model of mitochondrial dysfunction, Am. J. Hum. Genet. 83 (2008) 373–387.
[115] E. Perales-Clemente, P. Fernandez-Silva, R. Acin-Perez, A. Perez-Martos, J.A. Enriquez, Allotopic expression of mitochondrial-encoded genes in mammals: achieved goal, undemonstrated mechanism or impossible task? Nucleic Acids Res. 39 (2011) 225–234.
[116] H. Yu, R.D. Koilkonda, T.H. Chou, V. Porciatti, S.S. Ozdemir, V. Chiodo, S.L. Boye, S.E. Boye, W.W. Hauswirth, A.S. Lewin, J. Guy, Gene delivery to mitochondria by targeting modified adenoassociated virus suppresses Leber's hereditary optic neuropathy in a mouse model, Proc. Natl. Acad. Sci. U. S. A. 109 (2012) E1238–E1247.
[117] R.W. Taylor, P.F. Chinnery, D.M. Turnbull, R.N. Lightowlers, Selective inhibition of mutant human mitochondrial DNA replication in vitro by peptide nucleic acids, Nat. Genet. 15 (1997) 212–215.
[118] P.F. Chinnery, R.W. Taylor, K. Diekert, R. Lill, D.M. Turnbull, R.N. Lightowlers, Peptide nucleic acid delivery to human mitochondria, Gene Ther. 6 (1999) 1919–1928.
[119] A. Muratovska, R.N. Lightowlers, R.W. Taylor, D.M. Turnbull, R.A. Smith, J.A. Wilce, S.W. Martin, M.P. Murphy, Targeting peptide nucleic acid (PNA) oligomers to mitochondria within cells by conjugation to lipophilic cations: implications for

mitochondrial DNA replication, expression and disease, Nucleic Acids Res. 29 (2001) 1852–1863.
[120] A. Flierl, C. Jackson, B. Cottrell, D. Murdock, P. Seibel, D.C. Wallace, Targeted delivery of DNA to the mitochondrial compartment via import sequence- conjugatedpeptide nucleic acid, Mol. Ther. 7 (2003) 550–557.
[121] G. Wang, H.W. Chen, Y. Oktay, J. Zhang, E.L. Allen, G.M. Smith, K.C. Fan, J.S. Hong, S.W. French, J.M. McCaffery, R.N. Lightowlers, H.C. Morse 3rd, C.M. Koehler, M.A. Teitell, PNPASE regulates RNA import into mitochondria, Cell 142 (2010) 456–467.
[122] G. Wang, E. Shimada, J. Zhang, J.S. Hong, G.M. Smith, M.A. Teitell, C.M. Koehler, Correcting human mitochondrial mutations with targeted RNA import, Proc. Natl. Acad. Sci. U. S. A. 109 (2012) 4840–4845.
[123] S.R. Bacman, S.L. Williams, D. Hernandez, C.T. Moraes, Modulating mtDNA heteroplasmy by mitochondria-targeted restriction endonucleases in a 'differential multiple cleavage-site' model, Gene Ther. 14 (2007) 1309–1318.
[124] S.R. Bacman, S.L. Williams, D. Duan, C.T. Moraes, Manipulation of mtDNA heteroplasmy in all striated muscles of newborn mice by AAV9-mediated delivery of a mitochondria-targeted restriction endonuclease, Gene Ther. 19 (2012) 1101–1106.
[125] S. Srivastava, C.T. Moraes, Manipulating mitochondrial DNA heteroplasmy by a mitochondrially targeted restriction endonuclease, Hum. Mol. Genet. 10 (2001) 3093–3099.
[126] P.A. Gammage, J. Rorbach, A.I. Vincent, E.J. Rebar, M. Minczuk, Mitochondrially targeted ZFNs for selective degradation of pathogenic mitochondrial genomes bearing large-scale deletions or point mutations, EMBO Mol. Med. 6 (2014) 458–466.
[127] S.R. Bacman, S.L. Williams, M. Pinto, S. Peralta, C.T. Moraes, Specific elimination of mutant mitochondrial genomes in patient-derived cells by mitoTALENs, Nat. Med. 19 (2013) 1111–1113.
[128] M. Tanaka, H.J. Borgeld, J. Zhang, S. Muramatsu, J.S. Gong, M. Yoneda, W. Maruyama, M. Naoi, T. Ibi, K. Sahashi, M. Shamoto, N. Fuku, M. Kurata, Y. Yamada, K. Nishizawa, Y. Akao, N. Ohishi, S. Miyabayashi, H. Umemoto, T. Muramatsu, K. Furukawa, A. Kikuchi, I. Nakano, K. Ozawa, K. Yagi, Gene

therapy for mitochondrial disease by delivering restriction endonuclease SmaI into mito- chondria, J. Biomed. Sci. 9 (2002) 534–541.
[129] M.F. Alexeyev, N. Venediktova, V. Pastukh, I. Shokolenko, G. Bonilla, G.L. Wilson, Selective elimination of mutant mitochondrial genomes as therapeutic strategy for the treatment of NARP and MILS syndromes, Gene Ther. 15 (2008) 516–523.
[130] M.P. Bayona-Bafaluy, B. Blits, B.J. Battersby, E.A. Shoubridge, C.T. Moraes, Rapid directional shift of mitochondrial DNA heteroplasmy in animal tissues by a mitochondrially targeted restriction endonuclease, Proc. Natl. Acad. Sci. U. S. A. 102 (2005) 14392–14397.
[131] S.R. Bacman, S.L. Williams, S. Garcia, C.T. Moraes, Organ-specific shifts in mtDNA heteroplasmy following systemic delivery of a mitochondria-targeted restriction endonuclease, Gene Ther. 17 (2010) 713–720.
[132] Y.G. Kim, J. Cha, S. Chandrasegaran, Hybrid restriction enzymes: zinc finger fusions to Fok I cleavage domain, Proc. Natl. Acad. Sci. U. S. A. 93 (1996) 1156–1160.
[133] J. Smith, M. Bibikova, F.G. Whitby, A.R. Reddy, S. Chandrasegaran, D. Carroll, Requirements for double-strand cleavage by chimeric restriction enzymes with zinc finger DNA-recognition domains, Nucleic Acids Res. 28 (2000) 3361–3369.
[134] E.A. Schon, R. Rizzuto, C.T. Moraes, H. Nakase, M. Zeviani, S. DiMauro, A direct repeat is a hotspot for large-scale deletion of human mitochondrial DNA, Science 244 (1989) 346–349.
[135] M. Corral-Debrinski, T. Horton, M.T. Lott, J.M. Shoffner, M.F. Beal, D.C. Wallace, Mitochondrial DNA deletions in human brain: regional variability and increase with advanced age, Nat. Genet. 2 (1992) 324–329.
[136] N.W. Soong, D.R. Hinton, G. Cortopassi, N. Arnheim, Mosaicism for a specific somatic mitochondrial DNA mutation in adult human brain, Nat. Genet. 2 (1992) 318–323.
[137] A.S. Jun, I.A. Trounce, M.D. Brown, J.M. Shoffner, D.C. Wallace, Use of transmitochondrial cybrids to assign a complex I defect to the mitochondrial DNA-encodedNADH dehydrogenase subunit 6 gene mutation at nucleotide pair 14459 that causes Leber hereditary optic neuropathy and dystonia, Mol. Cell. Biol. 16 (1996) 771–777.

[138] S.G. Park, P. Schimmel, S. Kim, Aminoacyl tRNA synthetases and their connections to disease, Proc. Natl. Acad. Sci. U. S. A. 105 (2008) 11043–11049.
[139] C. De Luca, C. Besagni, L. Frontali, M. Bolotin-Fukuhara, S. Francisci, Mutations in yeast mt tRNAs: specific and general suppression by nuclear encoded tRNA interactors, Gene 377 (2006) 169–176.
[140] C. De Luca, Y. Zhou, A. Montanari, V. Morea, R. Oliva, C. Besagni, M. Bolotin- Fukuhara, L. Frontali, S. Francisci, Can yeast be used to study mitochondrial diseases? Biolistic tRNA mutants for the analysis of mechanisms and suppressors, Mitochondrion 9 (2009) 408–417.
[141] R. Li, M.X. Guan, Human mitochondrial leucyl-tRNA synthetase corrects mitochondrial dysfunctions due to the tRNALeu(UUR) A3243G mutation, associated with mitochondrial encephalomyopathy, lactic acidosis, and stroke-like symptoms and diabetes, Mol. Cell. Biol. 30 (2010) 2147–2154.
[142] J. Rorbach, A.A. Yusoff, H. Tuppen, D.P. Abg-Kamaludin, Z.M. Chrzanowska- Lightowlers, R.W. Taylor, D.M. Turnbull, R. McFarland, R.N. Lightowlers, Overexpression of human mitochondrial valyl tRNA synthetase can partially re- store levels of cognate mt-tRNAVal carrying the pathogenic C25U mutation, Nucleic Acids Res. 36 (2008) 3065–3074.
[143] E. Perli, C. Giordano, H.A. Tuppen, M. Montopoli, A. Montanari, M. Orlandi, A. Pisano, D. Catanzaro, L. Caparrotta, B. Musumeci, C. Autore, V. Morea, P. Di Micco, A.F. Campese, M. Leopizzi, P. Gallo, S. Francisci, L. Frontali, R.W. Taylor, G. d'Amati, Isoleucyl-tRNA synthetase levels modulate the penetrance of a homoplasmic m.4277TNC mitochondrial tRNA(Ile) mutation causing hypertrophic cardiomyopathy, Hum. Mol. Genet. 21 (2012) 85–100.
[144] H.T. Hornig-Do, A. Montanari, A. Rozanska, H.A. Tuppen, A.A. Almalki, D.P. Abg- Kamaludin, L. Frontali, S. Francisci, R.N. Lightowlers, Z.M. Chrzanowska- Lightowlers, Human mitochondrial leucyl tRNA synthetase can suppress non cognate pathogenic mt-tRNA mutations, EMBO Mol. Med. 6 (2014) 183–193.
[145] E. Perli, C. Giordano, A. Pisano, A. Montanari, A.F. Campese, A. Reyes, D. Ghezzi, A. Nasca, H.A. Tuppen, M. Orlandi, P. Di Micco, E. Poser, R.W. Taylor, G. Colotti, S.

Francisci, V. Morea, L. Frontali, M. Zeviani, G. d'Amati, The isolated carboxy- terminal domain of human mitochondrial leucyl-tRNA synthetase rescues the pathological phenotype of mitochondrial tRNA mutations in human cells, EMBO Mol. Med. 6 (2014) 169–182.
[146] O.A. Kolesnikova, N.S. Entelis, C. Jacquin-Becker, F. Goltzene, Z.M. Chrzanowska- Lightowlers, R.N. Lightowlers, R.P. Martin, I. Tarassov, Nuclear DNA-encoded tRNAs targeted into mitochondria can rescue a mitochondrial DNA mutation associated with the MERRF syndrome in cultured human cells, Hum. Mol. Genet. 13 (2004) 2519–2534.
[147] C. Comte, Y. Tonin, A.M. Heckel-Mager, A. Boucheham, A. Smirnov, K. Aure, A. Lombes, R.P. Martin, N. Entelis, I. Tarassov, Mitochondrial targeting of recombinant RNAs modulates the level of a heteroplasmic mutation in human mitochondrial DNA associated with Kearns Sayre Syndrome, Nucleic Acids Res. 41 (2013) 418–433.
[148] B. Mahata, S. Mukherjee, S. Mishra, A. Bandyopadhyay, S. Adhya, Functional delivery of a cytosolic tRNA into mutant mitochondria of human cells, Science 314 (2006) 471–474.
[149] J.R. Friedman, J. Nunnari, Mitochondrial form and function, Nature 505 (2014) 335–343.
[150] C. Alexander, M. Votruba, U.E. Pesch, D.L. Thiselton, S. Mayer, A. Moore, M. Rodriguez, U. Kellner, B. Leo-Kottler, G. Auburger, S.S. Bhattacharya, B. Wissinger, OPA1, encoding a dynamin-related GTPase, is mutated in autosomal dominant optic atrophy linked to chromosome 3q28, Nat. Genet. 26 (2000) 211–215.
[151] S. Zuchner, I.V. Mersiyanova, M. Muglia, N. Bissar-Tadmouri, J. Rochelle, E.L. Dadali, M. Zappia, E. Nelis, A. Patitucci, J. Senderek, Y. Parman, O. Evgrafov, P.D. Jonghe, Y. Takahashi, S. Tsuji, M.A. Pericak-Vance, A. Quattrone, E. Battaloglu, A.V. Polyakov, V. Timmerman, J.M. Schroder, J.M. Vance, Mutations in the mitochondrial GTPase mitofusin 2 cause Charcot–Marie–Tooth neuropathy type 2A, Nat. Genet. 36 (2004) 449–451.
[152] H. Chen, M. Vermulst, Y.E. Wang, A. Chomyn, T.A. Prolla, J.M. McCaffery, D.C. Chan, Mitochondrial fusion is required for mtDNA stability in skeletal muscle and tolerance of mtDNA mutations, Cell 141 (2010) 280–289.

[153] S. Cogliati, C. Frezza, M.E. Soriano, T. Varanita, R. Quintana-Cabrera, M. Corrado, S. Cipolat, V. Costa, A. Casarin, L.C. Gomes, E. Perales-Clemente, L. Salviati, P. Fernandez-Silva, J.A. Enriquez, L. Scorrano, Mitochondrial cristae shape determines respiratory chain supercomplexes assembly and respiratory efficiency, Cell 155 (2013) 160–171.
[154] G.A. Hakkaart, E.P. Dassa, H.T. Jacobs, P. Rustin, Allotopic expression of a mitochondrial alternative oxidase confers cyanide resistance to human cell respiration, EMBO Rep. 7 (2006) 341–345.
[155] R. El-Khoury, E. Dufour, M. Rak, N. Ramanantsoa, N. Grandchamp, Z. Csaba, B. Duvillie, P. Benit, J. Gallego, P. Gressens, C. Sarkis, H.T. Jacobs, P. Rustin, Alternative oxidase ex- pression in the mouse enables bypassing cytochrome c oxidase blockade and limits mitochondrial ROS overproduction, PLoS Genet. 9 (2013) e1003182.
[156] E. Perales-Clemente, M.P. Bayona-Bafaluy, A. Perez-Martos, A. Barrientos, P. Fernandez-Silva, J.A. Enriquez, Restoration of electron transport without proton pumping in mammalian mitochondria, Proc. Natl. Acad. Sci. U. S. A. 105 (2008) 18735–18739.
[157] E.P. Dassa, E. Dufour, S. Goncalves, V. Paupe, G.A. Hakkaart, H.T. Jacobs, P. Rustin, Expression of the alternative oxidase complements cytochrome c oxidase deficiency in human cells, EMBO Mol. Med. 1 (2009) 30–36.
[158] D.J. Fernandez-Ayala, A. Sanz, S. Vartiainen, K.K. Kemppainen, M. Babusiak, E. Mustalahti, R. Costa, T. Tuomela, M. Zeviani, J. Chung, K.M. O'Dell, P. Rustin, H.T. Jacobs, Expression of the Ciona intestinalis alternative oxidase (AOX) in Drosophila complements defects in mitochondrial oxidative phosphorylation, Cell Metab. 9 (2009) 449–460.
[159] A. Sanz, M. Soikkeli, M. Portero-Otin, A. Wilson, E. Kemppainen, G. McIlroy, S. Ellila, K.K. Kemppainen, T. Tuomela, M. Lakanmaa, E. Kiviranta, R. Stefanatos, E. Dufour, B. Hutz, A. Naudi, M. Jove, A. Zeb, S. Vartiainen, A. Matsuno-Yagi, T. Yagi, P. Rustin, R. Pamplona, H.T. Jacobs, Expression of the yeast NADH dehydrogenase Ndi1 in Drosophila confers increased lifespan independently of dietary restriction, Proc. Natl. Acad. Sci. U. S. A. 107 (2010) 9105–9110.
[160] K.K. Kemppainen, J. Rinne, A. Sriram, M. Lakanmaa, A. Zeb, T. Tuomela, A. Popplestone, S. Singh, A. Sanz, P. Rustin,

H.T. Jacobs, Expression of alternative oxidase in Drosophila ameliorates diverse phenotypes due to cytochrome oxidase deficiency, Hum. Mol. Genet. 23 (2014) 2078–2093.
[161] P. Rustin, H.T. Jacobs, Respiratory chain alternative enzymes as tools to better understand and counteract respiratory chain deficiencies in human cells and animals, Physiol. Plant. 137 (2009) 362–370.
[162] M. Tachibana, M. Sparman, H. Sritanaudomchai, H. Ma, L. Clepper, J. Woodward, Y. Li, C. Ramsey, O. Kolotushkina, S. Mitalipov, Mitochondrial gene replacement in primate offspring and embryonic stem cells, Nature 461 (2009) 367–372.
[163] M. Tachibana, P. Amato, M. Sparman, J. Woodward, D.M. Sanchis, H. Ma, N.M. Gutierrez, R. Tippner-Hedges, E. Kang, H.S. Lee, C. Ramsey, K. Masterson, D. Battaglia, D. Lee, D. Wu, J. Jensen, P. Patton, S. Gokhale, R. Stouffer, S. Mitalipov, Towards germline gene therapy of inherited mitochondrial diseases, Nature 493 (2013) 627–631.
[164] L. Craven, H.A. Tuppen, G.D. Greggains, S.J. Harbottle, J.L. Murphy, L.M. Cree, A.P. Murdoch, P.F. Chinnery, R.W. Taylor, R.N. Lightowlers, M. Herbert, D.M. Turnbull, Pronuclear transfer in human embryos to prevent transmission of mitochondrial DNA disease, Nature 465 (2010) 82–85.
[165] P.F. Chinnery, L. Craven, S. Mitalipov, J.B. Stewart, M. Herbert, D.M. Turnbull, The challenges of mitochondrial replacement, PLoS Genet. 10 (2014) e1004315.

Acknowledgements

This work was supported by the core grant from the MRC (MC_UP_1002/1), and by grants from: the Pierfranco and Luisa Mariani Foundation Italy (Ricerca2000), Telethon-Italy (GPP10005 and GGP11011 to M.Z.), Cariplo (2011-0526 to M.Z.), ERC (FP7-322424 to M.Z.), and Italian Ministry of Health (GR-2010-2306-756 to C.V.).

Chapter 5

Summary, conclusions and future perspectives

1. Summary

During my PhD program I have been involved in a project organized in two sections: in the first part, I generated and characterized the Ttc19 knockout mouse, a model of primary complex III deficiency; in the second part I applied an AAV-mediated gene therapy approach on the Mpv17 knockout mouse model, for the treatment of a mtDNA depletion syndrome mainly affecting the liver.

In order to achieve these aims, I initially focused on the molecular, biochemical and clinical characterization of the constitutive Ttc19$^{-/-}$ mouse. Similar to what reported in cells from patients and in the *Drosophila* model, knockout mice also showed complex III deficiency in all the tested tissues, as well as a compromised metabolism. This was associated to a clinical phenotype mainly characterized by neurological impairment, as demonstrated by several *in vivo* tests. Neuropathological analysis of the brain revealed accumulation of glial fibrillary acidic protein (GFAP), a marker of activated astrocytes., as well as accumulation of ubiquitinated proteins. Part of the pathogenetic mechanisms in Ttc19-associated diseases might be linked to oxidative stress since complex III is one of the main sites of ROS production within mitochondria [1]. This happens when electron transfer to cytochrome c cannot proceed through the respiratory chain, as, for instance, when the Rieske protein is not incorporated in cells carrying mutations in BCS1L [2]. Accordingly, isolated mitochondria from

Ttc19$^{-/-}$ tissues produced higher amounts of H_2O_2 in an *in vitro* assay.

The molecular analysis of cIII assembly in mouse mitochondria showed that Ttc19 is a $cIII_2$-associated protein, necessary to maintain a proper conformation of the enzyme and for the correct incorporation of the Rieske protein. Unlike other assembly factors (for instance BCS1L and MZM1L/LYRM7) [3, 4], TTC19 seems to be a chaperone that binds to cIII before the incorporation of the Rieske protein, an event mediated by BCS1L and MZM1L/LYRM7, but then remains in contact with cIII during its maturation, up to the formation of fully assembled dimeric $cIII_2$. In support to this view, lack of TTC19 causes a reduction in the incorporation of the catalytic Rieske protein, suggesting a role for TTC19 in the stabilisation of the pre-cIII. In summary, the characterization of the *Ttc19*$^{-/-}$ mouse model allowed us to confirm the involvement of Ttc19 in cIII biogenesis and mitochondrial dysfunction.

The second part of my PhD program was focused of the application of an AAV-mediated gene therapy approach on a mouse model of mtDNA depletion syndrome. In order to target the therapeutic gene to the liver, we constructed an AAV2/8 viral vector expressing the hMPV17 cDNA under the control of a liver-specific promoter and injected it in *Mpv17*$^{-/-}$ and wild type littermates mice. Interestingly, viral DNA was detected only in the liver of treated animals, thus confirming the high specific hepato-tropism of the serotype used. Accordingly, the expression and function of the protein were completely rescued

in *Mpv17*$^{-/-}$ mice, leading to the normalization of the mtDNA copy number in liver, and AST and ALT levels in blood, without any adverse effect on wild type littermates. In addition, we observed that, if exposed to a high fat ketogenic diet, *Mpv17*$^{-/-}$ mice develop fatal liver cirrhosis, likely due to decreased mitochondrial respiratory chain activity and inability to catabolize fat for energy supply through respiration. On the basis of this observation we exposed mice to ketogenic diet after AAV administration and we found that AAV treated, *Mpv17*$^{-/-}$ mice were fully protected from liver failure induced by ketogenic diet. Histological improvement of liver, restoration of normal mtDNA copy number and normalization of OXPHOS biochemical proficiency were present in AAV-treated knockout mice. We also investigated the potential ability of this therapy to correct an ongoing liver damage rather than prevent it. Mice underwent ketogenic diet and, once the hepatic damage was established, they were injected with AAV2/8-hMPV17, as in the first protocol. Although liver in these mice appeared already compromised, expression of the wild type gene was able to block the fatal progress of the disease even though we did not observe a complete regression of liver abnormalities. Taken together these observations suggest that the AAV based therapy is a promising strategy to combat mitochondrial diseases affecting specific, targetable organs.

2. Conclusions

The complexity of mitochondrial metabolism and of the disorders associated with their dysfunction stands as a formidable challenge for the development of effective treatments. Despite remarkable advances in the identification of the molecular mechanisms of primary mitochondrial diseases, their treatment options remain limited to supportive therapies rather than correction of the underlying deficiencies. The development of animal models that faithfully mimic human mitochondrial disease mutations is essential to understand the physiological role of the genes involved in the disease, to unravel the molecular basis of tissue specificity, and to develop therapeutic strategies. Although the last 20 years have been characterized by an exponential increase in understanding the genetic and biochemical mechanisms leading to mitochondrial diseases, this has not resulted in the development of effective therapeutic approaches that still remain focused on supportive interventions. However, new therapeutic strategies have recently been emerging, some of which have shown potential efficacy at the pre-clinical level; in particular, liver-specific AAV-based gene therapy has been successfully tested in several preclinical models [5, 6]. Targeting the liver is a promising approach either in liver specific disease (see Chapter 3) or in diseases characterized by systemic accumulation of toxic compounds [5, 6]. In the latter case, promising results have been achieved in Ethe1$^{-/-}$ mouse, a model of Ethylmalonic Encephalopathy (EE) [5]. EE is a fatal disease, characterized

by the accumulation of hydrogen sulfide (H_2S), a highly toxic compound. ETHE1, encoding a sulfur dioxygenase (SDO), which takes part in the mitochondrial pathway that converts H_2S into harmless SO_4^{2-}, is mutated in EE [7, 8]. At high concentrations, H_2S acts as a poison of several enzymes, such as cytochrome c oxidase [9] and short chain acyl-CoA dehydrogenase (SCAD) [8] and directly damages the vascular endothelium [10]. The re-expression of the wild type gene in the liver of constitutive knockout mice allowed the restoration of the H_2S detoxifying competency of the hepatic filter and reduced the plasma levels of thiosulfate, a biomarker of the disease, and restored cytochrome c oxidase activity in tissues, thus significantly prolonging lifespan of knockout mice [5]. Another effective AAV-liver specific therapy has been achieved in a mouse model of mitochondrial neurogastrointestinal encephalomyopathy (MNGIE). MNGIE is an autosomal recessive disorder caused by mutations in TYMP, encoding thymidine phosphorylase (TP) [11]. TP deficiency results in systemic accumulation of thymidine and deoxyuridine, which interferes with mtDNA replication and leads to mitochondrial dysfunction. AAV2/8-mediated transfer of the TYMP gene to the liver was shown to cause permanent reduction in plasma nucleoside levels to normal values, thus preventing the biochemical imbalances [6].

Successful treatments with the AAV8 have been reported also for non-mitochondrial diseases: rAAV vectors have provided long-term cures of hemophilia B in a number of large-animal

models [12-14], and patients [15]. Taken together, these and other observations strongly support the notion that adeno-associated vectors have emerged as one of the most versatile and most auspicious vectors for human gene therapy.

At the moment, a clinical trial with an AAV2-vector is ongoing for LHON [16]. The application of gene-therapy in LHON is mainly based on the nuclear, allotopic expression of mtDNA-encoded gene ND4 into the retinal ganglion cells. Although, and as already mentioned, limitations remain due to inefficient mitochondrial import of the highly hydrophobic mitohondrially encoded subunit [17], clinical trials sponsored by the University of Miami, Huazhong University of Science and Technology, and Gensight Biologics are currently recruiting patients with the 11778 mutation to assess the safety of gene therapy with an AAV vector carrying the wild-type ND4 gene (http://clinicaltrials.gov) [18]. These studies must demonstrate a tolerable safety profile and sufficient efficacy in protecting and restoring visual acuity in LHON patients. To this aim, a recent work demonstrated the safety of the vector for a phase 1 clinical trial in non-human primates that were intraocularly injected and followed up to one year without finding any serious adverse reactions [19]. In addition, a clinical trial with AAV8, involving our centre, is in early phases of development for the treatment of MNGIE.

3. Future perspectives

Although mitochondrial disorders are rare diseases, in recent years, next-generation sequencing (NGS) technologies characterised by high-throughput capacity and high accuracy, boosted the discovery of new mutations [20]. These studies further increased the biochemical complexity underlying mitochondrial diseases, with an ever-increasing number of genes involved. However, their function and their pathogenetic role remain in many cases elusive. For instance, FBXL4 [21], APOPT1 [22] and FASTKD2 [23] were recently discovered in our lab as new proteins involved in mitochondrial diseases, but their functions are still unknown.

My PhD work, demonstrates that new integrated approaches including, generation of appropriate animal models, mass-spec analysis of proteome and metabolome, are needed to unravel highly complex biological processes.

However, the increasing understanding of mitochondrial biology fed the first attempts to develop new therapies for these currently untreatable diseases. My results support the idea that AAV based gene therapy is a promising strategy to correct at least some mitochondrial diseases. Notably, AAV-mediated gene therapy has already been successfully used in the treatment of haemophilia B [24]. In addition, in 2012, the European Medicines Agency approved Glybera (alipogene tiparvovec), the first commercially human gene therapy product in the Western world, which is based on an AAV vector carrying the lipoprotein lipase gene [25]. Glybera is used for the

treatment of lipoprotein lipase deficiency (LPLD), a condition leading to lipid accumulation in the blood and pancreatitis. This approval made a great impact on the world, and it opened the door for a gene therapy market in the near future.

References

1. Drose, S. and U. Brandt, The mechanism of mitochondrial superoxide production by the cytochrome bc1 complex. J Biol Chem, 2008. 283(31): p. 21649-54.
2. Hinson, J.T., et al., Missense mutations in the BCS1L gene as a cause of the Bjornstad syndrome. N Engl J Med, 2007. 356(8): p. 809-19.
3. Fernandez-Vizarra, E., et al., Impaired complex III assembly associated with BCS1L gene mutations in isolated mitochondrial encephalopathy. Hum Mol Genet, 2007. 16(10): p. 1241-52.
4. Sanchez, E., et al., LYRM7/MZM1L is a UQCRFS1 chaperone involved in the last steps of mitochondrial Complex III assembly in human cells. Biochim Biophys Acta, 2013. 1827(3): p. 285-93.
5. Di Meo, I., et al., Effective AAV-mediated gene therapy in a mouse model of ethylmalonic encephalopathy. EMBO Mol Med, 2012. 4(9): p. 1008-14.
6. Torres-Torronteras, J., et al., Gene therapy using a liver-targeted AAV vector restores nucleoside and nucleotide homeostasis in a murine model of MNGIE. Mol Ther, 2014. 22(5): p. 901-7.
7. Tiranti, V., et al., Ethylmalonic encephalopathy is caused by mutations in ETHE1, a gene encoding a mitochondrial matrix protein. Am J Hum Genet, 2004. 74(2): p. 239-52.
8. Tiranti, V., et al., Loss of ETHE1, a mitochondrial dioxygenase, causes fatal sulfide toxicity in ethylmalonic encephalopathy. Nat Med, 2009. 15(2): p. 200-5.
9. Di Meo, I., et al., Chronic exposure to sulfide causes accelerated degradation of cytochrome c oxidase in ethylmalonic encephalopathy. Antioxid Redox Signal, 2011. 15(2): p. 353-62.
10. Giordano, C., et al., Morphologic evidence of diffuse vascular damage in human and in the experimental model of ethylmalonic encephalopathy. J Inherit Metab Dis, 2012. 35(3): p. 451-8.
11. Nishino, I., A. Spinazzola, and M. Hirano, Thymidine phosphorylase gene mutations in MNGIE, a human mitochondrial disorder. Science, 1999. 283(5402): p. 689-92.

12. Mount, J.D., et al., Sustained phenotypic correction of hemophilia B dogs with a factor IX null mutation by liver-directed gene therapy. Blood, 2002. 99(8): p. 2670-6.
13. Snyder, R.O., et al., Correction of hemophilia B in canine and murine models using recombinant adeno-associated viral vectors. Nat Med, 1999. 5(1): p. 64-70.
14. Nathwani, A.C., et al., Self-complementary adeno-associated virus vectors containing a novel liver-specific human factor IX expression cassette enable highly efficient transduction of murine and nonhuman primate liver. Blood, 2006. 107(7): p. 2653-61.
15. Nathwani, A.C., et al., Adenovirus-associated virus vector-mediated gene transfer in hemophilia B. N Engl J Med, 2011. 365(25): p. 2357-65.
16. Cwerman-Thibault, H., et al., Gene therapy for mitochondrial diseases: Leber Hereditary Optic Neuropathy as the first candidate for a clinical trial. C R Biol, 2014. 337(3): p. 193-206.
17. Perales-Clemente, E., et al., Allotopic expression of mitochondrial-encoded genes in mammals: achieved goal, undemonstrated mechanism or impossible task? Nucleic Acids Res, 2011. 39(1): p. 225-34.
18. Lam, B.L., et al., Leber hereditary optic neuropathy gene therapy clinical trial recruitment: year 1. Arch Ophthalmol, 2010. 128(9): p. 1129-35.
19. Koilkonda, R.D., et al., Safety and effects of the vector for the Leber hereditary optic neuropathy gene therapy clinical trial. JAMA Ophthalmol, 2014. 132(4): p. 409-20.
20. Taylor, R.W., et al., Use of whole-exome sequencing to determine the genetic basis of multiple mitochondrial respiratory chain complex deficiencies. JAMA, 2014. 312(1): p. 68-77.
21. Gai, X., et al., Mutations in FBXL4, encoding a mitochondrial protein, cause early-onset mitochondrial encephalomyopathy. Am J Hum Genet, 2013. 93(3): p. 482-95.
22. Melchionda, L., et al., Mutations in APOPT1, encoding a mitochondrial protein, cause cavitating leukoencephalopathy with cytochrome c oxidase deficiency. Am J Hum Genet, 2014. 95(3): p. 315-25.
23. Ghezzi, D., et al., FASTKD2 nonsense mutation in an infantile mitochondrial encephalomyopathy associated with

cytochrome c oxidase deficiency. Am J Hum Genet, 2008. 83(3): p. 415-23.
24. Manno, C.S., et al., Successful transduction of liver in hemophilia by AAV-Factor IX and limitations imposed by the host immune response. Nat Med, 2006. 12(3): p. 342-7.
25. Wirth, T., N. Parker, and S. Yla-Herttuala, History of gene therapy. Gene, 2013. 525(2): p. 162-9.

Publications

AAV-mediated liver-specific MPV17 expression restores mtDNA levels and prevents diet-induced liver failure*. Bottani E, Giordano C, Civiletto G, Di Meo I, Auricchio A, Ciusani E, Marchet S, Lamperti C, d'Amati G, Viscomi C, Zeviani M****. Mol Ther. 2014 Jan;22(1):10-7.***

Emerging concepts in the therapy of mitochondrial disease. *Viscomi C, Bottani E, Zeviani M****. Biochim Biophys Acta. 2015 Jun-Jul;1847(6-7):544-57. Review.***

Ttc19 is an assembly factor of respiratory complex III leading to slowly progressive neurodegeneration*. Bottani E, Giordano C, Cerutti R, Fearnly I, d'Amati G, Viscomi C, Fernandez-Vizarra E, Zeviani M.* ***In preparation***

The research presented in this thesis was performed at the Unit of Molecular Neurogenetics, of the Foundation IRCCS Neurological Institute Carlo Besta, Milan, Italy and at the Mitochondrial Medicine group, MRC Mitochondrial Biology Unit, Cambridge, United Kingdom since October 2012 to November 2015.

I want to thank Prof. Massimo Zeviani for giving me the opportunity to pursue a PhD in his lab, for his experience and precious advice; dr. Carlo Viscomi for having followed me throughout the period of PhD research; and all my colleagues.